Mid Holocene Climate Variability in Northern Germany and Adjacent Oceans

Dissertation zur Erlangung des Doktorgrades der Mathematisch-Naturwissenschaftlichen Fakultät der Christian-Albrechts-Universität zu Kiel

vorgelegt von

Veronica Rohde Krossa

Kiel, Dezember 2014

1. Gutachter und Betreuer:	Prof. Dr. Ralph Schneider
2. Gutachter:	PD Dr. Mara Weinelt
Komitee der Müntlichen Prüfung:	Prof. Dr. Birgit Schneider
Vorsitzender der müntlichen Prüfung:	Prof. Dr. Mojib Latif
Tag der Disputation:	23.02.2015
Zum Druck genehmigt:	23.02.2015
Der Dekan:	Prof. Dr. Wolfgang J. Duschl

Erklärung

Hiermit erkläre ich an Eides statt, dass die vorgelegte Dissertation „Mid Holocene Climate Variability in northern Germany and adjacent Seas“, abgesehen von der Beratung durch meine akademischen Betreuer, in Inhalt und Form meine eigene Arbeit darstellt. Ferner habe ich weder diese noch eine ähnliche Arbeit an einer anderen Hochschule im Rahmen eines Prüfungsverfahrens vorgelegt. Diese Arbeit ist unter Einhaltung der Regeln guter wissenschaftlicher Praxis der Deutschen Forschungsgemeinschaft entstanden.

Kiel, den 12.12.2014

Veronica Rohde Krossa

Table of contents

Summary

In northern Germany and southern Scandinavia, high temperatures, low precipitation rates, and associated retreating or lacking continental glaciers characterized the mid Holocene period, also referred to as the Climate Optimum. At around 4000 cal. yr BP, the Neoglacial started a long-term cooling, increased precipitation, and re-advancing ice sheets and glaciers. Several major developments in more recent human history in northern Germany and southern Scandinavia occurred during the mid and late Holocene. One of the most radical changes included the transition from hunter-gatherer-fisher communities to societies relying on farming. First farming elements occurred at ~6000 cal. yr BP, however, it is not well understood why farming appeared around 2000 years later in northern Germany and southern Scandinavia compared to its adjacent southern regions. Many studies attribute climate change as the potential causing hunter-gather-fisher societies to increasingly adapt farming techniques that late. However, the ultimate effect of climatic and environmental changes on shifts in the economy of northern settlements is still debated because of a dearth of high-resolution regional paleo-climate reconstructions.

Therefore, this PhD thesis focused on the reconstruction of past climate conditions using different biomarker approaches derived from sediment cores in order to assess the potential effect of climate change on the onset of farming. The sediment cores were from sites in the Skagerrak located close to the landmass and at the continent adjacent to the settlements of these human groups. Consistent with first farming elements occurring at ~6000 cal. yr BP, a pronounced cooling of ~5-6ºC reflecting an outflow of cold Baltic Sea water in the Skagerrak was documented. Concomitant, summers in northern Germany were most likely warm and dry, following a period of warm and wet climate conditions. This climate shift was probably associated with a major change from a maritime towards a more continental-dominated atmospheric pattern, manifested in strong seasonal contrast and more frequent cold winters and warm summers.

Such climate conditions and prevalent atmospheric circulation pattern over the Skagerrak and Baltic region most likely provoked invasive effects on the natural environment leading to a gradual restriction in natural food resources. Thereby, formerly hunter-gatherer-fisher societies were forced to adopt farming strategies to overcome periods of unfavourable climate conditions. Once fully adopted, the farming societies were even able to survive during periods of Baltic Sea hypoxia that largely affected the marine food resources, as evident in a human population density increase at ~5500 cal. yr BP.

The connection between regional climate change and the onset of human settlements relying on farming in northern Germany and southern Scandinavia promotes the hypothesis that climate change is an important factor within a succession of several events that resulted

in the adaption of agrarian techniques. Probably, a combination of multiple factors such as the vulnerability of natural ecosystems under Baltic Sea hypoxia and climatic stress as well as the better use of existing knowledge on agricultural strategies forced societies to adapt to changes in the environment. This was achieved by improving their living conditions that even caused an increase in human population on a regional scale under less hospitable climatic and environmental conditions, such as a strong seasonal temperature contrasts. This in turn suggests that climate change associated with a major shift in general atmospheric circulation pattern was a major factor leading to the establishment and expansion of fully developed farming groups in northern Germany and southern Scandinavia.

Zusammenfassung

Hohe Temperaturen, geringe Niederschlagsraten und dadurch zurücktretende, oder fehlende Gletscher charakterisierten das mittelholozäne Klima in Norddeutschland und Südskandinavien. Diese Periode wird häufig als das mittelholozäne Klimaoptimum beschrieben. Um ~4000 Kalender Jahre vor heute (v. H.). beendete die neoglaziale Periode das Klimaoptimum, welches charakterisiert ist, durch eine langanhaltende Abkühlung, erhöhte Niederschläge und erneute Gletschervorstöße. Viele wichtige Ereignisse in der Entwicklung zu modernen Gesellschaften in Norddeutschland und Südskandinavien geschahen genau während dieses Zeitraums. Eine der radikalsten Veränderungen der Menschheitsgeschichte ist der Übergang von einer Jäger-, Sammler- und Fischergemeinschaft zu einer Viehzucht und Ackerbau betreibenden Gemeinschaft. Erste landwirtschaftliche Strukturen entwickelten sich um ~6000 Kalender Jahre v. H., etwa 2000 Jahre später als in den südlich angrenzenden Gebieten. Die Ursachen für die späte Entwicklung der Landwirtschaft in diesen Regionen sind bisher nur wenig erforscht. Viele Studien führen Klimaveränderungen als potentiellen Auslöser für den späteren Beginn der Landwirtschaft an. Aufgrund mangelnder, hochauflösender, regionaler Paläoklimarekonstruktionen ist die Auswirkung von klimatischen und ökologischen Veränderungen auf die Lebensweise in den nördlichen Siedlungen, fortlaufender Gegenstand aktueller Diskussionen.

Das Ziel dieser Doktorarbeit war die Erstellung von Temperatur und Niederschlagsrekonstruktionen aus dem Mittel- bis Spätholozän mittels verschiedener Biomarkermethoden an Sedimentkernen. Dabei sollte eine mögliche Verbindung zwischen Klimawandel, dem späteren Beginn der Landwirtschaft in Norddeutschland und Südskandinavien untersucht werden. Die Sedimentkerne stammen aus dem Skagerrak und aus Norddeutschland, von Lokationen die so nah wie möglich an den prehistorischen Siedlungen liegen. Mit dem Beginn der Landwirtschaft in Norddeutschland und Südskandinavien war zeitgleich eine starke Abkühlung von 5-6ºC im Skagerrak zu erkennen, die mit einem verstärkten Ausstrom von Ostseewasser in Richtung Nordsee verbunden war. In Norddeutschland folgten damals warme und trockene Sommer auf eine Phase mit mildem und feuchtem Klima. Diese Veränderung beruhte wahrscheinlich auf einer großen Verschiebung des atmosphärischen Zirkulationsmusters, von einem maritimen- zu einem eher kontinental-dominierteren Klima. Daraus resultierten erhöhte Temperaturkontraste zwischen Sommer und Winter, sowie häufige auftretende warme Sommer und kalte Winter.

Solche Klimaverhältnisse und atmosphärischen Zirkulationsmuster über dem Skagerrak und der baltischen Region hatten vermutlich starke Auswirkungen auf die natürliche Um-

welt, was zu einer allmählichen Einschränkung der natürlichen Nahrungsressourcen führte. Dadurch wurde die ursprüngliche Gemeinschaft von Jägern, Sammlern und Fischern gezwungen, landwirtschaftliche Strategien zu nutzen, um Zeiten von ungünstigen Klimabedingungen zu überstehen. Der Anstieg der Bevölkerungsdichte nach ~5500 Kalender Jahre v. H. lässt darauf schließen, dass die landwirtschaftlichen Gesellschaften nach ihrer vollständigen Entwicklung sogar in der Lage waren, starke Verknappungen der marinen Nahrungsressourcen, u.a. bedingt durch Phasen der Sauerstoffarmut in der Ostsee, zu überstehen.

Der Zusammenhang zwischen Klimaveränderungen und die Entstehung der Landwirtschaft in Norddeutschland und Südskandinavien zeigt, dass der Klimawandel, zusammen mit vielen Faktoren, eine sehr entscheidende Rolle bei der Ausbreitung und Manifestation von Ackerbau und Viehzucht spielte. Wahrscheinlich führte eine Kombination mehrerer Faktoren, wie u.a. die Anfälligkeit von natürlichen Ökosystemen auf sauerstoffarme Bedingungen in der Ostsee, klimatischer Stress und die Anwendung von vorhandenem landwirtschaftlichem Wissen dazu, dass die ursprüngliche Gemeinschaft von Jägern, Sammlern und Fischern sich zu einer Gesellschaft mit landwirtschaftlich erzeugter Nahrungsversorgung entwickelte. Dieser Zusammenhang deutet darauf, dass regionale Klimaveränderungen eine wichtige Rolle bei der Verbreitung und Manifestation der Landwirtschaft in Norddeutschland und Südskandinavien spielten.

Acknowledgments

First of all, I am grateful to Prof. Dr. Ralph Schneider and Dr. Mara Weinelt for providing me the opportunity to work on this subject! Thank you to my supervisor for your assistance and guidance throughout my PhD studies.

This PhD thesis was mainly carried out within the framework of the multi-disciplinary SPP 1400 project "*Early Monumentality and Social Differentiation. On the origin and development of Neolithic large-scale buildings and the emergence of early complex societies in Northern Central Europe*" at the University of Kiel (2009-2011) and funded by the DFG (Deutsche Forschungsgesellschaft). Thank you to all SPP1400 members. Additionally, this PhD thesis was based on a co-operation with the BONUS EU+ "inflow" project (2009-2011) that aimed to reconstruct past changes in inflow and hypoxia in the Baltic Sea over the past 2000 years. Inflow members: thank you to all for lots of fun and fruitful discussions during the inflow meetings!

There are many people that have supported me over the past years. However, two persons deserve a very special thank you: Matthias Moros at the IOW (Germany) and Guillaume Leduc at C.E.R.E.G.E. (France). Thank you both for your support and assistance! Thank you for discussing; reading my manuscripts, for your ideas, and for improving my work. I am very grateful for your continuously supportive and constructive work. Thank you, Matthias, for inviting me to the inflow project!

Thank you to all of my colleagues: Jeroen, Janne, Renato, Yiming, Henrik, and Thomas for fruitful discussion, lots of coffee, fun, and for supporting me. Thank you Camille, for lots of fun (and serious) discussions, for your drawings (!), and for your cooperation during my PhD studies.

Thank you Silvia Koch for your assistance during my lab work at the biomarker laboratory (CAU Kiel). Thank you Thomas Blanz and Thomas Larsen for assistance with alkenones and stable hydrogen isotopes and providing me much information on the Skagerrak and Lake Belau. Thank you to all people working at the biomarker laboratory at the NIOZ for assistance. Thank you Huyn-Jung Kim for assistance during my stay at the NIOZ.

Thorsten Bauersachs: thank you for fruitful GDGT discussions and for improving my GDGT manuscript. I am very grateful.

A special thank you to Martin Hinz for giving me first-handed information on archaeology in northern Germany! Thank you, Jürgen Zahrer, Stephan Dreibrodt, Ingo Feeser, and Walter Dörfler for providing me lots of information and mud from Lake Belau!

Finally and quite important, my friends and family! Thank you Andrea for supporting me during my PhD work, for lots of fun, discussions, fun, and support! Thank you, Julia for sharing a lot of coffee with me! Mamma and pappa: Thank you for being supportive and believing in me during my studies and PhD thesis. Thank you to my mother and my mother-in-law for taking care of my child, Sigurd. Thank you Sebastian, for understanding my situation, for never giving up, for helping me with computer problems and chemistry, for discussions, and finally, for supporting me during my final and exhausting months of PhD writing!

List of Figures

List of Tables

1 Introduction

1.1 Holocene climate and towards an agrarian-based economy in northern Germany and southern Scandinavia

The Holocene interval covers the last 11700 cal. yr BP (Walker et al., 2012) and is generally regarded as a period of stable climate conditions (Mayewski et al., 2004; Wanner et al., 2008). The most prominent climate feature documented throughout the mid and late Holocene period is an insolation-driven progressive cooling trend that followed a temperature maximum in the early Holocene. This cooling is observed in many North Atlantic and European paleo-climate reconstructions (Calvo et al., 2002; Davis et al., 2003; Moros et al., 2004; Seppä et al., 2005; Sicre et al., 2008; Jansen et al., 2008; Risebrobakken et al., 2010) and is regarded as the major factor that modulated Holocene climate at northern high latitudes (Leduc et al., 2010; Schneider et al., 2010; Lohmann et al., 2013). The early Holocene period (11700 – 8200 cal. yr BP) was largely governed by ice sheet remnants and high boreal summer insolation. These features caused rapid retreats of the ice sheets, eustatic sea level rise, and glacial isostatic adjustments of the Scandinavian landmass that in turn provoked changes in climate and environment in northern Germany/southern Scandinavia and the Baltic Sea (Björck, 1995; Gyllencreutz, 2005). The mid Holocene interval (8200 – 4200 cal. yr BP) is often characterized by i.e. high temperatures, low precipitation rates, and associated reduced or lacking glaciers, and is often referred to as the Holocene Climate or Thermal Optimum (HCO or HTM) (Seppä and Birks, 2001; Calvo et al., 2002; Hammarlund et al., 2003; Moros et al., 2004; Bjune et al., 2005; Seppä et al., 2005; Bakke et al., 2008). At ~4500-4000 cal. yr BP, the Neoglacial cooling terminated the HCO (Magny and Haas, 2004; Mayewski et al., 2004; Wanner et al., 2008; Marcott et al., 2013), consequently initializing the late Holocene interval. In the North Atlantic and northern Europe, the Neoglacial period was generally associated with the insolation-driven cooling, increased precipitation, and consequently re-advancing glaciers in southern Norway (Seppä and Birks, 2001; Calvo et al., 2002; Hammarlund et al., 2003; Moros et al., 2004; Bjune et al., 2005; Seppä et al., 2005; Bakke et al., 2008; Nesje et al., 2001; Sicre et al., 2008).

In Europe, several major developments towards modern human societies occurred during the Holocene interval. One of the most important changes included the transition from hunter-gatherer-fisher based groups towards societies relying on animal husbandry and cereal cultivation. In northern Germany and southern Scandinavia, first agricultural elements occurred at ~6000 cal. yr BP (Sørensen and Karg, 2012), whereas a fully developed agrarian society is documented as late as ~5500 cal. yr BP (Dörfler et al., 2012; Kirleis et al., 2012; Feeser et al., 2012). In contrast, farming was manifested ~1500 years earlier in adjacent southern regions (Schier, 2009; Guilaine, 2000/2001), and consequently, the agrarian technology was most likely available to hunter-gatherer-fisher societies in northern Germany and

southern Scandinavia for more than one millennium. Many studies suggest that the late onset of an agricultural economy in northern Germany and southern Scandinavia was related to climate change (Bonsall et al., 2002; Hartz et al., 2007; Sørensen and Karg, 2012; Gronenborn et al., 2013). Northern hunter-gather-fisher groups were largely dependent on natural aquatic and terrestrial food resources, and therefore, environmental changes most likely had a strong impact on their economy. However, the ultimately effect of climate on changes in human subsidence technology at those sites is still debated because of a dearth of high-resolution regional paleo-climate reconstructions. Until now, a majority of climate reconstructions used for such comparisons are based on marine sedimentary records that are situated in large distances to the continental excavation sites (Shennan et al., 2013), and therefore do most likely not reflect climate conditions occurring over the landscape where those human groups settled. Consequently, establishing robust high-resolution paleo-climate reconstructions from sites located close to the continent or even on the continent is essential in order to understand potential changes in climate that might have affected past hunter-gatherer-fisher and early farming societies. Therefore, the overall aim of this PhD thesis was to establish paleo-climate reconstructions from sedimentary sequences located as close as possible to the landmasses (Skagerrak) and at the continent (Lake Belau) to determine the effect of climate change on both regional and local scales.

1.2 Structure of thesis

1.2.1 Aims and objectives

The mid Holocene period in northern Germany and southern Scandinavia roughly spans the time of human cultures responsible for early “neolithisation”, including i.e. fast spread of agriculture, animal husbandry, and exploitation of coastal environments. Economical opportunities, which finally controlled the development of these societies, were most likely substantially co-determined, not only by technological improvements, but also by climate change such as changes in temperature and/or precipitation. Therefore, this PhD study focused on the **reconstruction of past climate conditions using biomarker approaches in order to assess the potential effect and extent of climate change on human societies.** Taking advantage of biomarker proxies that can be used both in the marine and limnic sedimentary archives, this study aimed to compare marine and terrestrial climate signals in order to better understand the magnitude of regional and local climate change and if possible, to disentangle anthropogenic from natural climate changes observed in the lake record. Additionally, this PhD thesis aimed to test proxies for Baltic Sea outflow in the Skagerrak area. For this purpose, multi- and gravity-cores from the marine Skagerrak and Kattegat/Mecklenburg Bay as

well as a lake core retrieved from Lake Belau in northern Germany were investigated. The following main objectives of this PhD thesis will be addressed in single chapters:

- Testing proxies for past changes in Baltic Sea outflow in the Skagerrak.
- Establish high-resolution sea surface temperature (SST) reconstructions in order to evaluate the potential link between marine climate change and the onset of agriculture in northern Germany and southern Scandinavia.
- Compare marine temperature reconstructions to temperature and precipitation reconstructions on land from lake sediments in order to unravel significant differences that may be due to human impact on the lake climate record.
- Evaluate the potential link between past changes in temperature and precipitation on land and the onset of local farming societies.

1.2.2 Thesis outline

This PhD thesis is divided in 8 chapters. **Chapter 1** focuses the introduction and **Chapter 2** describes the study sites and regional climate. Material and methods are explained in **Chapter 3**. **Chapter 4** focuses on the application of tetra-unsaturated ketones ($C_{37:4}$ %) as a proxy for past Baltic Sea outflow changes in the Skagerrak and the reconstruction of outflow changes over the last 5000 years. Both multi-core and gravity-core sediments were evaluated in this study. The multi-core results mirror the modern salinity gradient observed in the Skagerrak, associated with lower $C_{37:4}$ % values close to the North Atlantic and higher $C_{37:4}$ % values closer to the Kattegat. To test the reliability of $C_{37:4}$ % back in time, gravity-core $C_{37:4}$ % reconstructions were compared to grain-size records from the Kattegat and Mecklenburg Bay, that are, based on a seismo-acoustic profile in the Kattegat channel, indicative of changes in outflow. All records document an increase in Baltic Sea outflow over the past ~3500 cal. yr BP, probably reflecting higher precipitation over the Baltic Sea catchment area owing to a re-organization of North Atlantic atmospheric circulation with increased influence of wintertime Westerlies over the Baltic catchment from the mid to the late Holocene. This manuscript is published online in *Boreas*.

Chapter 5 focuses on SST reconstructions in the Skagerrak to discuss the potential impact of climate change in the adjacent marine environment on the onset of farming at around 6000 cal. yr BP in northern Germany and southern Scandinavia. In this chapter, several gravity-core records from the northeastern, central, and western Skagerrak were evaluated to reconstruct past SST using the $U^{K'}_{37}$-temperature relationship. Over the mid and late Holocene, all Skagerrak records document an overall cooling. However, on millennial to multi-centennial time scales, diverging SST trends are observed, suggesting that climate condi-

tions prevailing over the North Atlantic and Baltic region differently modulated the SST in the western/central and northeastern Skagerrak, respectively. Consistent with a prominent cooling observed between ~6300 and 5600 cal. yr BP in the northeastern Skagerrak, first farming elements occur in northern Germany and southern Scandinavia. This suggests that the cooling might have provoked invasive effects on the natural environment that in turn caused formerly hunter-gatherer-fisher societies to adopt farming strategies in order to overcome periods of unfavorable climate conditions. Once fully adopted, the farming societies were even able to overcome such periods, as supported by an increase in human population during the coldest sea surface temperatures. This manuscript was submitted to *The Holocene* on October 22, 2014 and is now under revision.

Chapter 6 focuses on the reconstruction of past continental temperatures in order to disentangle anthropogenic impacts on the lake sedimentary sequence from natural climate changes and to discuss the potential effect of changes in temperature on the onset of local farming societies. In this chapter, a lake core from Lake Belau (northern Germany) with a well-established chronology was used to reconstruct past temperatures using branched glycerol dialkyl glycerol tetraethers (*br*GDGT). Although several periods of human interactions on the landscape and lake are documented throughout the period studies, there are no direct evidences that human activity might have perturbed the *br*GDGT-derived temperature reconstruction at that site. Overall, the temperature reconstruction documents the typical northern hemispheric mid to late Holocene cooling. However, opposite to the cooling interval observed in paleo-climate reconstructions from the northeastern Skagerrak and southern Sweden, a warming period is observed between ~5900 and 5300 cal. yr BP. This discrepancy in temperature trend at such short distances indicates that the *br*GDGTs might predominantly be biosynthesized during another period of the annual cycle. This warming interval matches the onset of local farming societies, suggesting that temperature played a pivotal role for the existence of such societies at the Lake Belau site. This manuscript is prepared for submission.

Chapter 7 focuses on the applicability of the TEX_{86}-proxy as a temperature proxy in the Skagerrak using both sub-surface and Holocene sediments by comparing to existing $U^{K'}_{37}$-SST records. Recently, a study from the northeastern Skagerrak covering the past ~110 years revealed a good match of TEX_{86} to mean annual SST. Therefore, this PhD project was motivated to use TEX_{86} together with the $U^{K'}_{37}$-SST as a multi-proxy approach to discuss the potential effect of climate change on the onset of farming in northern Germany and southern Scandinavia. However, in contrast to the good match of TEX_{86} to both mean annual SST and $U^{K'}_{37}$ in the sub-surface sediment, the TEX_{86}-temperature record covering the complete Holocene sequence, documented diverging trends and absolute values prior to ~2500 cal. yr BP when comparing to Skagerrak $U^{K'}_{37}$-SST reconstructions. Over the latest

Holocene, however, the absolute reconstructed temperatures ($U^{K'}_{37}$ and TEX_{86}) approach similar values and show the same cooling trend. As the $U^{K'}_{37}$-temperature relationship represents a robust paleo-climate signal, most likely reflecting mean annual SST conditions, these differences suggest that the TEX_{86} proxy might record a seasonal signal instead of the annual mean and/or even temperatures in the sub-surface waters. This chapter will be prepared as a forth manuscript for submission.

Chapter 8 focuses on the applicability of stable hydrogen isotope composition (δD) of specific *n*-alkanes as a proxy for continental precipitation and the reconstruction of changes in rainfall over northern Germany in order to discuss the potential effect of changes in precipitation on local farming societies. In this chapter, a lake core from Lake Belau (northern Germany) with a well-established chronology was used to reconstruct past precipitation using stable hydrogen isotopes (δD) from a suite of specific *n*-alkanes with different chain length (C_{27}, C_{29}, and C_{31}) derived from terrestrial plant leaf waxes. It turned out that in particular δD_{C29} can be used for the reconstruction of paleo-precipitation, as it seems less affected by anthropogenic-induced vegetation changes in the Lake Belau catchment area. Concomitant with the onset of local farming societies, the δD_{C29} documents dry climate conditions consistent with the warming period as showed by the *br*GDGT proxy. This implies that local warm and dry conditions were likely favorable for the existence of farming societies at that site.

Finally, in **Chapter 9**, conclusions and future outlook of the thesis are given.

2 Study sites and regional climate

2.1 Skagerrak

The Skagerrak lies in the north of the epicontinental North Sea and forms the only marine connection between the North Atlantic Ocean/North Sea and the landlocked Baltic Sea (Figure 2.1). In the north, the Skagerrak has a fjord-like shape (Thiede, 1987) and exceeds maximum water depths of more than 700 m (Rodhe, 1987), representing the deepest part of the otherwise shallow North Sea. In the present day Skagerrak, sea surface currents and temperatures are determined by the interplay between the inflow of North Atlantic water and Baltic Sea outflow (Figure 2.1). Therefore, sedimentary sequences from the northeastern Skagerrak that are closest to the Baltic region, provide an excellent archive for paleo-climate reconstructions that reflect changes in atmospheric circulation pattern over the Baltic region, while those from the western Skagerrak are more indicative of the overall maritime climate of the North Atlantic realm.

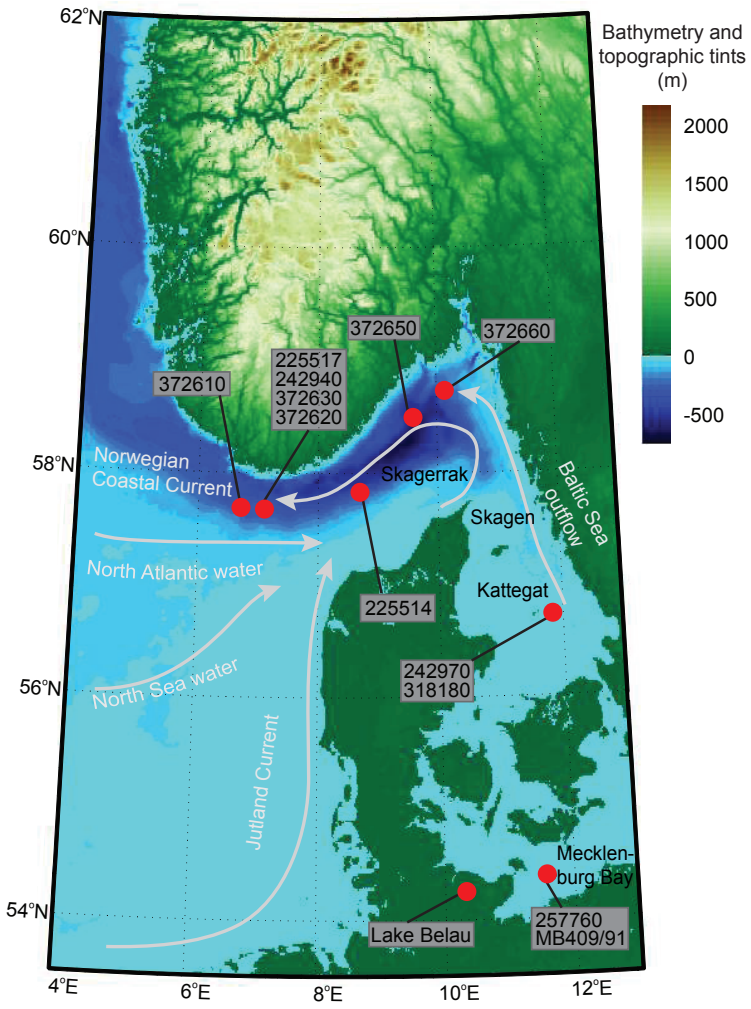

Fig. 2.1 Bathymetry and general ocean circulation pattern (pale grey arrows) in the North Sea and Skagerrak and core locations (see Table 3.1). The bathymetric and topographical lines are from (IOC et al., 2003).

Saline North Atlantic water enters the Skagerrak/North Sea between Scotland and Norway and via the English Channel. The South Jutland Current, consisting of water from the English Channel and southern North Sea, flows northwards along the Danish coast and mixes with the North Jutland Current that originates from the North Atlantic and central North Sea water. As the current passes Skagen (Figure 2.1) and enters the Skagerrak/Kattegat border, part of it mixes with fresher and colder Baltic Sea water. Thereupon, part of the current forms an anti-clockwise gyre that exits the Skagerrak, back flowing along the Norwegian coast as the Norwegian Coastal Current (Figure 2.1). The anti-clockwise current causes current speed reduction that allows fine-grained sediment to accumulate at high rates in the central and northeastern parts of the Skagerrak (Rodhe and Holt, 1996; van Weering, 1982).

2.2 SW Baltic Sea

The Baltic Sea is a semi-enclosed brackish water body located in a humid climatic zone in northern Europe. Today, the Baltic Sea is connected to the North Atlantic Ocean via the Skagerrak through the narrow and shallow Danish straits (Figure 2.1). As a consequence of the fresh water surplus and the strongly limited water exchange with the open ocean, the Baltic Sea has an estuarine circulation pattern characterized by outflowing low-salinity surface water and inflowing higher-salinity bottom water, causing a permanent salinity stratification. The Baltic Sea outflow causes a low-salinity environment in the Danish Straits and the Kattegat towards the Skagerrak (Danielssen et al., 1997). Due to the positive freshwater balance due to river runoff and net precipitation, quantities of outflowing Baltic Sea water are generally larger than inflowing water volumes. On a long-term average, the difference between outflowing and inflowing water volumes equals the freshwater surplus (Stigebrandt and Gustafsson, 2003). Model simulations suggest that an increase of the net freshwater supply to the Baltic Sea causes enhanced surface water outflow and a decrease of bottom water inflow in the Kattegat area (Stigebrandt, 1983; Stigebrandt and Gustafsson, 2003), although a weakening of inflow during periods of strong outflow is contradictory to a general estuarine circulation scheme.

Today, and probably in the past, the ecosystem health in the Baltic Sea is largely dependent on oxygen supply (HELCOM, 2007), and consequently, the occurrence of hypoxia (<2 ml/l O_2) in bottom waters induces major alternations in nutrient and other biogeochemical cycles (Vahtera et al., 2007), thereby destroying benthic faunal communities and fish habitats (Karlson et al., 2002; Conley et al., 2009). Today and probably since the initialization of the Baltic Sea estuarine circulation pattern at ~8500 cal. yr BP (Andren et al., 2000; Rößler et al., 2011), the inflow of saline and O_2-rich bottom water originating from the North Sea, or the lack of such, strongly controls the occurrence of hypoxia. Some studies argue that intensified

Baltic Sea outflow reduces the frequency and/or intensity of O_2-rich inflows (e.g., Stigebrandt, 1983; Matthäus and Schinke, 1999; Stigebrandt and Gustafsson, 2003; Krossa et al., 2014). In contrast, other studies argue that the generation of hypoxia is strongly related to intensified cyanobacteria blooms (Conley et al., 2009; Funkey et al., 2014) that most likely occur during warm summers (Kabel et al., 2012; Funkey et al., 2014). Yet, however, the direct causes and responses between these factors are still not completely understood and further studies are needed to understand the processes and feedbacks of hypoxia in the Baltic Sea.

2.3 Lake Belau

Lake Belau is a relatively small lake (surface area ~1.14 km^2) located in the young moraine landscape in northern Germany (10°16´E, 54°6´N) close to the southwestern Baltic Sea/Kattegat and Skagerrak (Figures 2.1 and 2.2). The maximum water depth is ~29 m and the lake surface area is ~1.13 km^2 (Müller, 1981). The catchment area compromises a size of ~3.37 km^2 (Naujokat, 1997) (Figure 2.2). Lake Belau is part of a connected system of kettle hole lakes that was formed during the Weichselian glaciation (Fränzle et al., 2008; Garbe-Schönberg et al., 1998). The Schwentine River that drains northwards into the Baltic Sea connects the lakes (Garbe-Schönberg et al., 1998).

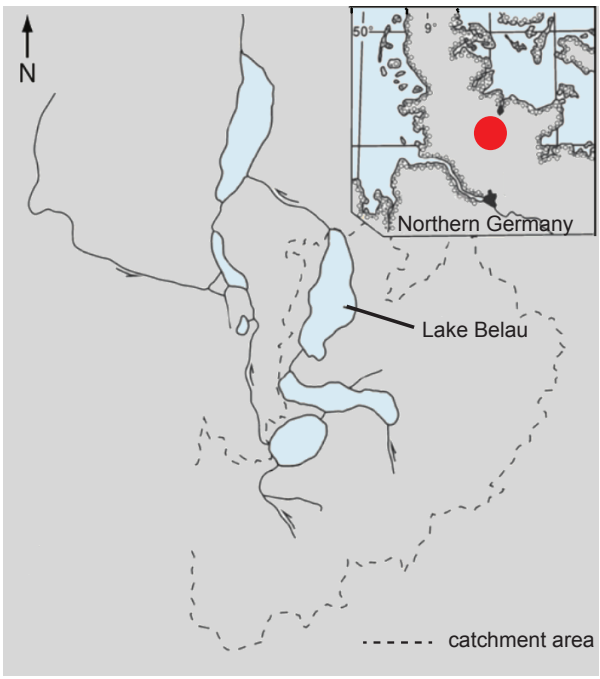

Fig. 2.2 Lake Belau (red dot) is located in northern Germany close to the Baltic Sea, Skagerrak, and the North Atlantic. Figure is slightly modified from Zahrer et al. (2013).

During the post-glacial period, major natural changes as well as human impact on the landscape surrounding Lake Belau are documented (Wiethold, 1998; Dörfler et al., 2012).

Prior to the first evidences of initial agrarian societies occurring at ~6000 cal. yr BP, shifts in vegetation pattern were probably mainly modulated by overall climate conditions that in turn most likely were driven by orbital parameters (Leduc et al., 2010; Schneider et al., 2010; Lohmann et al., 2013). During the early and partly mid Holocene period, a mixed deciduous forest dominated the Lake Belau catchment area. At ~5900 cal. yr BP, the palynological record documents an increase in micro-charcoal particles that clearly indicates the occurrence of early farming societies associated with “slash-and-burn” agricultural techniques for forest clearance (Wiethold, 1998; Dörfler et al., 2012). Between ~5500 and 5100 cal. yr BP, a period of intensified land use is documented in the Lake Belau area, as indicated in the occurrence of pioneer plants such as *Plantago lanceolata,* several grasses (both indicative of deforestation), and cereal pollen (Wiethold, 1998; Dörfler et al., 2012; Feeser et al., 2012). Also, geochemical records indicate a period of probably largely human-induced enhanced primary production and soil erosion (Dreibrodt and Wiethold, 2014). In contrast, between ~5100 and 2600 cal. yr BP, the landscape was characterized by reduced land use and woodland regeneration, interrupted by shorter periods of intensified land use, however, not reaching the same extent as between ~5500 and 5100 cal. yr BP (Dörfler et al., 2012). After ~2600 cal. yr BP, however, a re-intensification of agricultural activity during the Bronze Age is documented (Wiethold, 1998; Dörfler et al., 2012; Garbe-Schönberg et al., 1998).

2.4 Regional climate

The present day climate in northwest Europe and the Baltic region is strongly governed by large-scale atmospheric pressure systems that drive variations in strength and direction of wind fields (e.g., Hurrell, 1995; Hurrell et al., 2003; BACC, 2008). Such pressure systems include the Icelandic Low, the Azores High, and the winter High/summer Low over Russia, whereas variations in the occurrence of these pressure systems lead to a pre-dominance of maritime or continental climate. Periods of maritime-dominated climate are characterized by the strong influence of Westerlies directed towards northwest Europe that are driven by i.e. intensified pressure gradients between the Icelandic Low and Azores High. Such climate conditions cause mild and moist climate in northwest Europe that can affect large areas of the Baltic region. In contrast, a continental-dominated climate is marked by weaker Westerlies and a greater dominance of the continental anticyclone over Russia, thus provoking dry and warm summer and cold and dry winter conditions (e.g., Hurrell, 1995; Hurrell et al., 2003; BACC, 2008).

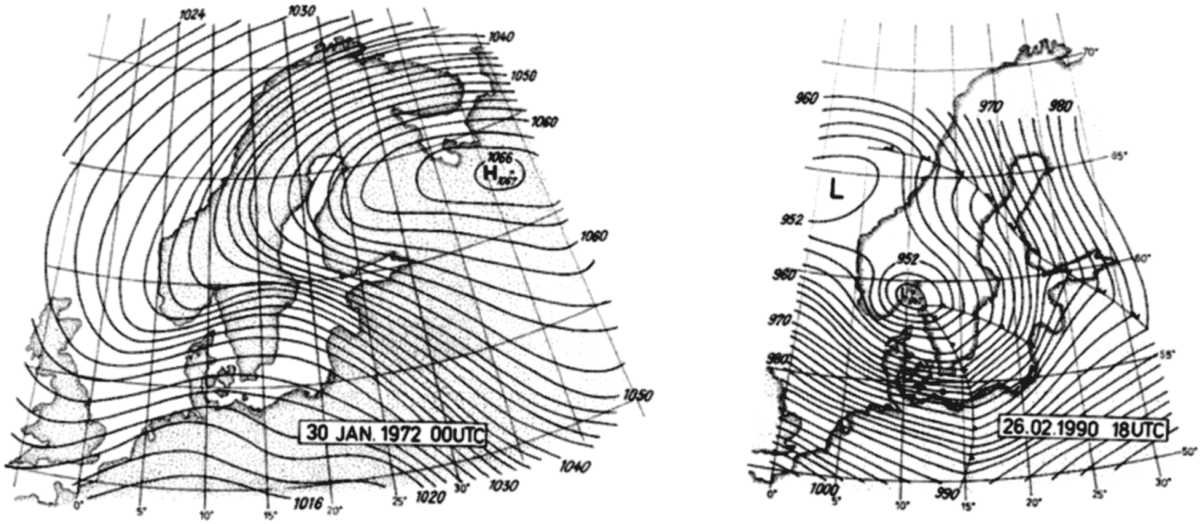

Fig. 2.3 Example of a major continental anti-cyclone (left) and a violent storm cyclone (right) over the Baltic Sea Basin. From BACC (2008). A high pressure system over the north European continent causes warm and dry summers and /or winters, whereas a strong low pressure system over the North Atlantic leads to milder and wetter climate conditions in north Europe.

3 Material and methods

3.1 Material

In this PhD thesis, a suite of gravity-cores and multi-cores from the Skagerrak, four gravity-cores from the Kattegat/Mecklenburg Bay, and one lake core from Lake Belau were analysed using different biomarker approaches (Table 3.1) and used in the chapters presented in this PhD study. The Institute of Warnemünde (IOW) provided all marine gravity- and multi-cores (Skagerrak, Kattegat, and Mecklenburg Bay), and the Institute of Pre- and Protohistoric Archaeology at the University of Kiel provided the Lake Belau samples.

Tab. 3.1 Location and biomarker methods of each core used in this PhD thesis (see also Figure 2.1).

Core	Latitude/ Longitude	Depth (m)	Cruise/year	Location	Biomarker	Used in Chapter
IOW372610 GC/MUC	57°41.05´N / 06°41.00´E	320	R/V Maria S Merian MSM12/4,	W Skagerrak	$U^{K'}_{37}$, $C_{37:4}$	4, 5, 7
IOW372620 MUC	57°40.06´N / 07°05.36´E	315	R/V Maria S Merian MSM12/4, 2009	W Skagerrak	$U^{K'}_{37}$, $C_{37:4}$	4
IOW372630 MUC	57°40.55´N / 07°09.97´E	330	R/V Maria S Merian MSM12/4, 2009	W Skagerrak	$U^{K'}_{37}$, $C_{37:4}$	4
IOW242940-4 MUC/GC	57°40.52´N / 07°10.00´E	316	R/V Poseidon 282, 2002	W Skagerrak	TEX_{86}, $C_{37:4}$	4, 7
IOW225514 GC	57°50.28´N / 08°42.226´E	420	R/V Alkor, 2000	C Skagerrak	$U^{K'}_{37}$, $C_{37:4}$	4, 5, 7
IOW372650 GC/MUC	58°29.76´N / 09°35.91´E	550	R/V Maria S Merian MSM12/4, 2009	NE Skagerrak	$U^{K'}_{37}$, $C_{37:4}$	4, 5
IOW372660 MUC	58°44.01´N / 10°11.96´E	227	R/V Maria S Merian MSM12/4, 2009	NE Skagerrak	$U^{K'}_{37}$, $C_{37:4}$	4
IOW318180 GC	56°43.58´N / 11°49.42´E	43	R/V Maria S Merian MSM 01/02, 2006	Kattegat	Grain-size	4
IOW242970 GC	56°43.58´N / 11°49.80´E	46	R/V Poseidon 282/ 2002	Kattegat	Grain-size	4
IOW257760 GC	54°22.54´N / 11°38.08´E	24	R/V Humboldt 1994	Meckl. Bay	Grain-size	4
MB409/91 GC	54°22.54´N / 11°33.00´E	24.5	R/V Humboldt 1991	Meckl. Bay	Grain-size	4
P2002	10°16´E / 54°6´N	28.3	2002	Lake Belau	*br*GDGTs, δD, $\delta^{13}C$	6, 8

All Skagerrak multi-cores were sub-sampled in 0.5 cm slices. Gravity-core IOW372650 in the northeastern Skagerrak was selected for high-resolution $U^{K'}_{37}$-SST (and $C_{37:4}$ %) studies and sub-sampled in 1 cm intervals, because of its proximity to the Baltic Sea, high sedimentation rate, and the well-established and robust age-depth model (see chapter 3.5). The gravity-cores in the western and central Skagerrak were sub-sampled in 10 to 2 cm intervals, depending on material available, for the analysis of $U^{K'}_{37}$-SST, $C_{37:4}$ %, and/or TEX_{86}. M. Moros (Institute of Warnemünde) provided the grain-size data in 1 cm resolution of the gravity-cores from the Kattegat (IOW318180 and IOW242970) and Mecklenburg Bay (IOW257760 and MB409/91). Bulk samples of 4x4 cm slices, representing an average of 20-25 years according to varve counting were sub-sampled on multi-centennial time scale in the Lake Belau composite sequence.

3.2 Alkenones

Alkenones are unsaturated ketones with 37 to 39 carbon atoms (C_{37}, C_{38}, C_{39}) as a basic chain, containing two to four alkene units (double bounds or 'unsaturations') causing variable degrees of unsaturation. They are exclusively biosynthesized by unicellular algae of the class Prymnesiophyceae, which require sunlight for photosynthesis and therefore generally dwell in the photic zone (Herbert, 2003). Today, they are almost ubiquitous in all marine settings but have also been observed in brackish and fresh water environments (see review of Castaneda and Schouten, 2011). In the marine environment, the cosmopolitan coccolithophorids *Emiliania huxleyi* and *Gephyrocapsa oceanica* (Volkman et al., 1995) are the main producers of alkenones during the last 150000 years.

3.2.1 Sea surface temperatures (SSTs)

Alkenones with 37 carbon atoms (C_{37}) are usually used to reconstruct past sea surface temperatures (SST) (Conte and Eglinton, 1993; Prahl and Wakeham, 1987; Ternois et al., 1997; Sicre et al., 2002). The paleo-thermometry is based on the response of coccolithophorids to changes in water temperature by altering the number of alkene units (two to four) in their cell membrane (Brassell et al., 1986; Prahl and Wakeham, 1987; Conte et al., 2006). In this paleo-thermometry, a higher number of three (or four) alkene units ($C_{37:3}$ and $C_{37:4}$) is produced at lower temperatures, while higher numbers of two alkene units ($C_{37:2}$) are formed at higher temperatures (Figure 3.1). Based on this relationship, unsaturation ratios (U^{K}_{37} and $U^{K'}_{37}$ indices, equations 3.1 and 3.2) have been defined for the sum of alkenones that can be extracted from marine sediments (Brassell et al., 1986; Prahl and Wakeham, 1987). As there is no empirical benefit in including tetra-unsaturated alkenones ($C_{37:4}$), the $U^{K'}_{37}$ index ignoring the latter alkenone is more commonly used for paleo-reconstructions:

$$U^{K}_{37}=(C_{37:2} - C_{37:4})/(C_{37:2} + C_{37:3} + C_{37:4}) \quad \text{(Brassell et al., 1986)} \quad (3.1)$$

$$U^{K'}_{37}=(C_{37:2})/(C_{37:2} + C_{37:3}) \quad \text{(Prahl and Wakeham, 1987)} \quad (3.2)$$

Laboratory cultures of *E. huxleyi*, modern plankton observations, and studies of surface sediment show a linear correlation of the $U^{K'}_{37}$ index to algal growth temperature (Prahl and Wakeham, 1987; Prahl et al., 1988; Conte et al., 1998; Müller et al., 1998). The $U^{K'}_{37}$ index is commonly converted to SST using the calibration of Müller et al. (1998):

$$SST=(U^{K'}_{37} - 0.44)/0.033 \quad \text{(Müller et al., 1998)} \quad (3.3)$$

Global core-top studies suggest the strongest correlation with modern mean annual SSTs (Müller et al., 1998; Conte et al., 2006; Rosell-Melé and Prahl, 2013). However, many studies argue that reconstructed SSTs at mid to high latitudes are seasonally skewed, as coccolithophorid growth strongly depends on light conditions and nutrient availability. Consequently, the $U^{K'}_{37}$-SST signal is skewed towards periods of the annual cycle when the algae bloom likely occurs (e.g., Leduc et al., 2010; Schneider et al., 2010; Lohmann et al., 2013). However, a recent review of previously published data suggests that globally distributed $U^{K'}_{37}$-based SST reconstructions correlate most significantly to modern mean annual sea surface temperatures rather than being seasonally skewed (Rosell-Melé and Prahl, 2013). The most straightforward explanation is that reconstructed SSTs might reflect seasons where the SST is similar to the mean annual SST (Müller et al., 1998). The own study in the Skagerrak area suggests that the $U^{K'}_{37}$-SST signal most likely reflects mean annual SSTs (see chapter 5).

3.2.2 $C_{37:4}$ % and Baltic Sea outflow (fresh water)

By contrast to the di- and tri-unsaturated alkenones, tetra-unsaturated ketones ($C_{37:4}$; Figure 3.1) are rare or absent outside of polar and sub-polar marine waters. Some studies from northern latitudes highlight an empirical relationship between the amount of $C_{37:4}$ and surface water salinity (e.g., Rosell-Melé, 1998; Rosell-Melé et al., 2002; Sicre et al., 2002; Harada et al., 2003; Blanz et al., 2005). Already, Rosell-Melé (1998) proposed that the relative abundance of the $C_{37:4}$ to the total C_{37} production ($C_{37:4}$ %; equation 3.4) could serve as an indicator of salinity at higher latitudes, whereas higher $C_{37:4}$ % values correspond to lower salinities of surface waters (e.g., Rosell-Melé, 1998; Sicre et al., 2002; Harada et al., 2003; Blanz et al., 2005). The proportion of tetra-unsaturated alkenones is expressed as:

$$C_{37:4}\,\% = (C_{37:4}/(C_{37:2}+C_{37:3}+C_{37:4}))*100 \qquad (3.4)$$

However, the application of $C_{37:4}$ % for reconstructing past salinities is controversially discussed (Sikes and Sicre, 2002). Several studies indicate that higher amounts of $C_{37:4}$ ketones are preferentially related to cold SSTs rather than simply being produced at higher rates in low salinity environments. According to Sikes and Sicre (2002), the observed correlation between $C_{37:4}$ % and salinity in the North Atlantic is probably an artefact of the strong link between low salinities and temperatures in these areas. Other studies, however, argue that the relative proportion of $C_{37:4}$ is a valid indicator for documenting qualitative changes in the influence of fresh water in surface waters in the North Atlantic and Pacific Ocean (Bendle et al., 2005; McClymont et al., 2008). For the Skagerrak, however, a coherence of changing pro-

portions of $C_{37:4}$ % in surface sediments and water samples related to salinity gradients has been observed (Schulz et al., 2000; Blanz et al., 2005).

3.2.3 Preparation technique and analysis

The total lipid extract containing the long-chained alkenones (C_{37}) was extracted from portions of freeze-dried and homogenized bulk sediment (~2-3 g) at the biomarker laboratory at the Christian Albrechts University of Kiel (Germany). Prior to extraction, the cells were loaded with cell-filling material (modified diatomaceous/Isolute HM-N, extraction grade and silicagel), and internal standards (1 µg of cholestane $C_{27}H_{48}$ and 0.5 µg of hexatriacontane $C_{36}H_{74}$) to quantify the organic compounds. Extraction proceeded with an Accelerated Solvent Extractor (Dionex^{TM} ASE-200) using a solvent mixture of 9:1 (v/v) of DCM:MeOH (dichloromethane:methanol) at 100°C and 100 bar N_2 pressure. After extraction, the samples were cooled to -20°C and subsequently taken to near dryness by vacuum rotary evaporation at 20°C and 65 mbar. The residues were dried over night and diluted using 100 µl hexane prior to injection.

The extracts were analysed using a multi-dimensional, double column gas chromatography setup (MD-GC) with two Agilent 6890 gas chromatographs (GC) for $C_{37:2}$, $C_{37:3}$, and $C_{37:4}$ identification and quantification (Etourneau et al., 2010). Both GCs have an independent oven and flame ionization detector (FID-1 and FID-2) connected via a transfer line. While the FID-1 operates as a monitor detector, only a small and pre-defined fraction, selectively cut from the first measurement (in the FID-1), reaches FID-2 (main detector), and consequently, the chromatogram recorded by the FID-2 only shows a few, pre-selected peaks. As the main detector only receives small portions from the monitor detector, both the memory effect and the level of contamination by co-eluates are reduced. It therefore has a much higher sensitivity than the monitor detector and allows a more precisely detection of the single alkenone chains. This technique using two running parallel GCs produces an accurate chromatography signal, even for very low alkenone signals (Etourneau et al., 2010), which is in particular crucial when determining the tetra-unsaturated C_{37} alkenone (Figure 3.1). The areas of $C_{37:2}$, $C_{37:3}$, and $C_{37:4}$ were graphically obtained from the main detector chromatograph and translated into concentrations using the internal standard added in each sample. The $U^{K'}_{37}$ index, SST, and $C_{37:4}$ % were calculated using equations 3.2 to 3.4.

Analytical precision based on duplicate analysis of internal laboratory sediment (Skagerrak) during the whole procedure was ±0.23 units of $C_{37:4}$ % and ±0.05 units of $U^{K'}_{37}$ that corresponds to ±0.12°C when using the calibration set of Müller et al. (1998) (equation 3.3).

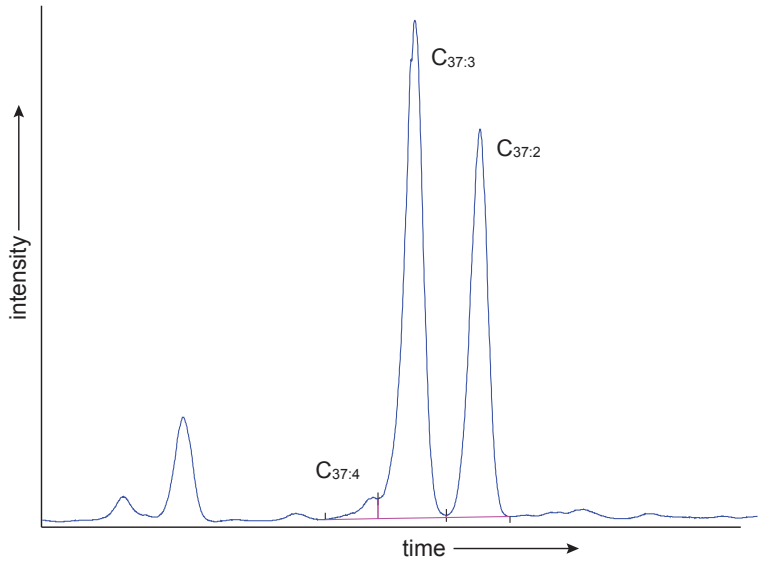

Fig. 3.1 Chromatogram from the main detector only showing a pre-defined fraction (Skagerrak sample). The $C_{37:4}$ ketone is left of the $C_{37:3}$ and is easily detectable in Skagerrak sediments when using this method (see text). When SST increases, the relative contribution of $C_{37:3}$ decreases and vice versa.

3.3 Glycerol dialkyl glycerol tetraethers

Glycerol dialkyl glycerol tetraethers (or GDGTs) are membrane lipids that are exclusively biosynthesized by Archaea. In addition, some Bacteria are thought to produce branched GDGTs (Weijers et al., 2006; Weijers et al., 2009; Sinninghe Damsté et al., 2011). These specific lipids were initially thought to be an adaption to harsh environments, as they are more stable than membrane lipids produced by other microorganisms. Over the past decade, however, studies have shown that GDGT-producing microorganisms are present and abundant in multiple realms of non-extreme environmental conditions (Schouten et al., 2013). These environments include i.e. the marine water column and sediments, peat and soils, lacustrine water columns and sediments and loess (e.g., Schouten et al., 2000; Sinninghe Damsté et al., 2000; Weijers et al., 2006; Peterse et al., 2009; Peterse et al., 2011; Tierney and Russell, 2009; Blaga et al., 2009; Tierney et al., 2010; Huguet et al., 2012). Detailed studies of the distribution and combination of specific GDGTs in different environments showed that they contain information on environmental conditions, such as i.e. seawater and air temperature, soil pH, and terrestrial soil input into marine environments (Schouten et al., 2002; Hopmans et al., 2004; Weijers et al., 2007).

3.3.1 TEX_{86} as a proxy for sea water temperature

Recently, the TEX_{86} index (TetraEther indeX with 86 carbon atoms, equation 3.5) was proposed as a proxy to infer past temperatures in marine settings (Schouten et al., 2002). It is

based on the relative abundance of isoprenoidal GDGTs, mainly biosynthesized by Thaumarchaeota that are abundant and present in many environmental settings, in particular the marine environment (e.g., Karner et al., 2001; Powers et al., 2004; Tierney et al., 2008; Blaga et al., 2009; Sinninghe Damsté et al., 2009). Since the introduction of the TEX_{86} index (equation 3.5) and temperature proxy, multiple studies have provided insight in understanding the paleo-thermometry (Kim et al., 2008; Kim et al., 2010; Kabel et al., 2012; Schouten et al., 2013). Recently, Kim et al. (2010) defined two novel TEX_{86} indices (equations 3.6 and 3.7) that are representative for ocean temperatures with modern mean annual SSTs ranging between 5-15ºC (TEX_{86}^{L} "low") and between 15-28ºC (TEX_{86}^{H} "high"), whereas both indices were highly correlated to mean annual SST (equations 3.8 and 3.9):

TEX_{86}=(GDGT-2+GDGT-3+Crenarchaeol-regio-isomer)/(GDGT-1+GDGT-2+GDGT-3+Crenarchaeol-regio-isomer)		Schouten et al. (2002)	(3.5)
TEX_{86}^{H}=log(TEX_{86})		Kim et al. (2010)	(3.6)
TEX_{86}^{L}=log(GDGT-2)/(GDGT-1+GDGT-2+GDGT-3)		Kim et al. (2010)	(3.7)
SST=64.8xTEX_{86}^{H}+38.6	(r^2=0.87, n=255)	Kim et al. (2010)	(3.8)
SST=67.5xTEX_{86}^{L}+46.9	(r^2=0.86, n=393)	Kim et al. (2010)	(3.9)

whereas the GDGT numbers refers to the isoprenoid GDGT structure (see Figure 3.2).

Recent studies have indicated that the temperature relationship proposed by Kim et al. (2010) might not be directly applicable in every setting and that a regional calibration including the TEX_{86}^{H} or TEX_{86}^{L} index is essential (Kabel et al., 2012; Schouten et al., 2013). Also, research has indicated that habitat depth of Thaumarchaeota is not restricted to the surface water but rather dwell in a range of water depths depending on location (Karner et al., 2001; Lincoln et al., 2014; Lopes dos Santos et al., 2010). In the North Sea, studies suggest that TEX_{86} most likely reflects winter temperatures rather than mean annual in the sub-surface waters (Herfort et al., 2006; Herfort et al., 2007; Wuchter et al., 2006; Bale et al., 2013). In contrast, in the Skagerrak area, Rueda et al. (2009) found best correlation to mean annual SST using surface and sub-surface sediments. However, this PhD project has indicated that this relationship to mean annual temperatures is probably not valid throughout the complete Holocene period in the Skagerrak (see chapter 7).

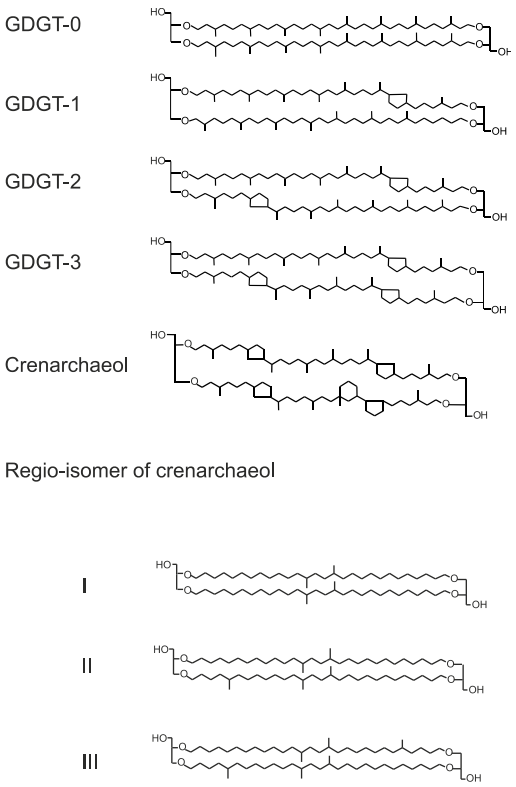

Fig. 3.2 Structure of isoprenoid GDGTs used in equations 3.5 to 3.9 and 3.19.

3.3.2 Branched GDGTs as a proxy for continental temperature using lake sediments

Branched glycerol dialkyl glycerol tetraethers (*br*GDGTs) are a variety of GDGTs presumably biosynthesized by bacteria (Weijers et al., 2006; Weijers et al., 2007; Sinninghe Damsté et al., 2011). *br*GDGTs are found worldwide in i.e. peat and soils, lacustrine water column and sediments (e.g., Sinninghe Damsté et al., 2000; Weijers et al., 2006; Blaga et al., 2009; Peterse et al., 2009; Tierney and Russell, 2009; Tierney et al., 2010). The *br*GDGT proxy is based on the idea that microorganisms that live in or near lakes produce a suite of *br*GDGTs, which reacts to changes in temperature (see review of Castaneda and Schouten, 2011). Consequently, the distribution of *br*GDGTs preserved in lake sediments provides a unique potential to infer past continental temperature changes. Originally, the proxy is based on the MBT (Methylation of Branched Tetraethers) and CBT (Cyclization of Branched Tetraethers) indices (equations 3.10 and 3.12). The CBT index correlates negatively to soil pH, whereas MBT primarily correlates positively with mean annual soil temperature that often equals mean annual air temperature (Weijers et al., 2007). The MBT/CBT calibrations are based on a dataset of globally distributed soil samples and correlated to mean annual air temperature (MAT; equation 3.13) and soil pH (Weijers et al., 2007). In 2012, Peterse et al. (2012) extended and re-calibrated the original MBT/CBT data set (equations 3.11 and 3.14):

MBT=(Ia+Ib+Ic)/(Ia+Ib+Ic+IIa+IIb+IIc+IIIa+IIIb+IIIc)	(Weijers et al., 2007)	(3.10)
MBT´=(Ia+Ib+Ic)/(Ia+Ib+Ic+IIa+IIb+IIIa)	(Peterse et al., 2012)	(3.11)
CBT=-log((Ib+IIb)/(Ia+IIa))	(Weijers et al., 2007)	(3.12)
MAT=(MBT-0.122-0.178xCBT)/0.020	(Weijers et al., 2007)	(3.13)
MAT=0.81-5.97xCBT+31.0xMBT´	(Peterse et al., 2012)	(3.14)

Since 2007, many studies have applied the *br*GDGT proxy to reconstruct both modern and past temperatures in lakes (e.g., Sinninghe Damsté et al., 2009; Tierney and Russell, 2009; Blaga et al., 2009; Blaga et al., 2010; Tierney et al., 2010; Zink et al., 2010; Loomis et al., 2011; Pearson et al., 2011). However, many studies argue that an in situ production of *br*GDGTs within the lake environment affects the reconstructed temperatures when using soil-based calibrations (Weijers et al., 2007; Peterse et al., 2012) (equations 3.13 and 3.14). Consequently, this led to alternative temperature equations developed for lake sediments (Tierney et al., 2010; Zink et al., 2010; Pearson et al., 2011) (equations 3.15 to 3.18). Equations 3.15 and 3.16 (MAT: mean annual air temperature and MST: mean summer temperature) include the MBT index, whereas equations 3.17 and 3.18 are based on the fractional abundance (*f*) of specific *br*GDGTs (roman numbers; Figure 3.3) that are most likely predominantly produced within the lake:

MAT=55.01xMBT-6.055	(Zink et al., 2010)	(3.15)
MST=49.658xMBT+0.207	(Zink et al., 2010)	(3.16)
MAT=50.47-74.18x*f*GDGTIIIa-31.60x*f*GDGTIIa-34.69x*f*GDGTIa	(Tierney et al., 2010)	(3.17)
MST=20.9+98.1x*f*GDGTIb-12.0x*f*GDGTIIa-20.5x*f*GDGTIIIa	(Pearson et al., 2011)	(3.18)

Hence, determining the dominant source of *br*GDGTs in the lake sediments is essential in order to decide which calibration equation (“aquatic vs. soil”) is most suitable for a given lake setting.

Nonetheless, recent studies have revealed the presence of structural isomers that partially co-elute with *br*GDGTs (De Jonge et al., 2013; 2014). Yet, however, it is unclear whether the isomers react differently to environmental factors. Consequently, it is possible that an improved chromatographic method applied on samples might reveal another temperature trend than the one estimated using the old method.

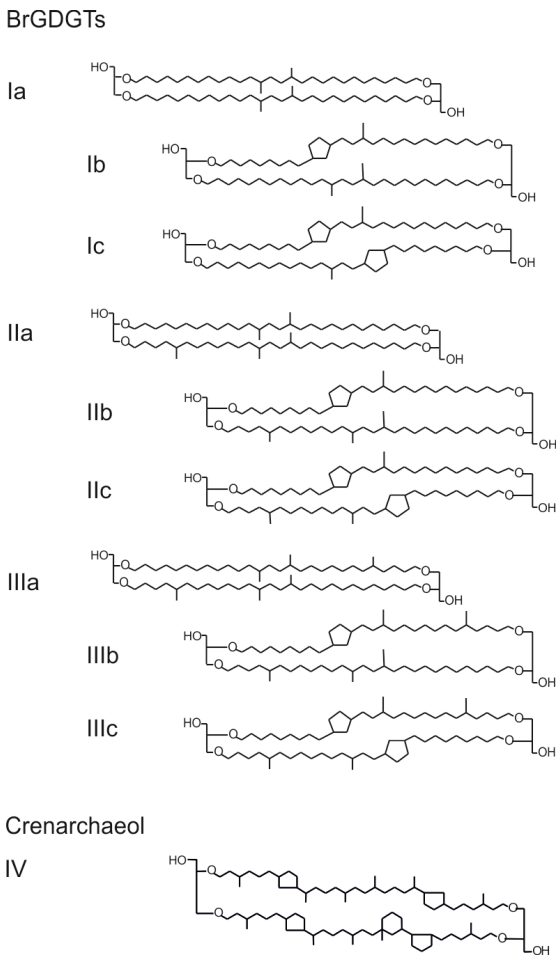

Fig. 3.3 Structure of branched GDGTs used in equations 3.10 to 3.18.

3.3.3 Preparation and analytical technique

GDGT samples were prepared and measured at the Department of Marine Biogeochemistry at the NIOZ (Royal Netherlands Institute for Sea research). 1 to 6 g of homogenized sediment were extracted by Dionex™ accelerated solvent extraction (Dionex™ ASE-200) using a solvent mixture of 9:1 (v/v) of dichloromethane:methanol (DCM:MeOH) at 100°C and at 100 bar N_2 pressure. The total lipid extracts (TLEs) were evaporated and subsequently dried under a pure N_2 flow. Thereupon, the TLEs were fractionated on activated Al_2O_3 columns using 9:1 (v/v) hexane:DCM, 1:1 (v/v) hexane:DCM and 1:1 (v/v) DCM:MeOH as solvents to yield the apolar, ketone, and polar fraction. Prior to the analysis, the polar fraction containing the GDGTs was concentrated under a pure N_2 flow, dissolved ultrasonically in 99:1 (v/v) hexane:isopropanol, and filtered through a 0.45 µm syringe filter. In each sample, an internal standard was added to subsequently determine the concentration of each GDGT compound.

The GDGTs were analysed using an Agilent 1100 series high performance liquid chromatography atmospheric pressure chemical ionisation/mass spectrometry (HPLC-APCI/MS) instrument equipped with automated injector and HP-Chemstation software

(Hopmans et al., 2000; Weijers et al., 2006; Weijers et al., 2007; Schouten et al., 2007). Peak areas of the single *br*GDGT compounds were determined by manual integration using the HP Chemstation software package. The isoprenoidal and branched GDGT indices were calculated according to equations 3.5 to 3.19 (see also Figure 3.2 and 3.3).

Analytical precision based on duplicate analyses of samples during the whole procedure was on average 0.004 units of TEX_{86}^{H} that corresponds to an averaged error of 0.29ºC when using the calibration of Kim et al. (2010).

The BIT index ("Branched vs. Isoprenoid Tetraethers") was also calculated in order to determine the potential influence of soil material in the lake samples (Hopmans et al., 2004):

BIT=(Ia+IIa+IIIa)/(Ia+IIa+IIIa+crenarchaeol) (Hopmans et al., 2004) (6.19)

3.4 Stable hydrogen and carbon isotopes on *n*-alkanes

Alkanes are hydrocarbons consisting of only hydrogen and carbon atoms linked by single bonds (saturated molecules). Long-chained *n*-alkanes (linear structure) with 21 to 37 carbon atoms in the molecule backbone (C_{21} – C_{37}) are major components in the epicuticular waxes of higher terrestrial plants that act as protection from water loss and physical damage (Eglinton and Hamilton, 1967). In contrast, shorter-chained *n*-alkanes are dominant in aquatic algae (Giger et al., 1980; Cranwell et al., 1987) and the mid-chained *n*-alkanes are common in submerged aquatic macrophytes (Ficken et al., 2000). *n*-alkanes are found in modern and fossil plant leafs, in soils/paleo-soils, and fluvial, lacustrine and marine sediments (see review of Castaneda and Schouten, 2011). In paleoecology and paleoclimatology, i.e. stable isotopic signatures ($\delta^{13}C$ and δD) and chain length of specific *n*-alkanes are often used for paleoenvironmental and vegetation type reconstructions.

3.4.1 Stable hydrogen isotopes

Variations in the relative abundance of stable hydrogen isotopes (δD), hydrogen (H) and deuterium (D), in precipitation is related to changes in the hydrological cycle and governed by condensation temperature, source and amount of precipitation, elevation, and distance from the ocean (Craig, 1961; Dansgaard, 1964; Gat, 1996). Stable hydrogen isotope compositions (δD) of specific molecules, as i.e. long-chain *n*-alkanes derived from terrestrial plant leaf waxes, are increasingly used to infer past changes in precipitation δD values as δD of plant leaf waxes reflects the δD of their primary hydrogen source (Huang et al., 2002; 2004; Sachse et al., 2004; Sachse et al., 2012). *n*-alkanes are biosynthesized within the leaf wax, and many studies show that the δD values are additionally governed by factors as plant life form (as tree, shrub, grasses), evapotranspiration from soil and leaf water, and different pho-

tosynthetic pathways (see review by Sachse et al., 2012). Stable hydrogen isotope compositions, mostly based on terrestrial plant *n*-alkanes with 29 carbon atoms (δD_{C29}), derived from surface lake sediments along a climatic gradient show strong positive correlation to mean annual precipitation δD values (e.g. Sachse et al., 2004; Huang et al., 2004). However, an offset between lipid and source water δD depending on plant life form (trees, shrubs, grasses), suggests that both climatic and biological factors differently modulated the δD_{C29} values.

3.4.2 Stable carbon isotopes

The stable carbon isotopic composition ($\delta^{13}C$) of long-chained *n*-alkanes (or other individual biomarker compounds) present in terrestrial plant leafs can vary based on different photosynthetic pathways used by the specific vegetation type. Plants that follow the C_3 pathway (Calvin-Benson) normally have an average isotopic composition of around -34.7‰ for the C_{29} n-alkane and -35.2‰ for the C_{31} *n*-alkane, while plants that utilize the C_4 carbon-fixation pathway (Hatch-Slack) are isotopically enriched (-21.4‰ for C_{29} and -21.7‰ for C_{31}) (Castaneda and Schouten, 2011). Therefore the isotopic signal ($\delta^{13}C$) of plant leaf waxes can be applied in reconstructing changes in vegetation type that is in turn related to altering environmental parameters, such as temperature, precipitation, and atmospherically carbon dioxide concentration (e.g. Castañeda and Schouten, 2011). Recently, research has shown that changes in photosynthetic pathway may alter δD values of *n*-alkanes (Wang et al., 2013) that is also the case in Lake Belau samples (see chapter 8).

3.4.3 Preparation and analytical technique

The *n*-alkane extraction and preparation were performed at the biomarker laboratory at the University of Kiel. The TLEs (Total Lipid Extracts), obtained at the Department of Marine Biogeochemistry at the NIOZ (Royal Netherlands Institute for Sea research) during *br*GDGT extraction was used to obtain the suite of n-alkanes (C_{27}, C_{29}, and C_{31}). Subsequently, elemental sulphur was removed by rotating the extract with activated copper beads in DCM under vacuum for ~30 minutes. The apolar fraction that compromises the suite of *n*-alkanes was achieved via fractionation on activated Al_2O_3 columns using 9:1 (v/v) hexane:DCM. Thereupon, the samples were measured on an Agilent 6890 N Gas Chromatograph (GC) with a Flame Ionization Detector in the biomarker laboratory at the University of Kiel to obtain concentration of each *n*-alkane compound. Quantification and identification of each specific *n*-alkane compound were conducted using a laboratory internal standard (comprehending a series of *n*-alkane mixtures).

The samples were analysed for stable carbon ($\delta^{13}C$) and hydrogen (δD) isotopic composition on a Thermo Finnigan GC combustion III unit (for $\delta^{13}C$) or High Temperature Conversion system (for δD) connected to a Thermo Fisher MAT253 mass spectrometer at the Leibniz laboratory at the University of Kiel. The method is fully described in Wang et al. (2013). δD is expressed in per mill relative to the VSMOW scale is $\delta^{13}C$ relative to the VPDB scale, established by using Arndt Schimmelmann´s stable isotope A2 reference mixture from 2009. The accuracy and precision of the system were determined daily by measuring an in-house mixture of nC_{28} to nC_{36} alkanes between samples; these mixtures had an average standard error of the mean (SEM) of 0.7‰ per day (n=7-8) for δD and 0.1‰ per day for $\delta^{13}C$ (n=5). For the samples, SEM values for nC_{27}, nC_{29}, nC_{31} were ≤0.9‰ per sample for δD (n=5-6) and ≤0.1‰ per sample for $\delta^{13}C$ (n=3).

3.5 Chronology

3.5.1 Skagerrak multi-cores

In this study, the Skagerrak multi-cores were dated using the AMS^{14}C method (Table 3.2). The radiocarbon dates were not converted into calendar years, as preliminary results from ^{210}Pb and ^{137}Cs measurements indicate that the standard 400 years marine reservoir age correction might not be applicable on sub-surface sediment in the Skagerrak (M. Moros pers. communication). However, the radiocarbon dates of several multi-cores indicated a “modern age” (“post bomb”) of surface and subsurface sediments (Table 3.2). Therefore, the uppermost sediment samples were used to discuss the near-modern $U^{K'}_{37}$-SST and spatial distribution of $C_{37:4}$ % in the Skagerrak.

3.5.2 Skagerrak and Kattegat gravity-cores

The Skagerrak and Kattegat gravity-cores used in this PhD project were dated using the AMS^{14}C method (Table 3.3). In order to compare with published results in the Skagerrak area (Jiang et al., 1998; Gyllencreutz, 2005; Gyllencreutz and Kissel, 2006; Erbs-Hansen et al., 2012), all radiocarbon ages were converted into calendar years (cal. yr BP) using the online software Calib Rev 7.0 with the Marine13 data set (Reimer et al., 2013), thereby applying the standard marine reservoir age of 400 years (Reimer et al., 2013). Age-depth models were established using interpolations between each calibrated radiocarbon age.

The age-depth models of gravity-cores IOW372610 and IOW372650 from the western and northeastern Skagerrak, respectively, are quite robust and consist of 13 and 14 radiocarbon dates.

Gravity-core IOW225514 was previously dated by Emeis et al. (2003) and re-calibrated for this PhD study.

In order to compare the $C_{37:4}$ % and TEX_{86}^{H} results from gravity-core IOW242940-4 (see chapters 4 and 7), a new chronology had to be established. For this purpose, the radiocarbon dated age-depth tie-points from the parallel core IOW242940-3 were applied for exactly the same depths in IOW242940-4 and converted into calendar years (see above). To further constrain the age-depth model for core IOW242940-4, log Ti/Ca records from XRF scanner measurements (C. Butruille, unpublished data) were compared to its counterpart from the well-dated gravity-core IOW225517 (Emeis et al., 2003; C. Butruille, unpublished data) at the same location (see chapter 7). An overall good relationship between the log Ti/Ca results of both cores was found, even though the matching between both cores could be improved by aligning common small-scale features in the XRF records. For this PhD study, however, the direct transfer of radiocarbon ages between the parallel cores IOW242940-3 and IOW242940-4 was sufficient since mainly the long-term trends were discussed.

The Kattegat gravity-cores (IOW318180 and IOW242970) consist of 5 and 11 radiocarbon dates (Table 3.3).

3.5.3 Mecklenburg Bay gravity-cores

The gravity-cores from the Skagerrak/Kattegat were compared with two grain-size records from the Mecklenburg Bay (MB409/91 and IOW257760). The upper 300 cm of core MB409/91 covers the last ~7900 cal. yr BP (Moros, 1998) and the upper 184 cm of core IOW257760 covers the last 6900 cal. yr BP (Rößler et al., 2011) (Table 3.3).

3.5.4 Lake Belau composite sequence and chronology

Both the stratigraphic connection and revised chronology is fully discussed in Dörfler et al. (2012) and will only be summarised in the following sub-chapter.

The Lake Belau sedimentary sequence was recovered from ~28 m water depth in 2002 and covered almost the complete Holocene period. The sediment core consisted of several combined segments from four parallel cores retrieved at the same location, whereas each segment was ~2 m in length. The segments were inter-connected by the identification of several specific markers (i.e. tephra layers) that were evident in several parallel segments of same age. Consequently, the composite sedimentary sequence consisted of sections of multiple segments from four different parallel cores with a total length of ~24 m (Dörfler et al., 2012).

A revised chronology based on varve counts (preserved during the early to late Holocene until ca. 1630 cal. yr BP and from AD1945 until AD2002), radiocarbon dates, and tephra analysis was recently established on the composite sedimentary sequence (Dörfler et al., 2012). The radiocarbon ages were converted into calibrated years (cal. yr BP) using OxCal 4.1, and varves and tephra layers were used to re-fine the age model (Dörfler et al., 2012).

Tab. 3.2 Age determination of each multi-core used in this PhD thesis. Radiocarbon ages were not calibrated (see text). Per cent modern (pMC) is reported when pMC values are larger than 100 pMC.

Sample (cm)	Dated material	Age (^{14}C yr BP)	Lab Ref.	C (mg)
	372610 (57°41.05´N, 06°41.00´E)			
0-2	Mixed benthic foraminifera	10±30	Poz-32521	0.41
19-21	Mixed benthic foraminifera	350±30	Poz-32962	0.5
42-44	Mixed benthic foraminifera	710±30	Poz-32522	0.61
	242940 (57°40.52´N, 07°10.00´E)			
0-1	Mixed benthic foraminifera	90±30	-	-
35-36	Mixed benthic foraminifera	895±30	-	-
	372620 (57°40.06´N, 07°05.36´E)			
0-2	Mixed benthic foraminifera	30±35	Poz-32523	0.39
	372630 (57°40.55´N, 07°09.97´E)			
0-1.5	Mixed benthic foraminifera	295±35	Poz-32525	0.4
10-12	Mixed benthic foraminifera	685±35	Poz-32960	-
	372650 (58°29.76´N, 09°35.91´E)			
0-1	Mixed benthic foraminifera	104.13±0.38 pMC	Poz-32530	0.48
10-11	Mixed benthic foraminifera	135±35	Poz-36311	0.35
15-16	Mixed benthic foraminifera	610±25	KIA 42424	0.6
25-26	Mixed benthic foraminifera	715±25	KIA42425	0.7
		372660 (58°44.01´N, 10°11.96´E)		
0-2	Mixed benthic foraminifera	101.82±0.39 pMC	Poz-32532	0.36
20-21	Mixed benthic foraminifera	600±35	Poz-36308	0.3
33-35	Mixed benthic foraminifera	1030±40	Poz-32533	0.52

Tab. 3.3 Age determination of each gravity-core used in this PhD study. Radiocarbon ages were calibrated (cal. yr BP) using the Calib Rev. 7.0 software program and the Marine13 calibration set (Reimer et al., 2013) with an assumed standard marine reservoir age of 400 years (see text). Omitted radiocarbon ages are in italics.

Sample depth (cm)	Dated material	Age (^{14}C yr BP)	Calibrated age min – max (1σ range, cal. yr BP)	Calibrated age med. (1σ range, cal. yr BP)	Lab Ref.	C (mg)
Skagerrak GC 372610 (57°41.05´N, 06°41.00´E)						
2-3	Mixed benthic foraminifera	715±25	314 - 397	359	KIA42411	0.7
20	Mixed benthic foraminifera	745±35	333 - 432	386	Poz-34467	0.42
55-56	Mixed benthic foraminifera	940±25	504 - 556	536	KIA42412	0.5
73-74	Mixed benthic foraminifera	1140±50	647 - 731	693	LuS 9540	1.07
100	Mixed benthic foraminifera	1510±40	1003 - 1123	1064	Poz-34553	0.37
124-125	Mixed benthic foraminifera	1960±50	1438 - 1577	1514	LuS 9539	0.53
155-156	Mixed benthic foraminifera	2385±25	1966 - 2060	2014	KIA 42413	1.0
174-175	Mixed benthic foraminifera	2550±50	2161 - 2292	2221	LuS 9538	0.78
200	Mixed benthic foraminifera	2710±30	2344 - 2444	2404	Poz-34468	0.67
255-256	Mixed benthic foraminifera	3195+35/-30	2935/2941 – 3055/3050	2995/2994	KIA 42414	0.8
300	Mixed benthic foraminifera	3820±40	3705 - 3826	3768	Poz-34554	0.5
354-356	Mixed benthic foraminifera	4530±35	4693 - 4807	4738	KIA 42415	0.6
424-426	Mixed benthic foraminifera	5505±35	5851 - 5933	5891	KIA 42416	0.5
Skagerrak GC 242940-3 (57°40.52´N, 07°10.00´E)						
0	Mixed benthic foraminifera	830 ± 30	445 - 494	468	KIA 18309	1.2
14.5	Mixed benthic foraminifera	1840±90	1297 - 1482	1395	Poz-45813	0.2
32	Mixed benthic foraminifera	2565±30	2195 - 2298	2240	KIA 18598	0.7
49.5	Mixed benthic foraminifera	2820±80	2468 - 2690	2561	Poz-45814	0.3
70	Mixed benthic foraminifera	3405±30	3232 - 3326	3277	KIA 18599	0.8
103.5	Mixed benthic foraminifera	4650±35	4822 - 4909	4871	KIA 18310	1.1
117.5	Mixed benthic foraminifera	4855±35	5113 - 5251	5163	KIA 18600	1.1
160	Mixed benthic foraminifera	5845±40	6213 - 6297	6263	KIA 18601	0.9
200	Mixed benthic foraminifera	6590±40	6787-6935	6865	KIA 18311	-
240	Mixed benthic foraminifera	7380±45	7590-7682	7644	KIA 18602	-
290	Mixed benthic foraminifera	8265±40	8467-8575	8520	KIA 18312	-
324	Mixed benthic foraminifera	9125±50	9516-9640	9583	KIA 18313	-
361	Mixed benthic foraminifera	*9890±55*	*10499-10593*	*10550*	*KIA 18314*	-
380	Mixed benthic foraminifera	9295±45	9719-9913	9830	KIA 18315	-
388	Shell	9810±50	10427-10538	10479	Poz-8187	-
412.5	Shell	10200±50	10909-11110	10985	Poz-8186	-

Sample depth (cm)	Dated material	Age (^{14}C yr BP)	Calibrated age min – max (1σ range, cal. yr BP)	Calibrated age med. (1σ range, cal. yr BP)	Lab Ref.	C (mg)
468	Shell	10800±50	11746-11969	11882	Poz-8183	-
478	Mixed benthic foraminifera	11200±55	12400-12455	12529	KIA 18316	-
Skagerrak GC 225514 (Emeis et al., 2003; 57°50.28´N, 08°42.226´E)						
10.5	Mixed benthic foraminifera	810±30	429 - 483	454	KIA 14028	-
105.5	Mixed benthic foraminifera	1780±35	1284 - 1353	1323	KIA 14029	-
135.5	Mixed benthic foraminifera	2710±35	2342 - 2451	2407	KIA 14031	-
155.5	Mixed benthic foraminifera	2755±45	2368 - 2545	2481	KIA 14033	-
250.5	Mixed benthic foraminifera	4280±45	4337 - 4480	4397	KIA 14034	-
310.5	Mixed benthic foraminifera	6400±45	6810 - 6939	6876	KIA 14035	-
Skagerrak GC 372650 (58°29.76´N, 09°35.91´E)						
24-26	Mixed benthic foraminifera	900±50	472 - 547	513	Poz-34465	0.26
55-57	Mixed benthic foraminifera	1200±25	699 - 767	736	KIA 42417	0.6
105-107	Mixed benthic foraminifera	1655±30	1186 - 1255	1222	KIA 42418	0.6
155-157	Mixed benthic foraminifera	2155±30	1703 - 1796	1749	KIA 42419	0.5
199-201	Mixed benthic foraminifera	2620±50	2240 - 2356	2303	Poz-34551	0.23
223-225	Mixed benthic foraminifera	2985±50	2713 - 2806	2762	LuS 9537	0.82
244-246	Mixed benthic foraminifera	3150±50	2855 - 3003	2935	Poz- 44174	0.6
255-257	Mixed benthic foraminifera	3470±35	3308 - 3404	3352	KIA 42420	0.5
273-275	Mixed benthic foraminifera	*3155±70*	*2847 - 3040*	*2946*	*LuS 9536*	*0.36*
284-286	Mixed benthic foraminifera	3760±50	3619 - 3770	3695	Poz-44175	0.2
299-301	Mixed benthic foraminifera	*3660±50*	*3492 - 3630*	*3566*	*KIA 42421*	*0.7*
323-325	Mixed benthic foraminifera	4230±90	4186 - 4440	4324	LuS 9535	0.27
355-357	Mixed benthic foraminifera	4945±35	5234 - 5325	5289	KIA 42422	0.6
415-417	Foraminifera	5880+40/-35	6256-6346	6298	KIA 42423	0.4
427-430	Foraminifera	6730±50	7202-7314	7261	Poz-44176	0.3
499-501	Foraminifera	10260±70	11161-11338	11261	Poz-34466	0.34
Kattegat GC 242970 (56°43.58´N, 11°49.80´E)						
18-19	Mollucs shells	765±20	384 - 456	416	KIA 29456	0.9
48-49	Mollucs shells	2605±25	2267 - 2334	2295	KIA 29454	1.1
68-69	Mollucs shells	2920±25	2691 - 2733	2711	KIA 29453	0.9
211	Mollucs shells	3590±25	3443 - 3529	3484	KIA 29451	0.7
531	Mollucs shells	6785±35	7266 - 7355	7313	KIA 29450	1.1
Kattegat GC 318180 (56°43.58´N, 11°49.42´E)						

Sample depth (cm)	**Dated material**	**Age (^{14}C yr BP)**	**Calibrated age min – max (1σ range, cal. yr BP)**	**Calibrated age med. (1σ range, cal. yr BP)**	**Lab Ref.**	**C (mg)**
8-9	*Turitella* shell	475±30	45 - 124	83	Poz-17915	-
29-30	*Arctica islandica*	1170±30	673 - 736	711	Poz-17916	-
61-62	*Turitella* shell	1565±35	1072 - 1172	1126	Poz-17908	-
111-112	*Turitella* shell	2650±35	2294 - 2377	2337	Poz-17909	-
146	Mixed benthic foraminifera	3390±40	3206 - 3321	3259	Poz-20727	0.32
180	Mixed benthic foraminifera	3665±35	3520 - 3628	3573	Poz-20728	-
214-215	*Turitella* shell	3850±35	3747 - 3868	3808	Poz-17912	-
270	Mixed benthic foraminifera	4680±40	4843 - 4947	4904	Poz-20729	-
315	Mixed benthic foraminifera	5890±50	6262 - 6367	6309	Poz-20731	-
375	Mixed benthic foraminifera	6120±40	6493 - 6608	6550	Poz-20732	-
424-425	Mollusc shells	6510±50	6948 - 7099	7022	Poz-17913	-
Mecklenburg Bay GC 257760 (Rößler *et al.* 2011; 54°22.54´N, 11°38.08´E)						
184	*Arctica islandica*	6440±35			KIA21604	-

4 Late Holocene Baltic Sea outflow changes reconstructed using $C_{37:4}$ content from marine cores

This chapter corresponds to the following manuscript published in Boreas: V. R. Krossa, M. Moros, T. Blanz, E. Jansen, and R. Schneider: Late Holocene Baltic Sea outflow changes reconstructed using $C_{37:4}$ content from marine cores, Boreas 2014

This study was written as a part of the co-operation to the BONUS EU+ "INFLOW" project. The first author has written the manuscript. The $C_{37:4}$ % measurements were done at the University of Kiel (Biomarker Laboratory) by the first author in cooperation with Thomas Blanz. Matthias Moros (Institute of Warnemünde, Rostock) provided the Kattegat and Mecklenburg Bay grain-size records. Ralph Schneider and Matthias Moros supervised the work. Eystein Jansen (Bjerknes Centre for Climate Research in Bergen, Norway) improved the manuscript before submission in February 2014.

4.1 Abstract

The Baltic Sea is an intra-continental brackish water body. Low saline surface water, the so-called Baltic outflow current, exits the Baltic Sea through the Kattegat into the Skagerrak. Ingressions of saline oxygen-rich bottom water enter the Baltic Sea basins via the narrow and shallow Kattegat and are of great importance for the ecological and ventilation state of the Baltic Sea. Over the past decades, progress has been made in studying Holocene changes in saline water inflow. However, reconstructions of past variations in Baltic Sea outflow changes are sparse and hampered due to the lack of suitable proxies. Here, we use the relative proportion of tetra-unsaturated C_{37} ketones ($C_{37:4}$ %) in long-chain alkenones produced by coccolithophorids as a proxy for outflowing Baltic Sea water in the Skagerrak. To evaluate the applicability of the proxy, we compare the biomarker results with grain-size records from the Kattegat and Mecklenburg Bay in addition to previously published salinity-reconstructions from the Kattegat over the last 5000 years. All Skagerrak records show an increase of $C_{37:4}$ % that is accompanied by enhanced bottom water currents in the Kattegat and western Baltic Sea over the past 3500 cal. yr BP, indicating an increase in Baltic Sea outflow. This likely reflects higher precipitation in the Baltic Sea catchment area due to a reorganization of North Atlantic atmospheric circulation with an increased influence of wintertime Westerlies over the Baltic catchment from the mid- to the late Holocene.

4.2 Introduction

The Baltic Sea is a semi-enclosed marginal sea located in a humid climatic zone in northern Europe and one of the largest brackish seas worldwide. At present, the Baltic Sea is connected to the North Atlantic Ocean via the Skagerrak through the narrow and shallow channels in the Kattegat and the Danish Straits, thus having strongly restricted water exchange with the open North Sea and North Atlantic Ocean (Figure 4.1). As a consequence of the fresh water surplus and the strongly limited water exchange with the open ocean, the Baltic Sea has an estuarine circulation pattern, characterized by outflowing low-salinity surface water and inflow of saline bottom water (Figure 4.1).

Based on oceanographic and meteorological observations, the inflow of saline bottom water that reaches the Baltic Sea has been intensively studied and described over the last decades (e.g., Matthäus and Schinke, 1999; Matthäus and Schinke, 1994; Schinke and Matthaus, 1998). Additionally, several studies have focused on ecological, physical, and biogeochemical consequences of enhanced inflows or the lack of such in the Baltic Sea in both modern and past settings (Conley et al., 2009; Kabel et al., 2012). So far, however, there are no high-resolution proxy-reconstructions for past variability of outflow beyond instrumental records due to the absence of suitable proxy methods. On the other hand, modelling studies provide insight into variations in freshwater supply and the consequent response of the Baltic Sea in terms of changes in water exchange dynamics and freshwater balance (Winsor et al., 2001; Gustafsson and Westman, 2002; Meier and Kauker, 2003). Model simulations suggest that an increase of the net freshwater supply to the Baltic Sea causes enhanced surface water outflow and a decrease of bottom water inflow in the Kattegat area (e.g., Stigebrandt, 1983; Stigebrandt and Gustafsson, 2003), supported by observations for the Kattegat area (Matthäus and Schinke, 1999). Simulations for past climatic conditions in the Baltic Sea also indicate a strong sensitivity to fresh water supply (e.g., Stigebrandt, 1983; Gustafsson and Westman, 2002; Meier and Kauker, 2003; Stigebrandt and Gustafsson, 2003). Gustafsson and Westman (2002) found close connections between variations in salinity and climate change throughout the last 8500 years. To verify such simulations of past changes by models, it is important to obtain empirical data of outflow variability and trends.

Until now, reconstructions of past Baltic Sea outflow changes have been hampered by a lack of suitable proxies that can be applied on sediments archives. In the Skagerrak, we attempt to use the relative proportion of tetra-unsaturated C_{37} ketones ($C_{37:4}$ alkenones) as a proxy for late Holocene outflow variability of Baltic Sea surface water. Alkenones are a series of long-chained unsaturated ketones that are biosynthesized mainly by the cosmopolitan coccolithophorids Emiliania huxleyi and Gephyrocapsa oceanica. The proportion of di-unsaturated ($C_{37:2}$) to tri-unsaturated ($C_{37:3}$) C_{37} alkenones (expressed as the $U^{K`}_{37}$ index) shows a linear correlation to algal growth temperature (Prahl and Wakeham, 1987; Prahl et

al., 1988; Conte et al., 1998). This relationship allows for the successful reconstruction of past sea surface temperatures (SST) in many marine settings (e.g., Brassell et al., 1986; Prahl and Wakeham, 1987; Conte and Eglinton, 1993; Müller et al., 1998; Sicre et al., 2002; Ternois et al., 1997). In contrast to the di- and tri-unsaturated alkenones, $C_{37:4}$ is rare or absent outside of polar and sub-polar waters. Some studies from northern latitudes highlight an empirical relationship between the amount of $C_{37:4}$ and surface water salinity (Rosell-Melé, 1998; Rosell-Melé et al., 2002; Sicre et al., 2002; Harada et al., 2003). However, the application of $C_{37:4}$ % for reconstructing past salinities is still controversially discussed (e.g., Sikes and Sicre, 2002). Several studies indicate that higher amounts of tetra-unsaturated C_{37} ketones are preferentially related to cold SSTs rather than simply being produced at higher rates in low salinity environments. According to Sikes and Sicre (2002), the observed correlation between $C_{37:4}$ % and salinity in the North Atlantic is probably an artefact of the strong link between salinity and temperature in these areas. Other studies, however, argue that the relative proportion of $C_{37:4}$ is a valid indicator for documenting qualitative changes in the influence of freshwater in surface waters in the North Atlantic and Pacific Ocean (Bendle et al., 2005; McClymont et al., 2008). In addition, in our study area, a coherence of changing proportions of $C_{37:4}$ % in surface sediment and water samples related to salinity gradients has been observed (Schulz et al., 2000; Blanz et al., 2005). Therefore, we regard the $C_{37:4}$ % signal derived from Skagerrak sediment cores characteristic for a specific, lower salinity water mass, rather than quantifying salinity units. In the following text we refer to “higher amounts of $C_{37:4}$ %” as being an indicator for low-salinity environments and vice versa, while recognizing that there is a complexity of $C_{37:4}$ % that hampers its utility as a pure signal of salinity.

To evaluate the significance of $C_{37:4}$ % as an indicator of Baltic Sea outflow, we will compare $C_{37:4}$ % records from the Skagerrak with grain-size records from the Kattegat and Mecklenburg Bay (southwestern Baltic Sea) that indicates bottom water current intensity. In addition, we will compare our results with previously published diatom-inferred salinity proxy-data from a gravity-core located east of Skagen (Figure 4.1) (Jiang et al., 1998).

4.3 Skagerrak and Baltic Sea freshwater budget

The Skagerrak is part of the epicontinental North Sea and is regarded as a transition area between the North Sea/North Atlantic and the Baltic Sea (Figure 4.1). In the northwest, the Skagerrak has a shape of a fjord (Thiede, 1987) and exceeds maximum depths of more than 700 m (Rodhe, 1987), while to the southeast the water depth is generally less than 150 m.

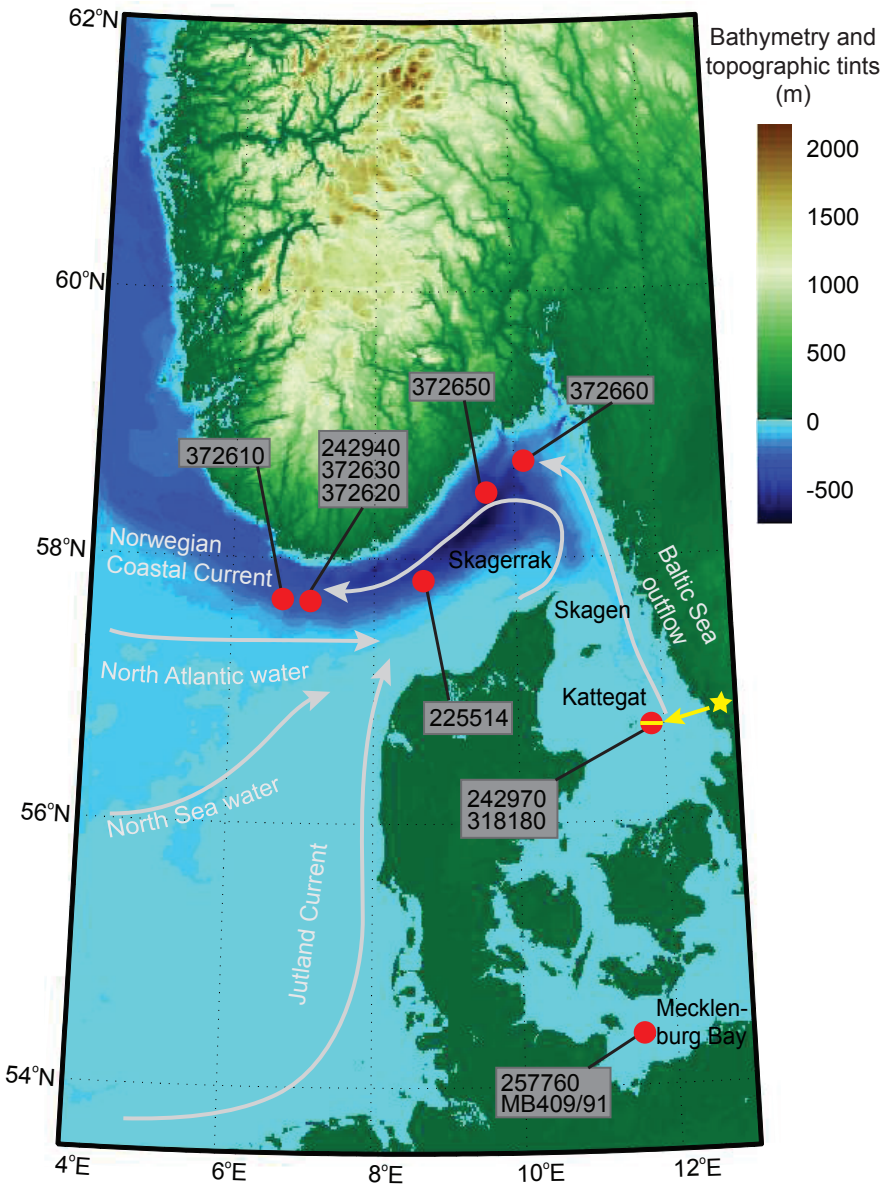

Fig. 4.1 Core locations in the Skagerrak, Kattegat and Mecklenburg Bay (core numbers in grey boxes, see Table 4.1). Pale grey arrow shows present-day mean surface currents in the Skagerrak and Kattegat. Yellow star indicates location of seismo-acoustic profile shown in Figure 4.5C. The bathymetric and topographical lines are from IOC et al. (2003).

The modern surface circulation pattern in the Skagerrak is mainly governed by large-scale coupled atmospheric and oceanic circulation systems, river runoff and brackish water discharges from the Baltic Sea (Svansson, 1975; Rodhe, 1987; 1988; Otto et al., 1990) (Figure 4.1). In general, circulation is marked by the inflow of saline water from the North Sea and North Atlantic and outflow of less saline water from the Baltic Sea. North Atlantic Water (35 psu) enters the Skagerrak from the west and north. Flowing along the northern part of the Danish west coast, it mixes with fresher southern North Sea water forming the North Jutland Current (NJC). East of Skagen (northern tip of Denmark, Figure 4.1) the NJC mixes with out-

flowing low-salinity Baltic Sea surface water. In the northeast Skagerrak, the water mass turns anti-clockwise, leading to a reduction of current speed, and allowing fine-grained sediment to accumulate at high rates (Rodhe and Holt, 1996; van Weering, 1982). The mixed surface water mass flows along the entire Norwegian coastline as the Norwegian Coastal Current (NCC) (Figure 4.1).

The Baltic Sea water that flows into the Skagerrak causes a low-salinity environment in the Danish Straits and the Kattegat towards the Skagerrak (e.g., Danielssen et al., 1997). It forms a brackish surface water layer with salinity increasing from about 20 psu in the southern Kattegat to around 28-30 psu at the Skagerrak border (e.g., Blanz et al., 2005). As a consequence of the positive freshwater balance due to river runoff and net precipitation, quantities of outflowing Baltic Sea water are generally larger than volumes of inflowing waters. On a long-term average, the difference between outflowing and inflowing water volumes equals the freshwater surplus (Stigebrandt and Gustafsson, 2003). At present day, the average annual river runoff into the Baltic Sea is around 428 km^3 yr^{-1} (Matthäus and Schinke, 1999). On an annual average, a water volume of roughly 950 km^3 yr^{-1} flows out of the Baltic Sea and is compensated by the inflow of about 470 km^3 yr^{-1} (Lindkvist et al., 2003).

Tab. 4.1 Location and water depth of each multi- and gravity-core used in this study (see also Figure 4.1).

Core number	Latitude	Longitude	Water depth (m)	Cruise/Year
IOW372610 GC/MUC	57°41.05´N	06°41.00´E	320	R/V Maria S Merian MSM12/4, 2009
IOW372620 MUC	57°40.06´N	07°05.36´E	315	R/V Maria S Merian MSM12/4, 2009
IOW372630 MUC	57°40.55´N	07°09.97´E	330	R/V Maria S Merian MSM12/4, 2009
IOW242940 GC	57°40.52´N	07°10.00´E	316	R/V Poseidon 282, 2002
IOW225514 GC	57°50.28´N	08°42.226´E	420	R/V Alkor, 2000
IOW372650 GC/MUC	58°29.76´N	09°35.91´E	550	R/V Maria S Merian MSM12/4, 2009
IOW372660 MUC	58°44.01´N	10°11.96´E	227	R/V Maria S Merian MSM12/4, 2009
IOW318180 GC	56°43.58´N	11°49.42´E	43	R/V Maria S Merian MSM 01/02, 2006
IOW242970 GC	56°43.58´N	11°49.80´E	46	R/V Poseidon 282/ 2002
IOW257760 GC	54°22.54´N	11°38.08´E	24	R/V Humboldt 1994
MB409/91 GC	54°22.54´N	11°33.00´E	24.5	R/V Humboldt 1991

4.4 Material and methods

Five multi-cores and four gravity-cores located on a west-central-northeast transect in the Skagerrak (Figure 4.1, Table 4.1) were used to document the distribution of $C_{37:4}$ % (relative amounts of $C_{37:4}$ from the total sum of C_{37} ketones) in surface and subsurface sediments and to reconstruct late Holocene changes in Baltic Sea outflow using the $C_{37:4}$ % relationship, respectively. The cores were retrieved during the cruises of R/V “Alkor” in 2000, R/V “Posei-

don" in 2002 and R/V "Maria S. Merian" MSM cruise 12/4 in September 2009 (Table 4.1). We analyzed grain-size distribution of bulk samples in four gravity-cores from the Kattegat and the Mecklenburg Bay, respectively (Figure 4.1, Table 4.1), in order to reconstruct late Holocene changes in bottom water dynamics. These cores were retrieved during the cruises of R/V "Maria S. Merian MSM" in 2006, R/V "Poseidon" in 2002, R/V "Humboldt" in 1991 and 1994 (Table 4.1).

4.4.1 Relative abundance of $C_{37:4}$

Long-chained alkenones (C_{37}) were extracted from portions of homogenized bulk sediment (approximately 2 to 3 g) using an Accelerated Solvent Extractor (Dionex ASE-200) with a mixture of 9:1 (v/v) of dichloromethane:methanol (DCM:MeOH) at 100°C and 100 bar N_2 (g) pressure each for 20 minutes at the University of Kiel. Extracts were cooled to approx. -20°C and subsequently taken to near dryness by vacuum rotary evaporation at 20°C and 65 mbar. We use a multi-dimensional, double gas column chromatography (MD-GC) set up with two Agilent 6890 gas chromatographs for $C_{37:2}$, $C_{37:3}$, and $C_{37:4}$ identification and quantification, which is described in Etourneau et al. (2010). Quantification of the organic compounds was achieved with the addition of an internal standard prior to extraction (cholestane ($C_{37}H_{48}$) and hexatriacontane ($C_{36}H_{74}$)). The proportion of each alkenone compound was obtained using the peak areas of the specific compounds. The proportion of the $C_{37:4}$ compound in the total amount of C_{37} ketones in one sample is expressed as $C_{37:4}$ %:

$$C_{37:4}\ \% = (C_{37:4} / (C_{37:4} + C_{37:3} + C_{37:2})) \times 100 \qquad (4.1)$$

Analytical precision based on duplicate analyses of internal laboratory sediment during the whole procedure was 0.30 units of $C_{37:4}$.

4.4.2 Grain size (sand content)

The relative weight percentage (wt. %) of sand fractions (63 µm – 2 mm) was determined by wet sieving of bulk sediment samples at the Institute of Warnemünde (IOW), Rostock/Germany. We did not perform any pretreatment of the bulk samples, as the carbonate content is very low.

4.4.3 Chronostratigraphy

The multi-cores in the Skagerrak and gravity-cores in the Skagerrak and Kattegat, respectively, were dated using the AMS ^{14}C method (Tables 4.2 and 4.3). We did not convert

the multi-core radiocarbon dates into calendar years, as ongoing studies on the Skagerrak multi-core chronology indicate that a standard marine reservoir age of 400 years might not be applicable (M. Moros). However, the radiocarbon dates of the several multi-cores indicate a “modern age” (“post bomb”) of surface and sub-surface sediments (Table 4.3), thus allowing a discussion on the spatial distribution of $C_{37:4}$ % in the Skagerrak area (Figure 4.3). However, the Skagerrak and Kattegat gravity-core chronologies presented in this study are based on radiocarbon ages that were converted into calendar years (cal. yr BP) applying the standard marine reservoir age of 400 years (Reimer et al., 2013), using the online software Calib Rev 7.0 with the Marine13 data set (Reimer et al., 2013) (Table 4.2). The application of the standard marine reservoir age on our gravity-cores allows direct comparison with previously published observations in the Skagerrak area (Jiang et al., 1998; Gyllencreutz and Kissel, 2006; Erbs-Hansen et al., 2012) that also applied a 400-year reservoir age. The age-depth models were established using linear interpolation between each calibrated radiocarbon ages (Figure 4.2).

Tab. 4.2 Age determination of each multi-core used in this study. Radiocarbon ages were not calibrated (see text). Per cent modern carbon (pMC) is reported when pMC values are larger than 100 pMC.

Sample (cm)	Dated material	Age (^{14}C yr BP)	Lab. Ref.	C (mg)
	MUC 372610 (57°41.05´N, 06°41.00´E, 320 m water depth)			
0-2	Mixed benthic foraminifera	10±30	Poz-32521	0.41
19-21	Mixed benthic foraminifera	350±30	Poz-32962	0.5
42-44	Mixed benthic foraminifera	710±30	Poz-32522	0.61
	MUC 372620 (57°40.06´N, 07°05.36´E, 315 m water depth)			
0-2	Mixed benthic foraminifera	30±35	Poz-32523	0.39
	MUC 372630 (57°40.55´N, 07°09.97´E, 330 m water depth)			
0-1.5	Mixed benthic foraminifera	295±35	Poz-32525	0.4
10-12	Mixed benthic foraminifera	685±35	Poz-32960	-
	MUC 372650 (58°29.76´N, 09°35.91´E, 550 m water depth)			
0-1	Mixed benthic foraminifera	104.13±0.38 pMC	Poz-32530	0.48
10-11	Mixed benthic foraminifera	135±35	Poz-36311	0.35
15-16	Mixed benthic foraminifera	610±25	KIA 42424	0.6
25-26	Mixed benthic foraminifera	715±25	KIA42425	0.7
	MUC 372660 (58°44.01´N, 10°11.96´E, 227 m water depth)			
0-2	Mixed benthic foraminifera	101.82±0.39 pMC	Poz-32532	0.36
20-21	Mixed benthic foraminifera	600±35	Poz-36308	0.3
33-35	Mixed benthic foraminifera	1030±40	Poz-32533	0.52

Records from the Skagerrak / Kattegat will be compared with grain-size records from two Mecklenburg Bay gravity cores, MB409/91 and IOW257760. The upper 300 cm of core MB409/91 covers the last approx. 7900 years (Moros, 1998) and the upper 184 cm of core IOW257760 covers the last 6900 cal. yr BP (Rößler et al., 2011) (Table 4.2).

Tab. 4.3 Age determination of each gravity-core used in this study (see also Figure 4.2). Radiocarbon ages were calibrated (cal. yr BP) using the Calib Rev 7.0 software program and the Marine13 calibration set (Reimer et al., 2013) with an assumed standard marine reservoir age of 400 years. Omitted radiocarbon ages are in italics.

Sample (cm)	Dated material	Age (^{14}C yr BP)	Calibrated age min – max (1σ range, cal. yr BP)	Calibrated age med. (1σ range, cal. yr BP)	Lab Ref.	C (mg)
Skagerrak GC 372610 (57°41.05´N, 06°41.00´E)						
2-3	Mixed benthic foraminifera	715±25	314 - 397	359	KIA42411	0.7
20	Mixed benthic foraminifera	745±35	333 - 432	386	Poz-34467	0.42
55-56	Mixed benthic foraminifera	940±25	504 - 556	536	KIA42412	0.5
73-74	Mixed benthic foraminifera	1140±50	647 - 731	693	LuS 9540	1.07
100	Mixed benthic foraminifera	1510±40	1003 - 1123	1064	Poz-34553	0.37
124-125	Mixed benthic foraminifera	1960±50	1438 - 1577	1514	LuS 9539	0.53
155-156	Mixed benthic foraminifera	2385±25	1966 - 2060	2014	KIA 42413	1.0
174-175	Mixed benthic foraminifera	2550±50	2161 - 2292	2221	LuS 9538	0.78
200	Mixed benthic foraminifera	2710±30	2344 - 2444	2404	Poz-34468	0.67
255-256	Mixed benthic foraminifera	3195+35/-30	2935/2941 - 3055/3050	2995/2994	KIA 42414	0.8
300	Mixed benthic foraminifera	3820±40	3705 - 3826	3768	Poz-34554	0.5
354-356	Mixed benthic foraminifera	4530±35	4693 - 4807	4738	KIA 42415	0.6
424-426	Mixed benthic foraminifera	5505±35	5851 - 5933	5891	KIA 42416	0.5
Skagerrak GC 242940-3 (57°40.52´N, 07°10.00´E)						
0	Mixed benthic foraminifera	830 ± 30	445 - 494	468	KIA 18309	1.2
14.5	Mixed benthic foraminifera	1840±90	1297 - 1482	1395	Poz-45813	0.2
32	Mixed benthic foraminifera	2565±30	2195 - 2298	2240	KIA 18598	0.7
49.5	Mixed benthic foraminifera	2820±80	2468 - 2690	2561	Poz-45814	0.3
70	Mixed benthic foraminifera	3405±30	3232 - 3326	3277	KIA 18599	0.8
103.5	Mixed benthic foraminifera	4650±35	4822 - 4909	4871	KIA 18310	1.1
117.5	Mixed benthic foraminifera	4855±35	5113 - 5251	5163	KIA 18600	1.1
160	Mixed benthic foraminifera	5845±40	6213 - 6297	6263	KIA 18601	0.9
Skagerrak GC 225514 (Emeis et al., 2003; 57°50.28´N, 08°42.226´E)						
10.5	Mixed benthic foraminifera	810±30	429 - 483	454	KIA 14028	
105.5	Mixed benthic foraminifera	1780±35	1284 - 1353	1323	KIA 14029	-
135.5	Mixed benthic foraminifera	2710±35	2342 - 2451	2407	KIA 14031	-

Sample (cm)	Dated material	Age (^{14}C yr BP)	Calibrated age min – max (1σ range, cal. yr BP)	Calibrated age med. (1σ range, cal. yr BP)	Lab Ref.	C (mg)
155.5	Mixed benthic foraminifera	2755±45	2368 - 2545	2481	KIA 14033	-
250.5	Mixed benthic foraminifera	4280±45	4337 - 4480	4397	KIA 14034	-
310.5	Mixed benthic foraminifera	6400±45	6810 - 6939	6876	KIA 14035	-
		Skagerrak GC 372650 (58°29.76´N, 09°35.91´E)				
24-26	Mixed benthic foraminifera	900±50	472 - 547	513	Poz-34465	0.26
55-57	Mixed benthic foraminifera	1200±25	699 - 767	736	KIA 42417	0.6
105-107	Mixed benthic foraminifera	1655±30	1186 - 1255	1222	KIA 42418	0.6
155-157	Mixed benthic foraminifera	2155±30	1703 - 1796	1749	KIA 42419	0.5
199-201	Mixed benthic foraminifera	2620±50	2240 - 2356	2303	Poz-34551	0.23
223-225	Mixed benthic foraminifera	2985±50	2713 - 2806	2762	LuS 9537	0.82
244-246	Mixed benthic foraminifera	3150±50	2855 - 3003	2935	Poz-44174	0.6
255-257	Mixed benthic foraminifera	3470±35	3308 - 3404	3352	KIA 42420	0.5
273-275	*Mixed benthic foraminifera*	*3155±70*	*2847 - 3040*	*2946*	*LuS 9536*	*0.36*
284-286	Mixed benthic foraminifera	3760±50	3619 - 3770	3695	Poz-44175	0.2
299-301	*Mixed benthic foraminifera*	*3660±50*	*3492 - 3630*	*3566*	*KIA 42421*	*0.7*
323-325	Mixed benthic foraminifera	4230±90	4186 - 4440	4324	LuS 9535	0.27
355-357	Mixed benthic foraminifera	4945±35	5234 - 5325	5289	KIA 42422	0.6
		Kattegat GC 242970 (56°43.58´N, 11°49.80´E)				
18-19	Mollucs shells	765±20	384 - 456	416	KIA 29456	0.9
48-49	Mollucs shells	2605±25	2267 - 2334	2295	KIA 29454	1.1
68-69	Mollucs shells	2920±25	2691 - 2733	2711	KIA 29453	0.9
211	Mollucs shells	3590±25	3443 - 3529	3484	KIA 29451	0.7
531	Mollucs shells	6785±35	7266 - 7355	7313	KIA 29450	1.1
		Kattegat GC 318180 (56°43.58´N, 11°49.42´E)				
8-9	*Turitella* shell	475±30	45 - 124	83	Poz-17915	
29-30	*Arctica islandica*	1170±30	673 - 736	711	Poz-17916	
61-62	*Turitella* shell	1565±35	1072 - 1172	1126	Poz-17908	
111-112	*Turitella* shell	2650±35	2294 - 2377	2337	Poz-17909	
146	Mixed benthic foraminifera	3390±40	3206 - 3321	3259	Poz-20727	0.32
180	Mixed benthic foraminifera	3665±35	3520 - 3628	3573	Poz-20728	
214-215	*Turitella* shell	3850±35	3747 - 3868	3808	Poz-17912	
270	Mixed benthic foraminifera	4680±40	4843 - 4947	4904	Poz-20729	
315	Mixed benthic foraminifera	5890±50	6262 - 6367	6309	Poz-20731	

Sample (cm)	Dated material	Age (^{14}C yr BP)	Calibrated age min – max (1σ range, cal. yr BP)	Calibrated age med. (1σ range, cal. yr BP)	Lab Ref.	C (mg)
375	Mixed benthic foraminifera	6120±40	6493 - 6608	6550	Poz-20732	
424-425	Mollusc shells	6510±50	6948 - 7099	7022	Poz-17913	
Mecklenburg Bay GC 257760 (Rößler et al., 2011; 54°22.54´N, 11°38.08´E)						
184	*Arctica islandica*	6440±35			KIA21604	

4.5 Results

4.5.1 Distribution of $C_{37:4}$ relative to the sum of C_{37} alkenones in the Skagerrak

Modern sea surface salinity data gradually decrease from 33 psu in the western Skagerrak to approximately 30-28 psu at the Skagerrak/Kattegat border (Blanz et al., 2005) and 24 psu in the Kattegat. In the multi-core records, which span the last millennium, minima in the relative abundance of $C_{37:4}$ ($C_{37:4}$ %) are found in the westernmost part of the Skagerrak, while maxima are detected in the northeast Skagerrak (Figure 4.3). Values of $C_{37:4}$ % gradually increase from the west towards the northeast Skagerrak close to the Kattegat and the Baltic Sea.

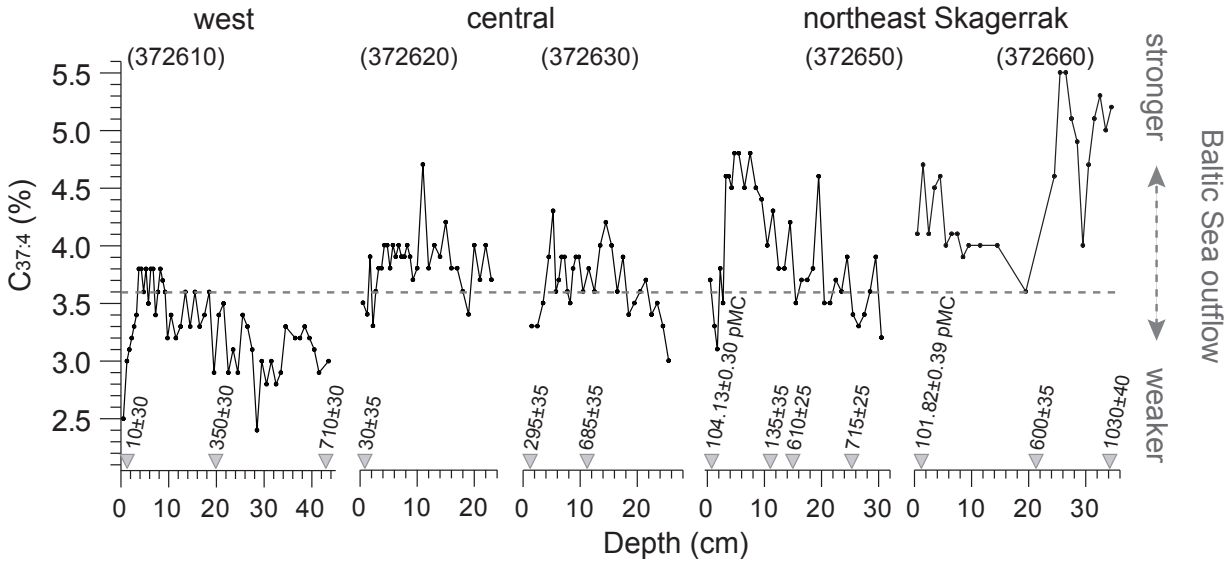

Fig. 4.2 The near-surface multi-core records showing a decrease of $C_{37:4}$ % from the northeastern towards the western Skagerrak, indicating a progressively decreasing contribution of Baltic Sea outflow from the Skagerrak/Kattegat border towards the North Atlantic. Grey horizontal dashed line shows average of all samples (3.6% $C_{37:4}$). Grey triangles indicate ^{14}C ages in the individual multi-cores, with pMC values reported only if >100 pMC.

All gravity-cores display a steady increase of $C_{37:4}$ % over the last ~3500 cal. a BP. As observed in the multi-core records, generally higher values of $C_{37:4}$ % are found in the north-east in contrast to the westernmost Skagerrak, thus also displaying a progressive decrease of $C_{37:4}$ % from locations adjacent to the Baltic Sea towards sites closer to the North Atlantic Ocean/North Sea (Figure 4.4), which supports a Baltic source for the higher $C_{37:4}$ % (see below).

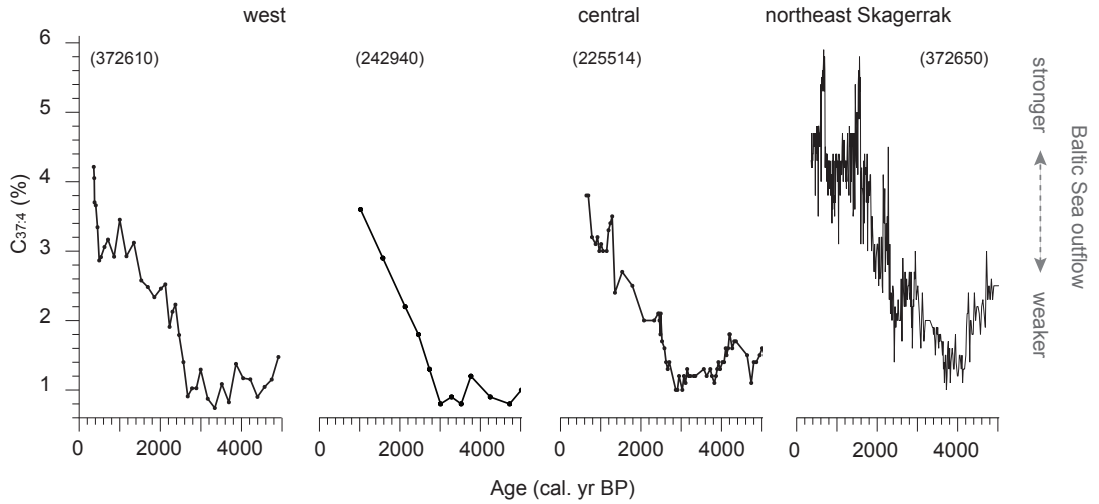

Fig. 4.3 A significant increase of $C_{37:4}$ % starting at ~3500 to 3000 cal. yr BP observed in four gravity-cores on a west-northeast transect, suggesting an increasing influence of Baltic Sea outflow in the Skagerrak during the late Holocene.

4.5.2 Grain-size distribution in the Kattegat and Mecklenburg Bay

Following a period of low percentages of sand (>63 µm; <20 wt. %), lithogenic grain-size records from the Kattegat (gravity-cores IOW242970 and IOW318180; Figure 4.1) are marked by a prominent increase in the sand fraction starting at ~3500 cal. a BP. In both records, the percentages of sand rapidly increase, reaching maximum values (>80 wt. %) during the last ~500 years (Figure 4.5A). In tandem with the increase in sand content, core IOW242970, which is located closer to the eastern channel margin than core IOW 318180 (Figure 4.5C), indicates a significant decrease in sedimentation rate (Figure 4.2), consistent with sediment winnowing. Reduced sediment accumulation is also evident from erosional discordances in mid- to late Holocene seismoacoustic reflection lines in the eastern part of the Kattegat channel (Figures 4.1 and 4.5C).

In the Mecklenburg Bay, the gravity-cores show an increase in the lithogenic sand fraction (maximum values around 15 – 30 wt. %) that is less prominent than the increase observed in the cores from the Kattegat. The increase starts in depths of around 100 cm, which corresponds to an approximate age of 3900 cal. yr BP (Figure 4.5B).

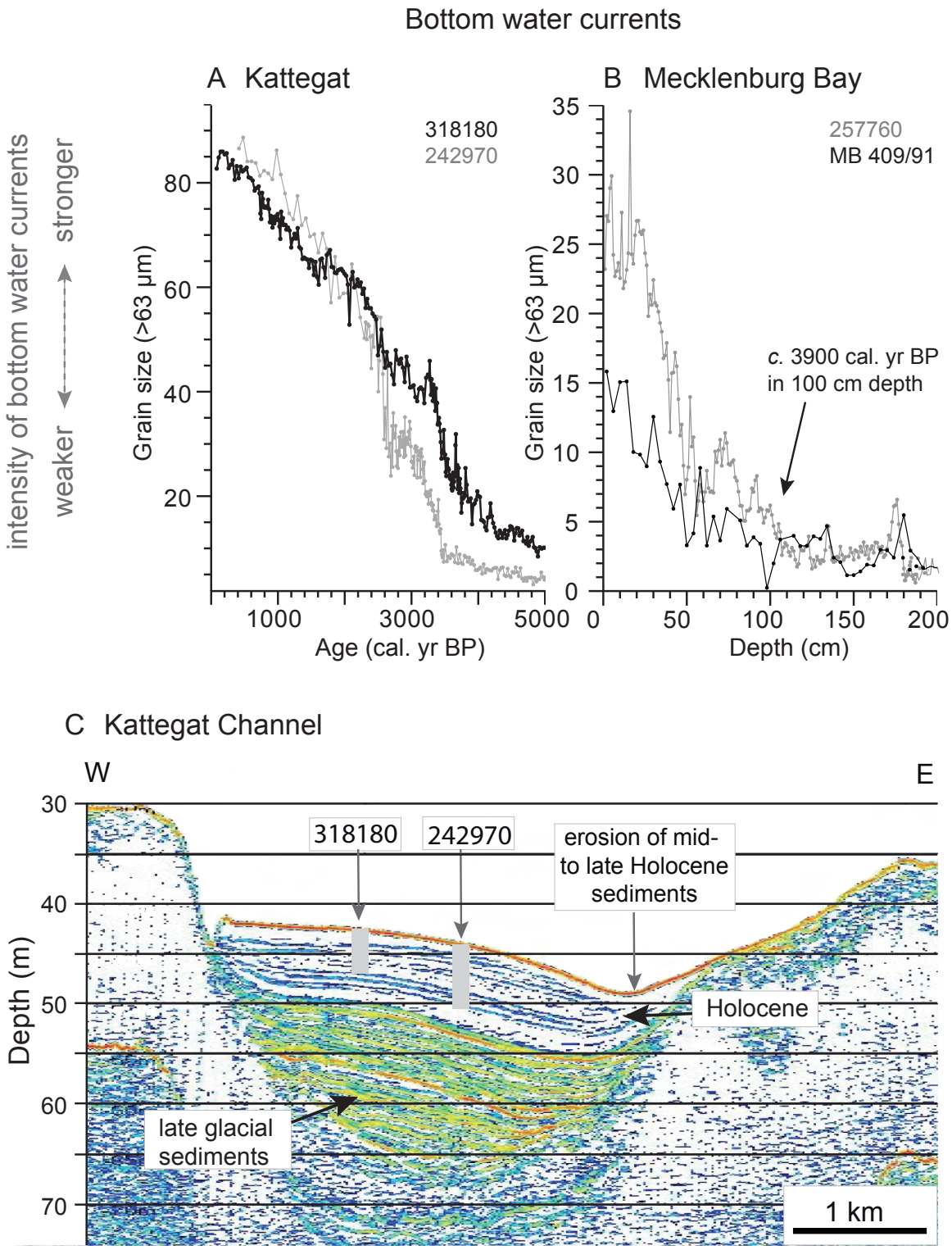

Fig. 4.4 An increase in sand particles (>63 µm) in gravity-core records from the Kattegat (A) and from the Mecklenburg Bay (B) at ~3500–3900 cal. yr BP suggesting strengthening in bottom water currents related to changes in water exchange between the Baltic Sea and the Skagerrak. C. High-resolution sub-bottom profile recorded during the RV 'Maria S. Merian' cruise MSM01/02 in 2006, using the parametric sediment echosounder system SES2000deep, INNOMAR Technology GmbH (see cruise report by Harff, 2006). The seismic reflector lines (blue and orange colours) indicate density changes between sedimentary successions, whereas the shift from orange to blue reflector lines represents a shift from harder to softer sediment successions. Based on radiocarbon dating on two sediment cores located on the seismo-acoustic profile (IOW242970 and IOW318180), we interpret that the lower sediment succession in the channel (orange reflector lines) represents late glacial sediments and the upper sediment succession (blue reflector lines) consists of Holocene deposits. At the eastern channel margin, mid- to late Holocene reflector lines are truncated, indicating erosion associated with increased bottom water currents in the Kattegat channel, presumably related to strengthening of the Baltic Sea outflow.

4.6 Discussion

4.6.1 Late Holocene variations in grain-size distribution in the Kattegat and Mecklenburg Bay

Changes in bottom water current dynamics can significantly affect sediment grain-size distribution (e.g., McCave et al., 1995). Accordingly, a strengthening in bottom water currents leads to an increase in the proportion of coarser sediments by winnowing of fine particles, and reducing overall sediment accumulation. In both Kattegat records, a significant rise in the sand fraction is documented at ~3500 cal. yr BP (Figure 4.5A) that presumably corresponds to the increase observed in both Mecklenburg Bay records starting at ~3900 cal. yr BP (Moros 1998; Rößler et al., 2011) (Figure 4.5B). The temporal discrepancy is likely due to the different quality of the age controls in the Kattegat and Mecklenburg Bay records (Table 4.2). However, the upward-coarsening trend documented in all gravity cores during the late Holocene, indicates an overall strengthening in bottom water currents presumably caused by changes in the water exchange dynamics between the Baltic Sea and North Sea.

In tandem with the increase in sand fraction, core IOW242970 located close to the eastern margin of the Kattegat channel (Figure 4.5C) indicates a significant decrease in sediment accumulation rate (Figure 4.2) presumably caused by erosion and winnowing. Supportingly, seismo-acoustic data on a west-east profile in the Kattegat channel (Figure 4.1) indicate intensified erosion at the eastern channel margin, as reflected in erosional discordancy of mid- and late Holocene reflector lines (Figure 4.5C). At the Northern Hemisphere, northwards directed currents are refracted towards the east due to Coriolis force. Therefore, the seismo-acoustic features observed at the eastern channel margin in addition to the pronounced decrease in sedimentation rate during the late Holocene in core IOW242970 hints to an increase in outflow rather than inflow. Although a weakening of inflow during periods of strong outflow is contradictory to a general estuarine circulation scheme, several model studies suggest that strong outflow reduces the occurrence of strong inflow into the Baltic Sea (Stigebrandt, 1983; Stigebrandt and Gustafsson, 2003) by lowering its salinity due to entrainment of low-salinity waters into the bottom water (Matthäus and Schinke, 1999). Also, the rather shallow sills in the south-western Baltic Sea hamper the inflow of bottom water. Therefore, large outflowing water volumes in the Kattegat can also cause a strengthening of the bottom water currents, the latter then affecting sediment deposition as apparent from Figure 4.5A-C. Yet, however, the relationship between outflowing and inflowing water masses in the Kattegat is not fully understood. To disentangle these processes in past settings, further studies are required to compare proxy results of both outflow and inflow.

4.6.2 $C_{37:4}$ % as an indicator for spatio-temporal changes in low-salinity Baltic Sea surface water contribution in the Skagerrak

Our core-top samples (upper 5 cm of each multi-core) reveal a gradual increase of $C_{37:4}$ % towards the Kattegat (Figure 4.3), mirroring the surface salinity gradient in the modern Skagerrak. Consequently, an occurrence of higher percentages of $C_{37:4}$ (approx. 5%) in multi-cores (cores 372650 and 372660; Figures 4.1 and 4.3) closer to the Kattegat implies that these records show higher contribution of less saline water, presumably originating from the Baltic Sea (see discussion below). In contrast, in the central and west Skagerrak multi-core records, lower $C_{37:4}$ % values (approx. 2.5%) and likely lower variability of $C_{37:4}$ %, reflect overall decreasing contributions of Baltic Sea water, regionally co-occurring with an increasing dominance of the saline North Atlantic water mass (Figure 4.3). This implies that the $C_{37:4}$ % can be used to characterize and track specific water masses (Bendle et al., 2005; Blanz et al., 2005). Combined multi- and gravity-cores (Figures 4.3 and 4.4) used in this study confirm coherent late Holocene and modern variations in $C_{37:4}$ %. This indicates that the spatial gradient of $C_{37:4}$ % from the northeast to the western Skagerrak observed in the core-top samples is also valid on a longer time scale, and that our interpretation of the $C_{37:4}$ % signal is applicable to older sediments in the Skagerrak. As apparent from Figure 4.4, this implies a more or less continuous increase in Baltic Sea outflow over the last 3500-3000 cal. yr BP. However, former studies suggest that selective biodegradation of ketones with higher number of double bounds can potentially bias the proportion of $C_{37:4}$ relative to the other ketone compounds (e.g., Gong and Hollander, 1999) and influence the unsaturation ratios (e.g., Gong and Hollander, 1999; Rontani et al., 2005; Rontani et al., 2008; Zabeti et al., 2010). To rule out that preferential degradation of tetra-unsaturated ketones over time is the principal factor causing the late Holocene trend in our gravity-core records (Figure 4.4), we applied two different approaches using the best-dated gravity-cores IOW372610 and IOW372650 (Figures 4.1 and 4.2; Table 4.2). First, we calculated the rate of change in $C_{37:4}$ to the sum of all ketones ($C_{37:4}$ %) back in time using intervals of 500 years and subsequently comparing the corresponding 500-year intervals between each core. Secondly, we compared the sedimentation rates to the rate of $C_{37:4}$ % change within each 500-year interval. Thereby we assumed that periods of lower sedimentation rates must show higher rates of (potential) preferential degradation in comparison to periods of higher sedimentation rates. Our calculations show that the gravity-cores do not indicate the same rate of $C_{37:4}$ % change downcore, on the contrary, the rate of change within each comparable 500-year interval is diverging. In addition, there is no coherence between lower/higher sedimentation rate and stronger/weaker decrease of $C_{37:4}$ % back in time. Therefore, we infer that the observed trends over the last 3500 cal. yr BP in our Skagerrak records reflect an increasing contribution of Baltic Sea out-

flow rather than being an artefact of selective degradation of tetra-unsaturated ketones downcore.

In consequence, all four Skagerrak gravity-cores studied suggest an increasing influence of the less saline Baltic Sea surface water mass starting at ~3500 cal. yr BP in the northeast and at ~2800 cal. yr BP in the western Skagerrak (Figure 4.4). Consistent with the increase of $C_{37:4}$ % observed in all Skagerrak records, grain-size records from the Kattegat/Mecklenburg Bay indicate a significant upward-coarsening trend (Figure 4.5A-B) in addition to reduced sediment accumulation and increased sand deposition at the eastern margin of the Kattegat channel (Figure 4.5C). As previously discussed, our grain-size and seismo-acoustic data hint to intensified outflow during the past 3500 cal. yr BP, although, we cannot completely rule out that the strengthening in bottom water currents could also be caused by enhanced inflow. The coherence in timing of the increase in $C_{37:4}$ % and the upward-coarsening trend documented by two independent proxies in the Skagerrak and Kattegat/Mecklenburg Bay, respectively, strongly suggests that the same signal, in our interpretation mainly the outflow, is documented by the two independent proxies.

Previous microfossil studies from gravity-cores at the Skagerrak/Kattegat border and in the northeast Skagerrak corroborate an increase of Baltic Sea outflow during the late Holocene (Jiang et al., 1998; Erbs-Hansen et al., 2012). Based on the occurrence of marine versus fresh water diatom assemblages, Jiang et al. (1998) report generally decreasing surface water salinity east of Skagen (Figure 4.1) over the last ~3000 cal. yr BP, likely related to enhanced outflow of Baltic Sea surface water. Also, Gustafsson and Westman (2002) suggest a reduction of salinity in the Baltic Sea over the past 5500 cal. yr BP. For the northeast Skagerrak, Erbs-Hansen et al. (2012) suggest enhanced productivity starting at ~3800 cal. yr BP as reflected in increased Total Organic Carbon (TOC), stable C/N ratio, and benthic foraminiferal flux. Potentially, the increase in productivity can be related to an intensified outflow of nutrient-rich Baltic Sea surface water (Danielssen et al., 1997) that may result in enhanced plankton blooms in the Skagerrak. Furthermore, based on magnetic properties of sediments from a gravity-core in the northeastern Skagerrak, Gyllencreutz and Kissel (2006) suggest a stronger contribution of Baltic Sea water and/or riverine input from the west coast of Sweden and south coast of Norway between 4000 and 1500 cal. yr BP that matches with the observed increase in $C_{37:4}$ % (Figure 4.4). During the last millennium, the influence of the North Atlantic water increased accompanied with reduced Baltic Sea water contribution (Gyllencreutz and Kissel, 2006) that is also indicated by a flattening of the $C_{37:4}$ % record in the northeast Skagerrak during the last 1500 cal. yr BP (Figure 4.4).

4.6.3 Possible causes of an enhanced Baltic Sea outflow during the late Holocene

The increase in $C_{37:4}$ % observed in the Skagerrak (Figure 4.4), increase in sand content (Figure 4.5A-B) and reduced sediment accumulation (Figure 4.5C) in the Kattegat/Mecklenburg Bay suggest intensified Baltic Sea outflow into the Skagerrak over the past ~3500 cal. yr BP (Figure 4.6B-C). This trend, supported by previous studies in the Skagerrak indicating reduced surface water salinity (Jiang et al., 1998) and increased contribution of Baltic Sea water until ~1500 cal. yr BP (Gyllencreutz, 2005; Gyllencreutz and Kissel, 2006; Erbs-Hansen et al., 2012), was accompanied by a general reduction in salinity in the Baltic Sea over the late Holocene (Gustafsson and Westman, 2002). Model and observational studies suggest that increased runoff strongly impacts the dynamics of water exchange processes between the Skagerrak and Baltic Sea. Thereby, intensification of the net outflow occurs, that, contradictory to an estuarine circulation pattern, likely hampers inflow of oceanic saline waters (Stigebrandt, 1983; Schinke and Matthaus, 1998; Matthäus and Schinke, 1999; Winsor et al., 2001; Gustafsson and Westman, 2002; Meier and Kauker, 2003). Enhanced runoff in the catchment area is presumably caused by increased precipitation and reduced evaporation associated with cool and moist climate conditions. Such climate conditions have been suggested for the late Holocene in the North Atlantic and northwestern Europe, including marine and terrestrial cooling (e.g., Davis et al., 2003; Moros et al., 2004; Bjune et al., 2005; Seppä et al., 2009), increased precipitation (Hammarlund et al., 2003; Bjune et al., 2005; Bakke et al., 2008; Heikkila et al., 2010), and re-advancing glaciers in southern Norway (Nesje et al., 2001; Bakke et al., 2008). Supportingly, raised lake levels during the late Holocene recorded in southern Sweden (e.g., Digerfeldt, 1988; Hammarlund et al., 2003) (Figure 4.6C) and reduced salinity in the Baltic Sea (Gustafsson and Westman, 2002) suggest colder and moister climate conditions and reduced evaporation. The shift to cooler and more moist climate conditions from the mid- to the late Holocene was presumably reinforced by a general re-organization of North Atlantic atmospheric circulation with an increased influence of wintertime Westerlies over northwestern Europe and the Baltic region (Hurrell, 1995; Hurrell et al., 2003). An enhanced influence of wintertime Westerlies would provoke milder temperatures causing less evaporation and also increased precipitation that in turn would cause intensified Baltic Sea outflow as also suggested by other studies (Zorita and Laine, 2000; Gustafsson and Westman, 2002). These paleo-climate reconstructions and model studies corroborate our conclusion that the increase in $C_{37:4}$ % and sand content in the Skagerrak and Kattegat/Mecklenburg Bay, respectively, is consistent with an intensification of Baltic Sea outflow over the past ~3500 cal. yr BP, probably caused by increased precipitation and runoff from land masses surrounding the Baltic Sea (Figure 4.6B-C).

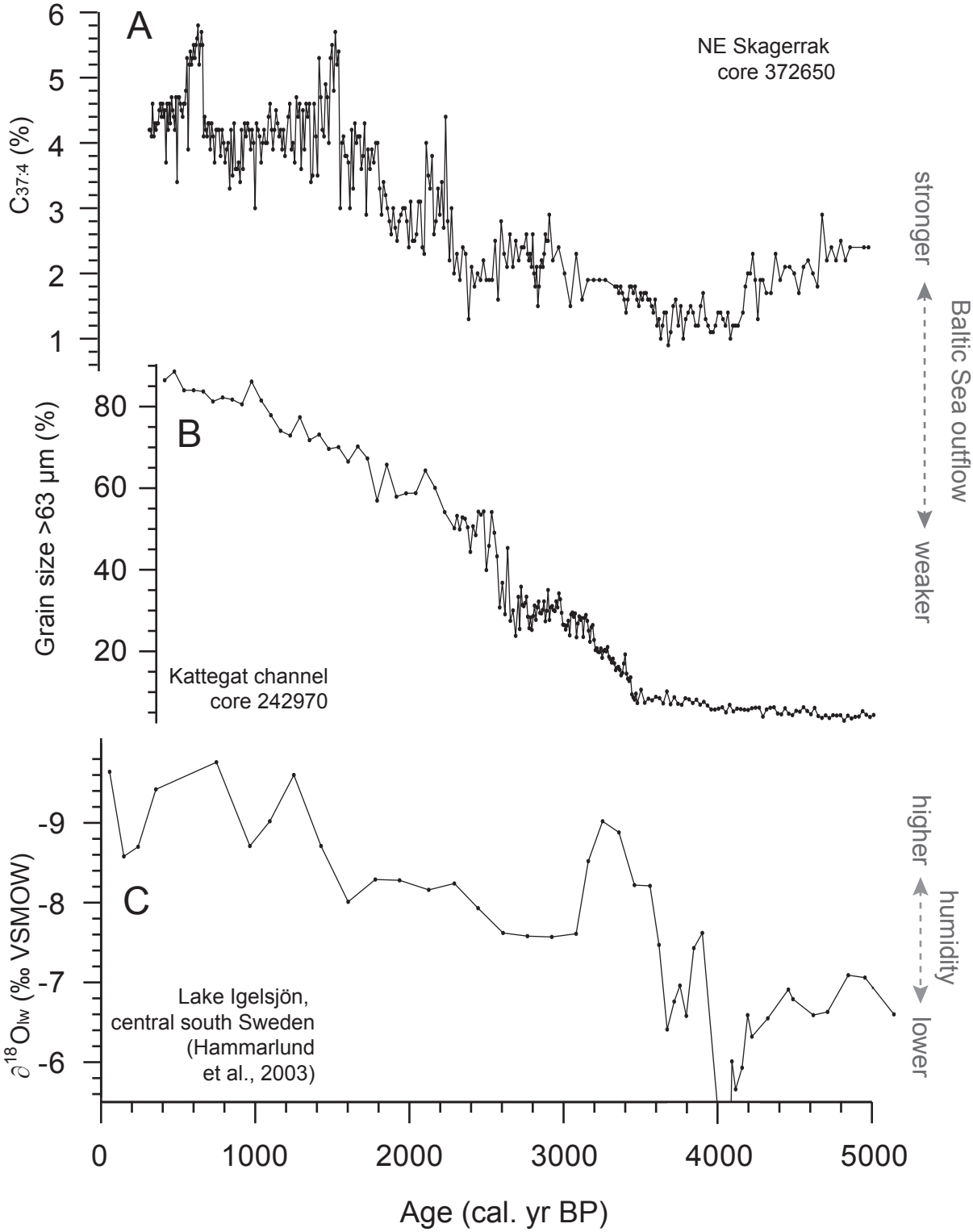

Fig. 4.5 An increase in both $C_{37:4}$ % (A) and sand particles (B) in the Skagerrak and Kattegat, respectively, suggesting strengthening of the Baltic Sea outflow starting at around 3500 cal. yr BP. Presumably, the strengthening in outflow is related to an increase in precipitation and/or reduced evaporation, as indicated in the $\delta^{18}O$ record from Lake Igelsjön (C) in central S Sweden (Hammarlund et al., 2003). Most likely, increased precipitation and consequently strengthening of the Baltic Sea outflow is induced by a major re-organization of the atmospheric circulation pattern over the North Atlantic over the past 3500 cal. yr BP.

4.7 Conclusions

Multi-core surface and subsurface samples collected along a transect display a significant increase in $C_{37:4}$ % from the west towards the northeast Skagerrak. The results imply that low saline surface waters influence sites located close to the Kattegat to a larger degree than those adjacent to the open ocean, thus mirroring the surface salinity gradient existing in the modern Skagerrak. Four gravity-cores studied, also suggest an increase in $C_{37:4}$ % amplitude from the west towards the northeast, confirming coherent late Holocene and surface and subsurface variations in $C_{37:4}$ % in the Skagerrak. In the northeast Skagerrak, an increase of $C_{37:4}$ % starts at ~3500 cal. yr BP. Concomitant, a significant rise in sand content is recorded in Kattegat/Mecklenburg Bay data accompanied by reduced sediment accumulation as evident from radiocarbon results and seismoacoustic data. The matching of two independent proxies (grain-size and $C_{37:4}$ %) suggests that the same process generated the proxy-signals. It is likely that a strengthening of Baltic Sea outflow led to an increase in $C_{37:4}$ % in the Skagerrak, an increase in grain-size in the Kattegat/Mecklenburg Bay, and reduced sediment accumulation rate in the Kattegat. Increased precipitation induced by a major re-organization of the atmospheric circulation pattern over the North Atlantic is the most likely cause for an increase in Baltic Sea outflow intensity over the past ~3500 cal. yr BP. Our results suggest that $C_{37:4}$ % derived from Skagerrak sediments can be used to infer past variations in Baltic Sea outflow in great detail, and should be compared with reconstructions of past changes in inflow.

Acknowledgments. – We thank the crews of Alkor, Poseidon, and Maria S. Merian research vessels for technical support during coring operations. We thank S. Koch for assistance with the alkenone analysis. We are grateful to all INFLOW members and Guillaume Leduc at C.E.R.E.G.E., Aix en Provence, for fruitful discussions. We are grateful to Kay-Christian Emeis and Richard Gyllencreutz for constructive reviews. The work has been founded by the DFG SPP 1400 ‘Early Monumentality and Social Differentiation’ and the EU BONUS+ ”Inflow” project.

5 Climate change triggers late onset of agrarian societies in northern Germany and southern Scandinavia

This chapter corresponds to the following manuscript submitted to The Holocene: V. R. Krossa, M. Moros, G. Leduc, M. Hinz, T. Blanz, and R. Schneider: Climate change triggers late onset of agrarian societies in northern Germany and southern Scandinavia

The first author has written the manuscript. The $U^{K'}_{37}$-SST analysis were done at the University of Kiel (Biomarker Laboratory) by the first author in cooperation with Thomas Blanz. Martin Hinz (Graduate School, University of Kiel) contributed to the archaeological discussion. Matthias Moros (Institute of Warnemünde, Rostock), Ralph Schneider (University of Kiel, Germany), and Guillaume Leduc (C.E.R.E.G.E., France) contributed to the manuscript by discussing. Ralph Schneider supervised the work.

5.1 Abstract

In northern Germany and southern Scandinavia, a shift from hunter-gatherer-fisher based communities into societies with an economy mainly relying on animal husbandry and cereal cultivation is evident as late as ~6000-5500 cal. yr BP. Many studies argue that climate change might have triggered the late onset of farming in those areas. Therefore, the aim of this study is to better document past sea surface temperature (SST) evolution in the western and northeastern Skagerrak region during that period in order to comment on potential climatic impacts on the landscape where those human groups settled. Prior to ~6300 cal. yr BP, similar warm SSTs are documented for the western and northeastern Skagerrak, suggesting dominance of North Atlantic water inflow. Between ~6300 and 5600 cal. yr BP, consistent with the shift in human economy, SSTs decreased by ~5-6ºC in the northeastern Skagerrak, approaching air temperature values reconstructed for central South Sweden. The pronounced SST drop suggests outflow of colder Baltic Sea water, probably reflecting a more continental-dominated atmospheric circulation pattern with stronger winter cooling of the Baltic Sea in general. Most likely, the cooling provoked invasive effects on the natural environment leading to a gradual restriction in natural food sources, thereby forcing formerly hunter-gatherer-fisher societies to adopt farming strategies to overcome periods of unfavorable climate conditions. Once fully adopted, the farming societies were even able to overcome periods of hypoxia largely affecting the marine food resources, as evident in a human population density increase. This correspondence suggests that climate change was most likely one factor that played a crucial role in the adoption of farming and animal husbandry in northern Germany and southern Scandinavia.

5.2 Introduction

The transition from hunter-gatherer-fisher communities to societies with an economy mainly relaying on animal husbandry and cereal cultivation was one of the most radical changes in more recent human history. In northern Germany and southern Scandinavia, first agricultural elements occur at ~6000 cal. yr BP (Sørensen and Karg, 2012), whereas evidence for a fully developed agrarian society is documented as late as ~5500 cal. yr BP (Dörfler et al., 2012; Feeser et al., 2012; Kirleis et al., 2012). In contrast, the agrarian economy was manifested at ~7500 cal. yr BP in adjacent southern regions (Schier, 2009; Guilaine, 2000/2001). Consequently, the agrarian technology was most likely available to hunter-gatherer-fisher societies in northern Germany and southern Scandinavia for more than one millennium.

Many studies have proposed climate change as a potential trigger for the late onset of farming in northern Germany and southern Scandinavia (Bonsall et al., 2002; Gronenborn, 2007; Hartz et al., 2007; Sørensen and Karg, 2012; Gronenborn et al., 2013). However, the ultimate effect of climatic and environmental changes on shifts in the economy at northern settlements is still debated because of a dearth of high-resolution regional paleo-environmental reconstructions. Often, the mid Holocene period (~8000-4000 cal. yr BP) is described as a stable interval of i.e. generally high temperatures, reduced precipitation, and reduced or lacking glaciers (Seppä and Birks, 2001; Hammarlund et al., 2003; Seppä et al., 2005). Many paleo-climate reconstructions, however, document a climate cooling within the North Atlantic region between ~6000 and 5000 cal. yr BP, consistent with the onset of first agricultural elements in northern Germany and southern Scandinavia (Bond et al., 2001; Zillén, 2003; Seppä et al., 2005; Bakke et al., 2008; Jansen et al., 2008).

Recently, Shennan et al. (2013) found little or no correlation between demographic proxies in northern Germany and southern Scandinavia and a set of paleoclimate reconstructions for Europe, and argued against a strong link between Holocene North Atlantic climate change and societal and cultural changes in Northern Europe. The paleoclimate reconstruction dataset used in Shennan et al. (2013) however includes reconstructions from distant locations, precluding a regional assessment of co-occurring environmental and demographic changes in northern Germany and southern Scandinavia. Here, we reconstruct the mid to late Holocene sea surface temperature ($U^{K'}_{37}$-SST) history from the western and central as well as from northeastern Skagerrak (Figure 5.1) close to areas where the proper timing of settlements of first agrarian communities in northern Germany and southern Scandinavia is well documented. The coring sites allow us to comment on the regional climate changes in the North Atlantic and Baltic region, and discuss the effect on the environmental changes occurring as closest as possible to the landscape where these communities settled.

5.3 Study site and regional climate

5.3.1 Skagerrak

The Skagerrak forms the only marine connection between the North Atlantic and the land-locked Baltic Sea (Figure 5.1). In the northwest, the Skagerrak has a fjord-like shape (Thiede, 1987) and reaches maximum water depths of more than 700 m (Rodhe, 1987), thus representing the deepest part of the otherwise shallow North Sea. In the present day NE Skagerrak, sea surface temperatures are determined by the interplay between the inflow of North Atlantic water and the Baltic Sea outflow. Therefore, sedimentary sequences from the NE Skagerrak provide excellent archives for paleo-climate reconstructions that reflect past changes in atmospheric circulation and precipitation pattern over the Baltic region, while those from the western Skagerrak are more indicative of the overall maritime climate of the North Atlantic realm.

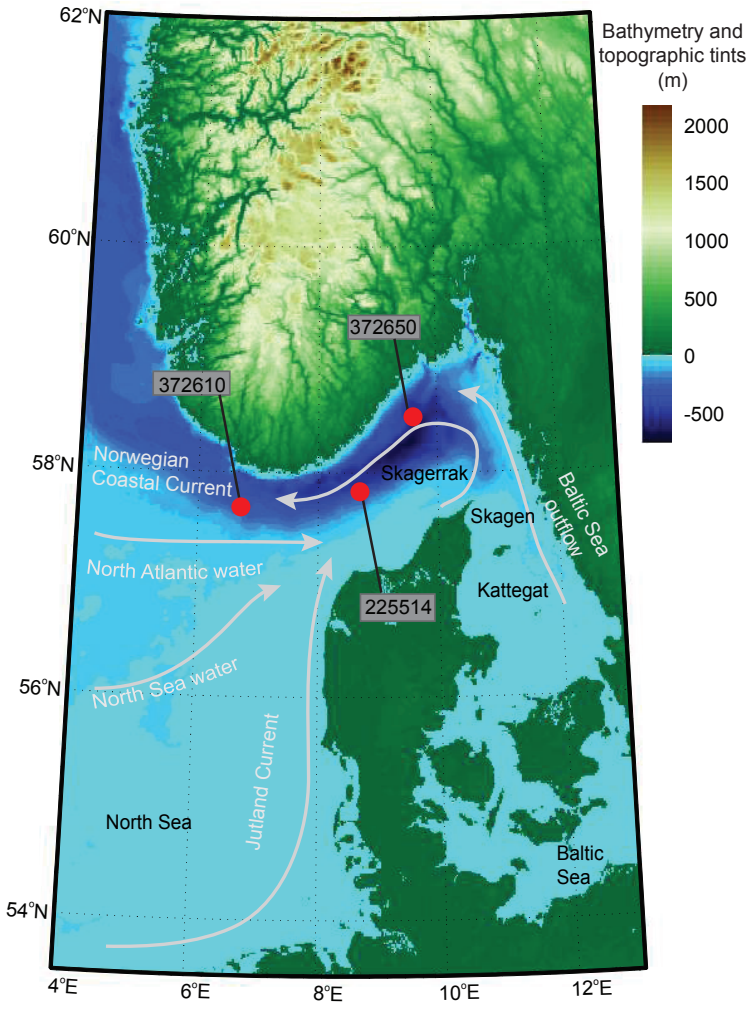

Fig. 5.1 Core locations in the Skagerrak (core numbers in grey boxes). White solid arrows indicate present day main surface currents in the Skagerrak and the Kattegat. The bathymetric and topographic lines are from IOC et al. (2003).

In general, the modern current circulation pattern in the Skagerrak/North Sea is largely governed by the inflow of North Atlantic and North Sea water and the outflow of Baltic Sea water (Svansson, 1975; Rodhe, 1987; 1988; Otto et al., 1990) (Figure 5.1). Saline North Atlantic water enters the Skagerrak/North Sea between Scotland and Norway and via the English Channel. The South Jutland Current, consisting of water from the English Channel and southern North Sea, flows northwards along the Danish coast and mixes with the North Jutland Current that originates from the North Atlantic and the central North Sea water. As the current passes Skagen (Figure 5.1) and enters the Skagerrak/Kattegat border, part of it mixes with fresher and colder Baltic Sea water. Thereupon, part of the current forms an anti-clockwise gyre that exits the Skagerrak, back flowing along the Norwegian coast as the Norwegian Coastal Current (Figure 5.1). The anti-clockwise current and the deep waters cause current speed reduction that allows fine-grained sediment to accumulate at high rates in the central and northeast parts of the Skagerrak (Rodhe and Holt, 1996; van Weering, 1982).

5.3.2 Baltic Sea outflow

The Baltic Sea semi-enclosed brackish water body is located in the humid climatic zone of northern Europe. At present day, it is connected to the North Atlantic Ocean via the Skagerrak through the narrow and shallow Kattegat and Danish straits, consequently having strongly restricted water exchange with the open ocean. As a consequence of the fresh water surplus and the strongly limited water exchange with the North Atlantic, the Baltic Sea has an estuarine circulation pattern characterized by outflowing low-salinity surface water and inflowing higher-salinity bottom water (Figure 5.1). The onset of this estuarine circulation pattern took place at around ~8500 cal. yr BP (Andren et al., 2000; Rößler et al., 2011) during the Litorina Sea transgression.

The Baltic Sea outflow that reaches the Skagerrak causes a low-salinity environment in the Danish Straits and the Kattegat towards the Skagerrak (Danielssen et al., 1997). As a consequence of the positive freshwater balance due to river runoff and net precipitation, quantities of outflowing Baltic Sea water are generally larger than inflowing water volumes. On a long-term average, the difference between outflowing and inflowing water volumes equals the freshwater surplus (Gustafsson and Westman, 2002). Model simulations suggest that an increase of the net freshwater supply to the Baltic Sea causes enhanced surface water outflow and a decrease of bottom water inflow in the Kattegat area (Stigebrandt, 1983; Gustafsson and Westman, 2002), although a weakening of inflow during periods of strong outflow is contradictory to a general estuarine circulation scheme.

5.3.3 Regional climate

The present day climate in northwest Europe and the Baltic region is strongly governed by large-scale atmospheric pressure systems that drive variations in strength and direction of wind fields (e.g., Hurrell, 1995; Hurrell et al., 2003; BACC, 2008)

. Such pressure systems include the Icelandic Low, the Azores High, and the winter High/summer Low over Russia, whereas variations in the occurrence of these pressure systems lead to a pre-dominance of maritime or continental climate. Periods of maritime-dominated climate are characterized by the strong influence of Westerlies directed towards northwest Europe that are driven by i.e. intensified pressure gradients between the Icelandic Low and Azores High. Such climate conditions cause mild and moist climate in northwest Europe that can affect large areas of the Baltic region. In contrast, a continental-dominated climate is marked by weaker Westerlies and a greater dominance of the continental anticyclone over Russia, thus provoking dry and warm summer and cold and dry winter conditions (e.g., Hurrell, 1995; Hurrell et al., 2003; BACC, 2008).

5.4 Material and methods

5.4.1 Skagerrak sediment cores

Two multi-cores (IOW372610 and IOW372650) and three gravity-cores (IOW372610, IOW225514, and IOW372650) located in the western, central, and northeastern Skagerrak (Figure 5.1) were used to reconstruct SST changes during the last decades and for the last 8000 years, respectively. The cores were retrieved during the cruises of “R/V Alkor” in 2000 and “R/V Maria S. Merian MSM” in September 2009 (Table 5.1).

Tab. 5.1 Location and water depth of each multi- and gravity-core used in this study (see also Figure 5.1).

Core number	Latitude	Longitude	Water depth (m)	Cruise/Year
372610 GC/MUC	57°41.05´N	06°41.00´E	320	R/V Maria S Merian MSM12/4, 2009
225514 GC	57°50.28´N	08°42.226´E	420	R/V Alkor, 2000
372650 GC/MUC	58°29.76´N	09°35.91´E	550	R/V Maria S Merian MSM12/4, 2009

5.4.2 $U^{K'}_{37}$-SST estimates

Total lipids were extracted from approximately 2 to 3 g of freeze-dried and homogenized bulk sediment, using an Accelerated Solvent Extractor (Dionex ASE-200) with a mixture of 9:1 (v/v) of dichloromethane:methanol (DCM:MeOH) at 100°C and 100 bar N_2 (g) pressure at the Biomarker Laboratory of the Geoscience Institute, Christian Albrechts University, Kiel. Extracts were cooled to -20°C and thereupon brought to near dryness by vacuum rotary evapo-

ration at 20°C and 65 mbar. We used a multi-dimensional, double gas column chromatography (MD-GC) set up with two Agilent 6890 gas chromatographs for $C_{37:3}$ and $C_{37:2}$ identification and quantification. The method is fully described in Etourneau et al. (Etourneau et al., 2010). Quantification of the organic compounds was achieved with the addition of an internal standard prior to extraction (cholestane ($C_{37}H_{48}$) and hexatriacontane ($C_{36}H_{74}$)). The alkenone unsaturation index ($U^{K`}_{37}$) was obtained by quantifying the peak areas of $C_{37:3}$ and $C_{37:2}$ and subsequently applying the equation of Prahl and Wakeham (1987):

$$U^{K`}_{37} = C_{37:2}/(C_{37:2}+C_{37:3}) \quad \text{(Prahl and Wakeham, 1987)} \quad (5.1)$$

The $U^{K`}_{37}$ index was translated into SST using a calibration based on a global set of 149 surface samples (Müller et al., 1998):

$$SST=(U^{K`}_{37} - 0.044)/0.033 \quad \text{(Müller et al., 1998)} \quad (5.2)$$

Analytical precision based on duplicate analyses of internal laboratory sediment standards during the whole procedure was approximately 0.12ºC.

5.4.3 Chronology

The surface sediments derived from multi-cores (Krossa et al., 2014) and gravity-cores (Emeis et al., 2003; Krossa et al., 2014) were dated using AMS ^{14}C dates (Table 5.2).

The radiocarbon dates of both multi-cores indicate a “modern age” (“post bomb”) of surface and subsurface sediments, thus allowing a comparison of estimated SST at the core-top with modern instrumental data (Krossa et al., 2014). Chronologies of the gravity-cores presented in this study are based on ^{14}C ages converted into calendar years using the online software Calib Rev 7.0 and the Marine13 calibration curve (Reimer et al., 2013). The application of the standard marine reservoir age of 400 years allows direct comparison with previously published paleo-climate records from the Skagerrak (Jiang et al., 1998; Gyllencreutz and Kissel, 2006; Erbs-Hansen et al., 2012; Krossa et al., 2014). Our results are presented on a calibrated age scale before Present (cal. yr BP, AD 1950). Age-depth models were established using linear interpolation between each calibrated radiocarbon date.

Tab. 5.2 Age determination of each gravity-core used in this study. The radiocarbon dates are published in Emeis et al. (2003) and Krossa et al. (2014) and supplemented by three new radiocarbon dates (the last three radiocarbon dates in core IOW372650). Radiocarbon ages were calibrated (cal. yr BP) using the Calib Rev 7.0 software program and the Marine13 calibration set (Reimer et al., 2013) with an assumed standard marine reservoir age of 400 years. Omitted radiocarbon ages are in italics.

Sample (cm)	Dated material	Age (^{14}C yr BP)	Calibrated age min – max (1σ range, cal. yr BP)	Calibrated age med. (1σ range, cal. yr BP)	Lab Ref.	C (mg)
Skagerrak GC 372610 (Krossa et al., 2014; 57°41.05´N, 06°41.00´E)						
2-3	Mixed benthic foraminifera	715±25	314 - 397	359	KIA42411	0.7
20	Mixed benthic foraminifera	745±35	333 - 432	386	Poz-34467	0.42
55-56	Mixed benthic foraminifera	940±25	504 - 556	536	KIA42412	0.5
73-74	Mixed benthic foraminifera	1140±50	647 - 731	693	LuS 9540	1.07
100	Mixed benthic foraminifera	1510±40	1003 - 1123	1064	Poz-34553	0.37
124-125	Mixed benthic foraminifera	1960±50	1438 - 1577	1514	LuS 9539	0.53
155-156	Mixed benthic foraminifera	2385±25	1966 - 2060	2014	KIA 42413	1.0
174-175	Mixed benthic foraminifera	2550±50	2161 - 2292	2221	LuS 9538	0.78
200	Mixed benthic foraminifera	2710±30	2344 - 2444	2404	Poz-34468	0.67
255-256	Mixed benthic foraminifera	3195+35/-30	2935/2941 - 3055/3050	2995/2994	KIA 42414	0.8
300	Mixed benthic foraminifera	3820±40	3705 - 3826	3768	Poz-34554	0.5
354-356	Mixed benthic foraminifera	4530±35	4693 - 4807	4738	KIA 42415	0.6
424-426	Mixed benthic foraminifera	5505±35	5851 - 5933	5891	KIA 42416	0.5
Skagerrak GC 225514 (Emeis et al., 2003; 57°50.28´N, 08°42.226´E)						
10.5	Mixed benthic foraminifera	810±30	429 - 483	454	KIA 14028	-
105.5	Mixed benthic foraminifera	1780±35	1284 - 1353	1323	KIA 14029	-
135.5	Mixed benthic foraminifera	2710±35	2342 - 2451	2407	KIA 14031	-
155.5	Mixed benthic foraminifera	2755±45	2368 - 2545	2481	KIA 14033	-
250.5	Mixed benthic foraminifera	4280±45	4337 - 4480	4397	KIA 14034	-
310.5	Mixed benthic foraminifera	6400±45	6810 - 6939	6876	KIA 14035	-
Skagerrak GC 372650 (Krossa et al., 2014; 58°29.76´N, 09°35.91´E)						
24-26	Mixed benthic foraminifera	900±50	472 - 547	513	Poz-34465	0.26
55-57	Mixed benthic foraminifera	1200±25	699 - 767	736	KIA 42417	0.6
105-107	Mixed benthic foraminifera	1655±30	1186 - 1255	1222	KIA 42418	0.6
155-157	Mixed benthic foraminifera	2155±30	1703 - 1796	1749	KIA 42419	0.5
199-201	Mixed benthic foraminifera	2620±50	2240 - 2356	2303	Poz-34551	0.23
223-225	Mixed benthic foraminifera	2985±50	2713 - 2806	2762	LuS 9537	0.82
244-246	Mixed benthic foraminifera	3150±50	2855 - 3003	2935	Poz- 44174	0.6
255-257	Mixed benthic foraminifera	3470±35	3308 - 3404	3352	KIA 42420	0.5

Sample (cm)	Dated material	Age (^{14}C yr BP)	Calibrated age min – max (1σ range, cal. yr BP)	Calibrated age med. (1σ range, cal. yr BP)	Lab Ref.	C (mg)
273-275	*Mixed benthic foraminifera*	*3155±70*	*2847 - 3040*	*2946*	*LuS 9536*	*0.36*
284-286	Mixed benthic foraminifera	3760±50	3619 - 3770	3695	Poz-44175	0.2
299-301	*Mixed benthic foraminifera*	*3660±50*	*3492 - 3630*	*3566*	*KIA 42421*	*0.7*
323-325	Mixed benthic foraminifera	4230±90	4186 - 4440	4324	LuS 9535	0.27
355-357	Mixed benthic foraminifera	4945±35	5234 - 5325	5289	KIA 42422	0.6
415-417	Mixed benthic foraminifera	5880+40/-35	6256-6346	6298	KIA 42423	0.4
427-430	Mixed benthic foraminifera	6730±50	7202-7314	7261	Poz-44176	0.3
499-501	Mixed benthic foraminifera	10260±70	11161-11338	11261	Poz-34466	0.34

5.5 Results

Modern data suggest sea surface temperatures ranging from approximately 4°C during winter to 16°C during summer months, with an annual average of approximately 9-10°C for the Skagerrak region (Locarnini et al., 2010). Our surface and subsurface sediments (upper 5 cm of each multi-core) reveal a mean SST value of 9.2±1.1ºC that is comparable with present-day mean-annual SST in the Skagerrak.

The Holocene SST records, which are located in the western (IOW372610), central (IOW225514), and northeastern Skagerrak (IOW372650) (Figure 5.1) reveal similar absolute SST values prior to ~6300 cal. yr BP and during the last millennium (Figure 5.2). In general, the western and central Skagerrak SST record show the typical orbital-forced mid to late Holocene cooling trend as documented in several North Atlantic and northern European paleo-climate records (Seppä and Birks, 2001; Calvo et al., 2002; Moros et al., 2004; Seppä et al., 2005; Jansen et al., 2008). Both records reveal a cooling of about 4.5°C from 13.5°C at 6500 cal. yr BP to 9°C at 500 cal. yr BP (Figure 5.2). In contrast, the SST evolution in the northeastern Skagerrak strongly diverged from that in the western and central regions towards much lower SST values of about 7°C for several periods between ~6300 and 1000 cal. yr BP. After a prominent 5-6°C decrease between ~6300 and 5600 cal. yr BP, only the northeastern Skagerrak SSTs converged with the much colder pollen-derived mean annual air temperature (MAT) record from central South Sweden (Seppä et al., 2005). This SST cooling was particularly prominent between ~6300 and 4700 cal. yr BP, and during several shorter periods at about, 4300, 2700, 2200, and 1500 cal. yr BP. After ~1000 cal. yr BP, the gravity- and multi-core SST records from both Skagerrak locations approach modern-time sea surface temperatures of 9-10ºC, diverging again from surface air temperatures of ~6ºC recorded in central South Sweden (Seppä et al., 2005).

The prominent SST drop from ~13°C to ~7 ºC that occurred between ~6300 and 4700 cal. yr BP brought SST values from the northeastern Skagerrak close to absolute MAT values estimated from central South Sweden (Seppä et al., 2005). Such a drop is not recorded in the western and central Skagerrak SST records (Figure 5.2) that rather track the overall long-term cooling trend seen in the MAT record in central South Sweden.

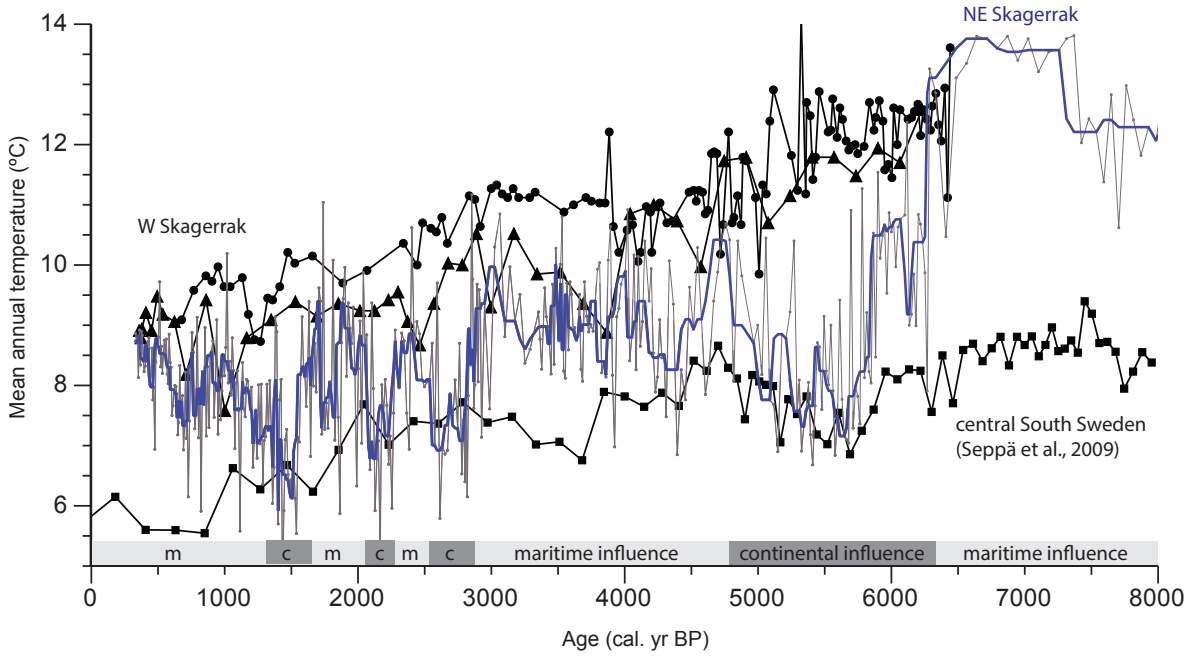

Fig. 5.2 Comparison of SST evolution in the western/central (upper black lines) and northeastern (grey lines, blue line represents 5 point running mean average) Skagerrak to mean annual air temperatures (MAT, black lower line) derived from a lake in central south Sweden (Seppä et al., 2005). Prior to ~6300 and during the last centuries, the Skagerrak SST records reveal similar absolute SST values, whereas during the mid and late Holocene (6300 to 1000 cal. yr BP), the northeastern SST evolution diverged from that recorded in the western Skagerrak, being more in harmony with the pollen-derived MAT record.

5.6 Discussion

5.6.1 Long-chain alkenone-derived SSTs in the Skagerrak

Long-chain alkenones (C_{37} to C_{39}) are unsaturated ketones exclusively biosynthesized by coccolithophorids, mainly the cosmopolitan species *Emiliania huxleyi* and *Gephyrocapsa oceanica*. The proportion of di-unsaturated ($C_{37:2}$) to tri-unsaturated ($C_{37:3}$) C_{37} alkenones (expressed as the $U^{K`}_{37}$ index) shows a linear correlation to algal growth temperature (Prahl and Wakeham, 1987; Prahl et al., 1988; Conte et al., 1998). Global core-top studies suggest the correlation between the $U^{K`}_{37}$ index and sea temperature is strongest when mean annual sea surface temperatures are considered (Müller et al., 1998; Conte et al., 2006; Rosell-Melé and Prahl, 2013). However, many studies argue that reconstructed SSTs are seasonally skewed, as the algae growth strongly depends on light conditions and nutrient availability (Leduc et al., 2010; Schneider et al., 2010; Lohmann et al., 2013). Although the maximum of

coccolithophorid bloom occurs during late spring and early summer in the modern Skagerrak area (Nanninga and Tyrrell, 1996; Blanz et al., 2005), our core-top SST estimates (upper 5 cm) match with observed mean annual sea surface temperature (approximately 9-10°C) and are slightly lower than spring/summer temperatures (Locarnini et al., 2010). Supportingly, Rosell-Melé et al. (2013) showed that the seasonality of maximum alkenone flux in globally distributed sediment traps do not follow any coherent spatial pattern, and conclude that alkenone-derived SST estimates are reflective of mean-annual SSTs. As we have no way to infer the seasonality of alkenone fluxes through the water column in the Skagerrak, we interpret the $U^{K`}_{37}$-derived SST values as a proxy for the mean annual temperature at this site. This is also appropriate for comparison with the pollen-derived MAT from Southern Sweden.

5.6.2 Diverging SST trends in the western and northeastern Skagerrak

All Skagerrak SST records presented in this study reveal similar absolute SST values prior to 6300 cal. yr BP and during the last millennium (Figure 5.2). Additionally, they all document a general cooling of 3 to 4ºC from the mid to late Holocene. This magnitude of cooling is observed in many North Atlantic and north European paleoclimate records (Magny and Haas, 2004; Wanner et al., 2008) and follows the pattern of a global temperature reconstruction in which the termination of the mid Holocene thermal optimum occurs between approximately 6000 and 5000 cal. yr BP (Marcott et al., 2013). In contrast, the SST evolution from 6300 to 1000 cal. yr BP in the northeastern Skagerrak, diverging from that in the western and central Skagerrak and periodically approaching temperature values very close to the MAT record from southern Sweden (Figure 5.2), requires a regional forcing, in particular to explain the prominent 6°C drop between 6300 and 5600 cal. yr BP.

Nowadays and probably over the last 8500 years, varying contributions of North Atlantic water inflow (Klitgaard-Kristensen et al., 2001; Gyllencreutz, 2005; Gyllencreutz and Kissel, 2006) and Baltic Sea water outflow (Krossa et al., 2014) dominated the Skagerrak circulation pattern as schematically indicated in Figure 5.1 (Klitgaard-Kristensen et al., 2001; Gyllencreutz, 2005; Gyllencreutz and Kissel, 2006). Temperature variations in regions dominated by continental climate are generally larger than those influenced by the open ocean climate because of the relatively high thermal inertia and heat capacity of the upper ocean relative to the land surface. Therefore, the SST evolution occurring in the western and central Skagerrak is likely determined by the inflowing North Atlantic waters, reflective of changes in North Atlantic, open-ocean temperature conditions. As the northeastern Skagerrak is strongly exposed to outflowing Baltic Sea water (Figure 5.1), it is therefore strongly impacted by climate variability prevailing over the continental landmasses and the Baltic Sea towards the East. Consequently, differences in climate evolution occurring over the North Atlantic Ocean

and the continental Baltic region probably modulated the Holocene SSTs in the western and northeastern Skagerrak differently (Krossa et al., 2014). In addition, or alternatively, processes causing strongly enhanced surface outflow of the much colder water masses from the southwestern Baltic Sea at certain periods could also explain the diverging SST evolution in the northeastern Skagerrak. Therefore, it may be used to track past shifts in the general atmospheric circulation pattern that predominantly governed the climate over northern Europe.

Overall warm Skagerrak SSTs prior to ~6300 cal. yr BP (Figure 5.2) suggest that North Atlantic (maritime) conditions affected the entire Skagerrak, as corroborated by multiple regional studies (Klitgaard-Kristensen et al., 2001; Gyllencreutz, 2005; Gyllencreutz and Kissel, 2006). Supportingly, paleoclimate records from the open North Atlantic and adjacent landmasses also indicate warm conditions prior to ~6000 cal. yr BP (Calvo et al., 2002; Seppä et al., 2005; Jansen et al., 2008). Warmer than modern SSTs found in the North Atlantic and all Skagerrak SST records prior to ~6300 cal. yr BP suggests that the Baltic region as a whole was influenced by mild climatic conditions of maritime origin (Seppä and Birks, 2001; Seppä et al., 2005).

The marked ~5-6°C cooling occurring between 6300 and 5600 cal. yr BP in the northeastern Skagerrak SST record (IOW372650) suggests the onset of a disconnection between climatic conditions prevailing in the Baltic region and those influencing the North Atlantic during this time interval (Figure 5.2 and 5.3). The culmination of this pronounced cooling trend is also recorded in the Swedish MAT record, and was followed by a smooth warming phase observed in both records (Figure 5.2 and 5.3). These common temperature features suggest that the northeastern Skagerrak region was much more influenced by continental climate conditions prevailing above the adjacent Swedish landmass and the southwestern Baltic region than before. As climate variability occurring over the Baltic region at both present day and over the past three millennia directly affects the northeastern Skagerrak (Krossa et al., 2014), we argue that the distinct SST decrease after 6300 cal. yr BP (Figure 5.2 and 5.3) was a direct response to changes in the Baltic Sea outflow during that period. Supportingly, apparent increases in the relative amount of $C_{37:4}$ compounds over the sum of C_{37} ketones in the northeastern Skagerrak sediment core (Figure 5.3B) are indicative of enhanced Baltic Sea outflow (Krossa et al., 2014). Therefore such peaks occurring at ~6200, 5800, and 5200 cal. yr BP suggest periods of increasingly enhanced Baltic Sea outflow concomitant with the prominent northeastern Skagerrak cooling between 6300 and 5600 cal. yr BP, and to a lesser extent with the slight warming phase that lasted until 4700 cal. yr BP. The first two pulses of cold Baltic Sea water outflow causing the temperature drop in the northeastern Skagerrak likely resulted from a more prevalent continental atmospheric circulation pattern. Antonsson and co-workers (2009) argued that a long-lived and recurrent high-pressure system that prevailed in the latitudinal belt of the Westerlies during the mid Holo-

cene period (Rimbu et al., 2007) blocked the winds bringing moist and mild air masses towards northern Europe, inducing a continental-dominated atmospheric circulation pattern above northern Europe. Consequently, the summers were warm and dry over the Baltic region and winters were cold and dry. Overall, large seasonal contrasts in temperature, especially when the winters are very cold, are likely to cause generally low mean annual temperatures over southern Sweden and the Baltic Sea, that in turn might have provoked the distinct local cooling period documented in the northeastern Skagerrak. Interestingly, a distinct increase in ice rafted debris (IRD) in North Atlantic sediments, culminating at ~5250 cal. yr BP (Bond et al., 2001), matches the maximum cooling in the northeastern Skagerrak (Figure 5.3C). This suggests that enhanced icebergs discharges in the North Atlantic resulted in a shift towards continental-dominated climate conditions in northern Europe, subsequently strengthening the outflow of colder Baltic surface waters as we observe in the northeastern Skagerrak (Figure 5.3).

5.6.3 Baltic Sea outflow, climate cooling, and development towards an agrarian-based society in northern Germany and southern Scandinavia

Between 6000 and 5500 cal. yr BP, strong evidences for the development towards an agrarian-based society in northern Germany and southern Scandinavia exist (Dörfler et al., 2012; Feeser et al., 2012; Kirleis et al., 2012; Sørensen and Karg, 2012). Probably as a consequence of the new economy, population densities in northern Germany and southern Scandinavia increased (Figure 5.3), as reflected by an increase in dated artefacts (Shennan and Edinborough, 2007; Hinz et al., 2012). Many studies attributed the onset of an agrarian-based society and associated growth in human populations in northern Germany and southern Scandinavia to climate change, suggesting that a climate shift provoked the development of agriculture and reduced foraging activities in human cultures (Bonsall et al., 2002; Hartz et al., 2007; Gronenborn, 2007; Sørensen and Karg, 2012). In contrast, Shennan and coworkers (2013) found no correlation between demographic evolution from several European sites and northern high-latitude climate change. However, as this study compares demographic results with climate records located at large geographical distances from the excavation sites than our sediment sequences, the paleo-climate proxies presented in Shennan et al. (2013) might not reflect the local climate situation occurring near the landscape where these people settled. Our multi-site study demonstrates that SST differences within the Skagerrak can vary much over short distances, and might depend on whether sedimentary sequences are from sites situated close to the continent/Baltic Sea or the open ocean/North Atlantic. It implies that caution is necessary when using climate records from remote sites to

comment on the likely climate impact that may have affected human societal, economic and cultural developments in north-central Europe.

In our case, our regional SST comparison suggests a connection between the onset of the severe cooling recorded in the northeastern Skagerrak at ~6300 cal. yr BP and a fundamental change in human strategies to secure sustainable food supply in the context of a growing population as evidenced by the increase in regional demography (Figure 5.3). Our results also suggest that such cooling (Figures 5.3 and 5.4), which was presumably associated with the outflow of cold Baltic Sea water reinforced by a general shift from a maritime to continental-dominated climate regime over the Baltic region, might have had an invasive effect on the natural environment leading to a gradual restriction in natural food sources, in turn negatively affecting human societies relying on hunting, gathering, and fishing. The increase in human population density (Hinz et al., 2012), strongly hints to alternative strategies to sustain the food supply for an increase in overall population, as i.e. agriculture and animal husbandry. Apparently, the cooling had already advanced before the first evidence for farming occurred (Figure 5.3), suggesting that the cooling was not an ultimate factor for explaining the recorded change in economy. Rather it likely progressively modified the environment to such an extent that new food supply techniques became increasingly efficient to counterbalance climate-induced diminution of natural food resources, particularly during harsh winters.

At the regional scale, archeological studies suggest that climate change causing restrictions in natural food resources might have forced agrarian food supply techniques to become increasingly efficient to balance diminution of natural food resources (Rowley-Conwy, 1984; Bonsall et al., 2002; Hartz et al., 2007; Gronenborn, 2007; Andersen, 2008; Bailey and Milner, 2008). In the southwestern Baltic Sea and Kattegat, some studies document a decline in the marine contribution (oysters, fish, and seals) in human diet at ~6000 cal. yr BP (Hartz et al., 2007; Bailey and Milner, 2008). Today, and probably in the past, the ecosystem health in the Baltic Sea is largely dependent on oxygen supply (HELCOM, 2007), and consequently, the occurrence of hypoxia (<2 ml/l O_2) in bottom waters induces major alternations in nutrient and other biogeochemical cycles (Vahtera et al., 2007), thereby altering benthic faunal communities and fish habitats (Karlson et al., 2002; Conley et al., 2009). In the Gotland Basin and Baltic Sea, hypoxic bottom water conditions, as indicated by the formation of C_{org}-rich laminated sediments, are documented between ~5700 and 4500 cal. yr BP (Lougheed et al., 2012), about 600 years after the onset of the NE Skagerrak SST cooling and during a period of maximum human population (Figure 5.3). This in turn suggests that the new economy was capable of sustaining the population even during a period of widespread hypoxic conditions in the adjacent Baltic Sea that most likely caused large-scale restrictions in the natural marine food resources. Today and probably since the initialization

of the Baltic Sea estuarine circulation pattern, the inflow of saline and O_2-rich bottom water originating from the North Sea, or the lack of such, strongly controls the occurrence of hypoxia. Some studies argue that intensified Baltic Sea outflow reduces the frequency and/or intensity of O_2-rich inflows (Stigebrandt, 1983; Stigebrandt and Gustafsson, 2003; Matthäus and Schinke, 1999; Krossa et al., 2014). However, on the contrary, the increases in $C_{37:4}$ documented in the northeastern Skagerrak, likely reflecting periods of enhanced Baltic Sea outflow, do not completely match the occurrence of hypoxia in the Gotland Basin (Figure 5.3B). This suggests that other factors might have generated hypoxia during that period rather than solely changes in water exchange dynamics in the Kattegat. Conley et al. (2009) and Funkey et al. (2014) have argued that periods of hypoxia are strongly related to intensified cyanobacteria blooms, presumably occurring during warm summers (Kabel et al., 2012; Funkey et al., 2014). Warmer summers in turn match a predominant continental atmospheric circulation pattern that most likely prevailed over the Baltic region during that period (see discussion above). Yet, however, the direct causes and responses between these factors are still not completely understood and further studies are needed to understand the processes and feedbacks of hypoxia in the Baltic Sea.

Nevertheless, the prominent SST drop occurring at ~6300 cal. yr BP probably associated with a continental climate regime over the Baltic region, was synchronous with first evidences of farming in northern Germany and southern Scandinavia. This suggests that the climate change was most likely one factor that led to a change in sustainable economy. The abrupt cooling may have progressively modified the environment to such an extent that farming and food storage during colder winters became more efficient to counter-balance environmental-related stress. This is further supported by the occurrence of widespread hypoxia in the Baltic Sea during a period of population increase, suggesting that farming was capable of sustaining a growing population.

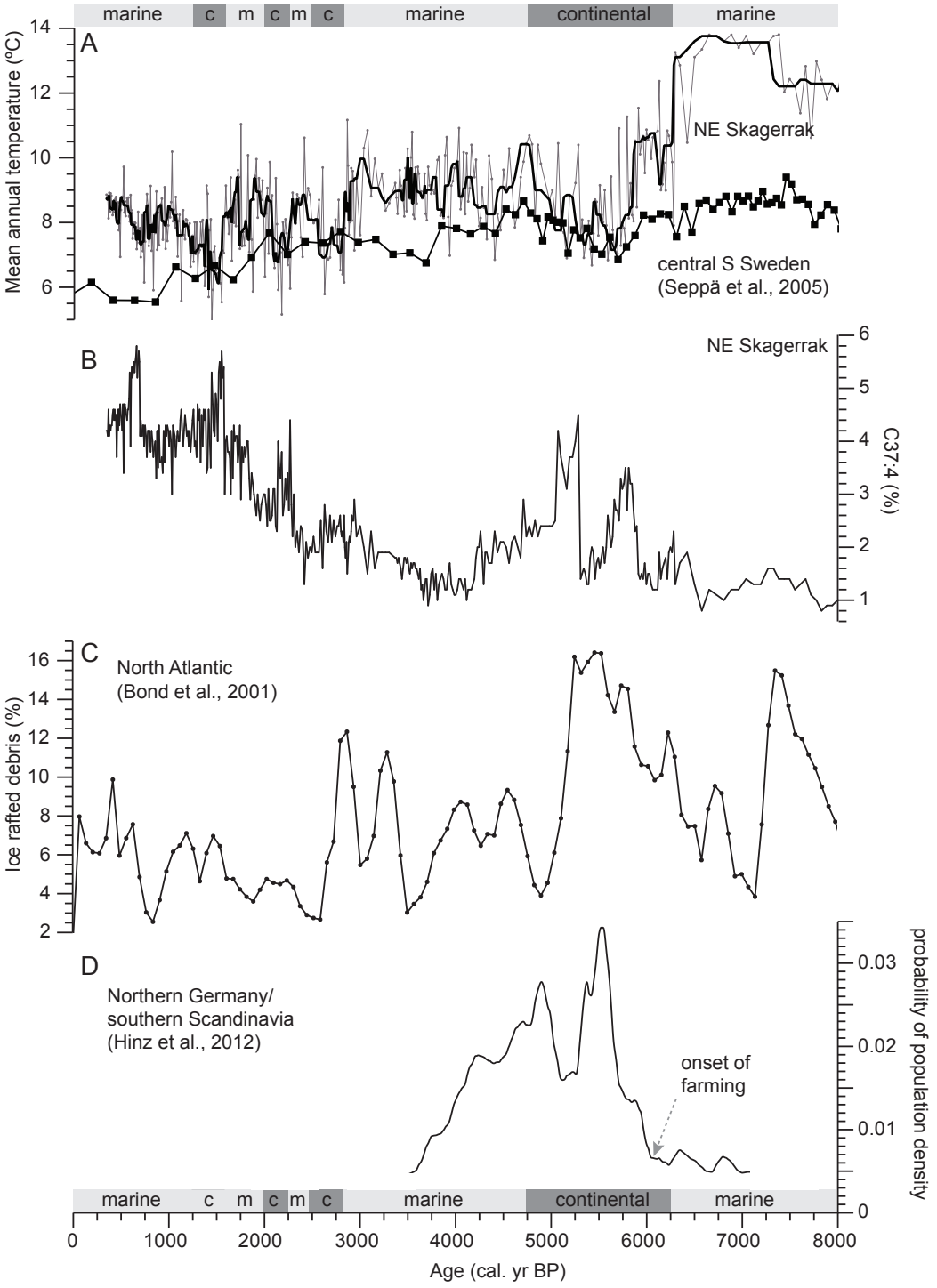

Fig. 5.3 A Alkenone-based SST from the NE Skagerrak (grey/black; IOW 372650), B pollen-based MAT from central south Sweden (blue; Seppä et al., 2005), C ice rafted debris from the Reykjanes Ridge in the North Atlantic (Bond et al., 2001), and D $C_{37:4}$ % from the NE Skagerrak (IOW372650). The paleoclimate records (A – C) demonstrate a cooling between ~6000 and 5000 cal. yr BP in the Skagerrak (A), southern Sweden (B), and North Atlantic (C) that is presumably related to a prevalent continental-dominated atmospheric circulation pattern. An increase in Baltic Sea outflow (D) is documented during the same period. The cooling and changes within the Baltic Sea match the onset of an agrarian-based economy in northern Germany and southern Scandinavia, suggesting that climate played a pivotal role.

5.7 Conclusions

We used a network of marine sediment cores in the Skagerrak to comment on regional and local changes in SST over the last 8000 years and modern time. Multi-core samples collected at sites in the western and northeastern Skagerrak, respectively, document a good match between estimated SSTs and modern mean annual sea surface temperatures. Gravity-cores show an overall SST decrease in the Skagerrak during the mid to late Holocene related to orbital-forced cooling. Outstanding is a notable SST drop of ~5-6°C recorded in the northeastern Skagerrak between ~6300 and 5600 cal. yr BP without any equivalent SST drop from the western Skagerrak sedimentary sequences. In addition, the northeastern Skagerrak record indicates constantly lower SSTs and more pronounced variability in contrast to the western Skagerrak records. These discrepancies within the Skagerrak suggest varying influences of continental and maritime-dominated atmospheric circulation pattern that contributed differently to the SST evolution in the Skagerrak. Therefore, the contrasting SST evolution implies a prominent shift from a more maritime towards a continental climate regime over the Baltic region occurring between 6300 and 5500 cal. y BP. This occurred synchronously with a fundamental change in sustainable economy in northern Germany and southern Scandinavia. Most likely, a succession of several events led to the onset of farming in those areas, whereas climate change was one important factor. The shift to a continental-dominated climate atmospheric circulation pattern associated with more frequent cold winters and warm summers, forced formerly hunter-gatherer-fisher societies to increasingly adopt farming strategies. Once fully adopted, the farming societies were even able to overcome periods of hypoxia largely affecting the marine food resources, as evident in a human population density increase. This in turn suggests that combination of several factors such as the vulnerability of natural ecosystems under hypoxia and climatic stress as well as the better use of existing knowledge on agricultural strategies caused societies to adapt through improving their living conditions that far that population even increased under less hospitable climatic and environmental conditions.

Acknowledgments. – We thank the crews of Alkor and Maria S. Merian research vessels for technical support during coring operations. We thank S. Koch for assistance with alkenone analysis. We are also thankful to all INFLOW and SPP 1400 members. The work has been founded by the DFG SPP 1400 “Early Monumentality and Social Differentiation” and the EU BONUS+ “Inflow” project.

6 Mid to late Holocene continental temperature reconstruction using branched glycerol dialkyl glycerol tetraetehers on lake sediments in Lake Belau (northern Germany)

This chapter corresponds to the following manuscript to be submitted: V. R. Krossa, G. Leduc, T. Bauersachs, J.-H. Kim, J. S. Sinninghe Damsté, and R. Schneider: Mid to late Holocene continental temperature reconstruction using branched glycerol dialkyl glycerol tetraethers on lake sediments in Lake Belau (northern Germany)

The first author has done the branched GDGT measurements in cooperation with Jung-Hyun Kim and Jaap S. Sinninghe Damsté (department of Marine Organic Biogeochemistry at the NIOZ, the Netherlands). The first author has written the manuscript under supervision of Ralph Schneider. Thorsten Bauersachs and Guillaume Leduc contributed to the manuscript by discussion.

6.1 Abstract

In northern Germany and southern Scandinavia, the shift from a hunter-gatherer-fisher based society into communities relying on animal husbandry and cereal cultivation is documented as late as ~6000 to 5500 cal. yr BP. The dearth of local high-resolution paleo-climate reconstructions has hampered a direct attribution of climate change to such societal shifts, as records from remote sites might not reflect the actual climate situation occurring over the landscape where those human groups settled. Here, we present a mid to late Holocene temperature record from a lake in northern Germany (Lake Belau) using the novel proxy based on branched glycerol dialkyl glycerol tetraethers (*br*GDGTs). The catchment area and the lake were influenced by periods of intensive human impact associated with farming over the time intervals studied. Despite that the temperature reconstruction at the Lake Belau site in general shows the typical mid to late Holocene cooling documented in many North Atlantic and north European records, we observe a warming between ~5900 and 5300 that is opposite to the cooling interval recorded in adjacent paleo-temperature reconstructions. Such contrasting temperature trends are surprising given the short geographical distances implied, suggesting that other processes than continental temperature might have influenced the Lake Belau *br*GDGT signal. We however do not detect any shift in the distribution of individual *br*GDGTs, suggesting that the *br*GDGT-derived temperature at the Lake Belau site might be a local signal, probably reflecting temperatures of the warmest seasons within the annual cycle. We argue that our lake-based temperature reconstruction reflects a connection between the onset and disappearance of local farming societies and climate change around Lake Belau, suggesting that the occurrence of warmer summers were favourable for cereal cultivation.

6.2 Introduction

Several major developments towards modern human societies in Europe occurred during the Holocene period, the onset of farming being one of the most important transitions. In northern Germany and southern Scandinavia, agricultural elements occur as late as ~6000-5500 cal. yr BP (Sørensen and Karg, 2012; Dörfler et al., 2012; Kirleis et al., 2012), i.e. ~1500 cal. yr BP later than in adjacent southern regions (Schier, 2009; Guilaine, 2000/2001). Previous studies have attributed the late onset of farming in northern Germany and southern Scandinavia to a change in the regional climate (Bonsall et al., 2002; Hartz et al., 2007; Gronenborn et al., 2013; Krossa et al., submitted). Until now, however, most of the climate reconstructions used for documenting climate variability impacting societies are based on marine sedimentary sequences, and are often located far from the continental excavation sites (Shennan et al., 2013). Consequently, they may not reflect the local or regional climate situation occurring at sites where the northern settlements evolved (Krossa et al., submitted). Local climate conditions were probably the key to the success of cereal cultivation, and hence may have had an important impact on farming societies in northern Germany and southern Scandinavia. Therefore, paleo-climate reconstructions from continental archives situated close to the archaeological excavation sites are essential to determine the potential impact of climate change on local societies.

Lake sediments potentially provide excellent archives for reconstructing past continental climate conditions (see review of Castaneda and Schouten, 2011). A majority of continental temperature reconstructions are based on pollen-transfer functions (e.g., Seppä and Birks, 2001; Davis et al., 2003; Seppä et al., 2005). However, these proxies can be influenced by other parameters than temperature such as by the anthropogenic alteration of the regional vegetation (Leng and Marshall, 2004; Seppä and Bennett, 2003). Interpolating in space and time a large data set of pollen time series can reduce the impact of non-climatic parameters such as anthropogenic factors (Seppä and Birks, 2001; Davis et al., 2003; Seppä et al., 2005), but also act to smooth the regional temperature reconstructions which make it difficult to detect abrupt climate changes that may have contributed to more rapid population adaptation in northern Europe (Krossa et al., submitted).

The recent development of organic tools used for paleothermometry have focused on a suite of organic molecules biosynthesized by Bacteria and Archaea (e.g., Brassell et al., 1986; Schouten et al., 2002). The distribution of membrane forming branched glycerol dialkyl glycerol tetraethers (*br*GDGTs) of bacterial origin (Weijers et al., 2006) that are preserved in lake sediments has provided a unique potential to infer past continental temperature changes. *br*GDGTs consist of three series of GDGTs (a, b, and c-series) that comprehend three structural isomers (I-III), with increasing degree of methyl branching (Weijers et al., 2006;

Sinninghe Damsté et al., 2012) (Figure 6.1). Originally, the proxy is based on two indices; the MBT (Methylation of Branched Tetraethers, equations 6.1 and 6.2) and CBT (Cyclization of Branched Tetraethers, equation 6.3) indices calculated from globally distributed soil samples (Weijers et al., 2007) and re-calibrated in 2012 (Peterse et al., 2012):

$$MBT=(Ia+Ib+Ic)/(Ia+Ib+Ic+IIa+IIb+IIc+IIIa+IIIb+IIIc) \quad \text{(Weijers et al., 2007)} \quad (6.1)$$

$$MBT'=(Ia+Ib+Ic)/(Ia+Ib+Ic+IIa+IIb+IIIa) \quad \text{(Peterse et al., 2012)} \quad (6.2)$$

$$CBT=-\log((Ib+IIb)/(Ia+IIa)) \quad \text{(Weijers et al., 2007)} \quad (6.3)$$

MBT and MBT´ refer to the number of methyl branches and CBT to the number of cyclopentyl moieties in the *br*GDGT alkyl chains and the roman numbers refer to each *br*GDGT compound (Figure 6.1). The MBT/MBT´ and CBT indices are correlated to mean annual air temperature (MAT) (Weijers et al., 2007; Peterse et al., 2012) (equations 6.4 and 6.5):

$$MAT=(MBT-0.122-0.178\times CBT)/0.020 \quad \text{(Weijers et al., 2007)} \quad (6.4)$$

$$MAT=0.81-5.97\times CBT+31.0\times MBT' \quad \text{(Peterse et al., 2012)} \quad (6.5)$$

Since 2007, many studies have applied the *br*GDGT proxy to reconstruct both modern and past temperatures in lakes (Sinninghe Damsté et al., 2009; Tierney and Russell, 2009; Blaga et al., 2009; Blaga et al., 2010; Tierney et al., 2010; Zink et al., 2010; Loomis et al., 2011; Pearson et al., 2011). However, many studies argue that an in situ (aquatic) production of *br*GDGTs within the lake environment affects the reconstructed MATs when using soil-based calibrations (Weijers et al., 2007; Peterse et al., 2012) (equations 6.4 and 6.5). Consequently, this led to alternative temperature equations developed for lake sediments (Tierney et al., 2010; Zink et al., 2010; Pearson et al., 2011) (equations 6.6 to 6.8). Equations 6.6 and 6.7 (MAT and mean summer temperature MST) include the MBT index, whereas equations 6.8 and 6.9 are based on the fractional abundance (*f*) of specific *br*GDGTs (roman numbers) that are most likely predominantly produced within the lake:

$$MAT=55.01\times MBT-6.055 \quad \text{(Zink et al., 2010)} \quad (6.6)$$

$$MST=49.658\times MBT+0.207 \quad \text{(Zink et al., 2010)} \quad (6.7)$$

$$MAT=50.47-74.18\times f\text{GDGTIIIa}-31.60\times f\text{GDGTIIa}-34.69\times f\text{GDGTIa} \quad \text{(Tierney et al., 2010)} \quad (6.8)$$

$$MST=20.9+98.1\times f\text{GDGTIb}-12.0\times f\text{GDGTIIa}-20.5\times f\text{GDGTIIIa} \quad \text{(Pearson et al., 2011)} \quad (6.9)$$

Hence, determining the dominant source of *br*GDGTs in the lake sediments is essential in order to decide which calibration equation (“aquatic vs. soil”) is most suitable for a given lake setting.

Here, we attempt to reconstruct mid to late Holocene (~7900 to 2300 cal. yr BP) continental temperatures using *br*GDGTs derived from a sedimentary sequence from Lake Belau in northern Germany in order to determine the impact of climate change on the onset of local farming activity occurring at ~5500 cal. yr BP. Past human settlements, in particular agrarian-based societies associated with intensive land use, strongly impacted the landscape in the lake catchment area. These changes might in turn have influenced biogeochemical cycles within the lake system (Dreibrodt and Wiethold, 2014), potentially affecting the production of *br*GDGTs. Therefore, any potential impact of human activity and land opening on the biomarker proxy has to be excluded prior to interpreting the temperature signal.

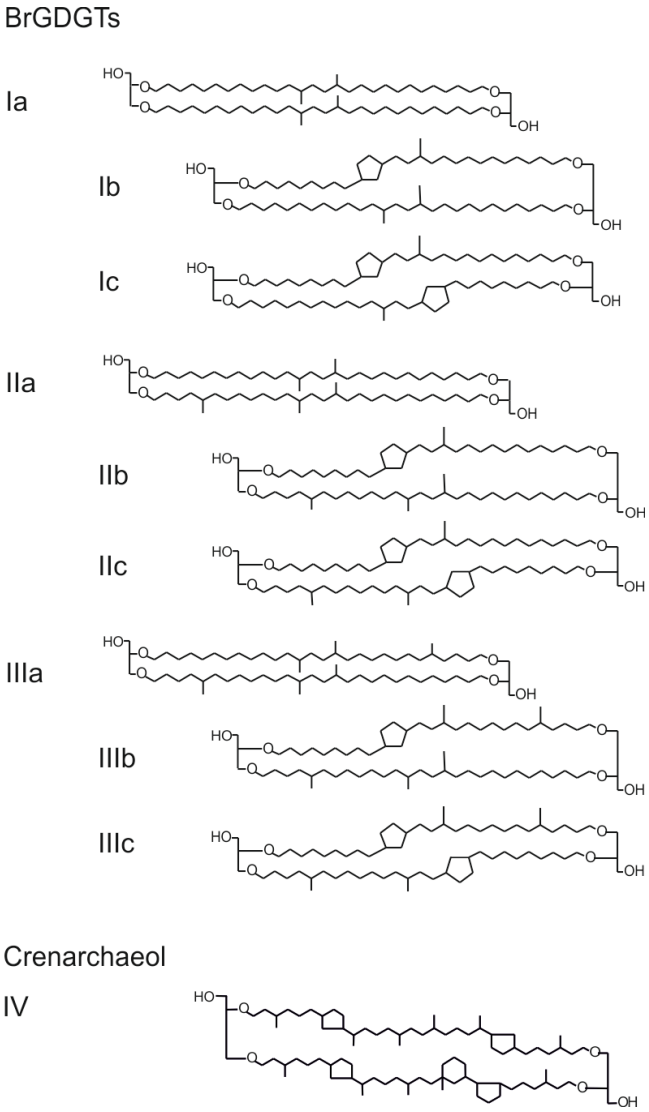

Fig. 6.1 Structures of branched GDGTs used in equations 6.1-6.10 (see text).

6.3 Study site

Lake Belau is a small lake located in the young moraine landscape in northern Germany (10°16´E, 54°6´N) close to the southwest Baltic Sea/Kattegat and Skagerrak (Figure 6.2). The maximum water depth is ~29 m and the surface area is around 1.13 km^2 (Müller, 1981). The catchment area comprises a size of ~3.37 km^2 (Naujokat, 1997). Lake Belau is part of a connected system of kettle hole lakes (Figure 6.2) that was formed during the Weichselian glaciation (Fränzle et al., 2008; Garbe-Schönberg et al., 1998). The Schwentine River that drains northwards into the Baltic Sea connects the lakes (Garbe-Schönberg et al., 1998). Lake Belau is an eutrophic lake as a consequence of its nutrient-rich conditions and intense plankton production (Landmesser, 1993; Landesamt, 2011). In the Lake Belau region, the modern air temperature within one annual cycle ranges from below zero during winter to 15-20°C in summer. Over the past ~130 years the average summer temperature (June to August) and the annual mean has been 16.1±0.9°C and 8.4±1.6°C, respectively (www.dwd.de meteorological data).

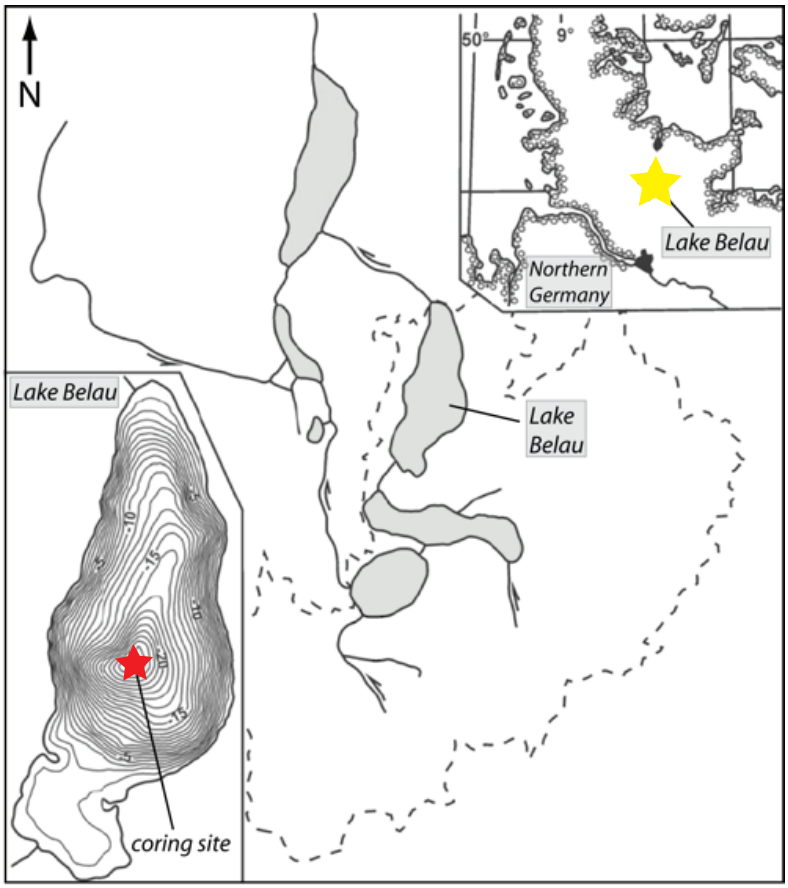

Fig. 6.2 Lake Belau (yellow star) is located in northern Germany between the Baltic Sea, Skagerrak, and North Atlantic. The coring position of the lake sedimentary sequence is marked with a red star. Figure is slightly modified from Zahrer et al. (2003).

During the post-glacial period that covers the complete Holocene interval, major changes in vegetation pattern around Lake Belau are documented (Wiethold, 1998; Dörfler et al., 2012). Prior to the first evidence of initial agrarian societies occurring at ~6000 cal. yr BP, shifts in the vegetation pattern were probably mainly impacted by regional climate conditions (Wiethold, 1998; Dörfler et al., 2012). Before the mid Holocene period, a mixed deciduous forest dominated the Lake Belau catchment area. At ~5900 cal. yr BP, the palynological record documents an increase in micro-charcoal particles that clearly indicates the occurrence of early farming societies associated with “slash-and-burn” agricultural techniques for forest clearance (Wiethold, 1998; Dörfler et al., 2012). Between ~5500 and 5100 cal. yr BP, a period of intensified land use is documented in the Lake Belau, as indicated in the occurrence of pioneer plants such as *Plantago lanceolata,* several grasses (both indicative of deforestation), and cereal pollen (Wiethold, 1998; Dörfler et al., 2012; Feeser et al., 2012; Kirleis et al., 2012). In contrast, between ~5100 and 2600 cal. yr BP, the landscape was characterized by reduced land use and woodland regeneration. After ~2600 cal. yr BP, a re-intensification of agricultural activity during the Bronze Age is documented (Garbe-Schönberg et al., 1998; Wiethold, 1998; Dörfler et al., 2012).

6.4 Material and methods

6.4.1 Soil and lake material

Six surface soil samples were collected from sites within the lake´s catchment area. All soils are of modern-age and are located both on the west and east side of the lake (Figure 6.2).
The lake sedimentary sequence was recovered from ~28.3 m water depth in 2002 (Figure 6.2) and covers almost the complete Holocene period. The sediment core consists of several combined segments from four parallel cores, whereas each segment is ~2 m in length. The segments were inter-connected by the identification of several specific markers (i.e. tephra layers) that are evident in several parallel segments of same age. Consequently, the composite sedimentary sequence consists of sections of multiple segments from four different parallel cores and has a total length of ~24 m. The stratigraphic connection between the different sections is fully discussed in Dörfler et al. (2012). Based on this composite sedimentary sequence, an age-depth model was developed. For the time period investigated in this study (~7900 to 2300 cal. yr BP), the age model is based on several AMS^{14}C dates, varve counting, and tephra layers. The radiocarbon dates were converted to calibrated years (cal. yr BP) using OxCal 4.1. We subsampled the lake core in ~4x4 cm slices that approximately covers a period of 20-25 years according to varve counting.

6.4.2 Branched glycerol dialkyl glycerol tetraethers (brGDGTs)

Ca. 4-5 g of freeze-dried and homogenized sediments (lake and soil samples) were extracted using an Accelerated Solvent Extractor (Dionex ASE-200) with a mixture of 9:1 (v/v) of dichloromethane:methanol (DCM:MeOH,) at 100 ºC and at 100 bar N_2 (g) pressure. The total lipid extracts (TLE) were dried under a gentle stream of pure N_2. Subsequently, we fractionated the TLE on activated Al_2O_3 columns. We used 9:1 (v/v) hexane:DCM, 1:1 (v/v) hexane:DCM, and 1:1 (v/v) DCM:MeOH as solvents to yield the apolar, ketone, and polar fractions, respectively. The fractions were subsequently dried under a gentle flow of pure N_2. Prior to analysis, the polar fraction that contains the *br*GDGTs was dissolved ultrasonically in 99:1 (v/v) hexane:isopropanol and filtered through an 0.45 µm syringe filter. The *br*GDGTs were analysed using High Performance Liquid Chromatography (HPLC-MS) using the method described in detail by Weijers et al. (2006; 2007). Peak areas of the single *br*GDGT compounds were determined by manual integration using the HP Chemstation software package. The MBT and CBT indices were calculated according to equations 6.1 to 6.3, the air and lake temperatures according to equations 6.4 to 6.9, equations 6.4 and 6.5 being soil-based calibrations (used for estimating air temperature) and 6.6 to 6.9 being lake-based calibrations (used for estimating lake temperature). Hereafter, temperatures are reported as Mean Annual Temperature (MAT) or Mean Summer Temperature (MST). We also calculated the BIT index ("Branched vs. Isoprenoid Tetraethers") (equation 6.10) in order to determine the potential influence of soil material in the lake samples (Hopmans et al., 2004):

BIT=(Ia+IIa+IIIa)/(Ia+IIa+IIIa+crenarchaeol) (Hopmans et al., 2004) (6.10)

6.5 Results

6.5.1 Distribution of brGDGTs in soil and lake samples

All soil and sediment samples contained *br*GDGTs. Both soil and lake samples, on average, show a clear dominance of *br*GDGTs without cyclopentyl moieties (a-series), followed by compounds with one or two rings (b- and c-series, respectively) (Figure 6.3). However, the relative abundance of each *br*GDGT within the a-series differs: IIa is most dominant in the averaged lake samples followed by IIIa and Ia, while the soil samples are dominated by Ia followed by IIa and IIIa. The b-series is more common in the lake samples with IIb and Ib as the most prominent ones, whereas it occurs only in minor abundances in the soil samples. Both, IIIb and IIIc were not detected in the soil samples, and only to a very small extent in the lake samples (Figure 6.3).

Throughout the time interval studied (~7900 to 2300 cal. yr BP), we do not record any major changes in the distribution of lake *br*GDGTs (Figure 6.3).

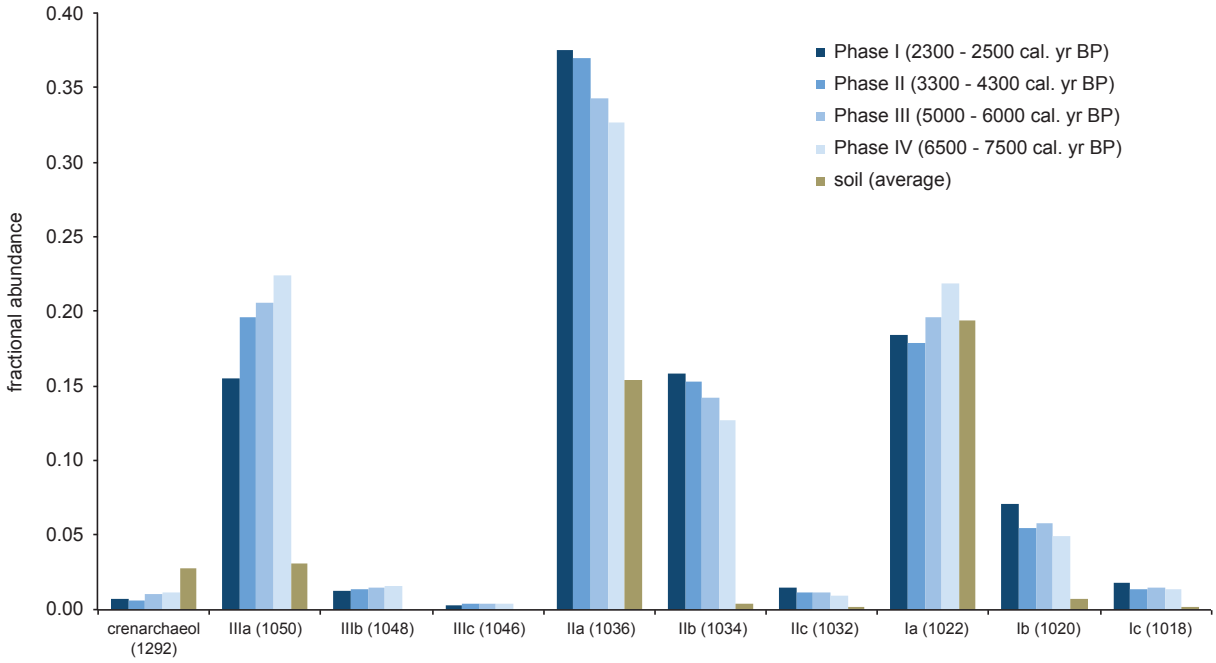

Fig. 6.3 Abundance of different fractions of *br*GDGTs for all lake sediments (blue colours) and soil samples (brown), whereas the lake samples are additionally reported in time series (~10 samples in each series; blue colours). In general, the a-series (Ia, IIa, and IIIa) contains the most abundant *br*GDGTs followed by the series b and c. The dominance of each *br*GDGT compound within the a-series differs in the soil and lake samples. Each lake time series represents a period of contrasting temperatures (Phase I: warm; phase II: cool/stable; phase III: warm; phase IV: cooling). There are no major changes between the different time series regarding the fractional abundance of each *br*GDGT homologue, and all differs from the *br*GDGT pattern in the soil samples. This suggests that there was no change in the major *br*GDGT source throughout the time interval measured (~7900 to 2300 cal. yr BP).

6.5.2 Temperature estimation in soil samples

In the six soil samples investigated in this study, the averaged MBT, MBT´, and CBT indices were 0.51±0.04, 0.51±0.04, and 1.56±0.28, respectively. Regardless which soil-based temperature equation we applied (Weijers et al., 2007; Peterse et al., 2012), we generally obtained a large scatter in absolute temperatures. When using the temperature equation of Weijers et al. (2007), we calculated an average for the MATs (mean annual air temperature) of 4.8±2.1ºC, which underestimates modern mean annual air temperatures (~8.4ºC). The recently modified soil-calibration of Peterse et al. (2012), which excludes IIIb and IIIc, shows averaged MAT of 7.3±1.4ºC that is in the range of present-day values. This suggests that the re-calibration of Peterse et al. (2012) is most reliable for estimating MATs in modern soils at the Lake Belau site.

6.5.3 Soil- and lake-based temperature estimations in lake samples

In the ~7900 to 2300 cal. yr BP time interval studied, the MBT, MBT´, and CBT indices documented averages of 0.27±0.02, 0.23±0.02, and 0.45±0.04, respectively. Lake MATs using the soil-based calibrations (Weijers et al., 2007; Peterse et al., 2012) ranged from of 4.7 to 6.4ºC and 1.9 to 5.8ºC, respectively (Figure 6.4). Thus both temperature equations are providing temperature estimates that are constantly colder than the MATs calculated from the modern soil samples and also lower compared to present day MAT (~8.4ºC).

Instead, when using the lake-based calibration of Zink et al. (2010) (Figure 6.4) to estimate past MATs and MSTs, the resulting values range from 7.0 to 12.3ºC and 12.0 to 16.0ºC, respectively, which are in the order of modern temperatures. Other lake calibrations indicate MATs (Tierney et al., 2010) and MSTs values ranging between 13.4 and 22.0ºC and 16.5 and 21.5ºC (Pearson et al., 2011). These represent MATs warmer than those observed today and MSTs within the range of present-day MST (Figure 6.4).

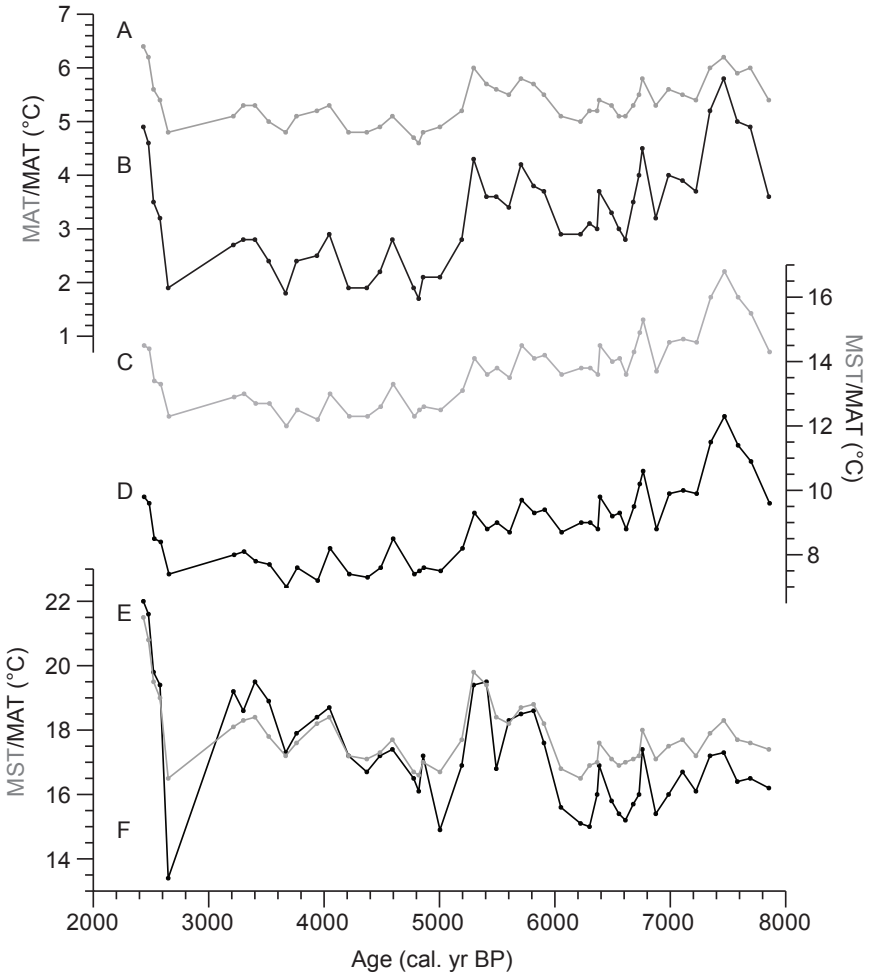

Fig. 6.4 Temperature estimations (MAT: mean annual air temperature/MST: mean summer air temperature) at the Lake Belau site using soil-based (A-B) and lake-based (C-F) temperature equations. The soil-inferred temperature equations are based on the calibration sets of Peterse et al. (2012; A) and Weijers et al. (2007; B), whereas the lake-inferred are based on Zink et al. (2010; C-D), Pearson et al. (2011; E), and Tierney et al. (2010; F).

6.6 Discussion

6.6.1 Sources of branched GDGTs at the Lake Belau site

The diverging *br*GDGT distribution between lake and soil samples suggests that the *br*GDGTs (Figure 6.3) are of aquatic origin (in situ production), as previously reported from other lake settings (e.g., Blaga et al., 2010; Tierney et al., 2010). Additionally, as we do not record any major changes in the distribution of lake *br*GDGTs throughout the complete mid to late Holocene record (Figure 6.3), we assume that the origin of lake *br*GDGTs did not significantly vary back in time. Although the lake BIT index, which has often been interpreted to reflect high terrestrial input (Hopmans et al., 2004; Niemann et al., 2012), is continuously high (0.98-0.99) throughout the complete record, we argue that this is not a straightforward evidence for non-aquatic production of the *br*GDGTs in the lake sediments, if assuming that *br*GDGTs are additionally produced within the lake and not only in soils (Schouten et al., 2013).

Given the comparison of modern soil and downcore lake *br*GDGTs distributions, we assume that in situ production of *br*GDGTs is the dominant contribution to Lake Belau sediments while a major terrestrial origin or *br*GDGTs is more unlikely. Therefore, we conclude that a lake-based calibration (Figure 6.4C-F) is probably more suitable for reconstructing past temperatures at the Lake Belau site.

6.6.2 Lake-based temperature estimations in the lake samples and general trends throughout the mid and late Holocene period (~7900 to 2300 cal. yr BP)

The Zink et al. (2010) MAT and MST lake-based calibrations (Figure 6.4C-D) indicate an overall non-monotonic cooling over the period studied that followed a warm early Holocene centred at ~7400 cal. yr BP. Following the warm peak at ~7400 cal. yr BP, these calibrations lead to an estimation of an warming interval until ~5300 cal. yr BP. After ~5300 cal. yr BP, the *br*GDGT-derived temperatures showed a cooling of ~2ºC until ~2600 cal. yr BP, followed by a 2.5ºC warming until ~2400 cal. yr BP (Figure 6.4C-D). In contrast, the other lake-based temperature equations (Tierney et al., 2010; Pearson et al., 2011) (Figure 6.4E-F) result in a long-term warming trend opposite to the results from the lake calibrations of Zink et al. (2010). Only the two prominent warming intervals occurring between ~6000 and 5000 cal. yr BP and after ~2600 cal. yr BP apparently match the warm intervals observed in the lake-based calibration of Zink et al. (2010) (Figure 6.4C-F). Furthermore, the overall Holocene MAT/MST warming trend of 1 to 2°C that results from the calibrations based on African and globally distributed lakes (Tierney et al., 2010; Pearson et al., 2011; MST; Figure 6.4E-F), is not comparable with any existing paleo-climate records from adjacent areas (Moros et al.,

2004; Seppä et al., 2005; Jansen et al., 2008; Krossa et al., submitted). To our knowledge, only increases in winter temperature estimated for NW Europe based on pollen counts (Davis et al., 2003) show a Holocene warming trend of similar amplitude as calculated when using the MAT and MST calibrations of Tierney et al. (2010) and Pearson et al. (2011). However, the absolute values of these two lake-based calibrations are much too high in terms of winter season temperatures for this period. In contrast, the Lake Belau MAT and MST reconstructions based on the equations of Zink et al. (2010) document an overall cooling that is coherent with other paleo-climate reconstructions from the region (Figure 6.4). This suggests that the equations 6.6-6.7 probably are the most suitable calibrations for the Lake Belau samples.

6.6.3 Implications of *br*GDGT-derived paleo-temperatures in the context of existing regional paleo-climate records

Over the mid to late Holocene (~7900 to 2300 cal. yr BP), our *br*GDGT-derived temperature reconstruction documents a non-monotonic temperature trend which mimics many orbital-related cooling observed elsewhere at such latitudes (Leduc et al., 2010; Schneider et al., 2010; Lohmann et al., 2013) (Figure 6.5). Paleo-temperature reconstructions from the adjacent northeastern Skagerrak (Krossa et al., submitted) and central South Sweden (Seppä et al., 2005) document millennial-scale temperature shifts that are not compatible with the Lake Belau record (Figure 6.5). In particular, the Lake Belau *br*GDGT-derived temperature record indicates a ~2ºC cooling after the warm early Holocene peak centred at ~7400 cal. yr BP and a slight warming between ~5900 and 5300 cal. yr BP that are both opposite to the warming and cooling intervals observed in the Skagerrak and south Sweden paleo-temperature records (Figure 6.5). Also, the warming occurring after ~2600 cal. yr BP in the Lake Belau record has no clear counterpart in the northeastern Skagerrak and central South Sweden. The Skagerrak and south Sweden temperature records most likely represent a shift from a maritime towards a continental-dominated atmospheric circulation pattern over the Baltic region at ~6300 cal. yr BP fostered by stronger outflow of cold Baltic Sea outflow (Krossa et al., submitted). As Lake Belau is located close to the Baltic Sea, we would expect that climate conditions occurring over the Baltic region should also impact the climate in the Lake Belau region. In this context, the opposite temperature trends between northeastern Skagerrak/central South Sweden and Northern Germany (Lake Belau) are surprising given the small geographical distances among these sites.

One possibility to explain the discrepancy between the Lake Belau and the Skagerrak/south Sweden sites might be that the main production of *br*GDGTs in lakes occurs during the summer season (Castaneda and Schouten, 2011; Sun et al., 2011) while the Skagerrak

and Swedish signals (Figure 6.5) reflect mean annual temperature conditions (Seppä et al., 2005; Krossa et al., submitted). Warmer summers over Schleswig-Holstein would in turn match a predominant continental atmospheric circulation pattern (Hurrell, 1995; Hurrell et al., 2003), as suggested for the Baltic region during the mid Holocene (Krossa et al., submitted). Therefore, it seems likely that the *br*GDGTs records the warmer period of the seasonal cycle rather than mean annual temperatures.

Nonetheless, as recent studies have revealed the presence of structural isomers that may co-elute with *br*GDGTs (De Jonge et al., 2013; 2014), it must be further checked whether the isomers react differently to environmental factors, and thus could bias the existing temperature calibrations. It might be possible that an improved chromatographic method to quantitatively isolate these isomers will reveal slightly another temperature trend in our Lake Belau record. For the moment, we assume that during this period of predominantly continental climate conditions between ~5900 and 5300 cal. yr BP was characterized by frequently cold winters and warm summers over Schleswig-Holstein. A similar atmospheric circulation pattern may have occurred at around ~7400 cal. yr BP and ~2500 cal. yr BP when the temperature records indicated large contrasts between Lake Belau and the Skagerrak (Figure 6.5).

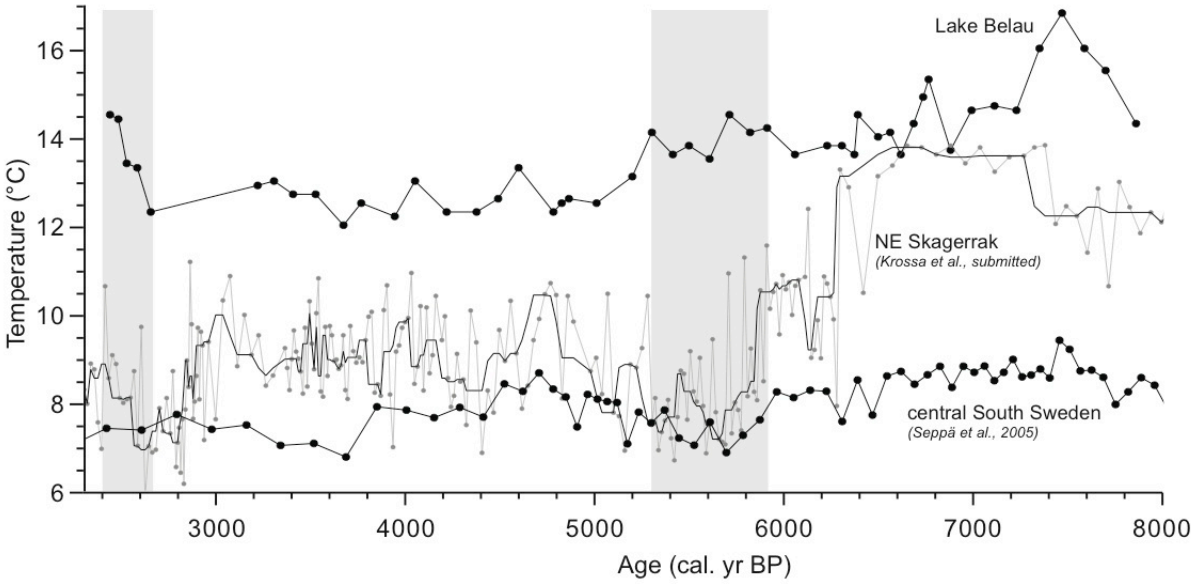

Fig. 6.5 Comparison of *br*GDGT-derived summer temperatures from Lake Belau (see Figure 5C) to adjacent paleo-temperature reconstructions (NE Skagerrak and central South Sweden; Seppä et al., 2005; Krossa et al., submitted) that reflect mean annual temperatures. The grey bars indicate periods of diverging temperature trends, when a cooling is recorded in the NE Skagerrak/S Sweden record opposite to the warming in the Lake Belau record.

6.6.4 Farming activity around Lake Belau and a possible impact on the biomarker signal

During both intervals with strong seasonal contrast under continental climate conditions at ~5900-5300 cal. yr BP and after ~2600 cal. yr BP, palynological and (bio)-geochemical records from Lake Belau and catchment soil samples document periods of intensified agricultural land use (Wiethold, 1998; Dörfler et al., 2012; Dreibrodt and Wiethold, 2014). First evidence for small-scaled agrarian-based societies occurred at ~6000 cal. yr BP in the Lake Belau area followed by a period of intense cultivation activity between ~5500-5100 cal. yr BP (Figure 6.6). In parallel, (bio-) geochemical records indicate intensified primary production in the lake inferred from increased biogenic silica and lowered C/N ratios, that in turn caused increased sedimentation and anoxic bottom water conditions (lowered Mn/Fe ratios) at ~5650 cal. yr BP (Wiethold, 1998; Dörfler et al., 2012; Dreibrodt and Wiethold, 2014) (Figure 6.6). The authors interpret the increase in lacustrine productivity as a clear response to agricultural land use. Additionally, there is evidence for increased soil erosion around Lake Belau, however; only low amounts of minerogenic input into the lake are described. The latter supports our result of no major changes in soil vs. aquatic *br*GDGTs during that time period (see above; Figure 6.3). Also an anthropogenic-forced lacustrine primary production seems unlikely to alter the distribution of brGDGTs within the lake since the temperature increase documented in the Lake Belau *br*GDGT record starts a few centuries earlier than the occurrence of intensified primary production (Dreibrodt and Wiethold, 2014).

After ~2600 cal. yr BP, we observe another *br*GDGT-derived temperature increase of several degrees that is not comparable with other paleo-temperature records from the region (Figure 6.5). During that period, the palynological record documents a re-opening of the landscape, while (bio-) geochemical records suggest an intensified primary production and input of (soil-derived) minerogenic material into the lake system, probably linked to intensified agriculture (Wiethold, 1998; Dörfler et al., 2012; Dreibrodt and Wiethold, 2014). Intensified soil erosion (Dreibrodt and Wiethold, 2014) may have also increased the input of soil-derived *br*GDGT. However, as we do not record any changes in distribution of *br*GDGT pattern prior to and after ~2600 cal. yr BP (Figure 6.3), we exclude that the input of soil-derived *br*GDGTs was likely to cause an artificial increase in the temperature signal. Since we have ruled out an impact of soil-derived *br*GDGTs on our Lake Belau temperature record during these two major warming intervals, we consider both intervals as phases of larger seasonal contrast between summer and winter temperatures in the Baltic and Schleswig-Holstein region as described above.

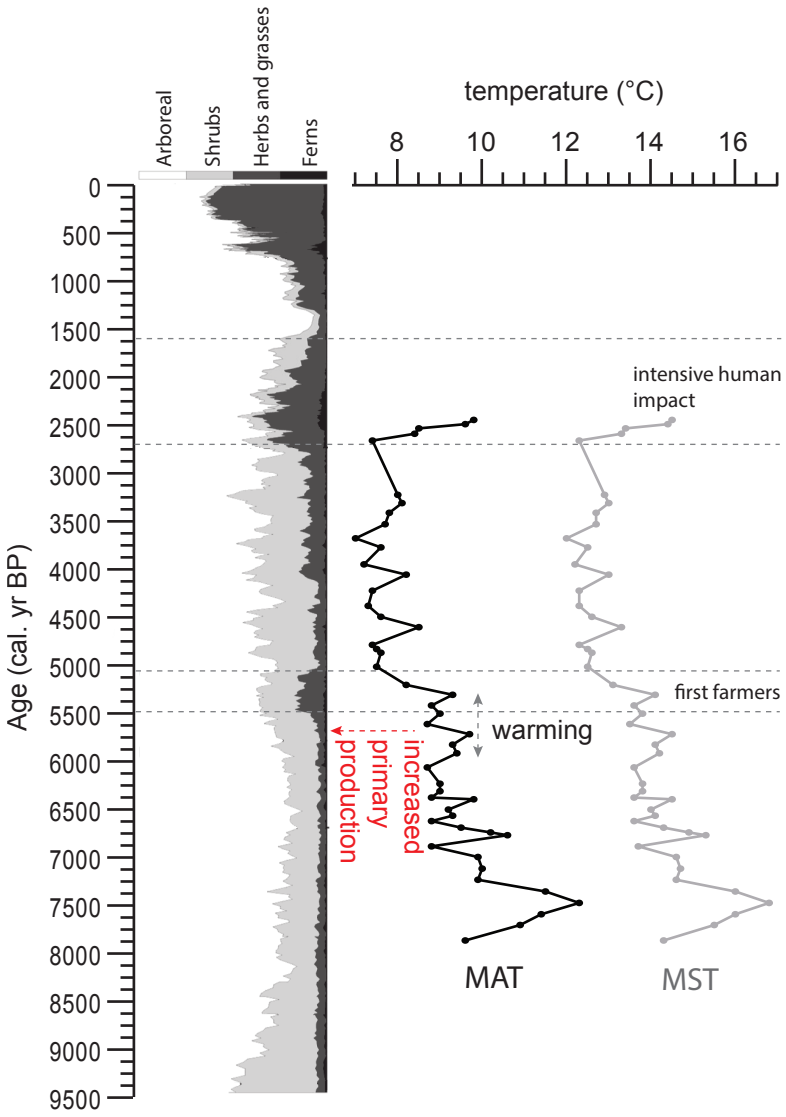

Fig. 6.6 Comparison of the temperature reconstruction (calibration sets based on Zink et al., 2010) to natural and human-induced changes in vegetation (analyses by Wiethold, 1998) at the Lake Belau site. Between ~5500 and 5100 cal. yr BP and after ~2600 cal. yr BP, clear indicators for forest clearance are documented in the increase in herbs and grasses An increase in lake primary production occurs at ~5650 cal. yr BP but ~100-200 years later than the *br*GDGT-inferred warming.

6.6.5 Implications of the brGDGT-derived temperature reconstruction and possible impact on the onset of first farming societies around Lake Belau during the mid Holocene period

The period of highest seasonal contrast between ~5900 and 5300 cal. yr BP matches the appearance of first agricultural elements in the Lake Belau area, whereas the disappearance of the fully developed local farming society occurs concomitantly with the ~1.5ºC cooling reaching lowest temperatures at around 4800 cal. yr BP (Figure 6.6). First agricultural elements occur at ~6000 cal. yr BP as indicated by “slash-and-burn” forest clearance, whereas

evidence for a fully developed agrarian society is documented between ~5500 cal. yr BP and 5100 cal. yr BP (Dörfler et al., 2012; Wiethold, 1998). Therefore, our Lake Belau temperature reconstruction implies a connection between the onset and disappearance of local farming societies in northern Germany and climate change during the mid Holocene. Our results hence suggest that the inferred summer warming and winter cooling provoked environmental conditions that were favourable for the fully establishment of farming in northern Germany.

6.7 Conclusion

We used a sedimentary record from Lake Belau in northern Germany to reconstruct past temperatures over a ~5600 year period (~7900-2300 cal. yr BP) to compare natural climate change to first periods of intensive land use. We used *br*GDGTs as a biomarker proxy to infer temperatures in lake sediments. We assume that the *br*GDGTs are most likely produced within the lake and not derived from the soil in the drainage area even under periods of intensive land opening and increase in soil erosion. We applied the lake calibration of Zink et al. (2010) to estimate past temperatures as it shows the best overall fit to published temperature reconstructions available in the region. We reconstruct intervals of warmth that are diverging from cooling periods documented in the adjacent northeastern Skagerrak and central South Sweden. At such short distances, we would expect that the climate conditions prevailing over the Baltic Sea region would lead to similar temperature records. Therefore, this discrepancy suggests either that the *br*GDGT are predominantly biosynthesized during warmer periods of the annual cycle than mean annual, or that the record is biased by a major input of soil-derived *br*GDGTs during periods of intensive land use. However, we do not find direct evidence that farming and landscape opening perturbed the *br*GDGT distribution in the lake system. Therefore, the prominent feature in the Lake Belau *br*GDGT-temperature record, the warm interval between ~5900 and 5300 cal. yr BP that was terminated by a ~1.5ºC cooling, is considered as a strong seasonal contrast under more severe continental climate conditions. Further more, the local temperature reconstruction implies a connection between the onset and disappearance of local farming societies around Lake Belau and local climate change, suggesting that the warming was favourable for growing crops in the Lake Belau area.

Acknowledgments. – We thank W. Dörfler and S. Dreibrodt (University of Kiel) for providing lake and soil material. We thank E. Hopmans and J. Ossebaar (NIOZ, Netherlands) for assistance with GDGT analysis. The work has been founded by the DFG SPP 1400 project “Early Monumentality and Social Differentiation”.

7 Implications on the TEX_{86} paleothermometry on Holocene sediments in the western Skagerrak

The first author has done the GDGT measurements in cooperation with Jung-Hyun Kim and Jaap S. Sinninghe Damsté at the department of Marine Organic Biogeochemistry at the NIOZ (the Netherlands). The first author has written the chapter. Ralph Schneider supervised the work.

7.1 Abstract

The TEX_{86}-temperature relationship has been applied in many marine settings in order to reconstruct both modern and past temperatures. In the Skagerrak area, previous studies have revealed a good match of reconstructed TEX_{86}-based sea surface temperatures using sediments covering the last ~100 years to observational and historical sea surface temperatures. In this study, we reconstructed TEX_{86}-temperatures using more recent sediments retrieved from a western Skagerrak multi-core sediment record. Further on, we attempted to test the applicability of the TEX_{86}-temperature proxy on early to late Holocene sediments retrieved from a gravity-core at the same site. Our sub-surface sediment results document a good match between present-day mean annual temperature and the sea surface temperature (SST) estimates based on the TEX_{86}^{H} calibration proposed for oceans with SSTs higher than 15ºC. In contrast, applying the TEX_{86}^{L} calibration (<15ºC) on the multi-core samples always results in SST estimates by 6 to 8ºC lower than ambient temperatures. This suggests that the TEX_{86}^{H} calibration is best suited for the modern conditions in the Skagerrak and does probably reflect mean annual SST. When applying the TEX_{86}^{H} calibration on the gravity-core sedimentary sequence that covers the complete Holocene, we document temperatures ranging from 7 to 12ºC. Over the last ~2500 cal. yr BP, the TEX_{86}^{H} temperature estimation in the gravity-core sediments provides values similar to $U^{K'}_{37}$-based temperatures and both methods document a prominent cooling trend. Prior to ~2500 cal. yr BP, the TEX_{86}^{H}-derived temperatures do not indicate the mid Holocene warming as apparent in the $U^{K'}_{37}$-based reconstruction. This difference suggests that the TEX_{86}^{H} and the $U^{K'}_{37}$ proxies, during generally warm climate conditions as the mid Holocene Climate Optimum, represent temperatures of different seasons and/or that the TEX_{86}^{H} then preferentially recorded sub-surface water temperatures.

7.2 Introduction

In northwestern Europe, the Skagerrak is a transitional area between the open North Atlantic and northern Europe, and therefore represents an excellent opportunity to document past changes in land-sea climate interactions. Over the past decades, a number of proxies based on a variety of biomarkers have been developed to infer past paleo-temperatures in marine settings. Among those, the alkenone unsaturation index $U^{K'}_{37}$ and its linear relationship to sea surface temperature (SST) has been applied virtually everywhere in the ocean and is considered as a robust SST proxy. More recently, the TEX_{86} index (TetraEther indeX with 86 carbon atoms, equation 7.1) and its relationship to temperature was proposed as an additional proxy to infer past temperatures from marine settings (Schouten et al., 2002). The TEX_{86}-temperature relationship is based on the relative abundance of isoprenoidal glycerol dialkyl glycerol tetraether (GDGTs), mainly biosynthesized by Thaumarchaeota (Sinninghe Damsté et al., 2002). Isoprenoidal GDGT lipids are membrane-forming compounds diagnostic for members of the archaeal domain that are abundant and present in many environmental settings, in particular in the marine environment (Karner et al., 2001; Powers et al., 2004; 2010; Tierney et al., 2008; Blaga et al., 2009; Sinninghe Damsté et al., 2009).

Since the introduction of the TEX_{86} temperature proxy, multiple studies have provided insights in understanding the paleo-thermometry (Kim et al., 2008; 2010; Liu et al., 2009; Kabel et al., 2012; Schouten et al., 2013). Most importantly, Kim et al. (2010) defined two novel TEX_{86} indices (equations 7.2 and 7.3) that are representable for oceans with modern mean annual SSTs ranging between 5-15ºC (TEX_{86}^{L} "low") and 15-28ºC (TEX_{86}^{H} "high"), whereas both indices are highly correlated to mean annual SST (equations 7.4 and 7.5) whereas the numbers correspond to the GDGT compounds (Figure 7.1):

TEX_{86}=(GDGT-2+GDGT-3+Crenarchaeol-regio-isomer)/(GDGT-1+GDGT-2+GDGT-3+Crenarchaeol-regio-isomer)		Schouten et al. (2002)	(7.1)
TEX_{86}^{H}=log(TEX_{86})		Kim et al. (2010)	(7.2)
TEX_{86}^{L}=log(GDGT-2)/(GDGT-1+GDGT-2+GDGT-3)		Kim et al. (2010)	(7.3)
SST=64.8xTEX_{86}^{H}+38.6	(r^2=0.87, n=255)	Kim et al. (2010)	(7.4)
SST=67.5xTEX_{86}^{L}+46.9	(r^2=0.86, n=393)	Kim et al. (2010)	(7.5)

However, some studies have indicated that the temperature relationship proposed by Kim et al. (2010) might not be directly applicable in every setting and that a regional calibration including the TEX_{86}^{H} or TEX_{86}^{L} indices is essential (Kabel et al., 2012; Schouten et al., 2013). Also, studies have indicated that Thaumarchaeota habitat depth is not restricted to the surface water but rather dwell in a range of water depths depending on location (Karner et al., 2001; Wuchter et al., 2006; Lincoln et al., 2014).

In the Skagerrak, first attempts have been performed to test the application of the TEX_{86}-temperature relationship using surface and sub-surface sediments (Rueda et al., 2009). These authors found a high correlation to present-day mean annual SST using the TEX_{86} index (and re-calibrated TEX_{86}^{H} index). Here, we attempt to test the applicability of the TEX_{86}-temperature relationship on past sediments using a gravity-core located in the central Skagerrak that covers the complete Holocene period. We also attempt to compare our results to existing alkenone-based SST temperatures ($U^{K'}_{37}$-SST) derived from a gravity-core in the central Skagerrak that covers the past 7000 years (Krossa et al., submitted).

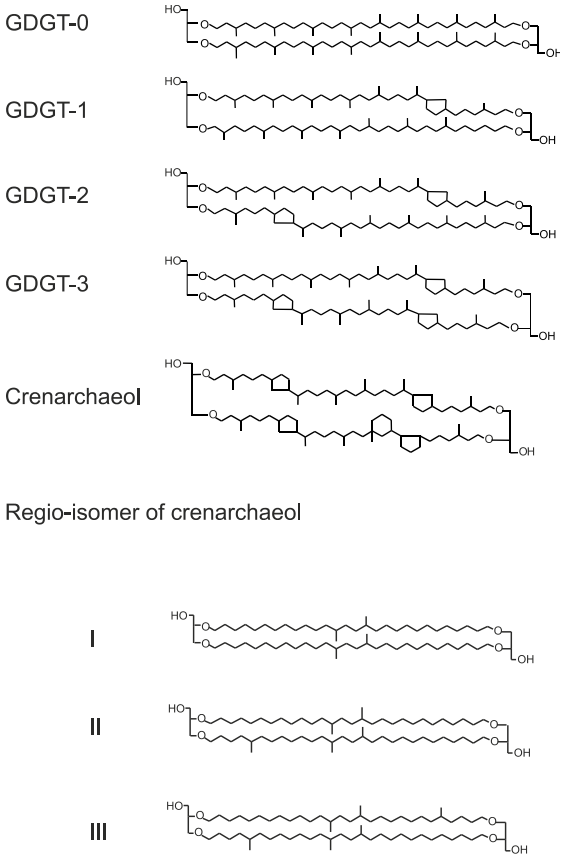

Fig. 7.1 Structure of isoprenoid GDGTs used for equations 7.1 to 7.3 in this study.

7.3 Study site

The Skagerrak lies in the north of the epicontinental North Sea and has a fjord-like shape (Thiede, 1987) that exceeds maximum water depths of more than 700 m (Rodhe, 1987), thus representing the deepest part of the otherwise shallow North Sea. In the present day Skagerrak, SSTs are mainly determined by the interplay between the inflow of North Atlantic water and the outflow of Baltic Sea water (Krossa et al., submitted). In the western and central Skagerrak, SSTs are most dominantly governed by the inflow of North Atlantic water rather

than the outflow of Baltic Sea water. Today, and probably over the last 8500 cal. yr BP (Gyllencreutz, 2005), a branch of saline North Atlantic water enters the Skagerrak/North Sea between Scotland and Norway and via the English Channel. The South Jutland Current, consisting of water from the English Channel and southern North Sea, flows northwards along the Danish coast and mixes with the North Jutland Current that originates from the North Atlantic and the central North Sea water. As the current passes Skagen (Figure 7.2) and enters the Skagerrak/Kattegat border, part of it mixes with fresher and colder Baltic Sea water. Thereupon, it forms an anti-clockwise gyre that exits the Skagerrak, back flowing along the Norwegian coast as the Norwegian Coastal Current (Figure 7.2). The North Atlantic branch mainly influences sub-surface and deeper waters.

Modern data suggest sea surface temperature ranging from ~4ºC during winter to ~16ºC during summer months, with an annual average of ~9-10ºC for the Skagerrak region (Locarnini et al., 2010).

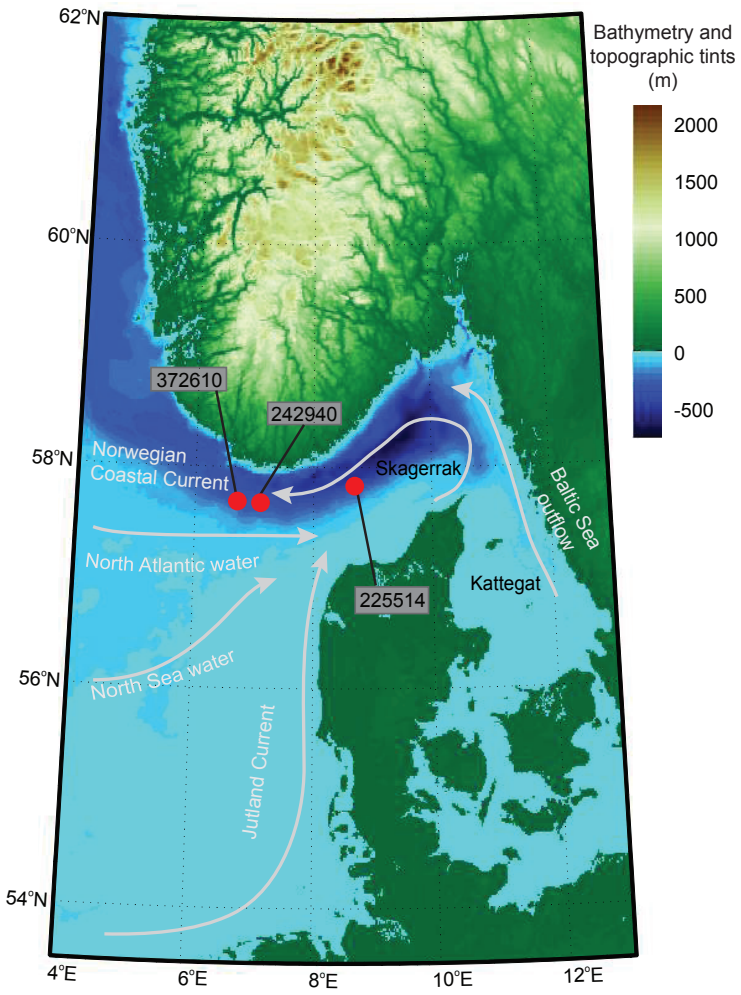

Fig. 7.2 Core locations in the Skagerrak area (core number in grey boxes). Pale grey arrows show present-day main surface current in the North Sea, Skagerrak, and Kattegat. The bathymetric and topographic lines are from IOC et al. (2003). The map is slightly modified from Krossa et al. (2014).

7.4 Material and methods

We used one multi-core and one gravity-core from site IOW242940-4 (57º40.52´N and 07º10.00´E, 316 m water depth) in the western Skagerrak (Figure 7.2) to reconstruct TEX_{86}-derived temperatures in both near-modern and past conditions. The multi- and gravity-cores were retrieved during a RV Poseidon cruise in 2002. To test the reliability of both near-modern and Holocene TEX_{86} temperature reconstructions, we compared the results with existing $U^{K'}_{37}$-SST records from the western and central Skagerrak at sites IOW372610 (57º41.05´N and 06º41.00´E, 320 m water depth, multi-core) and IOW225514 (57º50.28´N and 08º42.23´E, 420 m water depth, gravity-core) (Figure 7.2). All $U^{K'}_{37}$-SST records are already presented in Krossa et al. (submitted).

Glycerol dialkyl glycerol tetraethers

~1-2 g of freeze-dried and homogenized sediments were extracted using an Accelerated Solvent Extractor (Dionex ASE-200) with a mixture of 9:1 (v/v) of dichloromethane:methanol (DCM:MeOH,) at 100 ºC and at 100 bar N_2 (g) pressure. The extracts containing the Total Lipid Extract (TLE) were dried under a gentle stream of pure N_2. Subsequently, we fractionated the samples over an activated Al_2O_3 column. We used 9:1 (v/v) hexane:DCM, 1:1 (v/v) hexane:DCM, and 1:1 (v/v) DCM:MeOH as solvents to yield the apolar, ketone, and polar fractions. The fractions were subsequently dried under a gentle flow of pure N_2. Prior to the analysis, the polar fraction that contains the isoprenoid GDGTs was dissolved ultrasonically in 99:1 (v/v) hexane:isopropanol and filtered through an 0.45 µm syringe filter. The GDGTs were analysed using High Performance Liquid Chromatography (HPLC). Peak areas of the single GDGT compounds were determined by manual integration using the HP Chemstation software package. The TEX_{86} indices (TEX_{86}^{L}, and TEX_{86}^{H}) were calculated according to equations 7.1 to 7.2, the SST according to equations 7.3 to 7.4. Analytical precision based on duplicate analyses of samples during the whole procedure was on average 0.004 units of TEX_{86}^{H} that corresponds to an averaged error of 0.29ºC when using the calibration of Kim et al. (2010). The chemical pre-treatment and analyses were performed at the NIOZ organic geochemical laboratory (Texel, the Netherlands).

7.4.1 Chronology

The Skagerrak multi- and gravity-cores were dated using the $AMS^{14}C$ method, whereas parts of the age models are previously presented in Krossa et al. (2014) and supplemented by new $AMS^{14}C$ dates (Table 7.1).

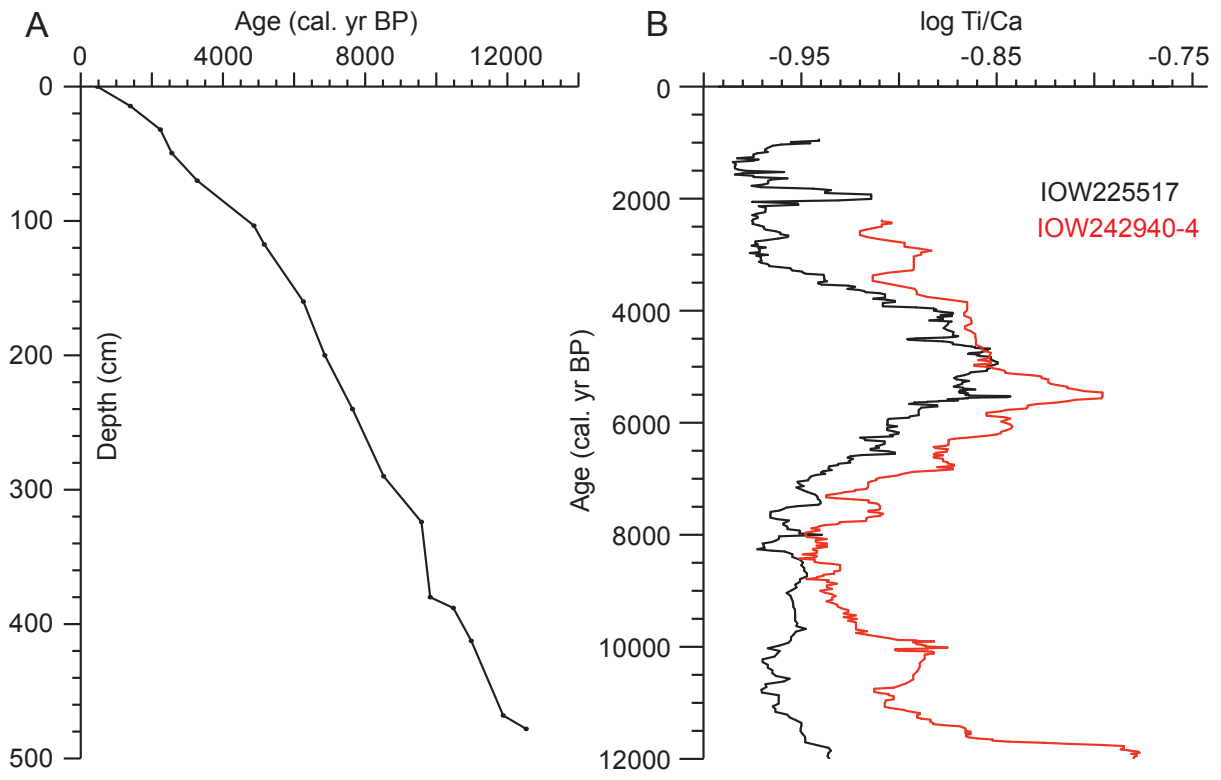

Fig. 7.3 A) Age-depth profile of the parallel core IOW242940-3 in the central Skagerrak (see also Table 7.1). The radiocarbon ages were converted into calendar years (cal. yr BP) using the online software Calib Rev 7.0, thereby applying the Marine13 data set and a standard reservoir age of 400 years (Reimer et al., 2013). The radiocarbon ages of IOW242940-3 were applied for exactly the same depths in IOW242940-4. B) To further constrain the age-depth model for IOW242940-4, we compared the log Ti/Ca from XRF scanner measurements to its counterpart from the well-dated gravity-core IOW225517 (Emeis et al., 2003; C. Butruille, unpublished data).

The multi-core age control is based on two radiocarbon dates in 0-1 cm (90±30 ^{14}C yr BP) and 35-36 cm core depth (895±30 ^{14}C yr BP). We did not convert the multi-core radiocarbon dates into calendar ages, as preliminary results from ^{210}Pb and ^{137}Cs measurements indicate that the standard 400 years marine reservoir age correction might not be applicable on sub-surface sediment in the Skagerrak (M. Moros pers. communication). In order to compare the TEX_{86}^{H} results from gravity-core IOW242940-4 with previously presented $U^{K'}_{37}$-SST records from the Skagerrak (Krossa et al., submitted), a new chronology had to be established. For this purpose, the radiocarbon dated age-depth tie points from the parallel core IOW242940-3 (Figure 7.3A) were applied for exactly the same depths in IOW242940-4 and the radiocarbon ages were converted into calendar years (cal. yr BP) applying the standard marine reservoir age of 400 years (Reimer et al., 2013), using the online software Calib Rev 7.0 with the Marine13 data set (Reimer et al., 2013) (Table 7.1). To further constrain the age-depth model for core IOW242940-4, we compared the log Ti/Ca record from XRF scanner measurements to its counterpart from the well-dated gravity-core IOW225517 (Emeis et al., 2003) at the same location (Figure 7.3B). We find an overall good relationship between the log Ti/Ca results of both cores, even though the matching between both cores could be improved

by aligning common small-scale features in the XRF records (Figure 7.3B). For this study, however, the direct age-depth transfer of radiocarbon ages between the parallel cores IOW242940-3 and IOW242940-4 is sufficient since we mainly discuss the long-term trends.

Tab. 7.1 Age determination of gravity-core IOW242930-3. The radiocarbon ages were calibrated (cal. yr BP) using the Calib Rev 7.0 software program and the Marine13 calibration set (Reimer et al., 2013) with an assumed standard marine reservoir age of 400 years. Omitted radiocarbon ages are in italics.

Depth (cm)	Dated material	Age (^{14}C yr BP)	Calibrated age min – max (1σ range, cal. yr BP)	Calibrated age med. (1σ range, cal. yr BP)	Lab Ref.	C (mg)	Reference
		Skagerrak GC 242940-3 (57°40.52´N, 07°10.00´E)					
0	Mixed benthic foraminifera	830±30	445-494	468	KIA 18309	1.2	Krossa et al. (2014)
14.5	Mixed benthic foraminifera	1840±90	1297-1482	1395	Poz-45813	0.2	Krossa et al. (2014)
32	Mixed benthic foraminifera	2565±30	2195-2298	2240	KIA 18598	0.7	Krossa et al. (2014)
49.5	Mixed benthic foraminifera	2820±80	2468-2690	2561	Poz-45814	0.3	Krossa et al. (2014)
70	Mixed benthic foraminifera	3405±30	3232-3326	3277	KIA 18599	0.8	Krossa et al. (2014)
103.5	Mixed benthic foraminifera	4650±35	4822-4909	4871	KIA 18310	1.1	Krossa et al. (2014)
117.5	Mixed benthic foraminifera	4855±35	5113-5251	5163	KIA 18600	1.1	Krossa et al. (2014)
160	Mixed benthic foraminifera	5845±40	6213-6297	6263	KIA 18601	0.9	Krossa et al. (2014)
200	Mixed benthic foraminifera	6590±40	6787-6935	7109	KIA 18311		This study
240	Mixed benthic foraminifera	7380±45	7590-7682	7847	KIA 18602		This study
290	Mixed benthic foraminifera	8265±40	8467-8575	8810	KIA 18312		This study
324	Mixed benthic foraminifera	9125±50	9516-9640	9878	KIA 18313		This study
361	*Mixed benthic foraminifera*	*9890±55*	*10499-10593*	*10843*	*KIA 18314*		*This study*
380	Mixed benthic foraminifera	9295±45	9719-9913	10140	KIA 18315		This study
388	Shell	9810±50	10427-10538	10729	Poz-8187		This study
412.5	Shell	10200±50	10909-11110	11193	Poz-8186		This study
468	Shell	10800±50	11746-11969	12281	Poz-8183		This study
478	Mixed benthic foraminifera	11200±55	12400-12455	12638	KIA 18316		This study

7.5 Results and discussion

7.5.1 TEX_{86} temperature estimates in the Skagerrak: comparing TEX_{86}^H and TEX_{86}^L of recent sediments

Even though the chronology of the multi-core is not fully completed (see chronology), we assume that our multi-core record from the central Skagerrak (IOW242940-4) probably covers the last centuries to millennium, whereas the uppermost samples most likely represent the last century. The uppermost samples indicate TEX_{86}^H-SST (equation 7.3) estimates of 8.5-10ºC, that is comparable to present-day mean annual sea surface temperature (Figure 7.2). In contrast, the TEX_{86}^L–based equation (equation 7.4) most likely underestimates ambient temperatures (Figure 7.4), even though this index is probably better suited for the reconstruction of past temperatures in ocean settings with present-day mean annual sea surface temperatures

lower than 15ºC (Kim et al., 2010). This is also supported by other core-top studies from the northeastern Skagerrak (Rueda et al., 2009), which documented the best correlation of TEX_{86}-SST (and re-calibrated TEX_{86}^{H}-SST) to modern and historical mean annual SST. This indicates that the TEX_{86}^{H} temperature equation (Kim et al., 2010) is best suited in the Skagerrak region for the modern situation.

Additionally, we observe TEX_{86}^{H}-temperatures similar to those of $U^{K'}_{37}$-based SSTs (Figure 7.4) derived from core-top and sub-surface samples of a nearby multi-core IOW372610 in the western Skagerrak (Figure 7.2). The latter indicates SST estimates of 9.5±0.9ºC on average that is comparable with present-day mean annual or early spring sea surface temperature in the Skagerrak (Krossa et al., submitted). Based on our core-top and sub-surface results, we therefore suggest that both $U^{K'}_{37}$- and TEX_{86}^{H} -derived temperatures probably recorded the same period of the annual cycle and the same water depth over the last centuries.

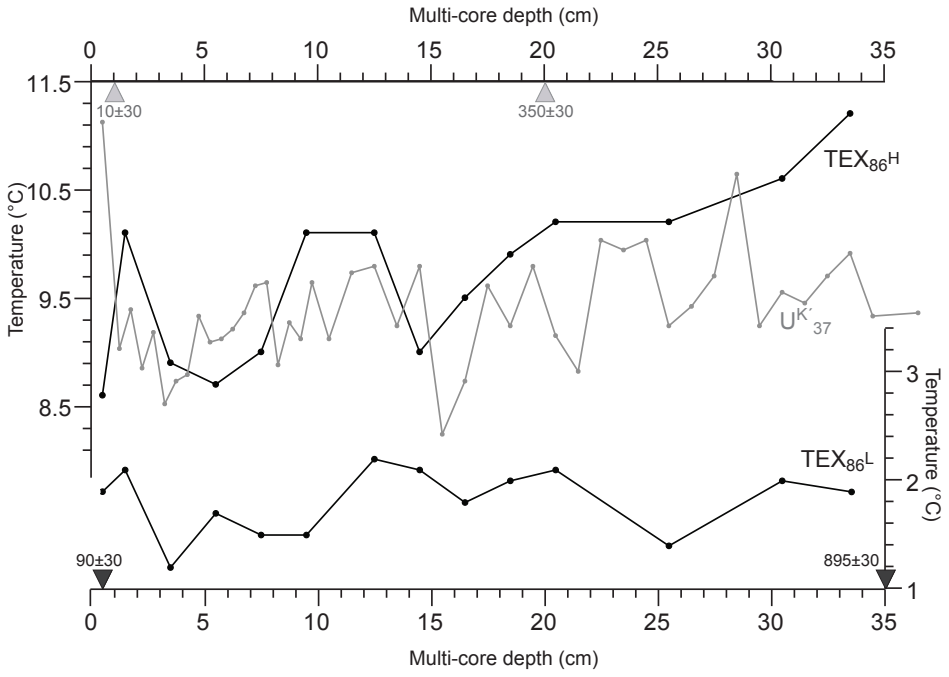

Fig. 7.4 Estimated TEX_{86}- and $U^{K'}_{37}$-temperatures from Skagerrak multi-core sediments (black/TEX_{86}: IOW242940-4; grey/$U^{K'}_{37}$: IOW372610). Multi-core radiocarbon dates, marked by black and grey triangles, were not calibrated (see text). We calculated TEX_{86}-temperatures using equations including the TEX_{86}^{H} and TEX_{86}^{L} indices (Kim et al., 2010). Present-day mean annual sea surface temperature is 9-10ºC (Locarnini et al., 2010) and fits well with both TEX_{86}^{H} and $U^{K'}_{37}$-derived temperatures. TEX_{86}^{L}-inferred temperatures are most likely underestimated.

7.5.2 Multi-proxy Holocene SST estimates using TEX_{86}-temperature relationship and comparison to gravity-core $U^{K'}_{37}$-SST reconstructions in the central Skagerrak

Similar to the recent sediment samples, early to late Holocene TEX_{86}^{H}-estimates indicate absolute reconstructed temperatures between 8.0 and 12.5ºC, whereas the TEX_{86}^{L}-temperature equation documents temperatures ranging between 0.5 and 5.0ºC (Figure 7.5). As observed in

the core-top and downcore samples, the TEX_{86}^{H} temperatures seems to provide reliable mean annual sea surface temperatures estimates, whereas the TEX_{86}^{L}–inferred temperatures appear much too cold (Figure 7.5), even if assuming that the temperature proxy might reflect winter conditions.

Even considering only the warm temperature calibration, we observe lower TEX_{86}^{H}-temperatures compared to the $U^{K'}_{37}$-SST estimates (Figure 7.6). While the central Skagerrak TEX_{86}^{H}-temperature reconstruction indicates temperatures oscillating between 7 and 9°C over the past ~7000 cal. yr BP (Figure 7.4), the $U^{K'}_{37}$-SST record from a nearby gravity-core located in the central Skagerrak (IOW225514) (Krossa et al., submitted) varies between 9 and 13ºC for the same period (Figure 7.6). In addition, the alkenone-derived temperature record in core IOW225514 documents a cooling trend over the last ~5000 cal. yr BP that is not observed in the TEX_{86}^{H} record presented in this study (Figure 7.6). The $U^{K'}_{37}$-SST and TEX_{86}^{H}-temperature reconstructions hence document diverging temperature trends prior to ~2500 cal. yr BP, while both proxies merge in absolute values after ~2500 cal. yr BP and in particular during the last centuries in multi-core samples (Figure 7.3). The diverging temperatures occurring until ~2500 cal. yr BP suggest that the season and/or water depth sampled by one or both of the two different signal carriers, Prymnesiophyta and Archaea, has changed over time in the Skagerrak.

Several studies argue that Thaumarchaeota are not restricted to the surface waters as are alkenone-producing organisms (coccolithophorids), but dwell in the sub-surface where the highest occurrence of ammonia is present (Wuchter et al., 2006; Huguet et al., 2007; Lee et al., 2008; Lopes dos Santos et al., 2010). In the Baltic Sea, preliminary studies have indicated that Thaumarchaeota probably dwell in deeper parts of the water column rather than the upper surface. Also, there have been some first indications that the Thaumarchaeota might even change their depth habitat (J. Kaiser, pers. communication). Therefore, a long-term change in the habitat depth of Thaumarchaeota, probably in association with oxic conditions in the Skagerrak, is a valid explanation for the differences prior to ~2500 cal. yr BP (Figure 7.6).

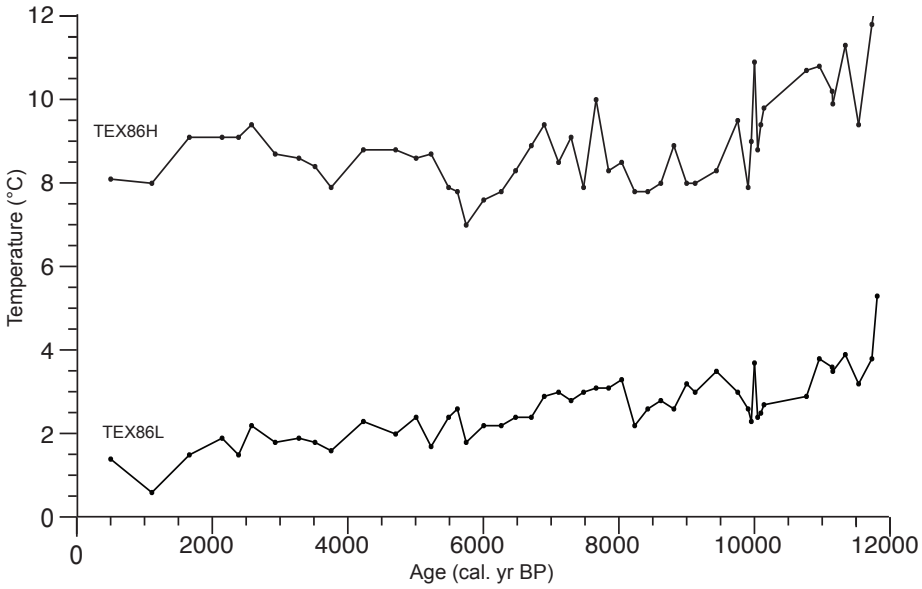

Fig. 7.5 Estimated SSTs using a gravity-core from the central Skagerrak (IOW242940-4). As for the multi-core sediments (see Figure 2), we used different temperature equations based on the TEX_{86}^{L} and TEX_{86}^{H} indices (Kim et al., 2010). The TEX_{86}^{L}-derived temperatures are most likely underestimated whereas those inferred from the TEX_{86}^{H} index are probably reliable.

Diverging absolute temperatures and trends between ~7000 and 2500 cal. yr BP might also be explained by the fact that the TEX_{86} proxy reflects another period of the annual cycle than $U^{K'}_{37}$. Previous studies have shown that in the adjacent North Sea Thaumarchaeota production is restricted to colder periods of the seasonal cycle (Wuchter et al., 2006; Herfort et al., 2007). In the Baltic Sea, however, some studies indicate that the main biomass production occurs during summer (Kabel et al., 2012; Funkey et al., 2014), whereas other studies argue that the TEX_{86} proxy reflects the phytoplankton productivity as Thaumarchaeota are dependent on recycled ammonia of phytoplankton origin and consequently depends on the timing of export productivity (J. Kaiser, personal comm.).

Based on our proxy-comparison, we consider the $U^{K'}_{37}$-temperature method more reliable for reflecting the Holocene surface temperature trends and absolute values in the Skagerrak while the TEX_{86} is more likely to reflect the sub-surface conditions.

7.5.3 Conclusion and future outlook

We estimated TEX_{86}-temperatures using multi- and gravity-core sediments located in the central Skagerrak. Based on the sub-surface sediments, we suggest that a temperature equation including the TEX_{86}^{H} index is more reliable than the TEX_{86}^{L} index. Despite the good correlation of the TEX_{86}^{H} temperature estimations to $U^{K'}_{37}$-SSTs over the near modern and past ~2500 cal. yr BP, we found diverging trends between ~2500 and ~7000 cal. yr BP. These diverging patterns suggest that the season and/or water depth sampled by the two proxies has changed over time at that location. Therefore, the need for a regional calibration set would provide more

reliable temperature reconstructions, in particular regarding seasonality. In addition, well-dated surface and downcore sediments are needed to fully understand the relationship of TEX_{86} to temperature proxy in the Skagerrak area. Also, a high-resolution reconstruction of TEX_{86} back in time would provide helpful information on the TEX_{86} proxy throughout the Holocene period.

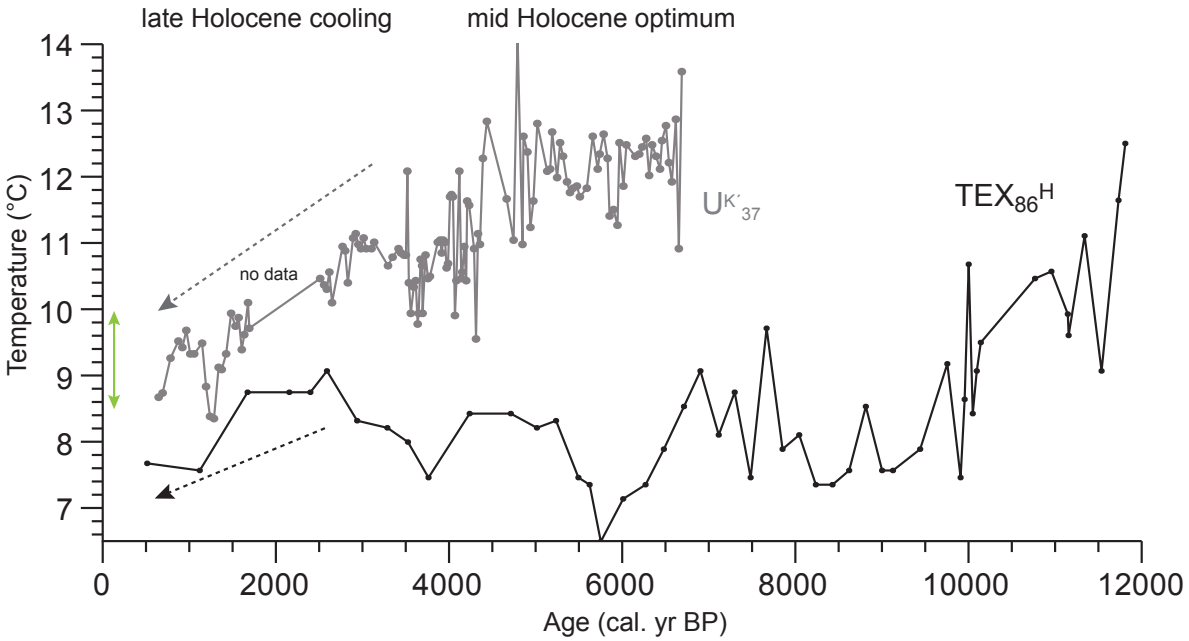

Fig. 7.6 Comparison of TEX_{86}^{H}- (black, IOW242940-4) and $U^{K'}_{37}$-based (grey, IOW225514) temperatures in the western and central Skagerrak, respectively. Black/grey arrows indicate temperature trends throughout the late Holocene, whereas the TEX_{86}^{H} record show a warming and the $U^{K'}_{37}$ record document the typical SST cooling. Green arrow indicates present day mean annual and early spring temperatures and the absolute temperatures (TEX_{86}^{H} and $U^{K'}_{37}$) in the uppermost multi-core samples (see Figure 7.3).

Acknowledgments. – We thank the crew of RV Poseidon research vessel for technical support during coring operations. We thank J. Ossebaar for assistance with GDGT analysis. We are also thankful to all INFLOW and SPP 1400 members. The work has been funded by the DFG SPP 1400 “Early Monumentality and Social Differentiation” and the EU BONUS+ “INFLOW” project.

8 Precipitation and vegetation changes in northern Germany from the mid to late Holocene

Veronica Rohde Krossa has done the preparation of all stable isotope samples and written the text. Hydrogen and carbon isotope measurements where performed by Thomas Larsen at the Leibniz institute in Kiel. Thomas Larsen and Yiming Wang contributed to the discussion. Ralph Schneider supervised the work.

8.1 Introduction

The transition from hunter-gatherer-fisher communities to societies based on an economy additionally relying on animal husbandry and cereal cultivation was most of the most radical changes in human history. It is not well understood why farming appeared much later in northern Germany and southern Scandinavia compared to its adjacent southern regions. First evidences of farming society in northern Germany and southern Scandinavia occurred at ~6000 cal. yr BP, whereas a fully developed farming society is documented as late as ~5500 cal. yr BP (Hartz et al., 2007; Sørensen and Karg, 2012; Dörfler et al., 2012) (see chapter 2.3). Evidence from high-resolution temperature reconstructions from the adjacent Skagerrak suggests that the onset of farming began concomitantly with a shift towards a continental-dominated atmospheric circulation pattern with warmer summers and colder winters (Krossa et al., submitted). However, little is known about past precipitation changes in the area, and therefore, establishing a precipitation record close to the landscape where those people settled would provide further information on the potential effect of local changes in precipitation on late hunter-gather-fisher societies and early farmers.

Stable hydrogen isotope compositions (δD) of specific molecules, as i.e. long-chain *n*-alkanes derived from terrestrial plant leaf waxes, are increasingly used to infer past changes in precipitation δD values as δD of plant leaf waxes reflects the δD of precipitation (e.g., Huang et al., 2002; Huang et al., 2004; Sachse et al., 2004). Variations in the relative abundance of stable hydrogen isotopes (δD), hydrogen (H) and deuterium (D), in precipitation is related to changes in the hydrological cycle and governed by condensation temperature, source and amount of precipitation, elevation, and distance from the ocean (Dansgaard, 1964; Gat, 1996; Craig, 1961). It is well established that precipitation strongly modulates δD values of lipids derived from terrestrial plants (e.g., Huang et al., 2004; Sachse et al., 2004). *n*-alkanes are lipids biosynthesized within the leaf wax, and the δD values of leaf wax *n*-alkanes are also governed by factors such as plant life form (tree, shrub, grasses), evapotranspiration from soil and leaf water, and different photosynthetic pathways (Sachse et al., 2012).

Here, we attempt to reconstruct past changes in δD of rainwater using a suite of specific *n*-alkanes (C_{27}, C_{29}, and C_{31}) from higher terrestrial plant leaf waxes derived from lake sediments (Lake Belau) in northern Germany. We will also compare our δD results with a temperature reconstruction from the same lake in order to potentially determine the effect of precipitation and temperature on the onset of local farming societies in the Lake Belau area. We also measured $\delta^{13}C$ on the same *n*-alkane homologues in order to determine any potential effect of major variations in photosynthetic pathway on the $\delta D_{leaf\ wax}$ signal (Wang et al., 2013).

8.2 Material and methods

8.2.1 Study site

We used a sediment core recovered from the pelagic of Lake Belau in 2002. Lake Belau is a relatively small lake (surface area ~1.14 km^2) located in the young moraine landscape in northern Germany (10°16´E, 54°6´N) close to the southwest Baltic Sea/Kattegat and Skagerrak (Figure 8.1). The maximum water depth is ~29 m (Müller, 1981), and the catchment area compromises a size of ~3.37 km^2 (Naujokat, 1997). Lake Belau is part of a connected system of kettle hole lakes (Figure 8.1) that was formed during the Weichselian glaciation (Fränzle et al., 2008; Garbe-Schönberg et al., 1998). The Schwentine River that drains northwards into the Baltic Sea connects the lakes (Garbe-Schönberg et al., 1998 and references therein). In present time the air temperature within one annual cycle ranges from below zero during winter to 15-20°C in summer with an annual average of 8.4±1.6°C over the past ~130 years in the Lake Belau region (Schleswig-Holstein, northern Germany). There is no evident seasonal-dependent pattern in amount of precipitation over the same period (meteorological data extracted from Deutscher Wetterdienst data).

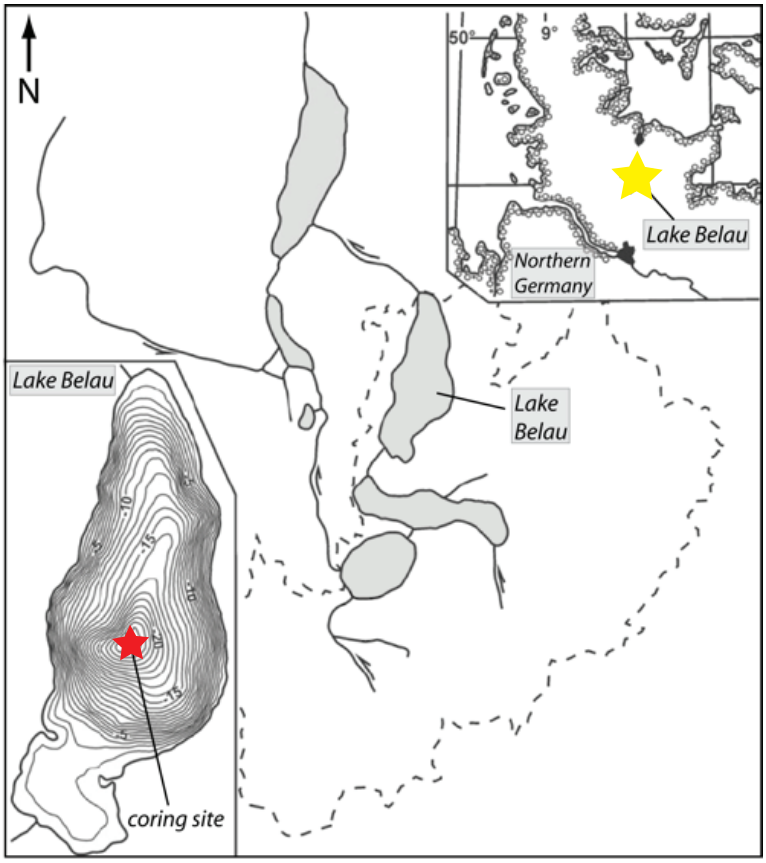

Fig. 8.1 Lake Belau (yellow star) is located in northern Germany close to the Baltic Sea, Skagerrak, and North Atlantic. The coring position of the lake sedimentary sequence is marked with a red star. Figure is slightly modified from (Zahrer et al., 2013).

8.2.2 Lake core and chronology

The lake sedimentary sequence was recovered from ~28.3 m water depth in 2002 (Figure 8.1) and covers almost the complete Holocene period (Dörfler et al., 2012). The sediment core consists of several combined segments from four parallel cores, whereas each segment is ~2 m in length. The segments were inter-connected by the identification of several specific markers (i.e. tephra layers) that are evident in several parallel segments of same depth and/or age. Consequently, the composite sedimentary sequence consists of sections of multiple segments from four different parallel cores and has a total length of ~24 m. The stratigraphic connection is fully discussed in Dörfler et al. (2012). In the time interval ~7900 to 2300 cal. yr BP, we subsampled the lake core in ~4x4 cm slices that approximately covers a period of 20-25 years according to varve counting.

An age-depth model was developed on the composite sedimentary sequence. In the time interval investigated in this study (~7900 to 2300 cal. yr BP), the age model is based on several AMS^{14}C dates, varve counting, and tephra layers. The radiocarbon dates were converted to calibrated years (cal. yr BP) using OxCal 4.1, and varves and tephra layers were used to refine the age model. The age model is fully discussed in Dörfler et al. (2012).

8.2.3 Method

The *n*-alkane extraction was performed at the Department of Marine Biogeochemistry at the NIOZ (Royal Netherlands Institute for Sea Research). We extracted ~6 g of homogenized sediment using a Dionex™ accelerated solvent extraction (Dionex™ ASE-200) with a solvent mixture of 9:1 (v/v) of dichloromethane:methanol (DCM:MeOH) at 100ºC and 100 bar N_2 pressure. The total lipid extracts (TLEs) were evaporated and subsequently dried under a pure N_2 flow. The following preparation was performed at the Biomarker Laboratory at the University of Kiel. After extraction, elemental sulphur was removed by rotating the extract with activated copper beads in DCM under vacuum for ~30 minutes. The apolar fraction that compromises the suite of *n*-alkanes (C_{27}, C_{29}, and C_{31}) was achieved via fractionation on activated Al_2O_3 columns using 9:1 (v/v) hexane:DCM. Thereupon, the samples were measured on an Agilent 6890 N Gas Chromatograph (GC) with a Flame Ionization Detector in the biomarker laboratory at the University of Kiel to obtain concentration of each *n*-alkane compound. Quantification and identification of each specific *n*-alkane compound were conducted using a laboratory internal standard (comprehending a series of *n*-alkane mixtures).

The samples were analysed for stable carbon (δ^{13}C) and hydrogen (δD) isotopic composition on a Thermo Finnigan GC combustion III (for δ^{13}C) or High Temperature Conversion systems (for δD) in the Leibniz laboratory at the University of Kiel. The method is fully described in Wang et al. (2013). δ^{13}C is expressed relative to the VPDB scale, established by using Arndt

Schimmelmann´s stable isotope A2 reference mixture from 2009. The accuracy and precision of the system were determined daily by measuring an in-house mixture of C_{28} to C_{36} alkanes between samples; these mixtures had an average standard error of the mean (SEM) of 0.7‰ per day (n=7-8) for δD and 0.1‰ per day for $\delta^{13}C$ (n=5). For the samples, SEM values for C_{27}, C_{29}, C_{31} were ≤ 0.9‰ per sample for δD (n=5-6) and ≤ 0.1‰ per sample for $\delta^{13}C$ (n=3).

8.3 Results

We measured three dominant long-chained odd-numbered *n*-alkanes (C_{27}, C_{29}, and C_{31}) regarding carbon ($\delta^{13}C$) and hydrogen (δD) isotopic composition, and concentration. At the Lake Belau site, C_{27} is the most common followed by C_{31} and C_{29}. Each *n*-alkane homologue shows overall similar relative trends in δD throughout the interval studied (~8000 to 2500 cal. yr BP), indicating an increase in enriched δD values towards ~5500 cal. yr BP followed by a period of depleted δD values. The absolute δD values are different and there is not a constant offset between each *n*-alkane homologue δD throughout the period investigated (~7600 to 2500 cal. yr BP). δD of C_{31} experienced the largest variations (29‰, -182 to -153‰) throughout the complete period measured followed by δD of C_{29} (24‰, -183 to -159‰), and δD of C_{27} (24‰, -171 to -147‰) (Figure 8.2).

All $\delta^{13}C$ records show similar patterns. C_{27} has the largest variations (~2.8‰), ranging from around -34 to -31.3‰, C_{31} varies from -33.8 to -31.3‰ (variation of ~2.4‰), and C_{29} has minor fluctuations of ~1.8‰ (between -32.4 and -30.6‰) (Figure 8.2). The depleted $\delta^{13}C$ values suggest the dominance of C_3 plants in the catchment of Lake Belau (Chikaraishi et al., 2004), and no apparent shift in plant in C_3 vs. C_4 plant. The relative small ranges of $\delta^{13}C$ values suggest that vegetation has a negligible effect on the δD values (Wang et al., 2013).

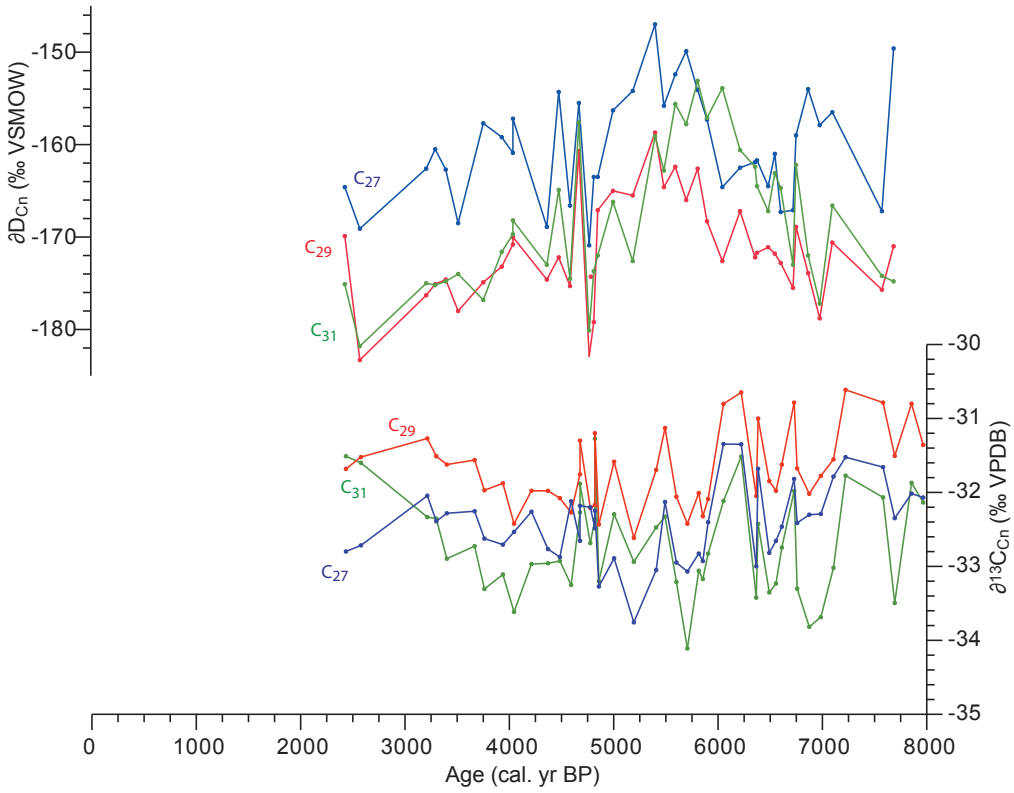

Fig. 8.2 δD (upper records) and $\delta^{13}C$ (lower records) from C_{27} (blue), C_{29} (red) and C_{31} (green) at the Lake Belau site.

8.4 Discussion

8.4.1 Distribution of *n*-alkane homologues (C_{27}, C_{29}, and C_{31}) and possible plant sources

Some studies suggest that the relative abundance of different *n*-alkane homologues, in particular C_{27}, C_{29}, and C_{31} are dominantly biosynthesized in grasses (C_{31}) or trees (C_{27} and C_{29}). Therefore, the ratio of C_{27} to C_{31} is often used to infer changes in vegetation type (Schwark et al., 2002; Hanisch et al., 2003). In the Lake Belau catchment area, a mixture of deciduous forest (Betula, Corylus, Alnus, Ulmus, Quercus) and grasses, in varying contributions, dominated the landscape between ~8000 and 2500 cal. yr BP (Wiethold, 1998; Dörfler et al., 2012). A deciduous forest, consisting of varying trees, is present throughout the entire record, whereas grasses are more common during periods of farming associated with forest clearance (Wiethold, 1998; Dörfler et al., 2012). In particular, between ~5500 and 5100 cal. yr BP, and after ~2700/2600 cal. yr BP, the contribution of grasses increased. The relative abundance of C_{27} to C_{31} reveals changes in the relative proportion of trees vs. grasses, and consequently, the C_{27}/C_{31} ratio matches major phases of forest clearance associated with increased grass between ~5500 and 5100 cal. yr BP, and after ~2700/2600 cal. yr BP (Wiethold, 1998; Dörfler et al., 2012) (Figure 9.3). This indicates that C_{27} is mainly biosynthesized by trees whereas C_{31} is probably more dominantly biosynthesized in grasses.

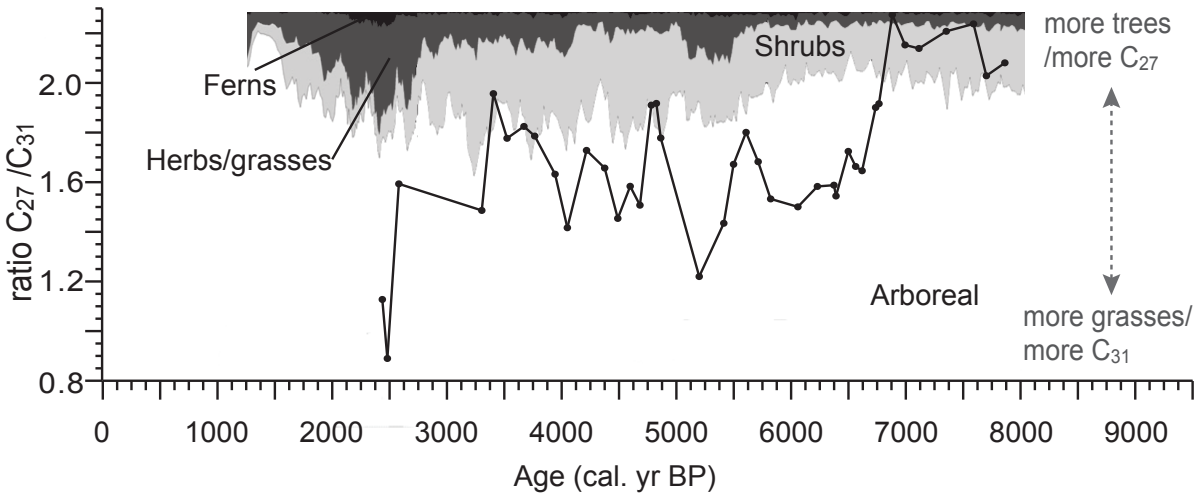

Fig. 8.3 Ratio of C_{27} to C_{31} in the Lake Belau sequence. An increase in C_{31} (C_{27}) occurs when the palynological record documents an increase in grasses (trees). Palynological record adopted from Dörfler et al. (2012).

8.4.2 Temperature dependency of precipitation δD values at the Lake Belau site

The temperature dependency on δD according to present day observational data at several stations in NW Europe is in the order of ~1.5-2‰ per ºC, although with a weak correlation. In contrast, other studies suggest temperature-dependency of δD of rainwater at oceanic-influenced, higher latitude sites of around ~14‰ per ºC (Dansgaard, 1964; Niggemann et al., 2003). In order to estimate potential past temperature variations at the Lake Belau sites, we used the same approach as Rach et al. (2014) using δD of *n*-alkanes derived from a lake in central Germany. First, we translated δD of each *n*-alkane compound (C_{27}, C_{29}, and C_{31}) into δD of meteoric water using the correlations proposed by Sachse et al. (2012). Thereby, we assumed a constant biological fractionation factor throughout the complete record for each compound and no significant change in photosynthetic pathways (C_3 vs. C_4 plants) (see results). We observe maximum variation in δD of reconstructed meteoric water of ~45‰ throughout the time interval recorded. If assuming that the determining factors on δD did not change in the past, reconstructed δD of meteoric water at the Lake Belau site suggests temperature variations of up to 30ºC when using a temperature-dependency of ~1.5-2‰ per ºC. This is highly unlikely given the relative temperature changes reconstructed from adjacent areas (Calvo et al., 2002; Moros et al., 2004; Jansen et al., 2008; Krossa et al., submitted). When using the temperature-dependency of ~14‰ per ºC (Dansgaard, 1964; Niggemann et al., 2003), we calculate relative changes of 2-3ºC that is reliable comparing to existing records, however, with diverging temperature trends (Calvo et al., 2002; Moros et al., 2004; Jansen et al., 2008; Krossa et al., submitted). Therefore, the variations in $\delta D_{n\text{-alk}}$ observed at the Lake Belau site cannot be solely explained by temperature changes.

8.4.3 Variations in $dD_{leaf\ wax}$ and anthropogenic vegetation shifts

Overall, the δD values of each *n*-alkane homologue indicate similar relative trends throughout the interval studied (~8000 to 2500 cal. yr BP). Although the absolute values differ, there is not a constant offset between the δD_{Cn} records. Prior to intensive human impact at 5500 cal. yr BP (see chapter 2.2), there is a poor correlation (r^2=0.03) of δD_{C27} to δD_{C31}, whereas they are well correlated after 5500 cal. yr BP (r^2=0.64). The correlation of δD_{C29} to both δD_{C31} and δD_{C27} is high throughout the complete record. If assuming that differences in $\delta D_{leaf\ wax}$ between the *n*-alkane homologues is mainly related to plant functional group, this indicates that C_{27} and C_{31} were biosynthesized mainly by different plant groups (trees/grasses, see discussion above) prior to 5500 cal. yr BP and most likely biosynthesized pre-dominantly by the same plant functional groups after 5500 cal. yr BP. It implies that forest clearance and the associated change in vegetation composition might have caused such shifts in the hydrogen isotopic composition. This does not necessary mean that the δD signal in the leaf wax *n*-alkanes is not reflecting changes in precipitation δD. Moreover, the natural background precipitation signal might still be present, however, there is no clear line which one of the δD records is most reliable and to what extent is the δD variation within each homologue reflective of natural precipitation change or caused by shifts in vegetation at the Lake Belau site. Nevertheless, as the correlation of δD_{C29} to both δD_{C31} and δD_{C27} is high throughout the complete record and not changing as the other *n*-alkane compounds (see above), we therefore suggest that the δD_{C29}, at the moment, is most suitable for paleo-implications at the Lake Belau site.

8.4.4 Paleo-implication on $\delta D_{leaf\ wax}$ at the Lake Belau site, comparison to *br*GDGT-derived temperature and late onset of farming

It is well established that δD values of leaf wax n-alkanes correlate with δD values of plant source water (precipitation) (Sachse et al., 2012), although with an additional effect of i.e. evaporation or plant-group related factors that might bias the δD signal in plant leaf waxes (Sachse et al., 2010; Feakins and Sessions, 2010; McInerney et al., 2011). Therefore, at the Lake Belau site, we interpret δD_{C29} values as a precipitation proxy, with an additional effect of such biasing factors.

Between ~7700 and 6000 cal. yr BP, we observe depleted δD_{C29} values suggesting wet climate conditions, and warm temperatures (*br*GDGTs, see manuscript 3) until ~7400 cal. yr BP. The most enriched δD_{C29} values occur between ~5800 and 4850 cal. yr BP, accompanied by a warming interval interrupted by a cooling at ~5100 cal. yr BP. Generally depleted δD_{C29} values, indicative of wet climate conditions, and colder temperatures characterize the late Holocene period. Supportingly, the Lake Belau δD_{C29} record matches a Holocene lake level reconstruction from southern Sweden (Digerfeldt, 1988), whereas depleted δD_{C29} values are recorded

during periods of higher lake levels and vice versa (Figure 8.4). This supports our interpretation of δD_{C29} as a precipitation proxy.

The onset of farming at ~6000-5500 cal. yr BP matches the interval of warm and dry climate conditions (Figure 8.4). As suggested in manuscript 2 (see chapter 5), we argue that the shift towards a more continental-dominated atmospheric circulation pattern caused changes in the environment, which in turn provoked a decline in natural food resources of late hunter-gather-fisher groups. Warm and dry climate conditions at the Lake Belau site, associated with such an atmospheric circulation pattern (Hurrell, 1995; Hurrell et al., 2003), might have been favourable for local cereal cultivation.

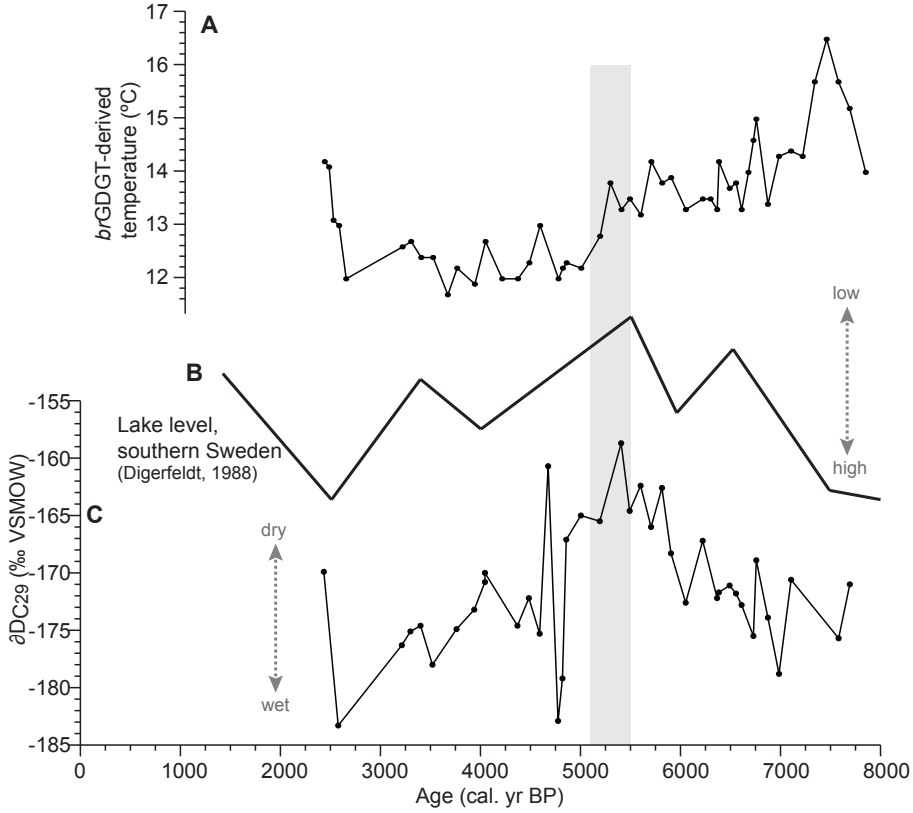

Fig. 8.4 Lowered lake level (Digerfeldt, 1988; B) matches dry periods as indicated by δD_{C29} (C) at the Lake Belau site. Evidences of first local farming groups are documented between ~5500 and 5100 cal. yr BP (Wiethold, 1998; Dörfler et al., 2012) (grey vertical bar), matching a period of both warm and dry climate conditions (A and C).

8.5 Conclusions

We measured δD and $\delta^{13}C$ on a suite of *n*-alkanes (C_{27}, C_{29}, and C_{31}) using the Lake Belau sedimentary sequence in northern Germany. Our $\delta^{13}C$ data indicate that there is no prominent change in photosynthetic pathway that can bias the δD values. We find correlations of C_{27}/C_{31} to changes in vegetation (grasses/trees), suggesting that C_{27} is predominantly biosynthesized by trees and C_{31} by grasses. We find no evidence that temperature can drive much of the δD varia-

tions observed in our δD *n*-alkane records, although we do not rule out that there is a temperature dependency of δD at such latitudes. The δD values of each *n*-alkane homologue show similar pattern over the period investigated, although with an offset that varies in time. Prior to first intensive farming activities at around 5500 cal. yr BP, we observe a low correlation of δD_{C27} and δD_{C31} variance, whereas the correlation is improved after 5500 cal. yr BP. This in turn suggests that anthropogenic changes in vegetation might cause changes towards more similar δD values. Consequently, we use δD_{C29} for paleo-precipitation interpretation, as it seems less affected by such changes. Our δD_{C29} matches a lake level record from southern Sweden, supporting our interpretation. We observe dry and warm climate conditions consistent with the onset of local farming around Lake Belau. This implies that such climate conditions were likely favorable for the adoption of the new economy.

Acknowledgments. – We thank Walter Dörfler for providing the Lake Belau samples. We are also thankful to all SPP 1400 members. The work has been funded by the DFG SPP 1400 “Early Monumentality and Social Differentiation” project.

9 Conclusions and future outlook

9.1 Conclusions

In this PhD thesis, paleo-climate conditions were reconstructed in order to assess the potential response and extent of climate change on the late onset of farming in northern Germany and southern Scandinavia. As paleo-climate records from remote sites might not reflect the actual climate situation occurring over the landscape where these societies settled, a network of marine sediment cores from the Skagerrak, Kattegat, and Mecklenburg Bay (Baltic Sea) as well as a lake core from northern Germany were used to reconstruct past climate change over the mid and late Holocene periods.

9.1.1 Main conclusions of each study (chapters 4 to 8)

- To reconstruct past changes in Baltic Sea outflow in the Skagerrak, tetra-unsaturated ketones ($C_{37:4}$ %) in comparison with grain-size records from the Kattegat channel were tested as a potential proxy over the late Holocene. An increase in both $C_{37:4}$ % and grain-size suggest enhanced outflow of Baltic Sea water during the last 3500 cal. yr BP. Probably, a strengthening in outflow was fostered by increased precipitation over the Baltic region induced by a major re-organization of the atmospheric circulation pattern over the North Atlantic.
- To test whether marine climate change had an impact on the late onset of farming in northern Germany and southern Scandinavia, past $U^{K'}_{37}$-SSTs in the Skagerrak were reconstructed. Outstanding was a notable ~5-6ºC SST drop between ~6300 and 5600 cal. yr BP, probably reflecting an outflow of colder Baltic Sea water associated with a prominent shift from a more maritime towards a continental climate regime over the Baltic region. The cooling matched the onset of farming in those areas, suggesting that climate change was an important factor for changes in economic strategies.
- In order to find a temperature proxy alternative to the $U^{K'}_{37}$ and applicable in Baltic Sea brackish conditions, the TEX_{86}-temperature proxy was tested in the Skagerrak over the Holocene and near-modern times. Over the last 2500 cal. yr BP both proxies provided similar values and trends, whereas in contrast, diverging trends and values were recorded during the early and mid Holocene. This latter difference suggests that before 2500 cal. yr BP, characterized by generally warm climate conditions, the $U^{K'}_{37}$ and TEX_{86} signals represented temperatures of different seasons and/or that the TEX_{86} preferentially recorded sub-surface water temperatures.
- To discuss the impact of marine and continental climate change on the late onset of farming, a continental temperature record from northern Germany was established. Intervals of diverging marine and continental temperature trends were documented, suggesting peri-

ods of strong seasonal contrasts associated with a predominantly continental atmospheric circulation pattern. A period of continental warmth followed by a 2.5ºC cooling matched the onset and disappearance of farming-based societies, suggesting that climate change played an important role in the expansion of agricultural techniques in northern Germany.

- In order to test whether changes in precipitation in addition to temperature affected the onset of farming, precipitation changes in northern Germany were reconstructed and compared to continental temperatures. Dry and warm climate conditions matched the onset of farming in northern Germany and were most likely associated with a more continental-dominated atmospheric circulation pattern. This suggests that both changes in temperature and precipitation pattern were important factors determining the onset and expansion of farming in those areas.

9.1.2 Impact of climate change on the late onset of farming in northern Germany

This PhD thesis has shown that paleo-climate reconstructions from sites close to or in Schleswig-Holstein are essential in order to reconstruct the impact of climate change on the late onset of farming in northern Germany. Consistent with the onset of first farming elements at ~6000 cal. yr BP, the northeastern Skagerrak experienced a pronounced 5-6ºC cooling reflecting an outflow of cold Baltic Sea water. Concomitant, summers were most likely warm and dry in northern Germany following a period of warm and wet climate conditions. This climate shift occurring at around 6000 cal. yr BP was associated with an increase in the dominating continental atmospheric circulation pattern, manifested itself in stronger seasonal temperature contrasts and more frequent cold winters and warm summers. Such climate conditions forced formerly hunter-gatherer-fisher groups to increasingly adopt farming strategies. Once fully adopted, the farming societies were even able to overcome periods of hypoxia in the Baltic Sea that largely negatively affected marine food resources, as evident in a human population density increase during periods of hypoxia.

The connection between climate change and the onset of farming groups on, both, local and regional scales shown in this PhD thesis indicated that climate change was an important factor within a succession of several events that led to the adaption of agrarian techniques in those areas. Probably, a combination of multiple factors such as the vulnerability of natural ecosystems under hypoxia and climatic stress as well as the better use of existing knowledge on agricultural strategies forced societies to adapt to changes in the environment. This was achieved by improving their living conditions that even caused an increase in human population on a regional scale under less hospitable climatic and environmental conditions. This suggests that a change in climate associated with a major shift in general atmos-

pheric circulation pattern led to the establishment and expansion of fully developed farming groups in northern Germany and southern Scandinavia.

9.2 Future outlook

9.2.1 Paleo-climate reconstructions in the marine environment

The North Atlantic/Skagerrak and Baltic Sea/Baltic region both largely impact climate conditions occurring over north-central Europe and southern Scandinavia. In order to further understand the link between these areas, high-resolution paleo-climate records on a transect from the western Skagerrak into the Baltic Sea should be developed:

- In order to improve the research on the link of water exchange dynamics between the Skagerrak and Baltic Sea, further studies of the $C_{37:4}$ % as a Baltic Sea outflow proxy in the Skagerrak by comparison to inflow proxies in the Baltic Sea should be carried out.
- To compare paleo-temperature records from the marine (Skagerrak) to the brackish (Baltic Sea) environment, proxies reflecting the same season and water depth should be applied. As the $U^{K'}_{37}$ proxy is probably not applicable in Baltic Sea sediments, a comparison of TEX_{86}-based temperature reconstructions in the Skagerrak to those in the Baltic Sea might be helpful as studies have shown that TEX_{86} can be applied for estimating past Baltic Sea surface water temperatures (Kabel et al., 2012). Therefore, further studies on TEX_{86} in the Skagerrak should be carried out in particular regarding the habitat depth of Thaumarchaeota and effects of seasonality on these microorganisms and possible changes of these factors within time. Studies of the modern the modern setting using sediment traps and surface sediments are necessary to better understand the modern conditions and temperature signal formation. Back in time, a comparison to modeling studies and the $U^{K'}_{37}$ proxy can be conducted to understand a possible effect of different seasons on the TEX86.

9.2.2 Paleo-climate reconstructions in the lacustrine environment

The present day climate in northwest Europe and the Baltic region is strongly governed by large-scale atmospheric pressure systems that drive variations in strength and direction of wind fields (e.g., Hurrell, 1995; Hurrell et al., 2003; BACC, 2008). Studies have shown that the North Atlantic Oscillation, which determines the flow of moist and mild air masses towards northwestern Europe, can be reconstructed over the modern period using diatom and varve studies in lake sediments (Lake Belau; Zahrer et al., 2013). These results should be compared to temperature and precipitation reconstructions in order to test if near-modern

precipitation and temperature changes if they follow the pattern of the North Atlantic Oscillation that governs the climate in northern Europe. To do so, paleo-climate records must be extended into historical time scales.

However, further studies are warranted for improving interpretations of precipitation and temperature proxies. For example, we do not fully understand how vegetation changes in the catchment may have affected both proxies. In the case of Lake Belau, it is well known that human activities and climate change altered vegetation composition over the Holocene period. Regarding the precipitation, these questions can be explored in conjunction with high-resolution pollen data time series and by comparison with near-by precipitation records independent of the lipid-based deuterium isotope signal. For the temperature reconstruction, the source(s) of the organic compounds in lake sediments and potential changes of those back in time, in particularly during intervals of intensive human impact on the landscape, must be carefully determined. This can be achieved by lipid analysis of the organic material preserved in the lake. Thereby, specific lipid biomarkers can be used to determine if the material is of predominantly aquatic or terrestrial origin. Nonetheless, as recent analytical techniques have improved the temperature estimation, the samples used for this study should be re-analysed.

9.2.3 Impact of climate change on the onset of farming northern Germany and southern Scandinavia

This PhD thesis has shown that climate change is one major factor to explain the late onset of farming in northern Germany and southern Scandinavia. To further explore the connection between climate change and major shifts in northern settlements, high-resolution paleo-climate records, regarding both temperature and precipitation and if possible, from both the continent and adjacent seas can be established. These records can be compared to existing continuous archaeological records, as for instance the population density proposed by Hinz et al. (2012) that is a good indicator for societal development. To do so, the continuation of the tight co-operation between archaeologists and paleo-climatologists would improve the understanding and connection of the results derived from both fields.

References

Andersen SH. (2008) The Mesolithic-Neolithic transition in Western Denmark seen from a kitchen midden perspective. A survey. *Analecta Praehistorica Leidensia* 40: 67-75.

Andren E, Andren T and Sohlenius G. (2000) The Holocene history of the southwestern Baltic Sea as reflected in a sediment core from the Bornholm Basin. *Boreas* 29: 233-250.

Antonsson K, Chen D and Seppä H. (2009) Anticyclonic atmospheric circulation as an analogue for the warm and dry mid-Holocene summer climate in central Scandinavia. *Climate of the Past* 4: 215-225.

BACC. (2008) *Assessment of Climate Change for the Baltic Sea Basin,* Berlin: Springer Verlag.

Bailey G and Milner N. (2008) *Molluscan archives from European prehistory*: BAR International Series.

Bakke J, Lie O, Dahl SO, et al. (2008) Strength and spatial patterns of the Holocene wintertime westerlies in the NE Atlantic region. *Global and Planetary Change* 60: 28-41.

Bale NJ, Villanueva L, Hopmans EC, et al. (2013) Different seasonality of pelagic and benthic Thaumarchaeota in the North Sea. *Biogeosciences* 10: 7195-7206.

Bendle J, Rosell-Mele A and Ziveri P. (2005) Variability of unusual distributions of alkenones in the surface waters of the Nordic seas. *Paleoceanography* 20.

Bjune AE, Bakke J, Nesje A, et al. (2005) Holocene mean July temperature and winter precipitation in western Norway inferred from palynological and glaciological lake-sediment proxies. *Holocene* 15: 177-189.

Björck S. (1995) A Review of the History of the Baltic Sea, 13.0-8.0 Ka Bp. *Quaternary International* 27: 19-40.

Blaga CI, Reichart GJ, Heiri O, et al. (2009) Tetraether membrane lipid distributions in water-column particulate matter and sediments: a study of 47 European lakes along a north-south transect. *Journal of Paleolimnology* 41: 523-540.

Blaga CI, Reichart GJ, Schouten S, et al. (2010) Branched glycerol dialkyl glycerol tetraethers in lake sediments: Can they be used as temperature and pH proxies? *Organic Geochemistry* 41: 1225-1234.

Blanz T, Emeis KC and Siegel H. (2005) Controls on alkenone unsaturation ratios along the salinity gradient between the open ocean and the Baltic Sea. *Geochimica Et Cosmochimica Acta* 69: 3589-3600.

Bond G, Kromer B, Beer J, et al. (2001) Persistent solar influence on North Atlantic climate during the Holocene. *Science* 294: 2130-2136.

Bonsall C, Macklin MG, Anderson DE, et al. (2002) Climate change and the adoption of agriculture in north-west Europe. *European Journal of Archaeology* 5: 9-23.

Brassell SC, Brereton RG, Eglinton G, et al. (1986) Paleoclimatic Signals Recognized by Chemometric Treatment of Molecular Stratigraphic Data. *Organic Geochemistry* 10: 649-660.

Calvo E, Grimalt JO and Jansen E. (2002) High resolution U(37)(K) sea surface temperature reconstruction in the Norwegian Sea during the Holocene. *Quaternary Science Reviews* 21: 1385-1394.

Castaneda I and Schouten S. (2011) A review of molecular organic proxies for examining modern and ancient lacustrine environments. *Quaternary Science Reviews* 30: 2851-2891.

Chikaraishi Y, Naraoka H and Poulson SR. (2004) Hydrogen and carbon isotopic fractionations of lipid biosynthesis among terrestrial (C3, C4 and CAM) and aquatic plants. *Phytochemistry* 65: 1369-1381.

Conley DJ, Bjorck S, Bonsdorff E, et al. (2009) Hypoxia-Related Processes in the Baltic Sea. *Environmental Science & Technology* 43: 3412-3420.

Conte MH and Eglinton G. (1993) Alkenone and Alkenoate Distributions within the Euphotic Zone of the Eastern North-Atlantic - Correlation with Production Temperature. *Deep-Sea Research Part I-Oceanographic Research Papers* 40: 1935-1961.

Conte MH, Sicre MA, Rühlemann C, et al. (2006) Global temperature calibration of the alkenone unsaturation index (UK`37) in surface waters and comparison with surface sediments. *Geopchemistry, Geophysics, Geosystems* 7: Q02005.

Conte MH, Thompson A, Lesley D, et al. (1998) Genetic and physiological influences on the alkenone/alkenoate versus growth temperature relationship in Emiliana huxleyi and Gephyrocapsa oceanica. *Geochimica Et Cosmochimica Acta* 62: 51-68.

Craig H. (1961) Isotopic variations in meteoric waters. *Science* 133: 1702–1703.

Cranwell PA, Eglinton G and Robinson N. (1987) Lipids of Aquatic Organisms as Potential Contributors to Lacustrine Sediments .2. *Organic Geochemistry* 11: 513-527.

Danielssen DS, Edler L, Fonselius S, et al. (1997) Oceanographic variability in the Skagerrak and Northern Kattegat, May-June, 1990. *CES Journal of Marine Science* 54: 753-773.

Dansgaard W. (1964) Stable Isotopes in Precipitation. *Tellus* 16: 436-468.

Davis BAS, Brewer S, Stevenson AC, et al. (2003) The temperature of Europe during the Holocene reconstructed from pollen data. *Quaternary Science Reviews* 22: 1701-1716.

De Jonge C, Hopmans EC, Stadnitskaia A, et al. (2013) Identification of novel penta- and hexamethylated branched glycerol dialkyl glycerol tetraethers in peat using HPLC–MS2, GC–MS and GC–SMB-MS. *Organic Geochemistry* 54: 78–82.

De Jonge C, Stadnitskaia A, Hopmans EC, et al. (2014) In situ produced branched glycerol dialkyl glycerol tetraethers in suspended particulate matter from the Yenisei River, Eastern Siberia. *Geochimica Et Cosmochimica Acta* 125: 476-491.

Digerfeldt G. (1988) Reconstruction and Regional Correlation of Holocene Lake-Level Fluctuations in Lake Bysjon, South Sweden. *Boreas* 17: 165-182.

Dreibrodt S and Wiethold J. (2014) Lake Belau and its catchment (northern Germany) – a northern central Europe key site of environmental history since the onset of agriculture. *Holocene*.

Dörfler W, Feeser I, van den Bogaard C, et al. (2012) A high-quality annually laminated sequence from Lake Belau, Northern Germany: Revised chronology and its implications for palynological and tephrachronological studies. *Holocene* 22: 1413-1426.

Eglinton G and Hamilton RJ. (1967) Leaf Epicuticular Waxes. *Science* 156: 1322-&.

Emeis KC, Struck U, Blanz T, et al. (2003) Salinity changes in the central Baltic Sea (NW Europe) over the last 10000 years. *Holocene* 13: 411-421.

Erbs-Hansen DR, Knudsen KL, Gary AC, et al. (2012) Holocene climatic development in Skagerrak, eastern North Atlantic: Foraminiferal and stable isotopic evidence. *Holocene* 22: 301-312.

Etourneau J, Schneider R, Blanz T, et al. (2010) Intensification of the Walker and Hadley atmospheric circulations during the Pliocene–Pleistocene climate transition. *Earth and Planetary Science Letters* 297: 103-110.

Feakins SJ and Sessions AL. (2010) Controls on the D/H ratios of plant leaf waxes in an arid ecosystem. *Geochimica Et Cosmochimica Acta* 74: 2128-2141.

Feeser I, Dörfler W, Averdieck F-R, et al. (2012) New insight into regional and local land-use and vegetation patterns in eastern Schleswig-Holstein during the Neolithic. In: Hinz M and Müller J (eds) *Siedlung, Grabenwerk, Großsteingrab. Studien zu Gesellschaft, Wirtschaft und Umwelt der Trichterbechergruppen im nördlichen Mitteleuropa. Frühe Monumentalität und Soziale Differenzierung.* Bonn, R. Habelt GmbH, 159–190.

Ficken KJ, Li B, Swain DL, et al. (2000) An n-alkane proxy for the sedimentary input of submerged/floating freshwater aquatic macrophytes. *Organic Geochemistry* 31: 745-749.

Fränzle O, Kappen L, Blume H-P, et al. (2008) *Ecosystem Ecosystem organisation of a complex landscape. Long term Research in the Bornhöved Lake District Germany,* Berlin: Springer.

Funkey CP, Conley DJ, Reuss NS, et al. (2014) Hypoxia Sustains Cyanobacteria Blooms in the Baltic Sea. *Environmental Science & Technology* 48: 2598-2602.

Garbe-Schönberg C-D, Wiethold J, Butenhoff D, et al. (1998) Geochemical and palynological record in annually laminated sediments from Lake Belau (Schleswig-Holstein) reflecting paleoecology and human impact over 9000 a. *Meyniania* 50: 47-70.

Gat JR. (1996) Oxygen and hydrogen isotopes in the hydrologic cycle. *Annual Review of Earth and Planetary Sciences* 24: 225-262.

Giger W, Schaffner C and Wakeham SG. (1980) Aliphatic and Olefinic Hydrocarbons in Recent Sediments of Greifensee, Switzerland. *Geochimica Et Cosmochimica Acta* 44: 119-129.

Gong C and Hollander DJ. (1999) Evidence for differential degradation of alkenones under contrasting bottom water oxygen conditions: Implication for paleotemperature reconstruction. *Geochimica Et Cosmochimica Acta* 63: 405-411.

Gronenborn D. (2007) Beyond the Models: 'Neolithization' in Central Europe. In: Whittle A and Cummings V (eds) *Going Over: the Mesolithic-Neolithic Transition in North-West Europe.* Proceedings of the British Academy, 73-98.

Gronenborn D, Strien HC, Dietrich S, et al. (2013) “Adaptive cycles” and climate fluctuations: a case study from Linear Pottery Culture in western Central Europe. *Journal of Archaeological Science*.

Guilaine J. (2000/2001) La diffusion de l’agriculture en Europe: une hypothèse arythmique. *Zephyrus: Revista de prehistoria y arqueología* 53/54: 267–272.

Gustafsson BG and Westman P. (2002) On the causes for salinity variations in the Baltic Sea during the last 8500 years. *Paleoceanography* 17.

Gyllencreutz R. (2005) Late Glacial and Holocene paleoceanography in the Skagerrak from high-resolution grain size records. *Palaeogeography Palaeoclimatology Palaeoecology* 222: 344-369.

Gyllencreutz R and Kissel C. (2006) Lateglacial and Holocene sediment sources and transport patterns in the Skagerrak interpreted from high-resolution magnetic properties and grain-size data. *Quaternary Science Reviews* 25: 1247-1263.

Hammarlund D, Bjorck S, Buchardt B, et al. (2003) Rapid hydrological changes during the Holocene revealed by stable isotope records of lacustrine carbonates from Lake Igelsjon, southern Sweden. *Quaternary Science Reviews* 22: 353-370.

Hanisch S, Ariztegui D and Püttmann W. (2003) The biomarker record of Lake Albano, central Italy—Implications for Holocene aquatic system response to environmental change. *Organic Geochemistry* 34: 1223–1235.

Harada N, Shin KH, Murata A, et al. (2003) Characteristics of alkenones synthesized by a bloom of Emiliania huxleyi in the Bering Sea. *Geochimica Et Cosmochimica Acta* 67: 1507-1519.

Harff J. (2006) Geoscientific investigation of Quarternary sediments from the Mecklenburgian Bright, Great Belt, southern Kattegat, Kriegers Flag, Arkona basin, and Hanö Bay (Bornholm basin). *Cruise report R/V Maria S. Merian Cruise MSM 01/02.* Warnemünde, 157.

Hartz S, Lübke H and Terberger T. (2007) From fish and seal to sheep and cattle: new research into the process of neolithisation in northern Germany. *Proceedings of the British Academy* 144: 567-594.

Heikkila M, Edwards TWD, Seppa H, et al. (2010) Sediment isotope tracers from Lake Saarikko, Finland, and implications for Holocene hydroclimatology. *Quaternary Science Reviews* 29: 2146-2160.

HELCOM. (2007) Baltic Sea action plan. Krakow, Poland: HELCOM Ministerial Meeting.

Herbert TD. (2003) *Alkenone paleotemperature determinations,* Amsterdam: Elsevier.

Herfort L, Schouten S, Abbas B, et al. (2007) Variations in spatial and temporal distribution of Archaea in the North Sea in relation to environmental variables. *Fems Microbiology Ecology* 62: 242-257.

Herfort L, Schouten S, Boon JP, et al. (2006) Application of the TEX86 temperature proxy to the southern North Sea. *Organic Geochemistry* 37: 1715-1726.

Hinz M, Feeser I, Sjögren KG, et al. (2012) Demography and the intensity of cultural activities: an evaluation of Funnel Beaker Societies (4200-2800 BC). *Journal of Archaeological Science* 29: 3331-3340.

Hopmans EC, Schouten S, Pancost RD, et al. (2000) Analysis of intact tetraether lipids in archaeal cell material and sediments by high performance liquid chromatography/atmospheric pressure chemical ionization mass spectrometry. *Rapid Communications in Mass Spectrometry* 14: 585-589.

Hopmans EC, Weijers JWH, Schefuss E, et al. (2004) A novel proxy for terrestrial organic matter in sediments based on branched and isoprenoid tetraether lipids. *Earth and Planetary Science Letters* 224: 107-116.

Huang YS, Shuman B, Wang Y, et al. (2002) Hydrogen isotope ratios of palmitic acid in lacustrine sediments record late Quaternary climate variations. *Geology* 30: 1103-1106.

Huang YS, Shuman B, Wang Y, et al. (2004) Hydrogen isotope ratios of individual lipids in lake sediments as novel tracers of climatic and environmental change: a surface sediment test. *Journal of Paleolimnology* 31: 363-375.

Huguet A, Wiesenberg GLB, Gocke M, et al. (2012) Branched tetraether membrane lipids associated with rhizoliths in loess: Rhizomicrobial overprinting of initial biomarker record. *Organic Geochemistry* 43: 12-19.

Huguet C, Schimmelmann A, Thunell R, et al. (2007) A study of the TEX86 paleothermometer in the water column and sediments of the Santa Barbara Basin, California. *Paleoceanography* 22.

Hurrell JW. (1995) Decadal Trends in the North-Atlantic Oscillation - Regional Temperatures and Precipitation. *Science* 269: 676-679.

Hurrell JW, Kushnir Y, Ottersen G, et al. (2003) An overview of the North Atlantic Oscillation. *American Geophysical Union* 134: 1-35.

IOC, IHO and BODC. (2003) Centenary Edition of the GEBCO Digital Atlas, published on CD-ROM on behalf of the Intergovernmental Oceanographic Commission and the International Hydrographic Organization as part of the General Bathymetric Chart of the Oceans. Liverpool: British Oceanographic Data Centre.

Jansen E, Andersson C, Moros M, et al. (2008) The early to mid-Holocene thermal optimum in the North Atlantic. In: Battarbee RW and Binney HA (eds) *Natural Climate Variability and Global Warming – A Holocene perspective.* Chichester: Wiley-Blackwell, 123-137.

Jiang H, Björck S and Svensson N-O. (1998) Reconstruction of Holocene sea-surface salinity in the Skagerrak-Kattegat: a climatic and environmental record of Scandinavia. *Journal of Quaternary Science* 13: 107-114.

Kabel K, Moros M, Porsche C, et al. (2012) Impact of climate change on the Baltic Sea ecosystem over the last 1000 years. *Nature Climate Change* 2: 871-874.

Karlson K, Rosenberg R and Bonsdorff E. (2002) Temporal and spatial large-scale effects of eutrophication and oxygen deficiency on benthic fauna in Scandinavian and Baltic waters – a review. *Oceanography and Marine Biology: an Annual Review* 40: 427-289.

Karner MB, DeLong EF and Karl DM. (2001) Archaeal dominance in the mesopelagic zone of the Pacific Ocean. *Nature* 409: 507-510.

Kim JH, Schouten S, Hopmans EC, et al. (2008) Global sediment core-top calibration of the TEX86 paleothermometer in the ocean. *Geochimica Et Cosmochimica Acta* 72: 1154-1173.

Kim JH, van der Meer J, Schouten S, et al. (2010) New indices and calibrations derived from the distribution of crenarchaeal isoprenoid tetraether lipids: Implications for past sea

surface temperature reconstructions. *Geochimica Et Cosmochimica Acta* 74: 4639-4654.
Kirleis W, Klooss S, Kroll H, et al. (2012) Crop growing and gathering in the northern German Neolithic: a review supplemented by new results. *Vegetation History and Archaeobotany* 21: 221-242.
Klitgaard-Kristensen D, Sejrup HP and Haflidason H. (2001) The last 89 kyr fluctuations in Norwegian Sea surface conditions and implications for the magnitude of climatic change: Evidence from the North Sea. *Paleoceanography* 16: 455-467.
Krossa VR, Moros M, Blanz T, et al. (2014) Late Holocene Baltic Sea outflow changes reconstructed using C37:4 content from marine cores. *Boreas*: n/a-n/a.
Krossa VR, Moros M, Leduc G, et al. (submitted) Climate change triggers late onset of agrarian societies in northern Germany and southern Scandinavia.
Landesamt. (2011) Available at: http://www.umweltdaten.landsh.de.
Landmesser B. (1993) Untersuchungen zur Struktur und zur Primärproduktion des Phytoplanktons im Belauer See. In: Hamburg DU (ed).
Leduc G, Schneider R, Kim JH, et al. (2010) Holocene and Eemian sea surface temperature trends as revealed by alkenone and Mg/Ca paleothermometry. *Quaternary Science Reviews* 29: 989-1004.
Lee KE, Kim JH, Wilke I, et al. (2008) A study of the alkenone, TEX(86), and planktonic foraminifera in the Benguela Upwelling System: Implications for past sea surface temperature estimates. *Geochemistry Geophysics Geosystems* 9.
Leng MJ and Marshall JD. (2004) Paleoclimate interpretation of stable isotope data from lake sediment archives. *Quaternary Science Reviews* 23: 811-831.
Lincoln SA, Wai B, Eppley JM, et al. (2014) Planktonic Euryarchaeota are a significant source of archaeal tetraether lipids in the ocean. *Proceedings of the National Academy of Sciences of the United States of America* 111: 9858-9863.
Lindkvist T, Björkert D, Andersson J, et al. (2003) Djupdata för havsområden 2003. *Rapporter Oceanografi* 11.
Liu ZH, Pagani M, Zinniker D, et al. (2009) Global Cooling During the Eocene-Oligocene Climate Transition. *Science* 323: 1187-1190.
Locarnini RA, Mishonov AV, Antonov JI, et al. (2010) *Volume 1: Temperature,* Washington, D.C: NOAA Atlas NESDIS 68, U.S. Government Printing Office.
Lohmann G, Pfeiffer M, Laepple T, et al. (2013) A model-data comparison of the Holocene global sea surface temperature evolution. *Climate of the Past* 9: 1807-1839.
Loomis S, Russell J and Sinninghe Damsté JS. (2011) Distributions of branched GDGTs in soils from western Uganda and implications for a lacustrine paleothermometer. *Organic Geochemistry* 42: 739-751.
Lopes dos Santos RA, Prange M, Castaneda I, et al. (2010) Glacial–interglacial variability in Atlantic meridional overturning circulation and thermocline adjustments in the tropical North Atlantic. *Earth and Planetary Science Letters* 300: 407-414.
Lougheed BC, Snowball I, Moros M, et al. (2012) Using an independent geochronology based on palaeomagnetic secular variation (PSV) and atmospheric Pb deposition to date Baltic Sea sediments and infer C-14 reservoir age. *Quaternary Science Reviews* 42: 43-58.
Magny M and Haas JN. (2004) A major widespread climate change around 5300 cal. yrs BP at the time of the Alpine Iceman. *Journal of Quaternary Science* 19: 423-430.
Marcott SA, Shakun JD, Clark PU, et al. (2013) A Reconstruction of Regional and Global Temperature for the Past 11,300 Years. *Science* 339: 1198-1201.
Matthäus W and Schinke H. (1994) Mean Atmospheric Circulation Patterns Associated with Major Baltic Inflows. *Baltic Sea* 46: 321-339.
Matthäus W and Schinke H. (1999) The influence of river runoff on deep water conditions of the Baltic Sea. *Hydrobiologia* 393: 1-10.
Mayewski PA, Rohling EE, Stager JC, et al. (2004) Holocene climate variability. *Quaternary Research* 62: 243-255.

McCave IN, Manighetti B and Robinson SG. (1995) Sortable Silt and Fine Sediment Size Composition Slicing - Parameters for Paleocurrent Speed and Paleoceanography. *Paleoceanography* 10: 593-610.

McClymont EL, Rosell-Mele A, Haug GH, et al. (2008) Expansion of subarctic water masses in the North Atlantic and Pacific oceans and implications for mid-Pleistocene ice sheet growth. *Paleoceanography* 23.

McInerney FA, Helliker BR and Freeman KH. (2011) Hydrogen isotope ratios of leaf wax n-alkanes in grasses are insensitive to transpiration. *Geochimica Et Cosmochimica Acta* 75: 541-554.

Meier HEM and Kauker F. (2003) Sensitivity of the Baltic Sea salinity to the freshwater supply. *Climate Research* 24: 231-242.

Moros M. (1998) Spätquartäre Sedimentation am Reykjanes Rücken und in der westlichen Ostsee - Rekonstruktion anhand hochauflösender sedimentphysikalischer Eigenschaften.: Ernst-Moritz-Arndt-University, 100.

Moros M, Emeis K, Risebrobakken B, et al. (2004) Sea surface temperatures and ice rafting in the Holocene North Atlantic: climate influences on Northern Europe and Greenland. *Quaternary Science Reviews* 23: 2113-2126.

Müller HE. (1981) Vergleichende Untersuchungen zur hydrochemischen Dynamik von Seen im Schleswig-Holsteinischen Jungmoränengebiet. *Kieler Geographische Schriften.* Kiel: Geographisches Institut der Christian-Albrechts-Universität Kiel.

Müller PJ, Kirst G, Ruhland G, et al. (1998) Calibration of alkenone paleotemperature index UK'37 based on core tops from the eastern South Atlantic and the global ocean (60°N-60°S). *Geochimica Et Cosmochimica Acta* 62: 1757-1772.

Nanninga HJ and Tyrrell T. (1996) Importance of light for the formation of algal blooms by Emiliania huxleyi. *Marine Ecology Progress Series* 136: 195-203.

Naujokat D. (1997) *Nährstoffbelastung und Eutrophierung stehender Gewässer,* Darmstadt: DDD Verlag.

Nesje A, Matthews JA, Dahl SO, et al. (2001) Holocene glacier fluctuations of Flatebreen and winter-precipitation changes in the Jostedalsbreen region, western Norway, based on glaciolacustrine sediment records. *Holocene* 11: 267-280.

Niemann H, Stadnitskaia A, Wirth SB, et al. (2012) Bacterial GDGTs in Holocene sediments and catchment soils of a high Alpine lake: application of the MBT/CBT-paleothermometer. *Climate of the Past* 8: 889-906.

Niggemann S, Mangini A, Mudelsee M, et al. (2003) Sub-Milankovitch climatic cycles in Holocene stalagmites from Sauerland, Germany. *Earth and Planetary Science Letters* 216: 539-547.

Otto L, Zimmermann TF, Furnes GK, et al. (1990) Review of the physical oceanography of the North Sea. *Netherlands Journal of Sea Research* 26: 161-238.

Pearson EJ, Juggins S, Talbot HM, et al. (2011) A lacustrine GDGT-temperature calibration from the Scandinavian Arctic to Antarctic: Renewed potential for the application of GDGT-paleothermometry in lakes. *Geochimica Et Cosmochimica Acta* 75: 6225-6238.

Peterse F, Hopmans EC, Schouten S, et al. (2011) Identification and distribution of intact polar branched tetraether lipids in peat and soil. *Organic Geochemistry* 42: 1007-1015.

Peterse F, Kim JH, Schouten S, et al. (2009) Constraints on the application of the MBT/CBT palaeothermometer at high latitude environments (Svalbard, Norway). *Organic Geochemistry* 40: 692-699.

Peterse F, van der Meer J, Schouten S, et al. (2012) Revised calibration of the MBT-CBT paleotemperature proxy based on branched tetraether membrane lipids in surface soils. *Geochimica Et Cosmochimica Acta* 96: 215-229.

Powers L, Werne JP, Vanderwoude AJ, et al. (2010) Applicability and calibration of the TEX86 paleothermometer in lakes. *Organic Geochemistry* 41: 404-413.

Powers LA, Werne JP, Johnson TC, et al. (2004) Crenarchaeotal membrane lipids in lake sediments: A new paleotemperature proxy for continental paleoclimate reconstruction? *Geology* 32: 613-616.

Prahl FG, Muehlhause LA and Zahnle DL. (1988) Further evaluation of long-chain alkenones as indicators of paleoceanographic conditions. *Geochimica Et Cosmochimica Acta* 52: 2303-2310.

Prahl FG and Wakeham SG. (1987) Calibration of unsaturation patterns in long-chain keton compositions for palaeotemperature assessment. *Nature* 330: 367-369.

Rach O, Brauer A, Wilkes H, et al. (2014) Delayed hydrological response to Greenland cooling at the onset of the Younger Dryas in western Europe. *Nature Geoscience* 7: 109-112.

Reimer PJ, Bard E, Bayliss A, et al. (2013) IntCal13 and Marine13 Radiocarbon Age Calibration Curves 0-50,000 Years cal BP. *Radiocarbon* 55: 1869-1887.

Rimbu N, Lohmann G and Grosfeld K. (2007) Blocking signature in ice core records from northern Greenland. *Geophysical Research Letters* 34: L09704.

Risebrobakken B, Moros M, Ivanova EV, et al. (2010) Climate and oceanographic variability in the SW Barents Sea during the Holocene. *Holocene* 20: 609-621.

Rodhe J. (1987) The large-scale circulation in the Skagerrak; interpretation of some observations. *Tellus* 39A: 245-253.

Rodhe J. (1988) The Baltic and North Seas: a process-oriented review of the physical oceanography. In: Robinson AR and Brink KH (eds) *The Sea.* New York: John Wiley and Sons, 699-732.

Rodhe J and Holt N. (1996) Observations of the transport of suspended matter into the Skagerrak along the western and northern coast of Jutland. *Journal of Sea Research* 35: 91-98.

Rontani JF, Bonin P, Jameson I, et al. (2005) Degradation of alkenones and related compounds during oxic and anoxic incubation of the marine haptophyte Emiliania huxleyi with bacterial consortia isolated from microbial mats from the Camargue, France. *Organic Geochemistry* 36: 603-618.

Rontani JF, Harji R, Guasco S, et al. (2008) Degradation of alkenones by aerobic heterotrophic bacteria: Selective or not? *Organic Geochemistry* 39: 34-51.

Rosell-Melé A. (1998) Interhemispheric appraisal of the value of alkenone indices as temperature and salinity proxies in high-latitude locations. *Paleoceanography* 13: 694-703.

Rosell-Melé A, Jansen E and Weinelt M. (2002) Appraisal of a molecular approach to infer variations in surface ocean freshwater inputs into the North Atlantic during the last glacial. *Global and Planetary Change* 34: 143-152.

Rosell-Melé A and Prahl FG. (2013) Seasonality of UK´37 temperature estimates as inferred from sediment trap data. *Quaternary Science Reviews* 72: 128-136.

Rowley-Conwy P. (1984) The laziness of the short-distance hunter: the origins of agriculture in Denmark. *Journal of Anthropological Archaeology* 3: 300-324.

Rueda G, Rosell-Mele A, Escala M, et al. (2009) Comparison of instrumental and GDGT-based estimates of sea surface and air temperatures from the Skagerrak. *Organic Geochemistry* 40: 287-291.

Rößler D, Moros M and Lemke W. (2011) The Littorina transgression in the southwestern Baltic Sea: new insights based on proxy methods and radiocarbon dating of sediment cores. *Boreas* 40: 231-241.

Sachse D, Billault I, Bowen GJ, et al. (2012) Molecular Paleohydrology: Interpreting the Hydrogen- Isotopic Composition of Lipid Biomarkers from Photosynthesizing Organisms. *Annual Review of Earth and Planetary Sciences, Vol 40* 40: 221-249.

Sachse D, Gleixner G, Wilkes H, et al. (2010) Leaf wax n-alkane delta D values of field-grown barley reflect leaf water delta D values at the time of leaf formation. *Geochimica Et Cosmochimica Acta* 74: 6741-6750.

Sachse D, Radke J and Gleixner G. (2004) Hydrogen isotope ratios of recent lacustrine sedimentary n-alkanes record modern climate variability. *Geochimica Et Cosmochimica Acta* 68: 4877-4889.

Schier W. (2009) Extensiver Brandfeldbau und die Ausbreitung der neolithischen Wirtschaftsweise in Mitteleuropa und Südskandinavien am Ende des 5. Jahrtausends v.Chr. *Praehistorische Zeitschrift* 84: 15-43.

Schinke H and Matthaus W. (1998) On the causes of major Baltic inflows - an analysis of long time series. *Continental Shelf Research* 18: 67-97.

Schneider B, Leduc G and Park W. (2010) Disentangling seasonal signals in Holocene climate trends by satellite-model-proxy integration. *Paleoceanography* 25.

Schouten S, Hopmans EC, Pancost RD, et al. (2000) Widespread occurrence of structurally diverse tetraether membrane lipids: Evidence for the ubiquitous presence of low-temperature relatives of hyperthermophiles. *Proceedings of the National Academy of Sciences of the United States of America* 97: 14421-14426.

Schouten S, Hopmans EC, Schefuß E, et al. (2002) Distributional variations in marine crenarchaeotal membrane lipids: a new tool for reconstructing ancient sea water temperatures? *Earth and Planetary Science Letters* 204: 265–274.

Schouten S, Hopmans EC and Sinninghe Damsté JS. (2013) The organic geochemistry of glycerol dialkyl glycerol tetraether lipids: A review. *Organic Geochemistry* 54: 19-61.

Schouten S, van der Meer MTJ, Hopmans EC, et al. (2007) Archaeal and bacterial glycerol dialkyl glycerol tetraether lipids in hot springs of Yellowstone National Park (USA). *Applied and Environmental Microbiology* 73: 6181–6691.

Schulz HM, Schoner A and Emeis KC. (2000) Long-chain alkenone patterns in the Baltic Sea - an ocean-freshwater transition. *Geochimica Et Cosmochimica Acta* 64: 469-477.

Schwark L, Zink K and Lechterbeck J. (2002) Reconstruction of postglacial to early Holocene vegetation history in terrestrial Central Europe via cuticular lipid biomarkers and pollen records from lake sediments. *Geology* 30: 463-466.

Seppä H and Bennett KD. (2003) Quaternary pollen analysis: recent progress in palaeoecology and palaeoclimatology. *Progress in Physical Geography* 27: 580-611.

Seppä H and Birks HJB. (2001) July mean temperature and annual precipitation trends during the Holocene in the Fennoscandian tree-line area: pollen-based climate reconstructions. *Holocene* 11: 527-539.

Seppä H, Bjune AE, Telford RJ, et al. (2009) Last nine-thousand years of temperature variability in Northern Europe. *Climate of the Past* 5: 523-535.

Seppä H, Hammarlund D and Antonsson K. (2005) Low-frequency and high-frequency changes in temperature and effective humidity during the Holocene in south-central Sweden: implications for atmospheric and oceanic forcings of climate. *Climate Dynamics* 25: 285-297.

Shennan S, Downey SS, Timpson A, et al. (2013) Regional population collapse followed initial agriculture booms in mid-Holocene Europe. *Nature communications* 4.

Shennan S and Edinborough K. (2007) Prehistoric population history: from the Late Glacial to the Late Neolithic in Central and Northern Europe. *Journal of Archaeological Science* 34: 1339-1345.

Sicre MA, Bard E, Ezat U, et al. (2002) Alkenone distributions in the North Atlantic and Nordic sea surface waters. *Geochemistry Geophysics Geosystems* 3.

Sicre MA, Yiou P, Eiriksson J, et al. (2008) A 4500-year reconstruction of sea surface temperature variability at decadal time-scales off North Iceland. *Quaternary Science Reviews* 27: 2041-2047.

Sikes EL and Sicre MA. (2002) Relationship of the tetra-unsaturated C-37 alkenone to salinity and temperature: Implications for paleoproxy applications. *Geochemistry Geophysics Geosystems* 3.

Sinninghe Damsté JS, Hopmans EC, Pancost RD, et al. (2000) Newly discovered non-isoprenoid dialkyl diglycerol tetraether lipids in sediments. *Journal of the Chemical Society, Chemical Communications* 23: 1683–1684.

Sinninghe Damsté JS, Hopmans EC, Schouten S, et al. (2002) Crenarchaeol: the characteristic core glycerol dibiphytanyl glycerol tetraether membrane lipid of cosmopolitan pelagic crenarchaeota. *Journal of Lipid Research* 43: 1641–1651.

Sinninghe Damsté JS, Ossebaar J, Abbas B, et al. (2009) Fluxes and distribution of tetraether lipids in an equatorial African lake: constraints on the application of the TEX86 palaeothermometer and branched tetraether lipids in lacustrine settings. *Geochimica Et Cosmochimica Acta* 73: 4232–4249.

Sinninghe Damsté JS, Ossebaar J, Schouten S, et al. (2012) Distribution of tetraether lipids in the 25-ka sedimentary record of Lake Challa: extracting reliable TEX86 and MBT/CBT paleotemperatures from an equatorial African lake. *Quaternary Science Reviews* 50: 43-54.

Sinninghe Damsté JS, Rijpstra WIC, Hopmans EC, et al. (2011) 13,16-Dimethyl octacosanedioic acid (iso-diabolic acid): a common membrane-spanning lipid of Acidobacteria subdivisions 1 and 3. *Applied and Environmental Microbiology* 77: 4147–4154.

Stigebrandt A. (1983) A Model for the Exchange of Water and Salt between the Baltic and the Skagerrak. *Journal of Physical Oceanography* 13: 411-427.

Stigebrandt A and Gustafsson BG. (2003) Response of the Baltic Sea to climate change - theory and observations. *Journal of Sea Research* 49: 243-256.

Sun Q, Chu GQ, Liu MM, et al. (2011) Distributions and temperature dependence of branched glycerol dialkyl glycerol tetraethers in recent lacustrine sediments from China and Nepal (vol 116, G02027, 2011). *Journal of Geophysical Research-Biogeosciences* 116.

Svansson A. (1975) *Physical and chemical oceanography of the Skagerrak and Kattegat*: Fishery Board of Sweden.

Sørensen L and Karg S. (2012) The expansion of agrarian societies towards the north – new evidence for agriculture during the Mesolithic/Neolithic transition in Southern Scandinavia. *Journal of Archaeological Science*.

Ternois Y, Sicre MA, Boireau A, et al. (1997) Evaluation of long-chain alkenones as paleo-temperature indicators in the Mediterranean Sea. *Deep-Sea Research Part I-Oceanographic Research Papers* 44: 271-286.

Thiede J. (1987) The Late Quaternary Skagerrak and its depositional environment. *Boreas* 16: 425-432.

Tierney JE and Russell JM. (2009) Distributions of branched GDGTs in a tropical lake system: Implications for lacustrine application of the MBT/CBT paleoproxy. *Organic Geochemistry* 40: 1032–1036.

Tierney JE, Russell JM, Eggemont H, et al. (2010) Environmental controls on branched tetraether lipid distributions in tropical East African lake sediments: a new lacustrine paleothermometer? *Geochimica et Cosmochimica Acta* 74: 4902–4918.

Tierney JE, Russell JM, Huang Y, et al. (2008) Northern hemisphere controls on tropical southeast African climate during the past 60,000 years. *Science* 322: 252–255.

Vahtera E, Conley DJ, Gustafsson BG, et al. (2007) Internal ecosystem feedbacks enhance nitrogen-fixing cyanobacteria blooms and complicate management in the Baltic Sea. *Ambio* 36: 186-194.

van Weering TCE. (1982) Recent sediments and sediment transport in the northern North Sea; pistoncores from Skagerrak. *Proceedings of the Koninklijke Nederlandse Akademie Van Wetenschappen* B 85: 155-201.

Volkman JK, Barrett SM, Blackburn SI, et al. (1995) Alkenones in Gephyrocapsa-Oceanica - Implications for Studies of Paleoclimate. *Geochimica Et Cosmochimica Acta* 59: 513-520.

Walker MJC, Berkelhammer M, Bjorck S, et al. (2012) Formal subdivision of the Holocene Series/Epoch: a Discussion Paper by a Working Group of INTIMATE (Integration of ice-core, marine and terrestrial records) and the Subcommission on Quaternary Stratigraphy (International Commission on Stratigraphy). *Journal of Quaternary Science* 27: 649-659.

Wang YMV, Larsen T, Leduc G, et al. (2013) What does leaf wax delta D from a mixed C-3/C-4 vegetation region tell us? *Geochimica Et Cosmochimica Acta* 111: 128-139.

Wanner H, Beer J, Butikofer J, et al. (2008) Mid- to Late Holocene climate change: an overview. *Quaternary Science Reviews* 27: 1791-1828.

Weijers JWH, Panoto E, van Bleijswijk J, et al. (2009) Constraints on the Biological Source(s) of the Orphan Branched Tetraether Membrane Lipids. *Geomicrobiology Journal* 26: 402-414.

Weijers JWH, Schouten S, Spaargaren OC, et al. (2006) Occurrence and distribution of tetraether membrane lipids in soils: Implications for the use of the TEX86 proxy and the BIT index. *Organic Geochemistry* 37: 1680-1693.

Weijers JWH, Schouten S, van den Donker JC, et al. (2007) Environmental controls on bacterial tetraether membrane lipid distribution in soils. *Geochimica Et Cosmochimica Acta* 71: 703-713.

Wiethold J. (1998) Studien zur jüngsten postglazialen Vegetations- und Siedlungsgeschichte im östlichen Schleswig-Holstein (mit einem Beitrag von H. Erlenkeuser). *Universitätsforschungen zur prähistorischen Archäologie.* Bonn.

Winsor P, Rodhe J and Omstedt A. (2001) Baltic Sea ocean climate: an analysis of 100 yr of hydrographic data with focus on the freshwater budget. *Climate Research* 18: 5-15.

Wuchter C, Schouten S, Wakeham SG, et al. (2006) Archaeal tetraether membrane lipid fluxes in the northeastern Pacific and the Arabian Sea: Implications for TEX86 paleothermometry. *Paleoceanography* 21.

Zabeti N, Bonin P, Volkman JK, et al. (2010) Potential alteration of U K-37' paleothermometer due to selective degradation of alkenones by marine bacteria isolated from the haptophyte Emiliania huxleyi. *Fems Microbiology Ecology* 73: 83-94.

Zahrer J, Dreibrodt S and Brauer A. (2013) Evidence of the North Atlantic Oscillation in varve composition and diatom assemblages from recent, annually laminated sediments of Lake Belau, northern Germany. *Journal of Paleolimnology* 50: 231-244.

Zillén L. (2003) *Setting the Holocene clock using varved lake sediments in Sweden,* Sweden: Lund University.

Zink K-G, Vandergoes MJ, Mangelsdorf K, et al. (2010) Application of bacterial glycerol dialkyl glycerol tetraethers (GDGTs) to develop modern and past temperature estimates from New Zealand lakes. *Organic Geochemistry* 41: 1060–1066.

Zorita E and Laine A. (2000) Dependence of salinity and oxygen concentrations in the Baltic Sea on large-scale atmospheric circulation. *Climate Research* 14: 25-41.

Appendix

Multi-cores

Appendix 1 Data of multi-cores IOW372610 (left) and IOW372620 (right) in the western and central Skagerrak. respectively.

Depth (cm)	$C_{37:4}$ %	$U^{K'}_{37}$	SST (ºC)	Depth (cm)	$C_{37:4}$ %	$U^{K'}_{37}$	SST (ºC)
372610				372620			
				:S			
0.50	2.47	0.411	11.12		3.54	0.381	10.21
1.25	2.99	0.342	9.03	1.25	3.39	0.391	10.52
1.75	3.12	0.354	9.39	1.75	3.90	0.313	8.15
2.25	3.24	0.336	8.85	2.25	3.29	0.391	10.52
2.75	3.26	0.347	9.18	2.75	3.62	0.358	9.52
3.25	3.42	0.325	8.52	3.25	3.79	0.340	8.97
3.75	3.76	0.332	8.73	3.75	3.77	0.375	10.03
4.25	3.78	0.334	8.79	4.25	3.95	0.380	10.18
4.75	3.59	0.352	9.33	4.75	4.04	0.345	9.12
5.25	3.80	0.344	9.09	5.25	3.83	0.368	9.82
5.75	3.50	0.345	9.12	5.75	3.96	0.370	9.88
6.25	3.75	0.348	9.21	6.25	3.86	0.375	10.03
6.75	3.76	0.353	9.36	6.75	3.95	0.375	10.03
7.25	3.44	0.361	9.61	7.25	3.89	0.363	9.67
7.75	3.60	0.362	9.64	7.75	3.95	0.356	9.45
8.25	3.77	0.337	8.88	8.25	4.00	0.364	9.70
8.75	3.71	0.35	9.27	8.75	3.93	0.374	10.00
9.25	3.60	0.345	9.12	9.25	3.75	0.370	9.88
9.75	3.17	0.362	9.64	10.00	3.79	0.361	9.61
10.50	3.39	0.345	9.12	11.00	4.67	0.296	7.64
11.50	3.15	0.365	9.73	12.00	3.83	0.382	10.24
12.50	3.26	0.367	9.79	13.00	4.02	0.353	9.36
13.50	3.56	0.349	9.24	14.00	3.89	0.342	9.03
14.50	3.26	0.367	9.79	15.00	4.23	0.331	8.70
15.50	3.61	0.316	8.24	16.00	3.79	0.359	9.55
16.50	3.32	0.332	8.73	17.00	3.80	0.349	9.24
17.50	3.38	0.361	9.61	18.00	3.57	0.366	9.76
18.50	3.65	0.349	9.24	19.00	3.40	0.383	10.27
19.50	2.86	0.367	9.79	20.00	4.02	0.359	9.55
20.50	3.41	0.346	9.15	21.00	3.67	0.331	8.70
21.50	3.48	0.335	8.82	22.00	4.00	0.306	7.94
22.50	2.95	0.375	10.03	23.00	3.70	0.315	8.21
23.50	3.12	0.372	9.94	24.00	3.63	0.344	9.09
24.50	2.91	0.375	10.03	25.00	3.37	0.368	9.82
25.50	3.42	0.349	9.24	26.00	3.45	0.338	8.91
26.50	3.29	0.355	9.42	27.00	3.70	0.335	8.82
27.50	3.11	0.364	9.70	28.00	3.85	0.311	8.09
28.50	2.36	0.395	10.64	29.00	3.67	0.346	9.15
29.50	2.97	0.349	9.24	30.00	3.15	0.363	9.67
30.50	2.81	0.359	9.55	31.00	2.80	0.368	9.82
31.50	3.01	0.356	9.45	32.00	2.73	0.377	10.09
32.50	2.77	0.364	9.70	33.00	2.54	0.379	10.15
33.50	2.89	0.371	9.91	34.00	2.70	0.380	10.18
34.50	3.33	0.352	9.33	35.00	2.55	0.351	9.30
36.50	3.22	0.353	9.36	36.00	2.41	0.383	10.27
37.50	3.21	0.345	9.12	37.00	2.57	0.383	10.27
38.50	3.28	0.35	9.27	38.00	2.37	0.372	9.94
39.50	3.23	0.335	8.82				
40.50	3.07	0.341	9.00				
41.50	2.86	0.352	9.33				
43.50	3.03	0.351	9.30				

Appendix 2 Data of multi-core IOW242940-4 in the central Skagerrak.

Depth (cm)	$C_{37:4}$ %	$U^{K'}_{37}$	$U^{K'}_{37}$-SST (ºC)	BIT	TEX_{86}^{L}	TEX_{86}^{H}	TEX_{86}^{L} (°C)	TEX_{86}^{H} (°C)
0.5	2.66	0.396	10.67	0.07	-0.667	-0.438	1.87	8.61
1.5	2.80	0.310	8.06	0.08	-0.663	-0.417	2.14	10.07
3.5	3.04	0.333	8.76	0.08	-0.678	-0.434	1.16	8.92
5.5	2.65	0.341	9.00	0.09	-0.670	-0.438	1.66	8.66
7.5	2.94	0.363	9.67	0.09	-0.673	-0.433	1.46	8.99
9.5	2.57	0.362	9.64	0.09	-0.673	-0.417	1.50	10.07
12.5	2.61	0.360	9.58	0.09	-0.663	-0.416	2.16	10.12
14.5	2.49	0.368	9.82	0.10	-0.664	-0.433	2.09	9.00
16.5	3.01	0.346	9.15	0.09	-0.668	-0.426	1.83	9.49
18.5	3.01	0.298	7.70	0.09	-0.665	-0.420	1.98	9.89
20.5	2.60	0.355	9.42	0.08	-0.664	-0.416	2.07	10.18
25.5	3.01	0.268	6.79	0.09	-0.673	-0.415	1.44	10.24
30.5	1.80	0.359	9.55	0.09	-0.666	-0.409	1.96	10.63
33.5	1.35	0.422	11.45	0.09	-0.666	-0.401	1.93	11.17

Appendix 3 Data of multi-core IOW372630 in the central Skagerrak.

Depth (cm)	$C_{37:4}$ %	$U^{K'}_{37}$	$U^{K'}_{37}$-SST (ºC)	Depth (cm)	$C_{37:4}$ %	$U^{K'}_{37}$	$U^{K'}_{37}$-SST (ºC)
1.50	3.31	0.386	10.36	33.5	3.53	0.331	8.70
2.50	3.31	0.380	10.18	34.5	3.55	0.329	8.64
3.50	3.53	0.378	10.12	35.5	3.16	0.350	9.27
4.50	3.92	0.365	9.73	36.5	3.45	0.341	9.00
5.25	4.28	0.352	9.33	37.5	3.43	0.320	8.36
5.75	3.56	0.374	10.00	38.5	3.11	0.321	8.39
6.25	3.74	0.347	9.18	39.5	3.26	0.324	8.48
6.75	3.90	0.357	9.48	40.5	2.29	0.364	9.70
7.25	3.87	0.347	9.18	41.5	2.89	0.314	8.18
7.75	3.61	0.359	9.55				
8.25	3.50	0.368	9.82				
8.75	3.82	0.362	9.64				
9.25	3.94	0.347	9.18				
9.75	3.91	0.351	9.30				
10.50	3.59	0.361	9.61				
11.50	3.77	0.366	9.76				
12.50	3.61	0.354	9.39				
13.50	4.05	0.353	9.36				
14.50	4.15	0.343	9.06				
15.50	4.03	0.335	8.82				
16.50	3.64	0.364	9.70				
17.50	3.87	0.334	8.79				
18.50	3.44	0.355	9.42				
19.50	3.54	0.340	8.97				
20.50	3.58	0.333	8.76				
21.50	3.66	0.331	8.70				
22.50	3.43	0.336	8.85				
23.50	3.48	0.336	8.85				
24.50	3.30	0.355	9.42				
25.50	2.97	0.355	9.42				
26.50	3.00	0.349	9.24				
27.50	3.14	0.344	9.09				
28.50	3.57	0.337	8.88				
29.50	3.02	0.364	9.70				
30.50	3.72	0.309	8.03				
31.50	3.28	0.347	9.18				
32.50	3.42	0.329	8.64				

Appendix 4 Data of multi-cores IOW372660 (left) and IOW372650 (right) in the northeastern Skagerrak.

Depth (cm)	$C_{37:4}$ %	$U^{K'}_{37}$	SST (ºC)	Depth (cm)	$C_{37:4}$ %	$U^{K'}_{37}$	SST (ºC)
	372660				372650		
0.5	4.08	0.390	10.48	0.50	3.71	0.305	9.42
1.5	4.70	0.324	8.48	1.25	3.34	0.344	10.52
2.5	4.15	0.388	10.42	1.75	3.08	0.345	10.39
3.5	4.50	0.356	9.45	2.25	3.76	0.314	9.73
4.5	4.62	0.346	9.15	2.75	3.46	0.346	10.61
5.5	4.04	0.385	10.33	3.25	4.59	0.216	7.00
6.5	4.05	0.385	10.33	3.75	4.64	0.240	7.76
7.5	4.06	0.387	10.39	4.25	4.49	0.273	8.76
8.5	3.93	0.384	10.30	4.75	4.80	0.248	8.06
9.5	3.99	0.372	9.94	5.50	4.81	0.241	7.88
11.5	4.04	0.387	10.39	6.50	4.50	0.287	9.18
14.5	4.02	0.402	10.85	7.50	4.84	0.256	8.36
19.5	3.60	0.402	10.85	8.50	4.48	0.301	9.64
24.5	4.62	0.371	9.91	9.50	4.39	0.287	9.15
25.5	5.47	0.311	8.09	10.50	3.97	0.322	10.06
26.5	5.47	0.326	8.55	11.50	4.25	0.307	9.73
27.5	5.14	0.345	9.12	12.50	3.79	0.324	10.06
28.5	4.88	0.351	9.30	13.50	3.82	0.330	10.27
29.5	4.01	0.395	10.64	14.50	4.17	0.301	9.48
30.5	4.75	0.358	9.52	15.50	3.50	0.338	10.39
31.5	5.06	0.331	8.70	16.50	3.66	0.321	9.94
32.5	5.27	0.329	8.64	17.50	3.72	0.337	10.42
33.5	5.04	0.341	9.00	18.50	3.77	0.331	10.27
34.5	5.23	0.330	8.67	19.50	4.57	0.271	8.70
				20.50	3.50	0.338	10.39
				21.50	3.47	0.340	10.45
				22.50	3.66	0.330	10.21
				23.50	3.55	0.325	10.00
				24.50	3.88	0.315	9.82
				25.50	3.36	0.334	10.18
				26.50	3.34	0.337	10.27
				27.50	3.36	0.343	10.48
				28.50	3.62	0.310	9.58
				29.50	3.91	0.310	9.67
				30.50	3.22	0.325	9.85
				31.50	3.62	0.326	10.06
				32.50	3.59	0.311	9.58
				33.50	3.19	0.322	9.76
				34.50	4.50	0.271	8.70
				35.50	3.25	0.328	9.94

Gravity-core data

Appendix 5 Data of Gravity-core IOW372610 in the western Skagerrak.

Depth (cm)	Age (cal. yr BP)	$\%C_{37:4}$	$U^{K'}_{37}$	SST (ºC)
	Gravity-core			
2.5	359	4.11	0.338	8.91
10.5	371	3.95	0.334	8.79
15.5	379	3.60	0.339	8.94
25.5	409	3.56	0.348	9.21
35.5	451	3.24	0.338	8.91
45.5	494	2.77	0.357	9.48
55.5	536	2.81	0.347	9.18
65.5	623	2.96	0.343	9.06
75.5	710	3.07	0.314	8.18
85.5	861	2.82	0.355	9.42
95.5	1001	3.35	0.294	7.58
105.5	1165	2.83	0.334	8.79
115.5	1349	3.02	0.344	9.09
125.5	1530	2.48	0.354	9.39
135.5	1691	2.38	0.346	9.15
145.5	1853	2.24	0.353	9.36
155.5	2014	2.36	0.349	9.24
165.5	2123	2.42	0.349	9.24
175.5	2228	1.81	0.355	9.42
185.5	2300	2.03	0.359	9.55
195.5	2372	2.13	0.343	9.06
205.5	2463	1.69	0.330	8.67
215.5	2569	1.30	0.353	9.36
225.5	2676	0.81	0.375	10.03
235.5	2782	0.92	0.374	10.00
245.5	2889	0.93	0.391	10.52
255.5	2995	1.19	0.351	9.30
265.5	3169	0.77	0.391	10.52
275.5	3343	0.64	0.369	9.85
285.5	3516	0.99	0.370	9.88
295.5	3690	0.72	0.353	9.36
305.5	3865	1.28	0.337	8.88
315.5	4041	1.07	0.402	10.85
325.5	4218	1.05	0.407	11.00
335.5	4394	0.80	0.398	10.73
345.5	4570	0.95	0.373	9.97
355.5	4746	1.05	0.431	11.73
365.5	4911	1.38	0.433	11.79
375.5	5075	1.21	0.397	10.70
385.5	5240	0.57	0.412	11.15
395.5	5405	0.74	0.433	11.79
405.5	5570	1.02	0.433	11.79
415.5	5734	1.18	0.423	11.48
425.5	5899	0.80	0.438	11.94
435.5	6064	0.67	0.430	11.70
445.5	6228	0.59	0.459	12.58
455.5	6393	0.52	0.379	10.15
465.5	6558	0.40	0.386	10.36
485.5	6887	0.54	0.420	11.39
505.5	7217	1.69	0.445	12.15
525.5	7546	2.43	0.416	11.27
545.5	7876	3.31	0.378	10.12

Appendix 6 Data of gravity-core IOW242940-4 in the central Skagerrak.

Depth (cm)	Age (cal. yr BP)	$C_{37:4}$ %	BIT	TEX_{86}^{L}	TEX_{86}^{H}	TEX_{86}^{L} (°C)	TEX_{86}^{H} (°C)
0.5	500	-	0.09	-0.674	-0.446	1.42	8.10
10	1107	3.55	0.08	-0.686	-0.448	0.57	7.97
20	1661	2.75	0.09	-0.673	-0.432	1.48	9.06
30	2143	2.08	0.09	-0.667	-0.431	1.86	9.09
40	2387	1.73	0.09	-0.673	-0.431	1.49	9.15
50	2578	1.18	0.09	-0.662	-0.427	2.18	9.36
60	2928	0.66	0.09	-0.668	-0.437	1.82	8.72
70	3277	0.78	0.09	-0.666	-0.438	1.93	8.63
75	3515	0.70	0.10	-0.669	-0.442	1.77	8.37
80	3753	1.10	0.10	-0.671	-0.448	1.62	7.94
90	4229	0.79	0.10	-0.661	-0.436	2.26	8.77
100	4704	0.72	0.11	-0.665	-0.435	2.04	8.85
110	5007	0.91	0.09	-0.660	-0.439	2.38	8.58
120	5228		0.09	-0.669	-0.437	1.72	8.73
130	5486		0.09	-0.659	-0.449	2.44	7.90
135	5616		0.10	-0.657	-0.450	2.58	7.79
140	5745		0.06	-0.669	-0.461	1.77	7.05
150	6004		0.08	-0.662	-0.453	2.19	7.62
160	6263		0.10	-0.663	-0.450	2.17	7.82
170	6475		0.09	-0.659	-0.443	2.39	8.32
181	6707		0.10	-0.660	-0.434	2.37	8.93
190	6898		0.10	-0.652	-0.427	2.86	9.37
200	7109		0.11	-0.650	-0.440	3.00	8.53
210	7294		0.10	-0.653	-0.431	2.83	9.11
220	7478		0.10	-0.651	-0.448	2.97	7.94
230	7663		0.11	-0.649	-0.417	3.12	10.05
240	7847		0.10	-0.649	-0.442	3.09	8.34
250	8040		0.10	-0.646	-0.440	3.27	8.53
260	8232		0.09	-0.663	-0.450	2.18	7.84
270	8425		0.10	-0.657	-0.450	2.57	7.82
280	8617		0.10	-0.653	-0.447	2.82	8.00
290	8810		0.10	-0.656	-0.434	2.61	8.89
296	8999		0.09	-0.648	-0.447	3.15	8.02
300	9124		0.09	-0.651	-0.447	2.97	8.01
310	9438		0.08	-0.644	-0.443	3.45	8.32
320	9752		0.08	-0.650	-0.426	3.04	9.46
330	9906		0.07	-0.657	-0.448	2.56	7.95
340	9953		0.07	-0.661	-0.433	2.30	9.01
350	10000		0.07	-0.640	-0.406	3.69	10.86
360	10046		0.07	-0.659	-0.436	2.42	8.79
370	10093		0.07	-0.657	-0.426	2.52	9.43
380	10140		0.08	-0.655	-0.421	2.68	9.82
390	10767		0.08	-0.652	-0.408	2.88	10.67
400	10956		0.10	-0.639	-0.407	3.76	10.75
410	11146		0.09	-0.641	-0.416	3.64	10.17
420	11340		0.09	-0.637	-0.400	3.88	11.25
430	11536		0.10	-0.648	-0.427	3.18	9.39
440	11732		0.11	-0.639	-0.392	3.79	11.81
444	11811		0.14	-0.617	-0.380	5.28	12.58
450	11928		0.20	-0.594	-0.329	6.79	16.12

Appendix 7 Data of Gravity-core IOW225514 in the central Skagerrak.

Depth (cm)	Age (cal. yr BP)	$\%C_{37:4}$	$U^{K'}_{37}$	SST (ºC)	Depth (cm)	Age (cal. yr BP)	$\%C_{37:4}$	$U^{K'}_{37}$	SST (ºC)
30.0	631	3.67	0.342	9.03	270.0	4671	1.27	0.436	11.88
35.0	677	3.67	0.344	9.09	271.5	4691	1.28	0.435	11.85
45.0	768	3.13	0.360	9.58	273.5	4718	1.40	0.380	10.18
55.0	859	2.96	0.368	9.82	275.0	4738	1.40	0.396	10.67
60.0	904	3.09	0.365	9.73	278.0	4779	1.40	0.447	12.21
65.0	950	2.87	0.373	9.97	280.0	4806	1.48	0.397	10.70
70.0	995	3.02	0.362	9.64	281.0	4819	1.53	0.400	10.79
75.0	1041	2.92	0.362	9.64	283.0	4846	1.22	0.412	11.15
85.0	1132	2.85	0.367	9.79	285.0	4873	1.51	0.396	10.67
90.0	1177	3.23	0.347	9.18	286.0	4886	1.52	0.433	11.79
95.0	1223	3.32	0.333	8.76	288.0	4913	1.62	0.431	11.73
100.0	1268	3.36	0.332	8.73	293.0	4981	1.68	0.411	11.12
106.0	1322	2.30	0.356	9.45	295.0	5008	1.86	0.369	9.85
111.0	1360	2.59	0.355	9.42	297.0	5034	1.97	0.418	11.33
118.0	1413	2.41	0.362	9.64	299.0	5061	1.71	0.413	11.18
126.0	1473	1.87	0.381	10.21	301.0	5088	1.85	0.453	12.39
133.0	1526	1.89	0.375	10.03	303.0	5115	1.75	0.47	12.91
138.0	1658	1.97	0.379	10.15	313.0	5250	2.03	0.434	11.82
143.0	1885	2.04	0.364	9.70	316.5	5297	2.72	0.415	11.24
147.0	2067	1.95	0.371	9.91	318.5	5324	2.47	0.510	14.12
153.0	2340	1.69	0.386	10.36	321.0	5357	3.80	0.413	11.18
155.0	2443	1.98	0.374	10.00	321.5	5364	4.35	0.463	12.70
157.0	2484	1.56	0.397	10.7	323.5	5391	6.21	0.456	12.48
160.0	2546	1.45	0.394	10.61	325.0	5411	6.80	0.421	11.42
162.0	2587	1.33	0.392	10.55	326.5	5431	7.51	0.433	11.79
164.0	2628	1.22	0.400	10.79	328.5	5458	6.56	0.469	12.88
166.0	2670	1.30	0.386	10.36	333.5	5526	6.16	0.447	12.21
174.0	2834	0.93	0.412	11.15	335.0	5546	6.19	0.448	12.24
176.0	2875	0.85	0.410	11.09	336.0	5559	5.31	0.465	12.76
178.0	2917	1.13	0.395	10.64	338.5	5593	5.02	0.444	12.12
182.0	2999	0.90	0.416	11.27	340.0	5613	4.08	0.460	12.61
184.0	3040	1.10	0.418	11.33	341.5	5633	4.77	0.454	12.42
186.0	3081	0.95	0.413	11.18	343.5	5660	5.12	0.442	12.06
188.0	3122	1.15	0.411	11.12	345.0	5681	1.27	0.437	11.91
190.0	3163	1.14	0.416	11.27	346.5	5701	1.44	0.439	11.97
192.0	3205	1.12	0.411	11.12	348.5	5728	1.14	0.440	12.00
196.0	3287	1.10	0.411	11.12	350.0	5748	1.05	0.435	11.85
198.0	3328	1.13	0.414	11.21	353.5	5795	1.25	0.439	11.97
208.5	3544	1.21	0.403	10.88	356.5	5835	1.03	0.463	12.70
212.0	3616	1.06	0.407	11.00	359.0	5869	0.82	0.448	12.24
216.5	3709	1.16	0.411	11.12	360.0	5882	0.85	0.455	12.45
218.5	3750	1.09	0.409	11.06	362.0	5909	0.73	0.464	12.73
221.5	3812	1.05	0.408	11.03	364.0	5936	0.90	0.453	12.39
223.5	3853	1.07	0.408	11.03	365.0	5950	0.87	0.426	11.58
225.0	3884	1.16	0.447	12.21	367.0	5977	0.81	0.429	11.67
226.5	3915	1.26	0.395	10.64	369.0	6004	0.94	0.422	11.45
228.5	3956	1.16	0.381	10.21	370.0	6017	0.95	0.460	12.61
231.5	4018	1.26	0.393	10.58	372.0	6044	0.85	0.440	12.00
233.5	4059	1.30	0.396	10.67	373.5	6064	0.69	0.459	12.58
235.5	4100	1.51	0.376	10.06	378.0	6125	0.82	0.454	12.42
236.5	4120	1.36	0.381	10.21	380.0	6152	0.74	0.455	12.45
238.5	4162	1.50	0.406	10.97	381.5	6172	0.78	0.458	12.55
240.0	4192	1.72	0.403	10.88	383.5	6199	0.68	0.462	12.67
240.5	4203	1.68	0.381	10.21	385.0	6219	0.76	0.445	12.15
243.5	4264	1.52	0.408	11.03	386.5	6239	0.62	0.459	12.58
246.0	4316	1.56	0.397	10.70	388.5	6266	0.83	0.454	12.42
248.0	4357	1.62	0.398	10.73	390.5	6293	0.71	0.448	12.24
256.0	4483	1.40	0.414	11.21	391.5	6306	0.67	0.461	12.64
258.5	4516	1.04	0.415	11.24	393.5	6333	0.00	0.468	12.85
260.0	4536	1.30	0.409	11.06	395.0	6354	0.00	0.451	12.33
261.5	4557	1.26	0.415	11.24	396.5	6374	0.00	0.442	12.06
263.5	4584	1.41	0.414	11.21	398.5	6401	0.00	0.471	12.94
265.0	4604	1.50	0.402	10.85	400.0	6421	0.00	0.411	11.12
266.5	4624	1.44	0.404	10.91	401.5	6441	0.00	0.493	13.61
268.5	4651	1.22	0.435	11.85					

Appendix 8 Data of gravity-core IOW372650 in the northeastern Skagerrak.

Depth (cm)	Age (cal. yr BP)	$\%C_{37:4}$	$U^{K'}_{37}$	SST (ºC)	Depth (cm)	Age (cal. yr BP)	$\%C_{37:4}$	$U^{K'}_{37}$	SST (ºC)
0.5	337	4.21	0.336	8.86	273.5	3559	1.74	0.312	8.12
1.5	344	4.23	0.332	8.74	274.5	3571	1.58	0.364	9.70
2.5	351	4.08	0.331	8.71	275.5	3583	1.64	0.328	8.59
3.5	358	4.56	0.312	8.13	276.5	3595	1.46	0.365	9.72
4.5	366	4.08	0.338	8.92	277.5	3606	1.44	0.358	9.51
5.5	373	4.32	0.319	8.34	278.5	3618	1.59	0.339	8.93
6.5	380	4.21	0.338	8.90	279.5	3630	1.24	0.340	8.96
7.5	387	4.34	0.335	8.83	280.5	3642	1.31	0.333	8.75
8.5	394	4.30	0.322	8.44	281.5	3654	1.00	0.336	8.83
9.5	401	4.50	0.315	8.23	282.5	3666	1.16	0.358	9.51
10.5	409	4.61	0.318	8.32	283.5	3677	1.43	0.317	8.27
11.5	416	4.45	0.330	8.67	284.5	3689	1.36	0.310	8.07
12.5	423	4.61	0.321	8.40	285.5	3703	0.93	0.365	9.72
13.5	430	4.38	0.332	8.73	286.5	3719	1.13	0.346	9.15
14.5	437	4.48	0.334	8.79	287.5	3735	1.45	0.338	8.89
15.5	445	3.66	0.308	8.01	288.5	3751	1.61	0.341	9.01
16.5	452	4.61	0.314	8.17	289.5	3768	1.20	0.338	8.90
17.5	459	4.20	0.329	8.62	290.5	3784	1.48	0.354	9.40
18.5	466	4.59	0.300	7.76	291.5	3800	1.02	0.372	9.93
19.5	473	4.32	0.307	7.97	292.5	3816	1.28	0.375	10.04
20.5	481	4.70	0.273	6.94	293.5	3832	1.41	0.315	8.21
21.5	488	4.53	0.321	8.39	294.5	3848	1.54	0.321	8.40
22.5	495	4.36	0.334	8.78	295.5	3864	1.37	0.313	8.14
23.5	502	4.19	0.329	8.65	296.5	3880	1.19	0.377	10.08
24.5	509	4.74	0.334	8.80	297.5	3897	1.18	0.395	10.64
25.5	517	3.43	0.365	9.72	298.5	3913	1.54	0.313	8.17
26.5	524	4.66	0.318	8.31	299.5	3929	1.68	0.274	6.98
27.5	531	4.67	0.330	8.65	300.5	3945	1.28	0.346	9.14
28.5	538	4.62	0.315	8.20	301.5	3961	1.21	0.350	9.28
29.5	545	4.54	0.325	8.53	302.5	3977	1.07	0.363	9.68
30.5	553	4.37	0.333	8.75	303.5	3993	1.14	0.368	9.81
31.5	560	4.60	0.325	8.51	304.5	4009	1.16	0.371	9.90
32.5	567	4.59	0.333	8.77	305.5	4026	1.41	0.404	10.92
33.5	574	4.83	0.314	8.19	306.5	4042	1.35	0.322	8.41
34.5	581	5.27	0.309	8.03	307.5	4058	1.31	0.334	8.80
35.5	589	3.94	0.336	8.85	308.5	4074	1.24	0.380	10.17
36.5	596	5.25	0.320	8.38	309.5	4090	1.37	0.317	8.26
37.5	603	5.41	0.318	8.30	310.5	4106	1.03	0.379	10.14
38.5	610	5.22	0.292	7.50	311.5	4122	1.23	0.330	8.65
39.5	617	5.30	0.297	7.66	312.5	4138	1.22	0.343	9.06
40.5	624	5.48	0.306	7.93	313.5	4155	1.20	0.387	10.40
41.5	632	5.27	0.308	8.00	315.5	4187	1.40	0.354	9.40
42.5	639	5.46	0.307	7.98	316.5	4203	1.75	0.372	9.94
43.5	646	5.58	0.303	7.86	317.5	4219	1.97	0.326	8.54
44.5	653	5.81	0.281	7.18	318.5	4235	2.02	0.304	7.89
45.5	660	5.20	0.287	7.38	319.5	4251	2.29	0.313	8.14
46.5	668	5.50	0.319	8.33	320.5	4267	1.89	0.344	9.09
47.5	675	5.66	0.290	7.47	321.5	4284	1.30	0.323	8.46
48.5	682	5.46	0.300	7.74	322.5	4300	1.90	0.325	8.51
49.5	689	4.15	0.302	7.83	323.5	4316	1.93	0.291	7.48
50.5	696	4.40	0.273	6.93	324.5	4339	1.68	0.376	10.07
51.5	704	4.19	0.286	7.33	325.5	4369	1.68	0.353	9.35
52.5	711	4.13	0.315	8.22	326.5	4399	2.33	0.270	6.85
53.5	718	4.25	0.279	7.12	327.5	4429	1.94	0.317	8.26
54.5	725	4.35	0.288	7.41	328.5	4460	2.09	0.300	7.76
55.5	732	3.88	0.247	6.15	329.5	4490	2.08	0.362	9.63
56.5	741	4.34	0.289	7.41	330.5	4520	2.01	0.339	8.93
57.5	751	4.09	0.319	8.32	331.5	4550	1.72	0.384	10.29
58.5	760	3.74	0.337	8.88	332.5	4580	2.13	0.344	9.10
59.5	770	4.19	0.326	8.55	333.5	4610	2.17	0.303	7.85
60.5	780	4.18	0.284	7.28	334.5	4641	1.99	0.320	8.37
61.5	789	4.21	0.292	7.50	335.5	4671	1.76	0.354	9.40
62.5	799	3.78	0.345	9.13	336.5	4701	2.87	0.370	9.88
63.5	809	4.24	0.279	7.13	337.5	4731	2.23	0.388	10.44
64.5	819	3.98	0.306	7.95	338.5	4761	2.42	0.397	10.69
65.5	828	3.71	0.239	5.91	339.5	4791	2.21	0.388	10.42

Depth (cm)	Age (cal. yr BP)	$\%C_{37:4}$	$U^{K'}_{37}$	SST (ºC)	Depth (cm)	Age (cal. yr BP)	$\%C_{37:4}$	$U^{K'}_{37}$	SST (ºC)
66.5	838	3.93	0.316	8.23	340.5	4822	2.54	0.311	8.08
67.5	848	4.02	0.298	7.68	341.5	4852	2.22	0.387	10.40
68.5	858	3.31	0.340	8.96	342.5	4882	2.41	0.368	9.82
69.5	867	4.18	0.280	7.16	345.5	4972	2.41	0.331	8.70
70.5	877	3.50	0.318	8.31	346.5	5002	2.35	0.341	9.00
71.5	887	4.26	0.285	7.30	347.5	5033	2.53	0.314	8.18
72.5	896	3.57	0.325	8.50	348.5	5063	4.18	0.389	10.45
73.5	906	3.64	0.326	8.56	349.5	5093	3.71	0.300	7.76
74.5	916	3.65	0.332	8.74	350.5	5123	3.42	0.298	7.68
75.5	926	3.36	0.290	7.47	351.5	5153	3.08	0.272	6.90
76.5	935	4.17	0.309	8.04	352.5	5183	3.65	0.336	8.85
77.5	945	3.60	0.344	9.09	353.5	5214	3.71	0.334	8.78
78.5	955	4.27	0.281	7.19	354.5	5244	4.04	0.348	9.22
79.5	964	4.09	0.311	8.09	355.5	5274	4.55	0.387	10.40
80.5	974	4.31	0.289	7.43	356.5	5298	1.43	0.294	7.57
81.5	984	4.21	0.305	7.91	357.5	5314	1.48	0.311	8.09
82.5	994	3.90	0.325	8.51	358.5	5331	1.64	0.272	6.91
83.5	1003	4.20	0.313	8.16	359.5	5348	1.50	0.286	7.32
84.5	1013	4.01	0.329	8.63	360.5	5365	1.28	0.294	7.58
85.5	1023	2.96	0.380	10.19	361.5	5382	1.32	0.310	8.05
86.5	1032	4.28	0.309	8.04	362.5	5398	1.78	0.281	7.18
87.5	1042	4.15	0.321	8.40	363.5	5415	1.96	0.264	6.68
88.5	1052	4.07	0.303	7.84	364.5	5432	1.94	0.297	7.66
89.5	1062	3.71	0.334	8.79	365.5	5449	1.41	0.331	8.71
90.5	1071	3.99	0.316	8.25	366.5	5466	1.70	0.329	8.64
91.5	1081	4.20	0.273	6.95	367.5	5483	1.81	0.295	7.60
92.5	1091	3.97	0.309	8.04	368.5	5499	1.60	0.346	9.15
93.5	1101	4.00	0.316	8.24	369.5	5516	1.76	0.316	8.24
94.5	1110	4.37	0.294	7.58	370.5	5533	2.00	0.308	8.01
95.5	1120	4.55	0.228	5.58	371.5	5550	1.70	0.341	9.00
96.5	1130	4.23	0.295	7.61	372.5	5567	2.01	0.305	7.91
97.5	1139	3.95	0.320	8.38	373.5	5583	2.60	0.270	6.84
98.5	1149	4.24	0.295	7.61	374.5	5600	2.25	0.291	7.48
99.5	1159	4.49	0.291	7.48	375.5	5617	2.00	0.355	9.42
100.5	1169	4.30	0.311	8.10	376.5	5634	2.17	0.300	7.77
101.5	1178	4.08	0.310	8.07	377.5	5651	2.90	0.280	7.16
102.5	1188	4.17	0.303	7.86	378.5	5668	2.73	0.278	7.10
103.5	1198	3.92	0.305	7.91	379.5	5684	2.67	0.276	7.04
104.5	1207	4.23	0.307	7.97	380.5	5701	2.45	0.404	10.91
105.5	1217	3.82	0.263	6.64	381.5	5718	3.29	0.285	7.29
107.5	1238	4.35	0.294	7.59	382.5	5735	3.08	0.308	7.99
108.5	1248	4.64	0.268	6.79	383.5	5752	3.21	0.302	7.82
109.5	1259	3.89	0.308	8.01	384.5	5768	3.55	0.287	7.36
110.5	1269	4.02	0.276	7.03	385.5	5785	2.66	0.416	11.27
111.5	1280	3.68	0.309	8.02	386.5	5802	3.52	0.312	8.13
112.5	1291	4.73	0.254	6.36	387.5	5819	3.19	0.348	9.21
113.5	1301	4.35	0.278	7.08	388.5	5836	3.24	0.316	8.23
114.5	1312	4.62	0.280	7.15	389.5	5852	2.74	0.309	8.04
115.5	1322	3.61	0.309	8.02	390.5	5869	2.26	0.391	10.53
116.5	1333	4.51	0.283	7.25	391.5	5886	2.39	0.324	8.47
117.5	1343	3.88	0.311	8.08	392.5	5903	1.48	0.425	11.54
118.5	1354	4.58	0.285	7.32	393.5	5920	1.42	0.378	10.11
119.5	1364	4.43	0.243	6.04	394.5	5937	1.48	0.390	10.49
120.5	1375	4.63	0.263	6.64	395.5	5953	1.38	0.396	10.67
121.5	1385	3.37	0.346	9.14	396.5	5970	1.65	0.358	9.53
122.5	1396	3.49	0.337	8.89	397.5	5987	1.30	0.403	10.87
123.5	1406	4.63	0.232	5.70	398.5	6004	1.46	0.392	10.55
124.5	1417	4.09	0.300	7.76	399.5	6021	1.51	0.397	10.71
125.5	1428	3.47	0.311	8.10	400.5	6037	1.31	0.373	9.97
126.5	1438	5.35	0.198	4.66	401.5	6054	1.23	0.395	10.63
127.5	1449	4.67	0.239	5.92	402.5	6071	1.18	0.399	10.76
128.5	1459	4.18	0.278	7.10	404.5	6105	1.16	0.401	10.83
129.5	1470	4.09	0.284	7.27	405.5	6122	1.93	0.452	12.37
130.5	1480	4.86	0.259	6.52	406.5	6138	1.36	0.341	9.00
131.5	1491	4.70	0.250	6.24	407.5	6155	1.59	0.347	9.18
132.5	1501	4.03	0.256	6.43	408.5	6172	1.70	0.369	9.85
133.5	1512	5.32	0.246	6.13	409.5	6189	1.79	0.341	8.99
134.5	1522	5.49	0.272	6.91	410.5	6206	1.40	0.402	10.84

Depth (cm)	Age (cal. yr BP)	$\%C_{37:4}$	$U^{K'}_{37}$	SST (ºC)	Depth (cm)	Age (cal. yr BP)	$\%C_{37:4}$	$U^{K'}_{37}$	SST (ºC)
135.5	1533	4.82	0.246	6.12	411.5	6222	1.86	0.397	10.68
136.5	1543	5.72	0.227	5.54	412.5	6239	1.99	0.386	10.38
137.5	1554	5.18	0.279	7.13	413.5	6256	1.95	0.370	9.87
138.5	1565	5.38	0.277	7.06	414.5	6273	2.33	0.305	7.91
139.5	1575	2.97	0.314	8.18	415.5	6290	1.31	0.482	13.26
140.5	1586	4.01	0.345	9.14	416.5	6336	1.70	0.468	12.86
141.5	1596	4.07	0.318	8.31	417.5	6413	1.93	0.390	10.47
142.5	1607	3.76	0.313	8.14	418.5	6490	1.32	0.477	13.11
143.5	1617	3.78	0.297	7.65	419.5	6567	0.85	0.485	13.35
144.5	1628	3.74	0.320	8.36	420.5	6644	1.20	0.499	13.80
145.5	1638	3.04	0.354	9.39	421.5	6721	1.12	0.498	13.76
146.5	1649	4.20	0.269	6.82	422.5	6798	1.02	0.493	13.60
147.5	1659	3.28	0.323	8.47	423.5	6875	1.24	0.500	13.80
148.5	1670	4.33	0.308	7.99	424.5	6952	1.23	0.486	13.40
149.5	1680	3.96	0.331	8.70	425.5	7030	1.36	0.498	13.76
150.5	1691	4.05	0.304	7.89	426.5	7107	1.26	0.480	13.21
151.5	1702	4.13	0.339	8.94	427.5	7184	1.31	0.491	13.54
152.5	1712	3.56	0.361	9.62	428.5	7261	1.57	0.492	13.57
153.5	1723	3.83	0.354	9.40	429.5	7317	1.57	0.498	13.76
154.5	1733	4.25	0.281	7.19	430.5	7373	1.44	0.500	13.81
155.5	1744	2.91	0.408	11.04	431.5	7429	1.36	0.441	12.03
156.5	1755	3.86	0.284	7.27	432.5	7485	1.35	0.454	12.43
157.5	1768	3.63	0.298	7.71	433.5	7541	1.25	0.447	12.21
158.5	1780	3.87	0.285	7.29	434.5	7597	1.27	0.419	11.38
159.5	1793	3.67	0.310	8.06	435.5	7653	1.38	0.467	12.83
160.5	1806	4.04	0.301	7.80	436.5	7709	1.14	0.395	10.62
161.5	1818	3.99	0.377	10.08	437.5	7765	0.98	0.472	12.98
162.5	1831	3.29	0.278	7.09	438.5	7820	0.84	0.454	12.41
163.5	1843	2.90	0.330	8.67	439.5	7876	0.90	0.434	11.82
164.5	1856	3.39	0.290	7.47	440.5	7932	0.85	0.449	12.29
165.5	1869	3.19	0.238	5.87	441.5	7988	1.04	0.442	12.07
166.5	1881	2.96	0.331	8.71	442.5	8044	0.96	0.468	12.86
167.5	1894	2.80	0.355	9.44	443.5	8100	1.02	0.451	12.33
168.5	1906	2.56	0.373	9.96	444.5	8156	1.11	0.425	11.54
169.5	1919	3.02	0.313	8.15	445.5	8212	0.99	0.439	11.96
170.5	1932	2.67	0.353	9.37	446.5	8268	0.82	0.474	13.02
171.5	1944	2.46	0.339	8.95	447.5	8324	1.52	0.480	13.23
172.5	1957	2.77	0.331	8.70	448.5	8380	0.95	0.480	13.20
173.5	1969	2.88	0.351	9.30	449.5	8436	3.51	0.475	13.07
174.5	1982	2.96	0.314	8.18	450.5	8492	2.97	0.487	13.43
175.5	1995	2.99	0.253	6.33	451.5	8548	5.33	0.487	13.44
176.5	2007	2.85	0.317	8.28	452.5	8604	2.55	0.490	13.53
177.5	2020	2.36	0.343	9.07	453.5	8660	2.14	0.480	13.22
178.5	2032	3.14	0.276	7.04	454.5	8716	2.80	0.474	13.02
179.5	2045	2.49	0.370	9.87	455.5	8771	3.64	0.477	13.11
180.5	2057	2.51	0.330	8.67	456.5	8827	3.13	0.479	13.19
181.5	2070	2.60	0.336	8.84	457.5	8883	2.15	0.486	13.40
182.5	2083	3.08	0.275	7.00	458.5	8939	2.01	0.503	13.92
183.5	2095	3.11	0.262	6.60	459.5	8995	2.51	0.486	13.41
184.5	2108	2.44	0.353	9.37	460.5	9051	2.88	0.482	13.28
185.5	2120	2.29	0.306	7.95	461.5	9107	2.79	0.485	13.35
186.5	2133	4.04	0.239	5.92	462.5	9163	3.27	0.466	12.78
187.5	2146	3.49	0.268	6.78	463.5	9219	3.02	0.467	12.83
188.5	2158	3.26	0.278	7.08	464.5	9275	2.93	0.466	12.79
189.5	2171	3.80	0.214	5.16	465.5	9331	4.00	0.466	12.79
190.5	2183	2.62	0.308	8.01	466.5	9387	4.26	0.470	12.90
191.5	2196	2.85	0.292	7.52	467.5	9443	3.50	0.463	12.69
192.5	2209	3.29	0.311	8.10	468.5	9499	3.75	0.453	12.40
193.5	2221	2.86	0.297	7.67	469.5	9555	3.72	0.442	12.07
194.5	2234	3.35	0.265	6.69	470.5	9611	3.78	0.441	12.03
195.5	2246	2.70	0.280	7.16	471.5	9667	4.72	0.446	12.18
196.5	2259	4.39	0.241	5.96	472.5	9723	4.58	0.443	12.09
197.5	2272	2.78	0.293	7.54	473.5	9778	4.96	0.435	11.84
198.5	2284	2.21	0.338	8.92	474.5	9834	5.39	0.434	11.80
199.5	2297	2.97	0.317	8.28	475.5	9890	4.60	0.434	11.81
200.5	2313	1.96	0.307	7.96	476.5	9946	6.90	0.431	11.73
201.5	2332	2.26	0.337	8.87	477.5	10002	4.62	0.438	11.93
202.5	2351	1.88	0.332	8.74	478.5	10058	4.18	0.449	12.29

Depth (cm)	Age (cal. yr BP)	$\%C_{37:4}$	$U^{K'}_{37}$	SST (ºC)	Depth (cm)	Age (cal. yr BP)	$\%C_{37:4}$	$U^{K'}_{37}$	SST (ºC)
203.5	2370	2.36	0.293	7.54	479.5	10114	4.05	0.455	12.45
204.5	2389	2.30	0.273	6.94	480.5	10170	4.18	0.457	12.51
205.5	2408	1.35	0.395	10.62	481.5	10226	4.03	0.460	12.60
206.5	2427	2.06	0.326	8.54	482.5	10282	4.02	0.459	12.57
207.5	2446	1.79	0.343	9.06	483.5	10338	4.24	0.469	12.89
208.5	2466	2.02	0.337	8.86	484.5	10394	3.67	0.473	12.99
209.5	2485	1.88	0.311	8.09	485.5	10450	3.57	0.475	13.07
210.5	2504	2.18	0.307	7.98	486.5	10506	3.69	0.477	13.11
211.5	2523	1.91	0.310	8.06	487.5	10562	3.65	0.462	12.66
212.5	2542	1.94	0.311	8.10	488.5	10618	3.35	0.471	12.94
213.5	2561	1.91	0.331	8.70	489.5	10674	3.74	0.454	12.44
214.5	2580	2.49	0.275	7.01	490.5	10730	3.75	0.457	12.51
215.5	2599	1.61	0.364	9.70	491.5	10785	3.90	0.455	12.46
216.5	2619	2.76	0.235	5.79	492.5	10841	4.14	0.443	12.08
217.5	2638	2.25	0.275	7.00	493.5	10897	4.07	0.446	12.19
218.5	2657	2.13	0.270	6.86	494.5	10953	4.64	0.433	11.79
219.5	2676	2.65	0.272	6.92	495.5	11009	4.41	0.439	11.96
220.5	2695	2.12	0.304	7.86	496.5	11065	3.92	0.447	12.22
221.5	2714	2.47	0.286	7.34	497.5	11121	3.92	0.443	12.08
222.5	2733	2.20	0.311	8.09	498.5	11177	4.00	0.452	12.35
223.5	2752	2.42	0.285	7.29	499.5	11233	3.96	0.450	12.31
224.5	2766	2.42	0.331	8.70	500.5	11309	4.13	0.439	11.97
226.5	2783	2.62	0.260	6.53	501.5	11405	4.37	0.428	11.65
227.5	2791	2.34	0.278	7.08	502.5	11500	4.15	0.433	11.80
228.5	2799	2.18	0.289	7.42	503.5	11596	4.49	0.417	11.31
229.5	2807	2.31	0.255	6.40	504.5	11691	4.28	0.420	11.40
230.5	2816	2.10	0.295	7.61	505.5	11786	3.66	0.452	12.36
231.5	2824	2.56	0.247	6.15	506.5	11882	4.03	0.443	12.08
232.5	2832	2.03	0.302	7.83	507.5	11977	3.90	0.442	12.06
233.5	2840	1.81	0.339	8.94	508.5	12073	3.97	0.441	12.04
234.5	2849	2.10	0.319	8.34	509.5	12168	3.72	0.441	12.02
235.5	2857	1.49	0.413	11.17	510.5	12264	3.20	0.448	12.24
236.5	2865	1.76	0.366	9.76	511.5	12359	3.96	0.417	11.31
237.5	2873	2.14	0.295	7.62	512.5	12454	3.48	0.445	12.16
238.5	2881	2.20	0.308	8.01	513.5	12550	3.66	0.421	11.41
239.5	2890	2.10	0.327	8.59	514.5	12645	3.41	0.440	11.99
240.5	2898	2.30	0.364	9.68	515.5	12741	3.57	0.440	12.01
241.5	2906	2.56	0.310	8.06	516.5	12836	4.29	0.415	11.23
242.5	2914	2.54	0.360	9.59	517.5	12932	3.92	0.427	11.61
243.5	2923	2.54	0.350	9.28	518.5	13027	3.34	0.438	11.93
244.5	2931	2.92	0.280	7.14	519.5	13122	3.07	0.438	11.94
245.5	2954	2.15	0.353	9.36	520.5	13218	3.18	0.446	12.19
246.5	2992	2.41	0.295	7.61	521.5	13313	3.42	0.449	12.28
247.5	3030	2.00	0.384	10.30	522.5	13409	4.07	0.417	11.30
248.5	3068	1.49	0.402	10.85	523.5	13504	3.99	0.448	12.24
249.5	3106	2.34	0.335	8.81	524.5	13600	3.93	0.440	12.01
250.5	3144	1.58	0.373	9.97	525.5	13695	3.36	0.451	12.34
251.5	3181	1.91	0.343	9.07	526.5	13790	3.26	0.463	12.71
252.5	3219	1.94	0.358	9.51					
253.5	3257	1.86	0.320	8.37					
254.5	3295	1.87	0.328	8.60					
256.5	3358	1.83	0.348	9.22					
257.5	3370	1.77	0.333	8.77					
258.5	3382	1.70	0.317	8.27					
259.5	3394	1.76	0.340	8.97					
260.5	3405	1.66	0.362	9.62					
261.5	3417	1.59	0.346	9.14					
262.5	3429	1.44	0.340	8.98					
263.5	3441	1.61	0.331	8.69					
264.5	3453	1.76	0.314	8.19					
265.5	3464	1.75	0.363	9.68					
266.5	3476	1.75	0.320	8.35					
267.5	3488	1.85	0.383	10.28					
268.5	3500	1.64	0.352	9.32					
269.5	3512	1.46	0.332	8.74					
270.5	3524	1.69	0.374	10.01					
271.5	3535	1.64	0.400	10.80					
272.5	3547	1.67	0.316	8.24					

Kattegat/Mecklenburg Bay

Appendix 9 Data of gravity-cores in the Kattegat (IOW318180/IOW242970) and Mecklenburg Bay (MB409/IOW257760).

Depth (cm)	Age (cal. yrs BP)	>63µm (%)	Depth (cm)	Age (cal. yrs BP)	>63µm (%)	Depth (cm)	>63µm (%)	Depth (cm)	>63µm (%)
318180			242970			MB409		257760	
0.5		78.3	0.5		82.3	2	15.8	1	23.2
1.5		80.9	1.5		82.7	6	13.0	2	27.0
2.5		83.4	2.5		87.3	10	15.1	3	26.6
3.5		82.8	3.5		87.4	14	15.1	4	29.0
4.5		82.3	4.5		86.3	18	10.0	5	29.9
5.5		81.5	5.5		85.0	22	9.8	6	24.2
6.5		82.8	6.5		86.1	26	9.0	7	22.7
7.5		82.1	7.5		86.1	30	12.6	8	23.1
8.5	83	82.7	8.5		82.9	34	9.3	9	23.6
9.5	113	84.8	9.5		85.7	38	7.7	10	22.5
10.5	143	86.0	10.5		83.7	42	5.9	11	27.3
11.5	173	86.0	11.5		86.1	46	7.7	12	21.8
12.5	203	85.4	12.5		85.7	50	3.3	13	22.3
13.5	233	85.7	13.5		86.2	54	4.2	14	23.1
14.5	262	82.8	14.5		83.2	58	8.9	15	24.3
15.5	292	83.4	15.5		85.6	62	3.3	16	34.6
16.5	322	84.4	16.5		87.6	66	5.4	17	24.3
17.5	352	80.6	17.5		84.5	70	3.6	18	23.6
18.5	382	83.2	18.5	416	86.6	74	5.9	19	25.6
19.5	412	80.9	19.5	479	88.7	78		20	26.7
20.5	442	83.1	20.5	541	84.1	82	5.1	21	26.7
21.5	472	82.2	21.5	604	84.1	86	3.3	22	25.9
22.5	502	82.5	22.5	667	83.8	90	3.9	23	25.7
23.5	532	82.9	23.5	729	81.3	94	3.4	24	26.0
24.5	561	81.1	24.5	792	82.3	98	0.2	25	24.3
25.5	591	80.9	25.5	854	81.8	102	2.0	26	23.5
26.5	621	80.4	26.5	917	80.6	106	3.7	27	19.8
27.5	651	78.5	27.5	980	86.2	110		28	21.4
28.5	681	79.0	28.5	1042	81.6	114	4.0	29	20.6
29.5	711	79.3	29.5	1105	78.0	118	3.2	30	22.4
30.5	724	78.0	30.5	1168	74.1	122	3.3	31	20.8
31.5	737	74.1	31.5	1230	73.0	126	3.9	32	20.6
32.5	750	73.1	32.5	1293	77.5	130	3.8	33	20.1
33.5	763	78.1	33.5	1355	71.9	134	4.7	34	19.3
34.5	776	76.9	34.5	1418	73.2	138	2.4	35	18.7
35.5	789	75.4	35.5	1481	69.7	142	2.1	36	16.8
36.5	802	75.2	36.5	1543	70.2	146	1.1	37	17.0
37.5	815	75.5	37.5	1606	66.6	150	1.1	38	17.9
38.5	828	75.4	38.5	1669	70.3	154	1.4	39	15.2
39.5	841	75.2	39.5	1731	67.4	158	1.9	40	11.4
40.5	854	76.7	40.5	1794	57.1	162	1.8	41	15.7
41.5	867	75.0	41.5	1856	65.8	166	3.0	42	15.8
42.5	880	72.5	42.5	1919	58.0	170	2.9	43	17.2
43.5	893	73.7	43.5	1982	58.8	174	2.4	44	16.2
44.5	906	72.4	44.5	2044	58.9	180	5.5	45	13.8
45.5	919	71.4	45.5	2107	64.4	184	2.9	46	11.2
46.5	931	73.4	46.5	2170	60.2	188	2.4	47	12.0
47.5	944	72.2	47.5	2232	54.2	192	1.5	48	9.0
48.5	957	73.6	48.5	2295	50.3	196	1.8	49	7.0
49.5	970	72.8	49.5	2312	53.3	200	1.7	50	8.0
50.5	983	73.2	50.5	2330	50.0			51	8.9
51.5	996	74.0	51.5	2347	52.9			52	14.0
52.5	1009	72.9	52.5	2364	52.6			53	10.4
53.5	1022	71.6	53.5	2381	50.5			54	11.1
54.5	1035	69.3	54.5	2399	44.5			55	7.9
55.5	1048	74.5	55.5	2416	50.8			56	5.4
56.5	1061	72.0	56.5	2433	48.6			57	6.5
57.5	1074	73.3	57.5	2451	54.3			58	7.6
58.5	1087	71.9	58.5	2468	53.6			59	7.2

Depth (cm)	Age (cal. yrs BP)	>63µm (%)	Depth (cm)	Age (cal. yrs BP)	>63µm (%)	Depth (cm)	>63µm (%)	Depth (cm)	>63µm (%)
59.5	1100	71.9	59.5	2485	54.4			60	6.4
60.5	1113	71.9	60.5	2502	40.0			61	7.1
61.5	1126	71.1	61.5	2520	45.9			62	8.7
62.5	1150	71.4	62.5	2537	54.2			63	7.4
63.5	1174	70.9	63.5	2554	49.2			64	7.1
64.5	1199	67.6	64.5	2572	43.4			65	7.2
65.5	1223	69.3	65	2589	30.8			66	7.1
66.5	1247	70.2	65.5	2606	36.9			67	10.1
67.5	1271	69.3	66	2624	29.2			68	9.3
68.5	1296	71.3	66.5	2641	45.4			69	10.1
69.5	1320	67.7	67	2658	27.6			70	10.9
70.5	1344	67.4	67.5	2675	30.1			71	9.0
71.5	1368	65.4	68	2693	23.9			72	10.3
72.5	1392	65.7	68.5	2710	33.4			73	11.4
73.5	1417	65.4	69	2719	25.6			74	10.7
74.5	1441	65.3	69.5	2728	35.9			75	9.2
75.5	1465	63.7	70.5	2736	31.5			76	9.1
76.5	1489	65.3	71.5	2745	31.2			77	9.3
77.5	1514	65.1	72.5	2754	31.9			78	9.4
78.5	1538	62.3	73.5	2763	33.5			79	8.2
79.5	1562	64.9	74.5	2771	28.6			80	7.9
80.5	1586	62.0	75.5	2780	25.8			81	7.2
81.5	1610	60.5	76.5	2789	28.4			82	6.1
82.5	1635	65.3	77.5	2798	25.3			83	6.1
83.5	1659	65.5	78.5	2806	28.7			84	5.1
84.5	1683	63.8	79.5	2815	31.3			85	5.1
85.5	1707	61.8	80.5	2824	27.8			86	5.8
86.5	1732	66.2	81.5	2833	30.8			87	5.8
87.5	1756	66.5	82.5	2842	32.3			88	5.9
88.5	1780	67.1	83.5	2850	29.5			89	7.4
89.5	1804	63.9	84.5	2859	29.4			90	7.1
90.5	1828	63.8	85.5	2868	30.2			91	8.0
91.5	1853	62.8	86.5	2877	32.3			92	8.3
92.5	1877	62.7	87.5	2885	27.5			93	5.7
93.5	1901	63.2	88.5	2894	30.0			94	6.0
94.5	1925	63.4	89.5	2903	35.1			95	5.9
95.5	1949	63.5	90.5	2912	27.8			96	4.9
96.5	1974	63.1	91.5	2920	30.9			97	5.3
97.5	1998	62.6	92.5	2929	31.2			98	5.8
98.5	2022	62.2	93.5	2938	30.2			99	5.8
99.5	2046	60.5	94.5	2947	30.0			100	6.2
100.5	2071	52.8	95.5	2956	32.4			101	5.5
101.5	2095	61.5	96.5	2964	30.9			102	4.7
102.5	2119	62.9	97.5	2973	34.3			103	4.1
103.5	2143	60.0	98.5	2982	32.9			104	3.8
104.5	2167	60.3	99.5	2991	29.5			105	4.8
105.5	2192	61.5	101	2999	26.6			106	4.3
106.5	2216	60.2	103	3008	26.5			107	2.6
107.5	2240	60.9	105	3017	25.4			108	3.2
108.5	2264	58.7	107	3026	26.4			109	3.5
109.5	2289	59.7	109	3034	27.6			110	3.3
110.5	2313	56.0	111	3043	24.0			111	2.8
111.5	2337	57.8	113	3052	29.1			112	2.5
112.5	2364	56.0	115	3061	29.6			113	3.1
113.5	2390	56.0	117	3070	28.6			114	2.9
114.5	2417	54.9	119	3078	29.4			115	2.3
115.5	2444	54.4	121	3087	23.5			116	1.8
116.5	2471	53.8	123	3096	26.9			117	2.0
117.5	2497	47.0	125	3105	28.6			118	3.2
118.5	2524	48.7	127	3113	27.8			119	2.9
119.5	2551	51.9	129	3122	28.2			120	2.9
120.5	2578	47.7	131	3131	23.6			121	3.2
121.5	2604	44.6	133	3140	28.3			122	3.2
122.5	2631	47.6	135	3149	29.0			123	3.9
123.5	2658	45.0	137	3157	27.6			124	2.4
124.5	2684	45.3	139	3166	25.1			125	1.6

Depth (cm)	Age (cal. yrs BP)	>63µm (%)	Depth (cm)	Age (cal. yrs BP)	>63µm (%)	Depth (cm)	>63µm (%)	Depth (cm)	>63µm (%)
125.5	2711	43.2	141	3175	22.4			126	2.2
126.5	2738	41.4	143	3184	26.0			127	1.7
127.5	2765	47.9	145	3192	26.5			128	2.5
128.5	2791	46.1	147	3201	22.9			129	2.2
129.5	2818	45.3	149	3210	20.4			130	2.0
130.5	2845	46.3	151	3219	20.8			131	2.2
131.5	2872	44.6	153	3227	20.0			132	2.2
132.5	2898	41.8	155	3236	19.9			133	2.9
133.5	2925	46.7	157	3245	20.8			134	4.7
134.5	2952	45.0	159	3254	18.5			135	4.7
135.5	2978	40.8	161	3263	20.2			136	3.2
136.5	3005	40.9	163	3271	20.4			137	2.2
137.5	3032	41.2	165	3280	20.1			138	2.1
138.5	3059	39.0	167	3289	21.1			139	2.2
139.5	3085	38.2	169	3298	18.7			140	2.5
140.5	3112	40.5	171	3306	18.2			141	2.4
141.5	3139	40.8	173	3315	17.3			142	3.2
142.5	3166	40.5	175	3324	18.3			143	2.6
143.5	3192	37.8	177	3333	17.2			144	2.2
144.5	3219	42.7	179	3341	15.5			145	2.5
145.5	3246	43.3	181	3350	16.0			146	
146.5	3264	42.9	183	3359	16.3			147	2.5
147.5	3273	45.9	185	3368	15.6			148	3.1
148.5	3282	42.3	187	3377	14.2			149	2.8
149.5	3291	39.4	189	3385	14.8			150	2.3
150.5	3301	42.4	191	3394	17.1			151	2.9
151.5	3310	41.0	193	3403	19.3			152	2.9
152.5	3319	38.2	195	3412	14.6			153	2.4
153.5	3328	41.3	197	3420	13.4			154	3.2
154.5	3337	38.7	199	3429	12.8			155	2.8
155.5	3347	38.1	201	3438	13.7			156	3.5
156.5	3356	36.3	203	3447	9.5			157	2.6
157.5	3365	40.6	205	3455	8.8			158	3.2
158.5	3374	37.9	207	3464	8.2			159	2.3
159.5	3384	37.8	209	3473	9.7			160	3.0
160.5	3393	33.7	211	3482	7.4			161	3.2
161.5	3402	34.2	213	3506	10.7			162	2.8
162.5	3411	35.0	215	3530	7.5			163	3.5
163.5	3421	33.8	217	3554	8.5			164	3.5
164.5	3430	32.4	219	3578	8.1			165	3.1
165.5	3439	30.3	221	3602	8.9			166	2.8
166.5	3448	27.2	223	3626	8.6			167	3.2
167.5	3458	28.3	225	3650	7.3			168	2.4
168.5	3467	28.8	227	3674	10.3			169	2.6
169.5	3476	28.5	229	3698	7.1			170	3.1
170.5	3485	32.7	231	3722	8.8			171	4.0
171.5	3494	27.3	233	3745	7.2			172	3.7
172.5	3504	28.0	235	3769	7.0			173	5.0
173.5	3513	24.6	237	3793	8.6			174	6.1
174.5	3522	23.8	239	3817	8.3			175	6.2
175.5	3531	26.4	241	3841	7.4			176	6.6
176.5	3541	27.1	243	3865	8.2			177	4.8
177.5	3550	25.4	245	3889	7.0			178	3.5
178.5	3559	25.1	247	3913	7.7			179	3.3
179.5	3568	24.0	249	3937	6.8			180	1.6
180.5	3576	23.4	251	3961	5.9			181	0.8
181.5	3583	24.0	253	3985	5.8			182	1.2
182.5	3590	23.2	255	4009	6.0			183	1.2
183.5	3597	22.2	257	4033	6.4			184	2.1
184.5	3604	21.4	259	4057	5.1			185	1.1
185.5	3610	21.1	261	4081	7.0			186	0.9
186.5	3617	22.6	263	4105	5.4			187	0.6
187.5	3624	24.5	265	4129	6.0			188	1.2
188.5	3631	21.7	267	4153	5.9			189	0.8
189.5	3638	22.8	269	4177	5.8			190	1.1
190.5	3645	24.2	271	4200	5.7			191	1.4

Depth (cm)	Age (cal. yrs BP)	>63µm (%)	Depth (cm)	Age (cal. yrs BP)	>63µm (%)	Depth (cm)	>63µm (%)	Depth (cm)	>63µm (%)
191.5	3651	23.8	273	4224	6.1			192	1.9
192.5	3658	29.8	275	4248	6.3			193	2.4
193.5	3665	31.9	277	4272	6.3			194	1.1
194.5	3672	24.5	279	4296	4.1			195	1.2
195.5	3679	23.9	281	4320	5.9			196	1.2
196.5	3685	25.9	283	4344	6.3			197	2.4
197.5	3692	21.4	285	4368	6.4			198	1.6
198.5	3699	23.2	287	4392	4.9			199	1.7
199.5	3706	25.4	289	4416	4.7			200	1.7
200.5	3713	20.6	291	4440	6.1				
201.5	3719	22.4	293	4464	4.8				
202.5	3726	23.3	295	4488	4.5				
203.5	3733	21.5	297	4512	5.5				
204.5	3740	20.7	299	4536	5.3				
205.5	3747	16.8	301	4560	6.4				
206.5	3753	18.7	303	4584	5.5				
207.5	3760	19.6	305	4608	4.7				
208.5	3767	19.5	307	4632	6.2				
209.5	3774	19.7	309	4656	4.2				
210.5	3781	19.7	311	4679	3.8				
211.5	3788	20.6	313	4703	4.4				
212.5	3794	20.3	315	4727	3.7				
213.5	3801	20.1	317	4751	4.4				
214.5	3808	25.4	319	4775	4.3				
215.5	3828	22.2	321	4799	4.4				
216.5	3848	19.0	323	4823	3.1				
217.5	3867	19.0	325	4847	4.3				
218.5	3887	19.6	327	4871	3.6				
219.5	3907	14.6	329	4895	4.0				
220.5	3927	18.4	331	4919	4.1				
221.5	3946	18.6	333	4943	5.4				
222.5	3966	19.3	335	4967	4.5				
223.5	3986	20.9	337	4991	4.0				
224.5	4006	20.0	339	5015	4.5				
225.5	4025	19.8	341	5039	4.7				
226.5	4045	15.4	343	5063	4.6				
227.5	4065	15.3	345	5087	3.4				
228.5	4085	15.1							
229.5	4104	14.1							
230.5	4124	13.5							
231.5	4144	15.9							
232.5	4164	16.0							
233.5	4183	18.6							
234.5	4203	16.2							
235.5	4223	14.8							
236.5	4243	14.0							
237.5	4262	13.0							
238.5	4282	12.3							
239.5	4302	11.9							
240.5	4322	13.4							
241.5	4341	13.0							
242.5	4361	12.0							
243.5	4381	12.8							
244.5	4400	13.5							
245.5	4420	11.9							
246.5	4440	12.5							
247.5	4460	13.4							
248.5	4479	14.2							
249.5	4499	14.1							
250.5	4519	13.6							
251.5	4539	11.5							
252.5	4558	12.9							
253.5	4578	13.9							
254.5	4598	13.8							
255.5	4618	12.5							
256.5	4637	13.0							

Depth (cm)	Age (cal. yrs BP)	>63µm (%)	Depth (cm)	Age (cal. yrs BP)	>63µm (%)	Depth (cm)	>63µm (%)	Depth (cm)	>63µm (%)
257.5	4657	13.4							
258.5	4677	11.4							
259.5	4697	11.4							
260.5	4716	10.9							
261.5	4736	12.2							
262.5	4756	10.5							
263.5	4776	11.3							
264.5	4795	11.5							
265.5	4815	12.2							
266.5	4835	10.2							
267.5	4855	10.0							
268.5	4874	9.4							
269.5	4894	8.5							
270.5	4920	10.2							
271.5	4951	10.0							
272.5	4982	10.1							
273.5	5013	10.1							
274.5	5044	10.5							

Appendix 10 branched GDGTs at the Lake Belau site.

Depth (m)	Age (cal. yr BP)	BIT	MBT	MBT´	CBT	MAT (ºC) (Weijers et al.. 2007)	MAT (ºC) (Peterse et al.. 2012)	MAT (ºC) (Zink et al.. 2010)	MST (ºC) (Zink et al.. 2010)	MAT (ºC) (Tierney et al.. 2010)	MST (ºC) (Pearson et al.. 2011)
10.29	2434	0.99	0.288	0.246	0.362	4.92	6.38	9.79	14.51	21.97	21.49
10.43	2478	0.99	0.285	0.243	0.377	4.62	6.20	9.62	14.36	21.62	20.82
10.59	2522	0.99	0.265	0.227	0.396	3.45	5.61	8.53	13.37	19.83	19.46
10.79	2578	0.99	0.263	0.225	0.415	3.16	5.42	8.41	13.26	19.38	19.00
11.00	2649	0.99	0.244	0.210	0.447	1.91	4.79	7.36	12.32	13.37	16.48
12.43	3214	0.99	0.256	0.218	0.431	2.65	5.12	8.01	12.90	19.22	18.07
12.63	3300	0.99	0.257	0.221	0.420	2.83	5.28	8.09	12.98	18.64	18.34
12.85	3401	0.99	0.252	0.216	0.396	2.79	5.28	7.79	12.71	19.50	18.40
13.09	3520	0.99	0.251	0.215	0.436	2.36	4.99	7.74	12.66	18.87	17.77
13.40	3667	0.99	0.238	0.205	0.425	1.81	4.76	7.03	12.02	17.33	17.21
13.60	3761	0.99	0.248	0.213	0.416	2.43	5.06	7.61	12.54	17.88	17.62
13.99	3938	0.99	0.241	0.210	0.370	2.48	5.22	7.20	12.17	18.41	18.23
14.22	4045	0.99	0.258	0.221	0.423	2.86	5.26	8.16	13.04	18.71	18.38
14.55	4212	0.99	0.244	0.210	0.450	1.88	4.77	7.35	12.31	17.20	17.23
14.84	4370	0.99	0.243	0.210	0.448	1.88	4.77	7.33	12.29	16.67	17.13
15.04	4484	0.99	0.249	0.214	0.445	2.18	4.91	7.63	12.56	17.16	17.32
15.23	4592	0.99	0.264	0.224	0.458	2.81	5.15	8.46	13.31	17.40	17.67
15.58	4776	0.99	0.244	0.210	0.455	1.86	4.73	7.39	12.34	16.48	16.72
15.66	4820	0.99	0.247	0.210	0.480	1.75	4.61	7.51	12.45	16.06	16.55
15.73	4858	0.99	0.249	0.213	0.455	2.10	4.84	7.64	12.57	17.16	16.97
16.02	5004	0.99	0.247	0.214	0.440	2.14	4.94	7.54	12.48	14.90	16.66
16.44	5193	0.99	0.259	0.221	0.430	2.84	5.22	8.20	13.07	16.86	17.66
16.67	5296	0.98	0.280	0.238	0.383	4.31	6.02	9.34	14.10	19.37	19.83
16.92	5407	0.98	0.269	0.231	0.403	3.60	5.69	8.76	13.58	19.52	19.43
17.09	5492	0.98	0.274	0.233	0.425	3.64	5.61	9.03	13.83	16.75	18.42
17.29	5601	0.99	0.268	0.228	0.421	3.38	5.48	8.70	13.53	18.35	18.21
17.47	5706	0.99	0.287	0.241	0.433	4.20	5.82	9.74	14.46	18.48	18.71
17.66	5815	0.99	0.279	0.236	0.437	3.77	5.65	9.31	14.07	18.56	18.81
17.82	5905	0.99	0.282	0.236	0.463	3.66	5.49	9.45	14.20	17.60	18.20
18.08	6052	0.99	0.269	0.226	0.479	2.86	5.09	8.74	13.56	15.60	16.80
18.38	6222	0.99	0.274	0.229	0.506	2.89	5.04	9.04	13.84	15.09	16.53
18.52	6300	0.99	0.274	0.230	0.477	3.13	5.24	9.01	13.80	15.01	16.88
18.63	6366	0.99	0.269	0.227	0.470	2.96	5.17	8.75	13.58	15.98	17.03
18.66	6384	0.98	0.288	0.239	0.494	3.68	5.42	9.79	14.51	16.87	17.57
18.84	6491	0.98	0.278	0.232	0.483	3.27	5.28	9.22	13.99	15.83	17.07
18.94	6555	0.98	0.280	0.233	0.519	3.04	5.10	9.33	14.10	15.41	16.88
19.03	6611	0.98	0.270	0.228	0.493	2.79	5.08	8.79	13.61	15.20	16.97
19.14	6679	0.98	0.283	0.235	0.493	3.46	5.29	9.54	14.28	15.65	17.12
19.23	6729	0.98	0.296	0.243	0.503	3.98	5.50	10.21	14.89	16.03	17.23
19.28	6758	0.99	0.303	0.251	0.492	4.47	5.80	10.63	15.27	17.43	17.96
19.48	6874	0.99	0.271	0.229	0.459	3.15	5.30	8.85	13.66	15.42	17.08
19.67	6985	0.98	0.289	0.241	0.469	3.98	5.61	9.86	14.57	16.01	17.54
19.88	7106	0.98	0.292	0.242	0.487	3.93	5.54	9.99	14.69	16.75	17.72
20.08	7222	0.98	0.290	0.240	0.503	3.69	5.40	9.89	14.60	16.08	17.22
20.28	7344	0.98	0.319	0.258	0.498	5.18	6.00	11.48	16.04	17.17	17.90
20.48	7463	0.98	0.334	0.269	0.512	5.80	6.24	12.29	16.77	17.30	18.30
20.68	7581	0.98	0.318	0.258	0.514	4.97	5.88	11.41	15.97	16.42	17.73
20.87	7693	0.98	0.309	0.252	0.468	4.95	5.95	10.92	15.53	16.48	17.63
21.12	7854	0.98	0.284	0.237	0.481	3.60	5.42	9.57	14.31	16.22	17.35

Appendix 11 Stable hydrogen and carbon isotope (δD and $\delta^{13}C$) compositions and concentration of *n*-alkanes (C_{27}. C_{29}. and C_{31}) at the Lake Belau site.

		$\delta^{13}C$ (‰ VPDB)			δD (‰ SMOW)			Concentration (%)		
depth (m)	Age (cal. yr BP)	C_{27}	C_{29}	C_{31}	C_{27}	C_{29}	C_{31}	C_{27}	C_{29}	C_{31}
10.29	2434	-31.5	-31.7	-32.8	-164.6	-169.9	-175.1	41.9	19.5	38.6
10.43								40.2	12.4	47.4
10.79	2578	-31.6	-31.5	-32.7	-169.1	-183.3	-181.8	48.3	20.5	31.2
12.43	3214	-32.3	-31.3	-32.0	-162.6	-176.3	-175.0	46.7	20.9	32.4
12.63	3300	-32.4	-31.5	-32.4	-160.5	-175.1	-175.2	52.6	19.9	27.5
12.85	3401	-32.9	-31.6	-32.3	-162.7	-174.6	-174.8	50.5	20.3	29.1
13.40	3667	-32.7	-31.6	-32.3	-168.5	-178.0	-174.0	51.2	20.1	28.7
13.60	3761	-33.3	-32.0	-32.6	-157.7	-174.9	-176.8	51.5	19.0	29.5
13.90					-159.2	-173.2	-171.6			
13.99	3938	-33.1	-31.9	-32.7	-160.9	-170.8	-169.7	48.1	21.7	30.2
14.22	4045	-33.6	-32.4	-32.5	-157.2	-170.0	-168.2	45.9	20.7	33.4
14.55	4212	-33.0	-32.0	-32.3				49.2	21.6	29.2
14.84	4370	-33.0	-32.0	-32.8	-168.9	-174.6	-173.0	49.5	19.8	30.7
15.04	4484	-32.9	-32.1	-32.9	-154.3	-172.2	-164.9	46.8	20.0	33.2
15.23	4592	-33.3	-32.3	-32.1	-166.6	-175.3	-174.5	48.1	20.7	31.2
15.39	4677	-32.3	-31.8	-32.7	-155.5	-160.7	-157.6	47.0	21.0	32.1
15.39	4677	-31.9	-31.3	-32.2						
15.58	4776	-32.7	-32.2	-32.2	-170.9	-182.9	-180.1	51.6	20.8	27.6
15.66	4820	-32.4	-32.2	-32.5	-163.5	-179.2	-173.7	52.3	19.8	27.9
15.66	4820	-31.3	-31.2	-32.2						
15.73	4858	-33.2	-32.4	-33.3	-163.5	-167.1	-172.0	50.2	20.9	28.9
16.02	5004	-32.3	-31.6	-32.9	-156.3	-165.0	-166.2			
16.44	5193	-32.9	-32.6	-33.8	-154.2	-165.5	-172.6	42.6	21.3	36.2
16.92	5407	-32.5	-31.7	-33.0	-147.0	-158.7	-159.1	45.7	21.5	32.8
17.09	5492	-32.3	-31.1	-32.1	-155.8	-164.6	-162.8	49.0	20.9	30.1
17.29	5601	-33.2	-32.1	-32.9	-152.4	-162.4	-155.6	51.1	19.9	29.1
17.47	5706	-34.1	-32.4	-33.1	-149.9	-166.0	-157.8	50.6	18.6	30.8
17.66	5815	-33.1	-32.0	-32.8	-154.1	-162.6	-153.1	48.2	19.4	32.4
17.73	5854	-33.2	-32.3	-32.9						
17.82	5905	-32.8	-32.1	-32.4	-157.3	-168.3	-157.1			
18.08	6052	-32.1	-30.8	-31.3	-164.6	-172.6	-153.9	47.9	19.2	32.9
18.38	6222	-31.5	-30.6	-31.3	-162.5	-167.2	-160.6	48.3	20.3	31.4
18.63	6366	-33.4	-32.0	-33.0	-161.9	-172.2	-162.4	48.9	19.5	31.6
18.66	6384	-32.4	-31.0	-31.7	-161.7	-171.7	-164.5	48.4	19.4	32.2
18.84	6491	-33.4	-31.8	-32.8	-164.5	-171.1	-167.2	50.4	19.6	30.0
18.94	6555	-33.2	-32.0	-32.7	-161.0	-171.8	-163.1	49.9	19.3	30.8
19.03	6611	-32.7	-31.6	-32.5	-167.3	-172.8	-164.7	49.6	19.5	30.9
19.23	6729	-32.0	-30.8	-31.8	-167.1	-175.5	-173.0	51.5	20.8	27.7
19.28	6758	-33.3	-31.7	-32.4	-159.0	-168.9	-162.2	51.3	21.4	27.4
19.48	6874	-33.8	-32.0	-32.3	-154.0	-173.9	-172.0	55.4	19.8	24.8
19.67	6985	-33.7	-31.8	-32.3	-157.9	-178.8	-177.2	54.2	20.1	25.7
19.88	7106	-33.0	-31.6	-31.8	-156.5	-170.6	-166.6	53.2	21.5	25.4
20.08	7222	-31.8	-30.6	-31.5				54.2	20.8	25.0
20.68	7581	-32.1	-30.8	-31.7	-167.2	-175.7	-174.2	54.1	21.2	24.7
20.87	7693	-33.5	-31.5	-32.3	-149.6	-171.0	-174.8	53.9	18.9	27.2
21.12	7854	-31.9	-30.8	-32.0				53.4	20.3	26.2